Impact and regulatory pathways of fatty acids in monocytes/macrophages and adipocytes

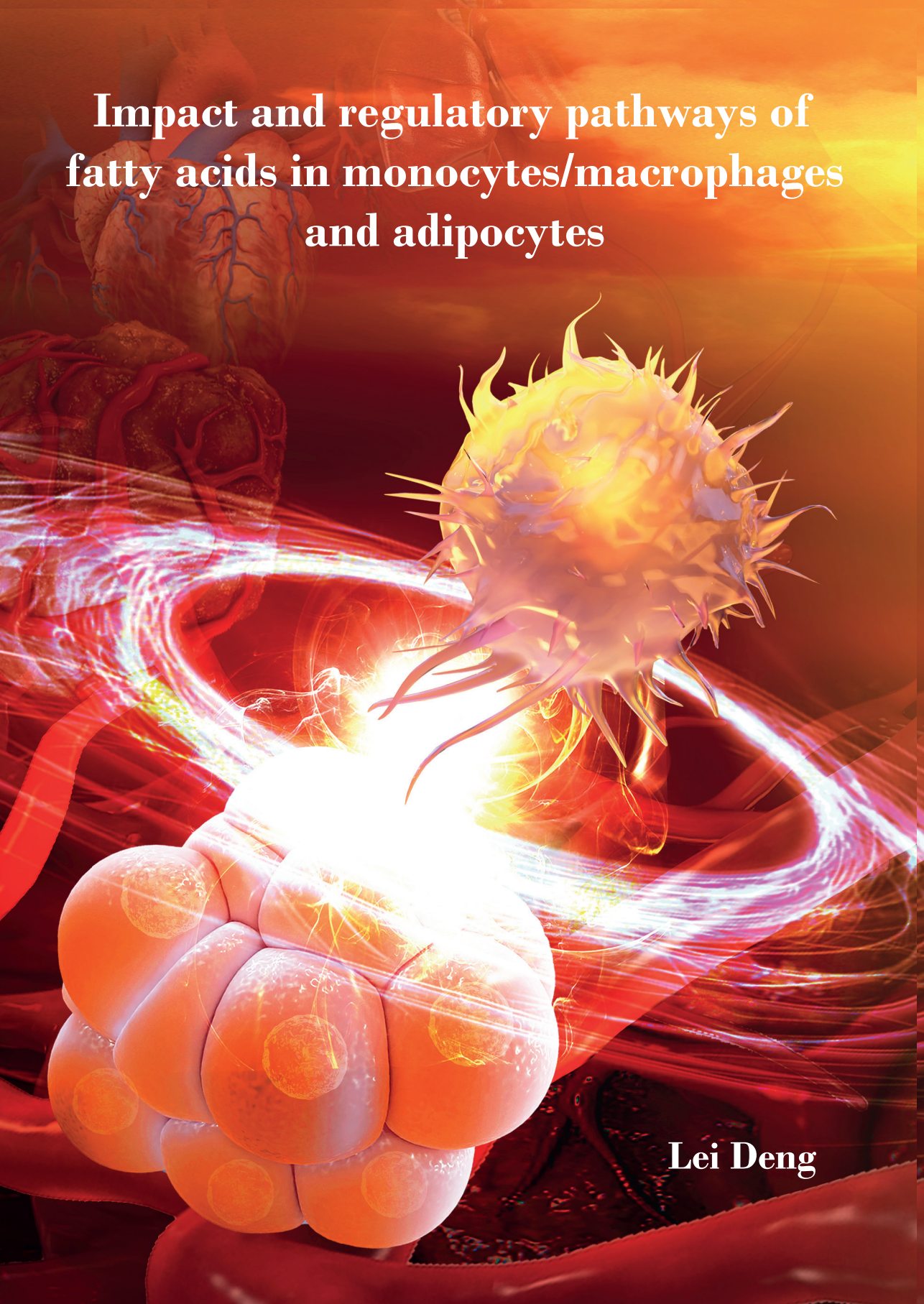

Lei Deng

Propositions

1. Secretion of fatty acids defines a new role of macrophages in immunometabolism.
   (this thesis)
2. HILPDA is essential for the autocrine feedback regulation of lipolysis.
   (this thesis)
3. Having lab members from different cultural backgrounds increases the quality of science in a laboratory.
4. Supervising MSc students is an essential component of the PhD student training and experience.
5. Intuition is an important element of good scientific practice.
6. The Dutch culture does not encourage working outside office hours.
7. Everybody develops biases because information sources are biased by region.

Propositions belonging to the thesis, entitled

"Impact and regulatory pathways of fatty acids in monocytes/macrophages and adipocytes"

Lei Deng

Wageningen, 22nd November, 2022

Impact and regulatory pathways of fatty acids in monocytes/macrophages and adipocytes

Lei Deng

Thesis committee

Promotors

Prof. Dr Sander (A.H.) Kersten

Professor of Nutrition, Metabolism and Genomics

Wageningen University & Research

Dr Lydia A. Afman

Associate Professor, Division of Human Nutrition and Health

Wageningen University & Research

Co-promotors

Dr. Anouk L. Feitsma

FrieslandCampina, Wageningen

Dr. Rinke Stienstra

Assistant Professor, Division of Human Nutrition and Health

Wageningen University & Research

Other members

Prof. Dr Mangala Srinivas – Wageningen University & Research

Prof. Dr Stine Marie Ulven - Oslo Metropolitan University, Norway

Prof. Dr Jogchum Plat - Maastricht University

Dr Eric Kalkhoven - University Medical Center Utrecht

Prof. Dr Bart van de Sluis – University Medical Center Groningen

This research was conducted under the auspices of the Graduate School VLAG

(Advanced Studies in Food Technology, Agrobiotechnology, Nutrition and Health Sciences).

Impact and regulatory pathways of fatty acids in monocytes/macrophages and adipocytes

Lei Deng

Thesis

submitted in fulfilment of the requirements for the degree of doctor
at Wageningen University
by the authority of the Rector Magnificus
Prof. Dr A.P.J. Mol,
in the presence of the
Thesis Committee appointed by the Academic Board
to be defended in public
on Tuesday 22 November 2022
at 4 p.m. in the Omnia Auditorium.

Lei Deng

Impact and regulatory pathways of fatty acids in monocytes/macrophages and adipocytes

PhD thesis, Wageningen University, Wageningen, the Netherlands (2022)
With references, with summary in English

ISBN: 978-94-6447-353-7
DOI: 10.18174/574976

When I walk along with two others, they may serve me as my teachers. I will select their good qualities and follow them, their bad qualities and avoid them.

——***Confucius***

Table of contents

CHARPTER 1

General Introduction

Lipid metabolism

Lipid homeostasis refers to the collective cellular processes involved in the metabolism of lipids, including lipid synthesis, trafficking, and degradation. Many different types of lipids are involved in lipid homeostasis, including fatty acids, monoglycerides, diglycerides, triglycerides (TG), and phospholipids. To maintain lipid homeostasis, the cell must achieve a proper balance between lipid synthesis and lipid degradation.

The synthesis of fatty acids starts with acetyl-CoA. Acetyl-CoA is produced by the breakdown of glucose through glycolysis and by the breakdown of fatty acids through β-oxidation. It can be oxidized in the mitochondria via the citric acid (TCA) cycle to provide energy. Under specific metabolic circumstances, acetyl-CoA can also be converted into malonyl-CoA and used as a building block for the synthesis of fatty acids. The synthesis of fatty acids is referred to as lipogenesis and mainly happens in the liver, yielding acyl-CoA as the end product. As indicated above, fatty acids can also be degraded via β-oxidation. In the liver, fatty acid oxidation is mainly active during fasting, whereas lipogenesis is only relevant following the intake of carbohydrates.

The synthesis of TG starts with acyl-CoA. In the endoplasmic reticulum (ER), acyl-CoA molecules are added one by one to Glycerol-3-Phosphate (G3P) to form TG through the successive action of glycerol-3-phosphate acyltransferase (GPAM, GPAT), acylglycerol-3-phosphate acyltransferase (AGPAT), phosphatidic acid phosphatase (PAP, LPIN), and diacylglycerol acyltransferase (DGAT). Alternatively, in the intestine, because of the abundance of monoglycerides, the acyl-CoA is directly coupled to monoacylglycerol to form diacylglycerol, followed by the conversion of diacylglycerol into TG via DGAT. Two evolutionarily unrelated DGAT isoforms are known to exist, DGAT1 and DGAT2, which each can catalyze the final step in TG synthesis.

TG are actively broken down into fatty acids in nearly all cells, which is important for the function of cells and organs (Guilherme et al., 2008; Unger, 2002; Ahmadian et al., 2010). In particular, TG hydrolysis allows cells to use their internal fat stores as fuel. According to our current understanding, only adipocyte actively export fatty acids, which enter the circulation and can be used as an energy source by other tissues. Three major lipase enzymes are involved in TG hydrolysis, starting with the adipose tissue triglyceride lipase (ATGL), which degrades TG into diacylglycerol, followed by hormone-sensitive lipase (HSL) and monoacylglycerol lipase (MGL), which liberate fatty acids from diacylglycerol and monoacylglycerol, respectively (Zimmermann et al., 2009; Coleman and Mashek, 2011). Many proteins are involved in the regulation of TG hydrolysis. For instance, ATGL can be inhibited by the G0S2 protein and activated by comparative gene identification-58 (CGI-58, aka

ABHD5). In addition, ATGL is regulated by phosphorylation via AMP-dependent protein kinase and AMP-activated protein kinase.

Lipid digestion in humans

Dietary fat is a major source of energy for humans. The majority of dietary fat is in the form of TG, complemented by small amounts of cholesterol and phospholipids. After being digested in the intestinal lumen to monoglycerides and fatty acids, the TG are reassembled in the enterocytes and exported as part of chylomicrons. The chylomicrons are secreted into the lymph and enter the bloodstream at the level of the subclavian vein. After entry in the blood, the chylomicrons are transported to peripheral tissues such as the heart, skeletal muscles, and adipose tissue, where the TG are hydrolyzed by the enzyme lipoprotein lipase. The ensuing chylomicron-remnant particles are cleared from the circulation by the liver. Chylomicrons contain the ApoB48 protein upon secretion from the intestine and pick up the ApoE and ApoC proteins in the bloodstream after interacting with HDL.

In the fasted state, TG are exclusively carried in the blood by very low-density lipoproteins (VLDL). Nascent VLDL is excreted by the liver and contains the ApoB100 protein. Its major lipid cargo consists of TG supplemented by free cholesterol, cholesterol esters, and surface phospholipids. Similar to chylomicrons, VLDL particles acquire ApoE and ApoC proteins in the bloodstream from HDL. After hydrolysis of the VLDL-TG by lipoprotein lipase, intermediate-density lipoproteins are formed, which are further metabolized to low-density lipoprotein, leading to a gradual loss of TG and an increase in the relative content of cholesterol and protein.

Adipocytes

Adipocytes are cells that are specialized in storing energy. Excess energy is stored in the form of TG, which occurs in specialized organelles called lipids droplets. There are two major types of adipocytes in mammals. White adipocytes contain one large lipid droplet and are mainly involved in energy storage. By contrast, brown adipocytes have many small lipid droplets and are involved in generating energy via the abundant mitochondria, thus contributing to the maintenance of body temperature during cold (Cohena and Spiegelmanb, 2016; Jung et al., 2019). When tissues need lipids as fuel, the TG stored in white adipocytes are broken down into fatty acids and released as such into circulation (Rosen and Spiegelman, 2006). In this process of intra-cellular lipolysis, two enzymes play a key role, which are adipose triglyceride lipase (ATGL) and hormone-sensitive lipases (HSL). Besides harboring the major lipid reservoir in the body, adipocytes also play an important role in endocrine

circulation by secreting various signaling molecules such as adipokines, lipokines, and exosomes (Coelho et al., 2013).

Lipid homeostasis and ER stress

Lipid homeostasis strives for harmony between the various metabolic pathways. When cells take up more fatty acids beyond their capacity to store or oxidize them, cells may become stressed (Lee et al., 2015). A similar situation could ensue when TG hydrolysis exceeds the capacity of the cell to secrete or oxidize the mobilized fatty acids (Chitraju et al., 2017). The cellular lipid overload is called lipotoxicity and can induce ER stress. The ER is a cellular organelle involved in many essential processes, including the synthesis of proteins and lipids. Conditions that disrupt ER homeostasis create a cellular state commonly referred to as ER stress. An important trigger for ER stress is the improper folding of proteins but other factors, including excess uptake of saturated fatty acids, can also induce ER stress. The cellular response to ER stress involves the activates of the unfolded protein response, which aims to adjust the ER folding capacity to restore protein homeostasis. Activation of the unfolded protein response leads to three major actions: inhibiting protein translation, degrading misfolded proteins, and increasing the production of molecular chaperones involved in protein folding. If these fail, the cell may enter into apoptosis (Yoshida, 2007).

The expression of ER stress-related genes and proteins was found to be increased in adipose tissue of obese, insulin-resistant people (Boden et al., 2008). Mechanistically, the elevated free fatty acid level in adipocytes may potentially trigger ER stress (Cnop et al., 2012; Jiao et al., 2011). The continuous ER stress and the failed unfolded protein response cause adipocyte dysfunction and necrosis, which further induce insulin resistance, thereby interfering with lipid homeostasis. Therefore, careful control of cellular lipolysis and lipid uptake is important for maintaining proper adipocyte function.

Autocrine negative feedback regulation of lipolysis in adipocytes

As indicated above, a proper balance between fatty acid uptake, lipolysis, fatty acid oxidation, and TG synthesis is essential for cellular homeostasis. Specific mechanisms are in place to safeguard cellular homeostasis when any of these pathways are altered. For instance, when fatty acid uptake or lipolysis is increased, fatty acids activate cellular signaling pathways to exert feedback inhibition of lipolysis. This type of regulation is called autocrine negative feedback regulation. Initially, adenosine was described as an autocrine inhibitory regulator of lipolysis (Jeanrenaud et al., 1970). However, subsequent studies found that oleic acid efficiently inhibited cAMP production in adipocytes (Fain and Shepherd, 1975). The antilipolytic effect of fatty acids appears to be independent of fatty acid β-oxidation and re-esterification (Burns et al., 1978; Kalderon et al., 2012). Recently, Jeppe et al.,

uncovered fatty acid receptor 4 (GPR120) as the main receptor in white adipocytes responsible for sensing FA and mediating negative feedback regulation of lipolysis (Husted et al., 2020). Specifically, it was shown that fatty acids excreted by adipocytes stimulate GPR120, which is one of the G protein uncoupled receptors, and initiate lipolysis inhibition. Although it was suggested that Gi signaling of GPR120 is involved in the regulation of lipolysis by activated cAMP-dependent protein kinase, more direct evidence for the key players in downstream signaling is needed, including the potential role of Gq signaling.

Lipid droplets-associated proteins

Lipid droplets are lipid-rich cellular organelles that regulate the storage and hydrolysis of neutral lipids. They are found in nearly all cells and can vary in size from 20 to 40 nm to 100 uM. The largest lipid droplets are found in adipocytes. The lipid droplets are coated by numerous proteins, called lipid droplet-associated proteins, most of which are involved in the regulation of lipid metabolism (Xu et al., 2018). The first and best-studied family of lipid droplet-associated proteins is the perilipin family, consisting of the five members PLIN1-PLIN5 (Sztalryd and Brasaemle, 2017). Another lipid droplet-associated protein is HILPDA, short for hypoxia-inducible associated. HILPDA is activated by hypoxia in several different cell types and plays an essential role in the regulation of lipid metabolism in lipid droplets (de la Rosa Rodriguez and Kersten, 2017). Specifically, HILPDA acts as a regulatory signal that blocks the breakdown of the internal fat stores in cells when the extracellular fatty acid supply is high or when the availability of oxygen is low (Grabner et al., 2021; Povero et al., 2020). In cells, HILPDA is located in the endoplasmic reticulum and around lipid droplets. HILPDA was found to promote fat storage in liver cells (Mattijssen et al., 2014), cancer cells (Li et al., 2020), and macrophages (van Dierendonck et al., 2020). This effect is mediated by suppression of TG triglyceride breakdown by inhibiting ATGL. The binding of HILPDA to ATGL occurs via the conserved N-terminal portion of HILPDA, which is similar to a region in the G0S2 protein (Padmanabha Das et al., 2018).

Immunometabolism

In the past few decades, it has become evident that metabolism and immunology interact at numerous levels, leading to the emergence of the novel field of immunometabolism. For example, common metabolic diseases, such as cardiovascular disease, obesity, and diabetes, are associated with disturbances in immune function. In particular, all these diseases are characterized by abnormal lipid metabolism in immune cells (Fullerton et al., 2013; Hotamisligil, 2017). Many immune cells, including macrophages/monocytes, dendritic cells, and lymphocytes, can take up and store lipids,

mainly in the form of TG and cholesteryl-esters. The catabolism and storage of lipids in these immune cells have been shown to impact their functional phenotype (van Eijk and Aerts, 2021; Hubler and Kennedy, 2016). For instance, excessive storage of lipids in macrophages can lead to a pro-inflammatory phenotype and promote pro-inflammatory cytokine secretion, which can further recruit more immune cells to the inflammatory sites (Cochain and Zernecke, 2017; Linton and Fazio, 2003). Furthermore, disruption of the normal metabolism of lipids can interfere with the function of mitochondria, thereby impacting numerous core catabolic pathways, including oxidative phosphorylation and the TCA cycle (Alaynick, 2008; Gao et al., 2018; Hubler and Kennedy, 2016). Recent studies have indicated that the core catabolic pathways are important drivers of immune cell behavior, illustrating the powerful link between cellular metabolism and immune cell function. Understanding the essential principles of lipid metabolism in immune cells is vital to developing strategies to treat immune-related and metabolic diseases and understanding how dietary lipids may influence these diseases.

Monocytes and macrophages

Monocytes are the largest type of leukocytes residing in the blood. In specific situations, they can differentiate into different types of macrophages, as well as into conventional dendritic cells. As an essential component of the innate immune system, monocytes can also influence adaptive immune responses. Because of their residence in the blood, monocytes are exposed directly to postprandial lipids, which makes monocytes an important type of immune cell at the crossroad between lipid metabolism and immunology. In recent years, many studies have revealed that exposure to lipids influences the functional phenotype of monocytes by altering the release of different cytokines and chemokines through multiple mechanisms, for example by activating PPAR receptors and Toll-like receptors (Chinetti et al., 2000; Chiurchiù et al., 2016). The differentiation of monocytes into macrophages can also be affected by exposure to lipids, which will further modulate the inflammatory status of monocytes/macrophages.

Macrophages represent the end-stage of monocyte differentiation. To an even stronger extent than monocytes, macrophages can take up all kinds of different lipids, including fatty acids, phospholipids, cholesterol, and entire lipoprotein particles. In several metabolic diseases, such as atherosclerosis (Lee-Rueckert et al., 2022), alcoholic and non-alcoholic fatty liver disease (Kazankov et al., 2018), and obesity (Dahik et al., 2020), the lipid-laden macrophages are a pathological hallmark throughout the initiation and progression of the disease. Hence, understanding how lipids are taken up, stored,

and metabolized in monocytes/macrophages may generate novel inlets for the prevention and treatment of these inflammation-related diseases.

Physiology of TG-rich lipoproteins uptake by macrophages

Lipids can be acquired by macrophages via two major routes. They can be taken up from the external environment or they can be synthesized de novo in the cell. Recent studies suggest that de novo lipogenesis is stimulated upon macrophage activation. Inhibition of the fatty acid synthesis pathway is associated with decreased secretion of various cytokines and impaired phagocytosis (Carroll et al., 2018; Ecker et al., 2010), indicating the importance of the lipogenic pathway for macrophage function.

Traditionally, lipid uptake and storage in macrophages have primarily been investigated in the context of atherosclerosis (de Gaetano et al., 2016). Macrophages take up oxidized LDL, which is considered a key event in the pathogenesis of atherosclerotic lesions (Poznyak et al., 2020). Apart from LDL particles, VLDL and VLDL remnants can also be taken up and retained in the intima, where they can interact with macrophages (Nordestgaard et al., 1995). This further contributes to atherosclerosis (Ginsberg et al., 2021a), possibly by carrying remnant cholesterol and/or by exerting a pro-inflammatory effect on macrophages (Saraswathi and Hasty, 2006).

As indicated above, the excessive uptake and accumulation of lipids in tissue-resident macrophages goes beyond atherosclerosis. For example, alcoholic and non-alcoholic fatty liver disease are characterized by lipid accumulation in Kupffer cells, the major type of hepatic macrophages, and specifically by increased lysosomal cholesterol (Bieghs et al., 2012) (Leroux et al., 2012). Interestingly, Kupffer cells likely play an important role in lipid accumulation in hepatocytes via the release of pro-inflammatory cytokines such as IL-1beta and TNF (Diehl et al., 2020; Stienstra et al., 2010). Another example is obesity. As the adipose tissue expands macrophages accumulate around adipocytes and adopt the morphology of foam cells (Shapiro et al., 2013). The foam cells have been suggested to contribute to the inflammatory phenotype of obese adipose tissue (Reilly and Saltiel, 2017), which in turn may promote the development of insulin resistance (Hotamisligil, 2006; Kotas and Medzhitov, 2015; Lumeng and Saltiel, 2011), although recent data have called this model into question (van Dierendonck et al., 2020).

Endocytic uptake of lipoprotein-TG by macrophages

Endocytosis describes the transport of extracellular substances or particles into cells. For cells, there are different solutions to take up the content of lipoproteins. One classic way is uptake after hydrolysis by lipoprotein lipase (LPL), which means that cells take up fatty acids. Alternatively, some cells can

take up entire lipoprotein particles via endocytosis. Endocytotic uptake of lipoproteins usually requires additional factors. For instance, for hepatocytes, apolipoprotein receptors and other receptors are essential for the uptake of lipoprotein particles (MANN et al., 1995; Zanoni et al., 2018).

In macrophages, the uptake of LDL and oxidized LDL depends on clathrin-mediated endocytosis (Lakadamyali et al., 2006), also called receptor-mediated endocytosis. Before being internalized as a complete lipoprotein particle, binding to a specific receptor is required. This includes the LDL receptor, as well as a group of structurally unrelated molecular pattern recognition receptors referred to as scavenger receptors, including SCARB1, CD36, and MSR1 (Dhaliwal and Steinbrecher, 1999). After endocytosis, the endosome fuses with the lysosome, followed by digestion of the lipoprotein by lysosomal lipase and transfer of the resulting fatty acids to other cellular compartments. Presently, whether macrophages take up TG-rich lipoproteins, including VLDL and chylomicrons, via a similar mechanism as oxidized LDL remains unclear.

Lysosomal processing of internalized TG in macrophages

Lysosomes are membrane-bound cell organelles that contain digestive enzymes. Initially, lysosomes were identified to destroy invading viruses and bacteria. Since then, the functional role of lysosomes has been expanded to the intracellular processing of internalized neutral lipids. It is found that after uptake by macrophages, LDL is degraded in lysosomes, releasing free cholesterol. The cholesterol binds to Niemann-Pick type C2 (NPC2) before being shuttled out of the lysosome via NPC1 (Mesmin et al., 2013) (Infante et al., 2008)(Thelen and Zoncu, 2017). Part of the cholesterol transported via this pathway may go to the plasma membrane, while another portion may go to the endoplasmic reticulum (ER). The lysosomal membrane protein STARD3 transports the cholesterol directly from the lysosome to the ER by interacting with vesicle-associated membrane protein-associated protein (VAP)A/B on the ER membrane (Alpy et al., 2013). Interestingly, STARD3 also promotes the reverse transport of cholesterol from the ER to the lysosome (Wilhelm et al., 2017), as well as the transfer of cholesterol from the lysosome to mitochondria (Charman et al., 2010). While there is thus substantial insight into how cholesterol is processed, transported, and stored in macrophages, our mechanistic understanding of the processing of TG-rich lipoproteins in macrophages is very limited.

Dairy fat consumption and immune health

Milk and other dairy products are consumed daily worldwide. In the last decades, consumption of full-fat milk and butter has been viewed as undesirable because of its naturally high levels of saturated fatty acids. Saturated fatty acids were shown to raise plasma levels of LDL cholesterol. In addition, saturated fatty acids have been shown to carry pro-inflammation properties (Huang et al., 2012).

However, in vitro and in vivo studies, including human studies, have shown that dairy lipids may possess anti-inflammatory properties due to their unique lipid composition and the enclosed milk fat globule membrane (MFGM) (Demmer et al., 2016a; Palmano et al., 2020).

MFGM is a complex and unique structure composed primarily of lipids and proteins, and physically helps the solubility and stability of the milk fat in the watery environment of the milk. The phospholipids in MFGM are considered bioactive. Indeed, the lipid fractions in goat and sheep products that carried anti-inflammatory activity were phosphatidylcholine and phosphatidylethanolamine lipid derivatives (Poutzalis et al., 2018). In the meantime, both in vitro and in vivo work in mice have also shown that phosphatidylcholine has several significant anti-inflammatory properties (Treede et al., 2007). Emerging evidence indicates that the phospholipids in MFGM exert an anti-inflammatory effect by inhibiting the production of inflammatory mediators, such as IL-6, IL-8, and PGE2 (Lordan et al., 2017; Rogers et al., 2017; Zanabria et al., 2014). In line with this, Demmer et al., investigated the effect of a dairy fraction rich in MFGM on the postprandial inflammatory response in overweight and obese adults by a randomized cross-over study. They found the additional intake of the milk fat fraction led to a lower plasma level of cholesterol, decreased inflammatory markers, and a decreased insulin response (Demmer et al., 2016b).

MFGM also has profound effects on the stability of fat globules during processing and digestion and this might limit the postprandial lipemia of milkfat consumption (Singh, 2019). In a study in mice, the consumption of a concept infant formula with large, phospholipid-coated lipid droplets protected against obesity by reducing fat accumulation and improving metabolic profiles (Oosting et al., 2012). In addition, MFGM may also influence the gut microbiota and was shown to attenuate metabolic endotoxemia in mice fed a high-fat diet (Li et al., 2018).

Although several mice and human studies point towards an immunomodulatory effect of MFGM, little is known about the underlying mechanisms. In addition, studies on humans are limited.

Milk fat is different from many other fats in that palmitate is mainly present in the sn-2 position. In contrast to fatty acids located in the sn-1,3 position, fatty acids located in the sn-2 position remain on the glycerol backbone as monoacylglycerol during digestion in the intestine (Hageman et al., 2019). Hence, intestinal digestion of milk fat leads to a lower release of free palmitic acid. Interestingly, the supplementation of a high sn-2 palmitate formula was found to be associated with a lower grade of intestinal erosion in mucin-2 deficient mice, which was modeled to reduce anti-inflammatory protection (Lu et al., 2013). The underlying cause was linked to an enhancement of T cell response

and up-regulation of Proliferator-activated Receptor Gamma (PPAR-gamma) and Enzymatic Antioxidants.

Postprandial lipemia

TG are a major source of energy in the human diet. After a meal, dietary TG enter the bloodstream packaged into large emulsion particles called chylomicrons. Most of the chylomicrons are processed in the adipose tissue, where the TG are hydrolyzed by the enzyme lipoprotein lipase. Elevated levels of triglycerides after a meal, referred to as postprandial lipemia, are associated with an increased risk of atherosclerotic cardiovascular disease (Ginsberg et al., 2021b; Nakamura et al., 2016).

Postprandial lipemia is considered the main factor causing postprandial inflammation, likely attributable to the lipidic environment around immune cells. Postprandial lipemia and inflammation are positively associated with several metabolic disorders, including cardiovascular diseases, diabetes (Bagdade et al., 1967), and obesity (Guerci et al., 2000; Vansant et al., 1999). As a consequence, major efforts are undertaken to try to develop strategies aimed at attenuating the postprandial lipemic response, for instance by enhancing LPL-mediated lipolysis (Tall et al., 2022).

A diet-based strategy can help to reduce postprandial lipemia and inflammation. It has been shown that consumption of different types of fats leads to differential effects on postprandial lipemia. For instance, hyperlipemia can be alleviated in adults with higher BMI ($\geq$30 kg/m^2), and/or who are older than 40 years old by replacing saturated fatty acids in the meal with unsaturated fatty acids (Neumann and Egert, 2022). Milk fat is considered to induce a relatively limited postprandial lipemic response, related to the specific fatty acid composition of milk fat and the presence of the MFGM (Michalski, 2009; Rogers et al., 2017).

Outline of the thesis

This thesis aims to gain more insights into the regulation of metabolic homeostasis by lipids in adipose tissue and the immune system. **Chapter 2** describes the involvement of Hypoxia-inducible lipid droplets-associated (HILPDA) in the maintenance of lipid homeostasis in adipocytes. The central role of HILPDA in the regulation of lipolysis is systematically investigated. **Chapter 3** explores how macrophages take up VLDL particles and shows that macrophages can excrete fatty acids after the internalization of the TG-rich lipoprotein particles. In **chapter 4** and **chapter 5**, a randomized cross-over study in human volunteers is described that is aimed at uncovering the postprandial effect of milk fat consumption on circulation lipid metabolites and monocytes. The investigation is based on the analysis of the postprandial plasma metabolome and the whole genome

transcriptome of the monocytes. Finally, in **chapter 6**, all findings will be discussed and integrated to provide a general conclusion of the thesis.

References

Ahmadian, M., Wang, Y., and Sul, H.S. (2010). Lipolysis in adipocytes. Int. J. Biochem. Cell Biol. *42*, 555–559.

Alaynick, W.A. (2008). Nuclear receptors, mitochondria and lipid metabolism. Mitochondrion *8*, 329–337.

Alpy, F., Rousseau, A., Schwab, Y., Legueux, F., Stoll, I., Wendling, C., Spiegelhalter, C., Kessler, P., Mathelin, C., Rio, M.C., et al. (2013). STARD3 or STARD3NL and VAP form a novel molecular tether between late endosomes and the ER. J. Cell Sci. *126*, 5500–5512.

Bagdade, J.D., Porte, D., and Bierman, E.L. (1967). Diabetic Lipemia. N. Engl. J. Med. *276*, 427–433.

Bieghs, V., Verheyen, F., van Gorp, P.J., Hendrikx, T., Wouters, K., Lütjohann, D., Gijbels, M.J.J., Febbraio, M., Binder, C.J., Hofker, M.H., et al. (2012). Internalization of modified lipids by CD36 and SR-A leads to hepatic inflammation and lysosomal cholesterol storage in kupffer cells. PLoS One *7*, e34378.

Boden, G., Duan, X., Homko, C., Molina, E.J., Song, W., Perez, O., Cheung, P., and Merali, S. (2008). Increase in endoplasmic reticulum stress-related proteins and genes in adipose tissue of obese, insulin-resistant individuals. Diabetes *57*, 2438–2444.

Burns, T.W., Langley, P.E., Terry, B.E., and Robinson, G.A. (1978). The role of free fatty acids in the regulation of lipolysis by human adipose tissue cells. Metabolism *27*, 1755–1762.

Carroll, R.G., Zasłona, Z., Galván-Peña, S., Koppe, E.L., Sévin, D.C., Angiari, S., Triantafilou, M., Triantafilou, K., Modis, L.K., and O'Neill, L.A. (2018). An unexpected link between fatty acid synthase and cholesterol synthesis in proinflammatory macrophage activation. J. Biol. Chem. *293*, 5509–5521.

Charman, M., Kennedy, B.E., Osborne, N., and Karten, B. (2010). MLN64 mediates egress of cholesterol from endosomes to mitochondria in the absence of functional Niemann-Pick Type C1 protein. J. Lipid Res. *51*, 1023–1034.

Chinetti, G., Fruchart, J.C., and Staels, B. (2000). Peroxisome proliferator-activated receptors (PPARs): Nuclear receptors at the crossroads between lipid metabolism and inflammation. Inflamm. Res. *49*, 497–505.

Chitraju, C., Mejhert, N., Haas, J.T., Diaz-Ramirez, L.G., Grueter, C.A., Imbriglio, J.E., Pinto, S., Koliwad, S.K., Walther, T.C., and Farese, R. V. (2017). Triglyceride Synthesis by DGAT1 Protects Adipocytes from Lipid-Induced ER Stress during Lipolysis. Cell Metab. *26*, 407-418.e3.

Chiurchiù, V., Leuti, A., Cencioni, M.T., Albanese, M., De Bardi, M., Bisogno, T., Centonze, D., Battistini, L., and Maccarrone, M. (2016). Modulation of monocytes by bioactive lipid anandamide in multiple sclerosis involves distinct Toll-like receptors. Pharmacol. Res. *113*, 313–319.

Cnop, M., Foufelle, F., and Velloso, L.A. (2012). Endoplasmic reticulum stress, obesity and diabetes. Trends Mol. Med. *18*, 59–68.

Cochain, C., and Zernecke, A. (2017). Macrophages in vascular inflammation and atherosclerosis. Pflugers Arch. Eur. J. Physiol. *469*, 485–499.

Coelho, M., Oliveira, T., and Fernandes, R. (2013). Biochemistry of adipose tissue: An endocrine organ. Arch. Med. Sci. *9*, 191–200.

Cohena, P., and Spiegelmanb, B.M. (2016). Cell biology of fat storage. Mol. Biol. Cell *27*, 2523–2527.

Dahik, V.D., Frisdal, E., and Goff, W. Le (2020). Rewiring of lipid metabolism in adipose tissue macrophages in obesity: Impact on insulin resistance and type 2 diabetes. Int. J. Mol. Sci. *21*, 1–30.

Demmer, E., Van Loan, M.D., Rivera, N., Rogers, T.S., Gertz, E.R., Bruce German, J., Smilowitz, J.T., and Zivkovic, A.M. (2016a). Addition of a dairy fraction rich in milk fat globule membrane to a high-saturated fat meal reduces the postprandial insulinaemic and inflammatory response in overweight and obese adults. J. Nutr. Sci. *5*, 1–11.

Demmer, E., Van Loan, M.D., Rivera, N., Rogers, T.S., Gertz, E.R., Bruce German, J., Smilowitz, J.T., and Zivkovic, A.M. (2016b). Addition of a dairy fraction rich in milk fat globule membrane to a high-saturated fat meal reduces the postprandial insulinaemic and inflammatory response in overweight and obese adults. J. Nutr. Sci. *5*, 1–11.

Dhaliwal, B.S., and Steinbrecher, U.P. (1999). Scavenger receptors and oxidized low density lipoproteins. In Clinica Chimica Acta, (Clin Chim Acta), pp. 191–205.

Diehl, K.L., Vorac, J., Hofmann, K., Meiser, P., Unterweger, I., Kuerschner, L., Weighardt, H., Förster, I., and Thiele, C. (2020). Kupffer Cells Sense Free Fatty Acids and Regulate Hepatic Lipid Metabolism in High-Fat Diet and Inflammation. Cells *9*.

van Dierendonck, X.A.M.H., de la Rosa Rodriguez, M.A., Georgiadi, A., Mattijssen, F., Dijk, W., van Weeghel, M., Singh, R., Borst, J.W., Stienstra, R., and Kersten, S. (2020). HILPDA Uncouples Lipid Droplet Accumulation in Adipose Tissue Macrophages from Inflammation and Metabolic Dysregulation. Cell Rep. *30*, 1811-1822.e6.

Ecker, J., Liebisch, G., Englmaier, M., Grandl, M., Robenek, H., and Schmitz, G. (2010). Induction of fatty acid synthesis is a key requirement for phagocytic differentiation of human monocytes. Proc. Natl. Acad. Sci. U. S. A. *107*, 7817–7822.

van Eijk, M., and Aerts, J.M.F.G. (2021). The unique phenotype of lipid-laden macrophages. Int. J. Mol. Sci. *22*, 4039.

Fain, J.N., and Shepherd, R.E. (1975). Free fatty acids as feedback regulators of adenylate cyclase and cyclic 3':5' AMP accumulation in rat fat cells. J. Biol. Chem. *250*, 6586–6592.

Fullerton, M.D., Steinberg, G.R., and Schertzer, J.D. (2013). Immunometabolism of AMPK in insulin resistance and atherosclerosis. Mol. Cell. Endocrinol. *366*, 224–234.

de Gaetano, M., Crean, D., Barry, M., and Belton, O. (2016). M1- and M2-type macrophage responses are predictive of adverse outcomes in human atherosclerosis. Front. Immunol. *7*, 275.

Gao, X., Lee, K., Reid, M.A., Sanderson, S.M., Qiu, C., Li, S., Liu, J., and Locasale, J.W. (2018). Serine Availability Influences Mitochondrial Dynamics and Function through Lipid Metabolism. Cell Rep. *22*, 3507–3520.

Ginsberg, H.N., Packard, C.J., Chapman, M.J., Borén, J., Aguilar-Salinas, C.A., Averna, M., Ference, B.A., Gaudet, D., Hegele, R.A., Kersten, S., et al. (2021a). Triglyceride-rich lipoproteins and their remnants: Metabolic insights, role in atherosclerotic cardiovascular disease, and emerging therapeutic strategies-a consensus statement from the European Atherosclerosis Society. Eur. Heart J. *42*, 4791–4806.

Ginsberg, H.N., Packard, C.J., Chapman, M.J., Borén, J., Aguilar-Salinas, C.A., Averna, M., Ference, B.A., Gaudet, D., Hegele, R.A., Kersten, S., et al. (2021b). Triglyceride-rich lipoproteins and their remnants: Metabolic insights, role in atherosclerotic cardiovascular disease, and emerging therapeutic strategies-a consensus statement from the European Atherosclerosis Society. Eur. Heart J. *42*, 4791–4806.

Grabner, G.F., Xie, H., Schweiger, M., and Zechner, R. (2021). Lipolysis: cellular mechanisms for lipid mobilization from fat stores. Nat. Metab. *3*, 1445–1465.

Guerci, B., Vergès, B., Durlach, V., Hadjadj, S., Drouin, P., and Paul, J.L. (2000). Relationship between altered postprandial lipemia and insulin resistance in normolipidemic and normoglucose tolerant obese patients. Int. J. Obes. *24*, 468–478.

Guilherme, A., Virbasius, J. V., Puri, V., and Czech, M.P. (2008). Adipocyte dysfunctions linking obesity to insulin resistance and type 2 diabetes. Nat. Rev. Mol. Cell Biol. *9*, 367–377.

Hageman, J.H.J., Danielsen, M., Nieuwenhuizen, A.G., Feitsma, A.L., and Dalsgaard, T.K. (2019). Comparison of bovine milk fat and vegetable fat for infant formula: Implications for infant health. Int. Dairy J. *92*, 37–49.

Hotamisligil, G.S. (2006). Inflammation and metabolic disorders. Nature *444*, 860–867.

Hotamisligil, G.S. (2017). Foundations of Immunometabolism and Implications for Metabolic Health and Disease. Immunity *47*, 406–420.

Huang, S., Rutkowsky, J.M., Snodgrass, R.G., Ono-Moore, K.D., Schneider, D.A., Newman, J.W., Adams, S.H., and Hwang, D.H. (2012). Saturated fatty acids activate TLR-mediated proinflammatory signaling pathways [S]. J. Lipid Res. *53*, 2002–2013.

Hubler, M.J., and Kennedy, A.J. (2016). Role of lipids in the metabolism and activation of immune cells. J. Nutr. Biochem. *34*, 1–7.

Husted, A.S., Ekberg, J.H., Tripp, E., Nissen, T.A.D., Meijnikman, S., O'Brien, S.L., Ulven, T., Acherman, Y., Bruin, S.C., Nieuwdorp, M., et al. (2020). Autocrine negative feedback regulation of lipolysis through sensing of NEFAs by FFAR4/GPR120 in WAT. Mol. Metab. *42*.

Infante, R.E., Wang, M.L., Radhakrishnan, A., Hyock, J.K., Brown, M.S., and Goldstein, J.L. (2008). NPC2 facilitates bidirectional transfer of cholesterol between NPC1 and lipid bilayers, a step in cholesterol egress from lysosomes. Proc. Natl. Acad. Sci. U. S. A. *105*, 15287–15292.

Jeanrenaud, B., Hepp, D., and Renold, A.E. (1970). The influence of lipolysis on energy metabolism of isolated fat cells. Horm. Metab. Res. *2*.

Jiao, P., Ma, J., Feng, B., Zhang, H., Alan Diehl, J., Eugene Chin, Y., Yan, W., and Xu, H. (2011). FFA-induced adipocyte inflammation and insulin resistance: Involvement of ER stress and IKKβ pathways. Obesity *19*, 483–491.

Jung, S.M., Sanchez-Gurmaches, J., and Guertin, D.A. (2019). Brown adipose tissue development and metabolism. In Handbook of Experimental Pharmacology, (NIH Public Access), pp. 3–36.

Kalderon, B., Azazmeh, N., Azulay, N., Vissler, N., Valitsky, M., and Bar-Tana, J. (2012). Suppression of adipose lipolysis by long-chain fatty acid analogs. J. Lipid Res. *53*, 868–878.

Kazankov, K., Jørgensen, S.M.D., Thomsen, K.L., Møller, H.J., Vilstrup, H., George, J., Schuppan, D., and Grønbæk, H. (2018). The role of macrophages in nonalcoholic fatty liver disease and nonalcoholic steatohepatitis. Nat. Rev. Gastroenterol. Hepatol. 2018 163 *16*, 145–159.

Kotas, M.E., and Medzhitov, R. (2015). Homeostasis, Inflammation, and Disease Susceptibility. Cell *160*, 816–827.

de la Rosa Rodriguez, M.A., and Kersten, S. (2017). Regulation of lipid droplet-associated proteins by peroxisome proliferator-activated receptors. Biochim. Biophys. Acta - Mol. Cell Biol. Lipids *1862*, 1212–1220.

Lakadamyali, M., Rust, M.J., and Zhuang, X. (2006). Ligands for clathrin-mediated endocytosis are differentially sorted into distinct populations of early endosomes. Cell *124*, 997–1009.

Lee-Rueckert, M., Lappalainen, J., Kovanen, P.T., and Escola-Gil, J.C. (2022). Lipid-Laden Macrophages and Inflammation in Atherosclerosis and Cancer: An Integrative View. Front. Cardiovasc. Med. *9*, 777822.

Lee, J., Ellis, J.M., and Wolfgang, M.J. (2015). Adipose fatty acid oxidation is required for thermogenesis and potentiates oxidative stress-induced inflammation. Cell Rep. *10*, 266–279.

Leroux, A., Ferrere, G., Godie, V., Cailleux, F., Renoud, M.L., Gaudin, F., Naveau, S., Prévot, S., Makhzami, S., Perlemuter, G., et al. (2012). Toxic lipids stored by Kupffer cells correlates with their pro-inflammatory phenotype at an early stage of steatohepatitis. J. Hepatol. *57*, 141–149.

Li, P., Lu, M., Shi, J., Gong, Z., Hua, L., Li, Q., Lim, B., Zhang, X.H.F., Chen, X., Li, S., et al. (2020). Lung mesenchymal cells elicit lipid storage in neutrophils that fuel breast cancer lung metastasis. Nat. Immunol. *21*, 1444–1455.

Li, T., Gao, J., Du, M., and Mao, X. (2018). Milk fat globule membrane supplementation modulates the gut microbiota and attenuates metabolic endotoxemia in high-fat diet-fed mice. J. Funct. Foods *47*, 56–65.

Linton, M.F., and Fazio, S. (2003). Macrophages, inflammation, and atherosclerosis. In International Journal of Obesity, (Nature Publishing Group), pp. S35–S40.

Lordan, R., Tsoupras, A., and Zabetakis, I. (2017). Phospholipids of animal and marine origin:

Structure, function, and anti-inflammatory properties. Molecules *22*, 1964.

Lu, P., Bar-Yoseph, F., Levi, L., Lifshitz, Y., Witte-Bouma, J., de Bruijn, A.C.J.M., Korteland-van Male, A.M., van Goudoever, J.B., and Renes, I.B. (2013). High Beta-Palmitate Fat Controls the Intestinal Inflammatory Response and Limits Intestinal Damage in Mucin Muc2 Deficient Mice. PLoS One *8*.

Lumeng, C.N., and Saltiel, A.R. (2011). Inflammatory links between obesity and metabolic disease. J. Clin. Invest. *121*, 2111–2117.

MANN, W.A., MEYER, N., WEBER, W., RINNINGER, F., GRETEN, H., and BEISIEGEL, U. (1995). Apolipoprotein E and lipoprotein lipase co-ordinately enhance binding and uptake of chylomicrons by human hepatocytes. Eur. J. Clin. Invest. *25*, 880–882.

Mattijssen, F., Georgiadi, A., Andasarie, T., Szalowska, E., Zota, A., Krones-Herzig, A., Heier, C., Ratman, D., De Bosscher, K., Qi, L., et al. (2014). Hypoxia-inducible Lipid Droplet-associated (HILPDA) is a novel Peroxisome Proliferator-activated Receptor (PPAR) target involved in hepatic triglyceride secretion. J. Biol. Chem. *289*, 19279–19293.

Mesmin, B., Antonny, B., and Drin, G. (2013). Insights into the mechanisms of sterol transport between organelles. Cell. Mol. Life Sci. *70*, 3405–3421.

Michalski, M.C. (2009). Specific molecular and colloidal structures of milk fat affecting lipolysis, absorption and postprandial lipemia. Eur. J. Lipid Sci. Technol. *111*, 413–431.

Nakamura, K., Miyoshi, T., Yunoki, K., and Ito, H. (2016). Postprandial hyperlipidemia as a potential residual risk factor. J. Cardiol. *67*, 335–339.

Neumann, H.F., and Egert, S. (2022). Impact of Meal Fatty Acid Composition on Postprandial Lipemia in Metabolically Healthy Adults and Individuals with Cardiovascular Disease Risk Factors: A Systematic Review. Adv. Nutr. *13*, 193–207.

Nordestgaard, B.G., Wootton, R., and Lewis, B. (1995). Selective Retention of VLDL, IDL, and LDL in the Arterial Intima of Genetically Hyperlipidemic Rabbits In Vivo. Arterioscler. Thromb. Vasc. Biol. *15*, 534–542.

Oosting, A., Kegler, D., Wopereis, H.J., Teller, I.C., Van De Heijning, B.J.M., Verkade, H.J., and Van Der Beek, E.M. (2012). Size and phospholipid coating of lipid droplets in the diet of young mice modify body fat accumulation in adulthood. Pediatr. Res. *72*, 362–369.

Padmanabha Das, K.M., Wechselberger, L., Liziczai, M., De La Rosa Rodriguez, M., Grabner, G.F., Heier, C., Viertlmayr, R., Radler, C., Lichtenegger, J., Zimmermann, R., et al. (2018). Hypoxia-inducible lipid droplet-associated protein inhibits adipose triglyceride lipase. J. Lipid Res. *59*, 531–541.

Palmano, K.P., Macgibbon, A.K.H., Gunn, C.A., and Schollum, L.M. (2020). In vitro and in vivo anti-inflammatory activity of bovine milkfat globule (MFGM)-derived complex lipid fractions. Nutrients *12*, 1–21.

Poutzalis, S., Lordan, R., Nasopoulou, C., and Zabetakis, I. (2018). Phospholipids of goat and sheep origin: Structural and functional studies. Small Rumin. Res. *167*, 39–47.

Povero, D., Johnson, S.M., and Liu, J. (2020). Hypoxia, hypoxia-inducible gene 2 (HIG2)/HILPDA, and intracellular lipolysis in cancer. Cancer Lett. *493*, 71–79.

Poznyak, A. V., Nikiforov, N.G., Markin, A.M., Kashirskikh, D.A., Myasoedova, V.A., Gerasimova, E. V., and Orekhov, A.N. (2020). Overview of OxLDL and Its Impact on Cardiovascular Health: Focus on Atherosclerosis. Front. Pharmacol. *11*.

Reilly, S.M., and Saltiel, A.R. (2017). Adapting to obesity with adipose tissue inflammation. Nat. Rev. Endocrinol. *13*, 633–643.

Rogers, T.S., Demmer, E., Rivera, N., Gertz, E.R., German, J.B., Smilowitz, J.T., Zivkovic, A.M., and Van Loan, M.D. (2017). The role of a dairy fraction rich in milk fat globule membrane in the suppression of postprandial inflammatory markers and bone turnover in obese and overweight adults: an exploratory study. Nutr. Metab. *14*, 1–9.

Rosen, E.D., and Spiegelman, B.M. (2006). Adipocytes as regulators of energy balance and glucose homeostasis. Nature *444*, 847–853.

Saraswathi, V., and Hasty, A.H. (2006). The role of lipolysis in mediating the proinflammatory effects of very low density lipoproteins in mouse peritoneal macrophages. J. Lipid Res. *47*, 1406–1415.

Shapiro, H., Pecht, T., Shaco-Levy, R., Harman-Boehm, I., Kirshtein, B., Kuperman, Y., Chen, A., Blüher, M., Shai, I., and Rudich, A. (2013). Adipose tissue foam cells are present in human obesity. J. Clin. Endocrinol. Metab. *98*, 1173–1181.

Singh, H. (2019). Symposium review: Fat globules in milk and their structural modifications during gastrointestinal digestion. In Journal of Dairy Science, (Elsevier), pp. 2749–2759.

Stienstra, R., Saudale, F., Duval, C., Keshtkar, S., Groener, J.E.M., Van Rooijen, N., Staels, B., Kersten, S., and Müller, M. (2010). Kupffer cells promote hepatic steatosis via interleukin-1β-dependent suppression of peroxisome proliferator-activated receptor α activity. Hepatology *51*, 511–522.

Sztalryd, C., and Brasaemle, D.L. (2017). The perilipin family of lipid droplet proteins: Gatekeepers of intracellular lipolysis. Biochim. Biophys. Acta - Mol. Cell Biol. Lipids *1862*, 1221–1232.

Tall, A.R., Thomas, D.G., Gonzalez-Cabodevilla, A.G., and Goldberg, I.J. (2022). Addressing dyslipidemic risk beyond LDL-cholesterol. J. Clin. Invest. *132*.

Thelen, A.M., and Zoncu, R. (2017). Emerging Roles for the Lysosome in Lipid Metabolism. Trends Cell Biol. *27*, 833–850.

Treede, I., Braun, A., Sparla, R., Kühnel, M., Giese, T., Turner, J.R., Anes, E., Kulaksiz, H., Füllekrug, J., Stremmel, W., et al. (2007). Anti-inflammatory effects of phosphatidylcholine. J. Biol. Chem. *282*, 27155–27164.

Unger, R.H. (2002). Lipotoxic diseases. Annu. Rev. Med. *53*, 319–336.

Vansant, G., Mertens, A., and Muls, E. (1999). Determinants of postprandial lipemia in obese women. Int. J. Obes. *23*, 14–21.

Wilhelm, L.P., Wendling, C., Védie, B., Kobayashi, T., Chenard, M., Tomasetto, C., Drin, G., and Alpy, F. (2017). STARD 3 mediates endoplasmic reticulum-to-endosome cholesterol transport at membrane contact sites. EMBO J. *36*, 1412–1433.

Xu, S., Zhang, X., and Liu, P. (2018). Lipid droplet proteins and metabolic diseases. Biochim. Biophys. Acta - Mol. Basis Dis. *1864*, 1968–1983.

Yoshida, H. (2007). ER stress and diseases. FEBS J. *274*, 630–658.

Zanabria, R., Tellez, A.M., Griffiths, M., Sharif, S., and Corredig, M. (2014). Modulation of immune function by milk fat globule membrane isolates. J. Dairy Sci. *97*, 2017–2026.

Zanoni, P., Velagapudi, S., Yalcinkaya, M., Rohrer, L., and von Eckardstein, A. (2018). Endocytosis of lipoproteins. Atherosclerosis *275*, 273–295.

Zimmermann, R., Lass, A., Haemmerle, G., and Zechner, R. (2009). Fate of fat: The role of adipose triglyceride lipase in lipolysis. Biochim. Biophys. Acta - Mol. Cell Biol. Lipids *1791*, 494–500.

CHARPTER 2

HILPDA mediates autocrine negative feedback regulation of adipose tissue lipolysis by fatty acids and GPR120

Lei Deng, Sander Kersten

To be submitted

ABSTRACT

Lipolysis is a key metabolic pathway in adipocytes that renders stored triglycerides available for use by other cells and tissues. Fatty acids are known to exert feedback inhibition on adipocyte lipolysis by activating the fatty acid receptor GPR120. Here, we present evidence that the ATGL inhibitor HILPDA underlies the autocrine negative feedback regulation of adipose tissue lipolysis by NEFA via GPR120. Elevation of extra- and intracellular fatty acid levels, as well as the GPR120 agonist TUG891, markedly increased HILPDA levels in primary mouse adipocytes. The induction of HILPDA by fatty acid was markedly attenuated by the GPR120 antagonist AH7614. Deficiency of HILPDA upregulated ATGL protein levels under conditions of extra- and intracellular fatty acid overload and GPR120 activation, which was associated with elevated glycerol release and induction of ER stress markers. In vivo deficiency of HILPDA deficiency in adipocytes minimally impacted metabolic parameters after low- or high-fat feeding, yet increased the expression of markers of ER stress in adipose tissue after fasting/refeeding. In conclusion, we show that HILPDA is a central node in a fatty acid- and GPR120-induced autocrine feedback loop in adipocytes that aims to limit intracellular lipolysis under conditions of excess intra- or extracellular fatty acid supply.

Keywords: Hypoxia-inducible lipid droplet associated, GPR120, Negative feedback regulation of lipolysis, ATGL, Adipocytes

INTRODUCTION

The main function of adipose tissue is to store excess energy as triglycerides. An average human adult carries sufficient amounts of triglycerides to survive at least 4 weeks of complete food deprivation. The amount of triglycerides stored in the adipose tissue is determined by the balance between triglyceride synthesis and triglyceride hydrolysis (lipolysis), e.g. triglyceride turnover. Estimates of the daily turnover rate of triglycerides for an averaged sized adult vary from 50-100 g/d (Hellerstein et al., 1991; Klein et al., 1986; Strawford et al., 2004).

The fatty acids used to synthesize triglycerides in adipose tissue are mainly derived from the circulating triglyceride-rich lipoproteins VLDL and chylomicrons. The triglycerides in these lipoproteins are hydrolyzed by the enzyme lipoprotein lipase (LPL), which is secreted by adipocytes and subsequently delivered to the endothelial surface (Kersten, 2014). After uptake by adipocytes, the fatty acids are transported to the endoplasmic reticulum where they are re-esterified to triglycerides through the sequential addition of fatty acyl moieties to a glycerol-3-phosphate (G3P) backbone. The last, and reportedly rate-limiting, step in triglyceride synthesis involves the addition of acyl-CoA to diacylglycerol and is catalyzed by diglyceride acyltransferase (DGAT). Two evolutionarily distinct DGAT isoenzymes exist, DGAT1 and DGAT2 (Bhatt-Wessel et al., 2018). It was shown that DGAT1 and DGAT2 can largely compensate for each other to support triglyceride storage in adipocytes (Chitraju et al., 2019). However, DGAT1 is unique in being able to protect the ER from the lipotoxic effects of high-fat diets (Chitraju et al., 2017). Following DGAT-catalyzed triglyceride synthesis, the lipids are stored in a single large lipid droplet surrounded by a phospholipid monolayer and decorated with numerous lipid-droplet-associated proteins.

As part of regular triglyceride turnover, a portion of the triglycerides stored in lipid droplets is hydrolyzed to fatty acids. The sequential removal of fatty acids from the triglyceride molecule is catalyzed by the enzymes adipose triglyceride lipase, hormone-sensitive lipase, and monoglyceride lipase (Young and Zechner, 2013). A portion of the liberated fatty acids is secreted and ends up in the bloodstream, accounting for most of the non-esterified fatty acid (NEFA) pool in the plasma. The other part is re-esterified to triglycerides in the adipocyte (Kalderon et al., 2000). Since glycerol released by lipolysis cannot be re-used by the adipocyte, the molar ratio of fatty acids to glycerol released provides an estimate of the relative rate of fatty acid re-esterification. In weight-stable, never-obese control subjects, this ratio of FFA:glycerol leaving the adipocytes was reported to be 1.4:1, suggesting that under baseline conditions most of the fatty acids are re-esterified (Leibel et al., 1985).

Adipose tissue lipolysis is under tight hormonal control (Goodman and Knobil, 1961). Cortisol, (nor)epinephrine, and growth hormone stimulate the activity of lipolytic enzymes, whereas insulin has the opposite effect. The effects of metabolic hormones on the activities of lipolytic enzymes are mainly mediated by post-translational mechanisms. The regulatory pathways mainly converge on ATGL, which is considered rate-limiting for lipolysis (Jenkins et al., 2004; Villena et al., 2004; Zimmermann et al., 2004). In addition to activation via PKA and AMPK-mediated phosphorylation, ATGL is regulated through the physical interaction with (in)activating proteins such as CGI-58 and G0S2. CGI-58 is a catalytically inactive member of the family of α/β hydrolase domain-containing proteins that binds and activates ATGL (Lass et al., 2006), whereas G0S2 inhibits ATGL (Yang et al., 2010). A more recently identified co-regulatory protein of ATGL is HILPDA (Gimm et al., 2010). HILPDA (Hypoxia Induced Lipid Droplet Associated) is a small lipid droplet-associated protein that is expressed in macrophages, hepatocytes, cancer cells, and adipocytes (de la Rosa Rodriguez and Kersten, 2020). The levels of HILPDA are increased by various stimuli including hypoxia, β-adrenergic activation, and fatty acids. Consistent with the ability of ATGL to bind to and inhibit ATGL (Padmanabha Das et al., 2018; Zhang et al., 2017), gain and loss of function studies have shown that HILPDA promotes triglyceride accumulation in hepatocytes (de la Rosa Rodriguez et al., 2021; DiStefano et al., 2015; Mattijssen et al., 2014), macrophages (Maier et al., 2017; van Dierendonck et al., 2020; van Dierendonck et al., 2022), and cancer cells (VandeKopple et al., 2019; Zhang et al., 2017). Currently, the physiological role of HILPDA in adipose tissue is not fully clear (Dijk et al., 2017; DiStefano et al., 2016). Previous studies did not reveal a clear effect of adipocyte-specific HILPDA-deficiency on in vivo lipolysis under conditions of fasting, cold exposure, or β3-adrenergic activation (Dijk et al., 2017).

In addition to via hormonal cues, lipolysis is also regulated by fatty acids, which are the products of the lipolytic reaction. Specifically, it was found that fatty acids exert feedback inhibition on lipolysis by suppressing cAMP levels (Burns et al., 1978; Fain and Shepherd, 1975; Kalderon et al., 2012). Recent data suggest that this feedback inhibition by fatty acids is mediated by FFAR/GPR120 (Husted et al., 2020). It was found that plasma NEFA levels in mice were decreased by activation of GPR120 using the synthetic GPR120 agonist CpdB, whereas plasma NEFA levels were increased in GPR120-deficient mice (Husted et al., 2020).

Here we explored the hypothesis that the feedback inhibition of lipolysis by fatty acids is mediated by GPR120-mediated induction of HILPDA, leading to inhibition of ATGL. In addition, we explored

the effect of adipocyte-specific HILPDA deficiency under conditions of low fat/high fat feeding or fasting/refeeding.

EXPERIMENTAL PROCEDURES

Animal study

Mice and diets

All animal experiments were approved by the animal welfare committee of Wageningen University (AVD104002015236; 2016.W-0093.002, 2016.W-0093.007). *Hilpda*$^{flox/flox}$ mice (Jackson Laboratories, Bar Harbor, ME; Hilpda$^{tm1.1Nat}$/J, RRID:IMSR_JAX:017360) were crossed with Adiponectin-Cre transgenic mice (Jackson Laboratories, Bar Harbor, ME; B6.FVB-Tg (Adipoq-cre)1Evdr/J, RRID:IMSR_JAX:028020) and backcrossed onto a C57BL/6J background in our facility for at least 5 generations. *Hilpda*$^{flox/flox}$ mice are characterized by LoxP sites flanking the second exon of *Hilpda*, followed by the open reading frame for membrane-tethered human placental alkaline phosphatase (ALPP) after the second loxP site. Following Cre recombination, ALPP is expressed under the control of the *Hilpda* promoter. *Hilpda*$^{flox/flox}$ mice were crossed with *Hilpda*$^{flox/flox}$ mice heterozygous for Adiponectin-Cre, yielding 50% *Hilpda*$^{flox/flox}$ and 50% adipocyte-specific HILPDA-deficient (*Hilpda*$^{\Delta ADIPO}$) mice, equally distributed among males and females. The *Hilpda*$^{flox/flox}$ and *Hilpda*$^{\Delta ADIPO}$ mice used in the studies were littermates.

Mice were group housed at 21-22ºC under specific pathogen-free conditions and according to a 6:00-18:00 day-night cycle. Mice had ad libitum access to regular chow and water unless otherwise indicated.

In the first study, male *Hilpda*$^{\Delta ADIPO}$ mice aged 10-13 weeks and their male *Hilpda*$^{flox/flox}$ littermates were randomly allocated using an online randomization tool to either a standardized high-fat diet or a low-fat diet (formula D12451 and formula D12450H respectively, Research Diets Inc., New Brunswick, USA; γ-irradiated with 10-20 kGy) for 20 weeks. The mice were housed individually in type 2 cages. Body weight and food intake were assessed weekly. The number of mice per group (4) was 9-12. After 16 weeks of high-fat feeding, an intraperitoneal glucose tolerance test was carried out.

In the second study, *Hilpda*$^{\Delta ADIPO}$ and *Hilpda*$^{flox/flox}$ mice aged 4-5 months were subjected to 24 hours of fasting or 20 hours of fasting followed by 4 hours of refeeding with chow. Water was available ad libitum during the entire period of fasting/refeeding. The number of mice per group (4) was 9-13.

At the end of both studies, the mice were anesthetized with isoflurane. Blood was collected via orbital puncture in tubes containing EDTA (Sarstedt, Nümbrecht, Germany). Immediately thereafter, mice were euthanized by cervical dislocation, after which tissues were excised, weighed, and frozen in liquid nitrogen or prepared for histology. Frozen samples were stored at -80 °C.

All animal experiments were approved by the Institutional Animal Care and Use Committee of Wageningen University (AVD104002015236; 2016.W-0093.002, 2016.W-0093.007).

Intraperitoneal glucose tolerance test

The mice fasted for 5 hours after which blood was collected via tail bleeding for baseline blood glucose measurement. Shortly thereafter, the mice received an intraperitoneal injection of glucose at 1g/kg body weight, followed by blood collection via tail bleeding at 15, 30, 45, 60, 90, and 120 min. Blood glucose was measured with a GLUCOFIX Tech glucometer and glucose sensor test strips (GLUCOFIX Tech, Menarini Diagnostics, Valkenswaard, the Netherlands).

Plasma measurements

Blood collected in EDTA tubes (Sarstedt, Numbrecht, Germany) was centrifuged for 10 min at 2,000 g at 4 °C. Plasma was collected, aliquoted, and stored at -80 °C. After thawing, plasma was analyzed for cholesterol (Liquicolor, Human GmbH, Wiesbaden, Germany), triglycerides (Liquicolor), glucose (Liquicolor), glycerol (Liquicolor), NEFAs (NEFA-HR set R1, R2 and standard, WAKO Diagnostics, Instruchemie, Delfzijl, The Netherlands), adiponectin (ELISA duoset kit, R&D Systems, Bio-techne, MN, USA), leptin (ELISA duoset kit, R&D Systems) and insulin (ultra-sensitive mouse insulin ELISA kit, Crystal Chem Inc., IL, USA) following manufacturer's instructions.

Liver triglyceride measurement

Two-percent liver homogenates were prepared in buffer (10 mM Tris, 2 mM EDTA and 0.25 M sucrose, pH 7.5) using a Tissue Lyser II (Qiagen, Hilden, Germany). Liver triglyceride content was quantified using a Triglyceride LiquiColor mono kit from HUMAN Diagnostics (Wiesbaden, Germany) according to the manufacturer's instructions.

Cell culture

3T3-L1 adipocytes

3T3-L1 fibroblasts were amplified in DMEM supplemented with 10% FCS and 1% penicillin/streptomycin (culture medium) and subsequently seeded into six-well plates (15,000 cells/cm^2). Two days after the cells reached confluence, the medium was changed to DMEM supplemented with 10% FCS containing 0.5 mM 3-isobutyl-1-methylxanthine (Sigma-Aldrich; I5879), 2 µg/ml insulin (Sigma-Aldrich; I2643), 0.5 µM dexamethasone (Sigma-Aldrich; D4902), and 1 µM rosiglitazone (Sigma-Aldrich; R2408). After 2 days, the medium was changed to culture medium supplemented with 2 µg/ml insulin and 1 µM rosiglitazone until the cells were fully differentiated.

Mouse primary adipocytes

Primary adipocytes were differentiated from the stromal vascular fraction, which was obtained from inguinal white adipose tissue of *Hilpda*$^{\Delta ADIPO}$ and *Hilpda*$^{flox/flox}$ mice. Briefly, dissected adipose tissue depots were kept and cleaned in ice-cooled transport medium (DMEM plus 1% fatty acid-free BSA (Sigma-Aldrich)). Cleaned adipose tissue samples were minced into small pieces and incubated with collagenase solution (DMEM, 3.2 mM CaCl2, 15 mM HEPES, 0.5% BSA, 10% FCS, and 1.5 mg/mL collagenase type II (Sigma-Aldrich; C6885)) at 37 °C for 30 min. The digested tissue suspensions were then filtered using a 100-mm cell strainer and centrifuged at 300 g for 10 min at room temperature. The pellet stromal vascular fractions (SVF) were resuspended and grown in cell culture flasks until around 90% confluency. Cells were seeded in the culture plate with a density of 15,000 cells/cm^2 in DMEM, 10% FCS, and 1% penicillin/streptomycin. Two to 3 days post-seeding (at full confluency), differentiation was started by supplementing with 0.5 mM of 3-isobutyl-1-methylxanthine (Sigma-Aldrich; I5879), 1 mM of dexamethasone (Sigma-Aldrich; D4902), 7 mg/mL of human insulin (Sigma-Aldrich; I2643), and 1 µM of rosiglitazone (Sigma-Aldrich; R2408). After 3 days of stimulation, cells were further cultured in insulin medium (DMEM containing 7 mg/mL human insulin) for another 3 days followed by a normal growth medium (DMEM, 10% FCS, and 1% penicillin/streptomycin).

Fatty acids treatment

A 2:1 mixture of oleate (Sigma-Aldrich; P0500) and palmitate (Sigma-Aldrich; O1008) was added to the cells for 12 hours. Fatty acids were dissolved in ethanol and diluted with 70 mM KOH to a 25 mM stock solution for cell culture application.

Agonist, antagonist, and inhibitor assays

Mouse primary mature adipocytes were treated with 10 μM isoproterenol (Sigma-Aldrich; I6504) for 3 hours and 10 μM forskolin (Sigma-Aldrich; F6886) for 2 hours to stimulate lipolysis. Cells were treated with 20 μM DGAT1 inhibitor T863 (Sigma-Aldrich; AML0539) and 10 μM DGAT2 inhibitor PF-06424439 (Merck; PZ0233) for the desired time durations to inhibit cellular DGAT1 and DGAT2, respectively. Atglistatin (50 μM, Sigma-Aldrich; 5.30151) was used to inhibit ATGL, and GW9662 (5 nM, Tocris; 1508) was used as a PPARγ antagonist in combination with the treatment of the cells with free fatty acids. The GPR120 agonist TUG891 (20 μM, Tocris; 4601) and antagonist AH6714 (10 μM, Tocris; 5256) were added to cells for the desired time durations.

The antagonists and inhibitors were applied to cells 30 min before the treatments. After pre-incubation, cells were washed with culture medium twice. After the treatment, the medium was collected for glycerol and free fatty acids analysis using relevant kits (Instruchemie, The Netherlands), following the manufacturer's protocols. The cells were washed with PBS twice for either protein or mRNA extractions.

Quantitative RT-PCR

Total RNA was isolated using TRizol Reagent (Thermo Fisher Scientific, 15596018). cDNA was synthesized using the iScript cDNA Synthesis Kit (Bio-Rad Laboratories, Inc., 1708890) following the manufacturer's protocol. Real-Time polymerase chain reaction (RT-PCR) was performed on the CFX 384 Touch Real-Time detection system (Bio-Rad Laboratories, Inc., California, United States), using the SensiMix (BioLine, BIO-83005) protocol for SYBR green reactions. Mouse 36B4 expression was used for normalization.

Immunoblotting

The cell lysates were prepared using RIPA Lysis and Extraction Buffer (Thermo Fisher Scientific, 89901) supplemented with protease inhibitor (Thermo Fisher Scientific; A32965) and phosphatase inhibitor (Roche; 4906845001) and quantified with Pierce BCA Protein Assay Kit (Thermo Fisher Scientific, Massachusetts, United States). The gonadal white adipose tissue homogenates were prepared in the same butter by tissue lyser. The fat was removed by centrifuging 3 times at 11,000 rpm for 10 min at 4 °C. The protein lysates were separated by electrophoresis on pre-cast 4-15% polyacrylamide gels and transferred onto nitrocellulose membranes using a Trans-Blot Semi-Dry transfer cell (Bio-Rad Laboratories, Inc., California, United States), blocked in 5% skim milk in TBS-T (TBS buffer supplied with 1 ‰ TWEEN 20) and incubated with HILPDA antibody (Rabbit antisera

against the C-terminal half (aa 37e64) of murine HILPDA generated by Pineda (Berlin, Germany)), ATGL antibody (Cell Signaling Technology; 2138S), and DGAT2 antibody (Bio-tech; Q-254644) overnight at 4ºC. Secondary antibody incubation was performed at room temperature for 1 hour. HSP90 was used for normalization (Cell Signaling Technology; 4874S). Images were acquired using the ChemiDoc MP system (Bio-Rad Laboratories, Inc., United States).

Cytokine secretion by adipose tissue explants

Epididymal white adipose tissue explants were taken into culture for 24h in DMEM, supplemented with 10% fetal calf serum (FCS, BioWest, Nuaillé, France) and 1% P/S. The supernatant was used for measurement of IL6 and IL10 by ELISA. DuoSet sandwich ELISA kits for IL6 and IL10 (Cat#DY417/Cat#DY406, R&D systems) were used to measure cytokine concentrations in explant supernatant according to the manufacturer's instructions. Data were normalized to the weight per explant.

Statistical analysis

Data were analyzed using unpaired Student's t-test or two-way ANOVA analysis followed by Tukey's multiple comparisons test. A value of $p<0.05$ was considered statistically significant. Details are presented in the figure legends.

RESULTS

To examine the regulation of HILPDA by fatty acids in adipocytes, we treated mouse 3T3-L1 adipocytes with a combination of oleic acid and palmitic acid (OA:PA). As observed in hepatocytes, macrophages, and cancer cells, OA:PA treatment markedly increased HILPDA protein levels (Fig. 1A). The increase in HILPDA protein by OA:PA was not accompanied by any change in *Hilpda* mRNA (Fig. 1B), indicating that fatty acids induce HILPDA at the post-transcriptional level. In agreement with this notion, oleic acid did not influence *Hilpda* mRNA expression in 3L3-L1 adipocytes but did markedly increase the expression of *Angptl4*, *Cpt1a*, and *Hmgcs2*, as observed by transcriptomics (Fig. 1C). Similar to the observation in 3T3-L1 adipocytes, OA:PA upregulated HILPDA protein but not mRNA levels in primary mouse adipocytes (Fig. 1D, E). Interestingly, despite a massive decrease in HILPDA protein level upon blocking DNA transcription, the induction of HILPDA by OA:PA was maintained under these conditions (Fig. 1F). These data suggest that active transcription is needed to maintain HILPDA protein levels but that the increase in HILPDA protein by fatty acids is not mediated by increased HILPDA transcription.

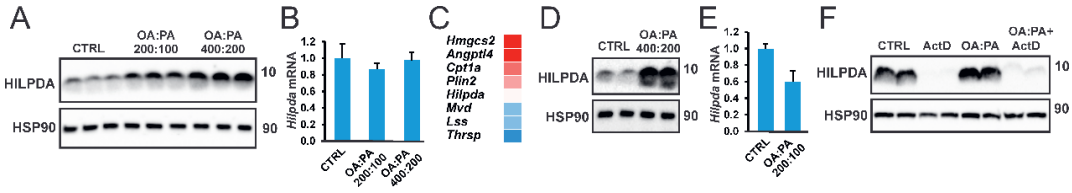

Fig 1. Fatty acids induce HILPDA expression in adipocytes. A). HILPDA protein level and B) mRNA expression of *Hilpda* in 3T3L-1 adipocytes treated with a 2:1 mixture of oleate and palmitate (total concentration 600 µM and 300 µM, respectively) for 12 hours. C) Lipid-sensitive gene expression in 3T3-L1 adipocytes treated with 1 mM oleate for 24 hours. D) HILPDA protein level and E) mRNA expression of *Hilpda* in mouse primary adipocytes treated with a 2:1 mixture of oleate and palmitate. F) HILPDA protein level in *Hilpda*$^{flox/flox}$ mouse primary adipocytes treated with 2:1 mixture of oleate and palmitate (total concentration 600 µM and 300 µM, respectively) for 6 hours, in presence of 5ug/ml actinmysin D.

We previously showed that isoproterenol and forskolin markedly increase HILPDA levels in 3T3-L1 adipocytes but were unable to identify the mechanism (Dijk et al., 2017). Similarly, we found that isoproterenol markedly upregulates HILPDA protein levels in primary mouse adipocytes (Fig. 2A). Consistent with an inhibitory effect of HILPDA on intracellular lipolysis, the release of glycerol (Fig.

2B) and NEFA (Fig. 2C) was significantly higher in HILPDA-deficient adipocytes obtained from *Hilpda*$^{\Delta ADIPO}$ mice compared to control adipocytes obtained from *Hilpda*$^{flox/flox}$ mice. Considering the marked induction of HILPDA by fatty acids, we hypothesized that forskolin and ISO may induce HILPDA by raising the intracellular concentration of fatty acids via activation of ATGL-catalyzed lipolysis and/or inhibition of DGAT-catalyzed esterification. To study the role of enhanced lipolysis in the induction HILPDA by forskolin and ISO, cells were treated with forskolin/ISO in the absence and presence of ATGL inhibitor. As expected, ISO and forskolin increased HILPDA protein level (Fig. 2D, E). Intriguingly, the induction of HILPDA by forskolin was completely abolished by ATGL inhibition (Fig. 2D), pointing to a crucial role of lipolysis and thus endogenous fatty acids in the induction of HILPDA by forskolin. By comparison, the induction of HILPDA by ISO was partly abolished by ATGL inhibition (Fig. 2E), suggesting that besides via activation of lipolysis, ISO upregulates HILPDA via another mechanism. Interestingly, the chemical inhibition of either DGAT1 or DGAT2 in cells treated with ISO further increased HILPDA protein levels, supporting the potent stimulatory effect of endogenous fatty acids on HILPDA levels (Fig. 2F). Taken together, these data show that both exogenous and endogenous fatty acids potently stimulate HILPDA protein levels in adipocytes.

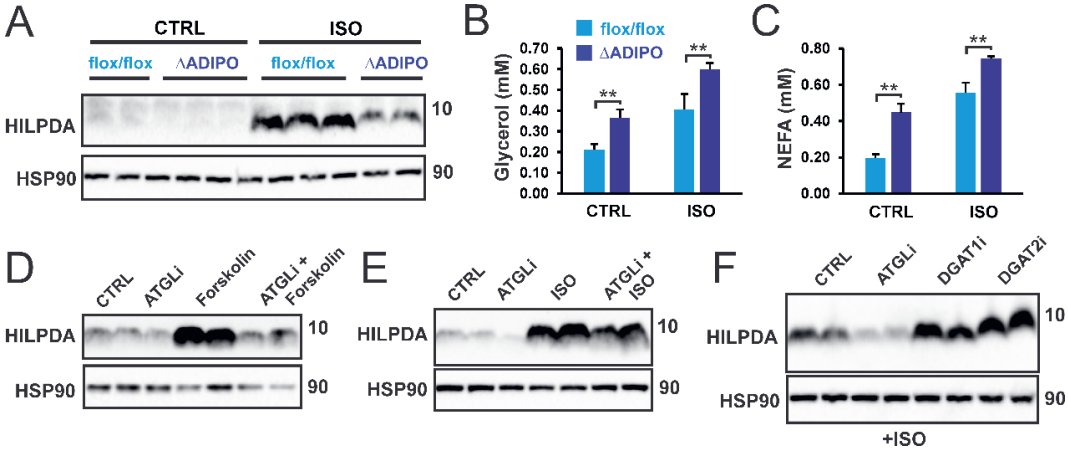

Fig 2. Lipolysis-induced HILPDA expression requires ATGL. A) HILPDA protein level in *Hilpda*$^{flox/flox}$ *and Hilpda*$^{\Delta ADIPO}$ mouse primary adipocytes treated with 10 µM isoproterenol for 3 hours. B) Free glycerol and C) non-esterified fatty acids concentration in the culture medium. HILPDA protein levels in *Hilpda*$^{flox/flox}$ mouse primary adipocytes treated with D) 10 µM forskolin for 2 hours and E) 10 µM isoproterenol for 3 hours, in the presence and absence of 50 µM atglistatin. Cells were pre-incubated with atglistatin for 30 min before the treatments. F) HILPDA protein levels in *Hilpda*$^{flox/flox}$ mouse primary adipocytes treated with 50 µM

atglistatin, or 20 µM T863 (DGAT1i), or 10 µM PF-06424439 (DGAT2i) for 2 hours, in the presence of 10 µM isoproterenol. The cells were pre-incubated with the inhibitors for 30 min.

Fatty acids are known to activate PPARγ (Kliewer et al., 1997; Krey et al., 1997). Since the expression of *Hilpda* is controlled by PPARγ (Dijk et al., 2017), it can be hypothesized that fatty acids increase HILPDA protein via PPARγ activation. While HILPDA protein levels in adipocytes were induced by the PPARγ agonist Rosiglitazone (Fig. 3A), the increase in HILPDA protein by OA:PA was not affected by the PPARγ antagonist GW9662 (Fig. 3B). These data suggest that fatty acids upregulate HILPDA in adipocytes independently of PPARγ.

It is well recognized that fatty acids exert feedback inhibition on lipolysis. A recent study indicates that this effect is mediated by the fatty acid receptor GPR120 (Husted et al., 2020). In line with this study, we found that the GPR120 activation TUG891 decreased glycerol release by primary adipocytes (Fig. 3C). Accordingly, it can be hypothesized that fatty acids upregulate HILPDA via activation of GPR120. To study the role of GPR120 in HILPDA regulation, we first treated adipocytes with the GPR120 agonist TUG891. TUG891 markedly increased HILPDA protein in primary mouse adipocytes (Fig. 3D) and 3T3-L1 adipocytes (Fig. 3E), suggesting that HILPDA levels are controlled by GPR120. Importantly, the increase in HILPDA protein by OA:PA was markedly attenuated by the GPR120 antagonist AH7614 (Fig. 3F), suggesting that the stimulatory effect of fatty acids on HILPDA levels in adipocytes is at least partly mediated by GPR120.

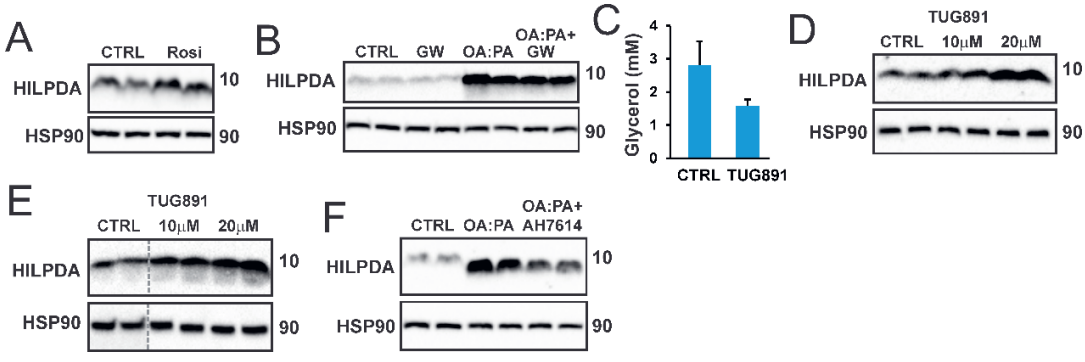

Fig 3. HILPDA is induced by GPR120 activation. HILPDA expression in mouse primary adipocytes treated with A) 10 µM rosiglitazone (PPARγ agonist) for 12 hours, B) a 2:1 mixture of oleate and palmitate (600 µM) in the presence and absence of 5 nM GW9662 (PPARγ antagonist) for 12 hours. C) Glycerol level of the culture medium of mouse primary adipocytes treated with 20 µM TUG891 for7 hours. HILPDA expression after the treatments of TUG891 for 24 hours in D) 3T3-L1 adipocytes and E) mouse primary adipocytes. F)

HILPDA expression in mouse primary adipocytes treated with a 2:1 mixture of oleate and palmitate (600 μM) for 12 hours, in the presence or absence of 10 μM AH7614.

HILPDA has been shown to be an inhibitor of ATGL (Padmanabha Das et al., 2018; Zhang et al., 2017). Interestingly, data from macrophages suggest that under certain conditions, the interaction between HILPDA and ATGL leads to a reduction in ATGL protein levels (van Dierendonck et al., 2020; van Dierendonck et al., 2022). Accordingly, we hypothesized that the induction of HILPDA by exogenous fatty acids may be associated with a decrease in ATGL protein. Consistent with this notion, treatment of primary adipocytes with OA:PA markedly increased HILPDA protein levels, while decreasing ATGL protein levels (Fig. 4A) Furthermore, ATGL protein levels were elevated in HILPDA-deficient adipocytes compared to control adipocytes. It should be noted, though, that even in HILPDA-deficient adipocytes, treatment with OA:PA decreased ATGL protein (Fig. 4A).

To study the impact of induction of HILPDA by endogenous fatty acids on ATGL protein levels, we assessed ATGL protein levels in HILPDA-deficient and control adipocytes treated with DGAT inhibitors. Similar to the fatty acid treatment, the increase in HILPDA protein by DGAT inhibitors was associated with a marked decrease in ATGL protein (Fig. 4B). Moreover, after treatment with DGAT inhibitors, ATGL protein levels were higher in HILPDA-deficient than control adipocytes, which was accompanied by increased glycerol release (Fig. 4C). As observed for OA:PA treatment, DGAT inhibitors decreased ATGL protein in HILPDA-deficient adipocytes, concurrent with an increase in HILPDA protein. These data indicate that exogenous and endogenous fatty acids upregulate HILPDA protein levels, which at least partly accounts for a concurrent reduction in ATGL protein.

The collective data presented so far are suggestive of a feedback mechanism in which elevations in fatty acids may suppress lipolysis by downregulating ATGL protein levels via induction of HILPDA. This notion suggests that under conditions of increased intracellular fatty acids, the absence of HILPDA may lead to intracellular lipid overload and associated lipotoxicity. Consistent with this notion, the expression of spliced XBP1, a marker of ER stress, was higher in fatty acid-treated HILPDA-deficient adipocytes compared to floxed adipocytes. Similarly, the expression of spliced XBP1, as well as other ER stress markers, was higher in HILPDA-deficient adipocytes treated with DGAT inhibitors compared to floxed adipocytes. These data support the notion that HILPDA maintains intracellular fatty acid homeostasis under conditions of increased fatty acid load by suppressing ATGL-mediated lipolysis

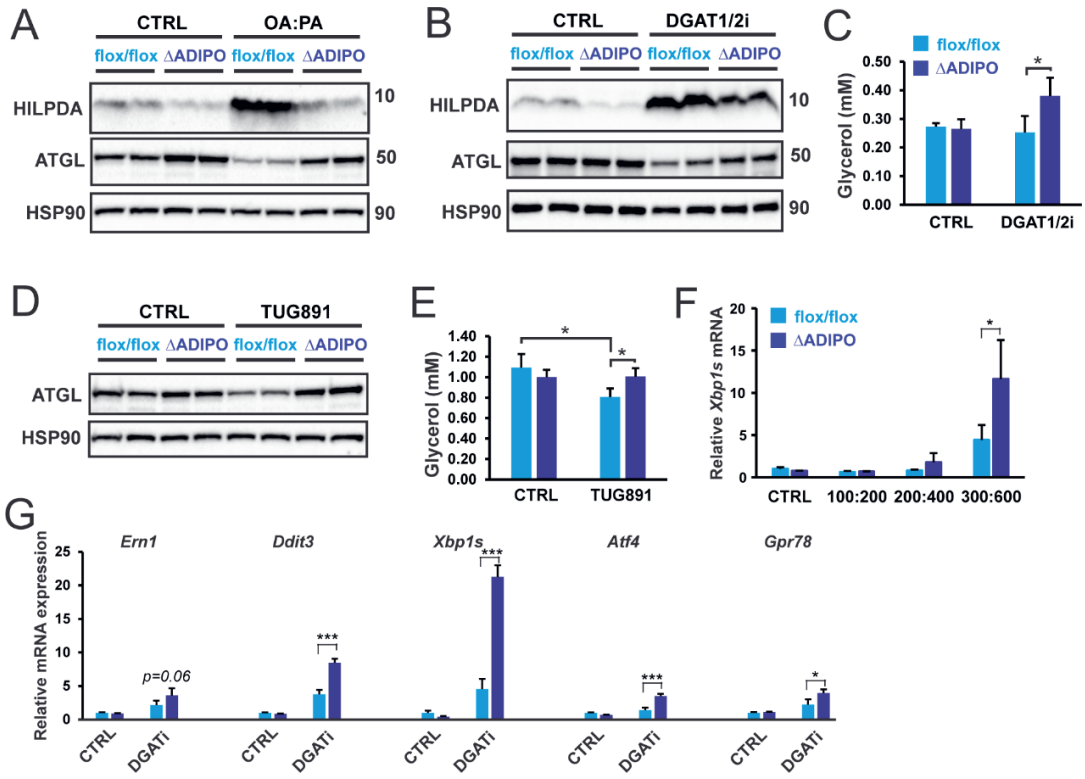

Fig 4. GPR120 activation downregulates ATGL levels via induction of HILPDA. HILPDA expression and ATGL expression in *Hilpda*$^{flox/flox}$ and *Hilpda*$^{\Delta ADIPO}$ mouse primary adipocytes treated with A) a 2:1 mixture of oleate and palmitate (600 μM) for 12 hours, B) 20 μM T863 (DGAT1i) and 10 μM PF-06424439 (DGAT2i) for 2 hours. C) Glycerol level in medium of *Hilpda*$^{flox/flox}$ and *Hilpda*$^{\Delta ADIPO}$ mouse primary adipocytes treated with 20 μM T863 (DGAT1i) and 10 μM PF-06424439 (DGAT2i) for 2 hours. D) HILPDA expression and ATGL expression in *Hilpda*$^{flox/flox}$ and *Hilpda*$^{\Delta ADIPO}$ mouse primary adipocytes treated with 20 μM TUG 891 for 24 hours. E) Glycerol level in medium of *Hilpda*$^{flox/flox}$ and *Hilpda*$^{\Delta ADIPO}$ mouse primary adipocytes treated with 20 μM TUG891 for 7 hours. ER stress-related gene expression in *Hilpda*$^{flox/flox}$ and *Hilpda*$^{\Delta ADIPO}$ mouse primary adipocytes treated with F) different concentrations of fatty acids for 24 hours, G) 20 μM T863 (DGAT1i) and 10 μM PF-06424439 (DGAT2i) for 12 hours.

To investigate whether HILPDA may play a similar role in vivo, we studied *Hilpda*$^{\Delta ADIPO}$ mice and *Hilpda*$^{flox/flox}$ mice fed a high-fat diet for 20 weeks, with mice fed a low-fat diet serving as controls. After both low-fat and high-fat feeding, *Hilpda* mRNA levels in adipose tissue but not liver were markedly reduced in *Hilpda*$^{\Delta ADIPO}$ mice compared to *Hilpda*$^{flox/flox}$ mice (Fig. 5A). The lower *Hilpda* expression in whole adipose tissue of *Hilpda*$^{\Delta ADIPO}$ mice could be attributed to a reduction in *Hilpda*

mRNA in the adipocyte as opposed to the stromal vascular fraction (Fig. 5B). High-fat feeding was associated with a pronounced increase in HILPDA protein levels in adipose tissue. Interestingly, adipose tissue HILPDA protein levels were similar in *Hilpda*$^{\Delta ADIPO}$ and *Hilpda*$^{flox/flox}$ mice (Fig. 5C), likely because foamy macrophages are the major source of HILPDA protein in adipose tissue of mice fed a high-fat diet (paper Xanthe). The tissue fractionation data (Fig. 5B) and reduced HILPDA protein levels in *Hilpda*$^{\Delta ADIPO}$ primary adipocytes (Fig. 4) suggest that HILPDA was effectively silenced in *Hilpda*$^{\Delta ADIPO}$ adipocytes in the low-fat/high-fat feeding study.

No differences in weight gain (Fig. 5D) and food intake (Fig. 5E) were observed between *Hilpda*$^{\Delta ADIPO}$ and *Hilpda*$^{flox/flox}$ mice on either the low-fat diet or high-fat diet. The relative weights of the liver, gonadal adipose tissue, inguinal adipose tissue, and brown adipose tissue were also not significantly different between the two genotypes on either the low-fat diet or high-fat diet (Fig. 5F). Furthermore, plasma cholesterol, triglycerides, glucose, and non-esterified fatty acid levels were similar in *Hilpda*$^{\Delta ADIPO}$ and *Hilpda*$^{flox/flox}$ mice in the low-fat and high-fat diet group (Fig. 5G). By contrast, after high-fat feeding, plasma glycerol levels were significantly elevated in *Hilpda*$^{\Delta ADIPO}$ compared to *Hilpda*$^{flox/flox}$ mice (Fig. 5G). These data suggest that adipocyte HILPDA deficiency increases plasma glycerol levels, reflecting an increase in adipose tissue lipolysis, but does not impact the levels of other relevant plasma metabolites.

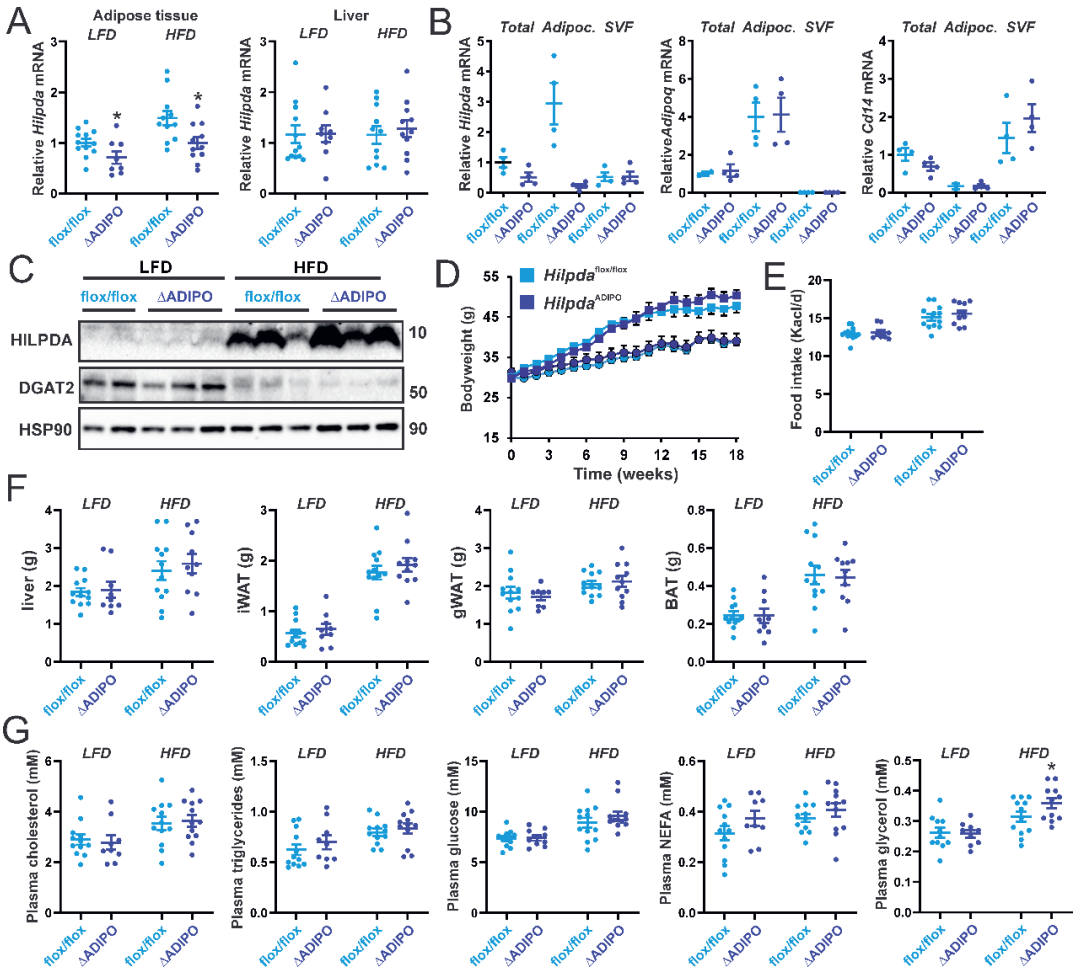

Fig 5. Minimal impact of adipocyte-specific Hilpda deficiency in mice fed a low- or high- fat diet. A) Relative *Hilpda* mRNA expression in adipose tissue and liver of *Hilpda*$^{flox/flox}$ and *Hilpda*$^{\Delta ADIPO}$ mice fed a low- or high-fat diet for 20 weeks (n=9-12 per group). B) Expression of *Hilpda*, *Adipoq* and *Cd14* in whole gonadal adipose tissue, freshly separated adipocytes, and the stromal vascular fraction of SVF of *Hilpda*$^{flox/flox}$ and *Hilpda*$^{\Delta ADIPO}$ mice. C) HILPDA and DGAT2 protein levels in epididymal white adipose tissue. D) Body weight. E) Food intake. F) Weight of liver and adipose tissue. G) Plasma concentration of glucose, glycerol, triglycerides, choleste .rol, and non-esterified fatty acids (NEFA). In the graphs, the horizontal bar represents the mean and the error bars represent SEM. Asterisk indicates significantly different from *Hilpda*$^{flox/flox}$ mice according to Tukey's posthoc test. *P<0.05.

Further analysis of the metabolic phenotype did not reveal any differences between *Hilpda*$^{\Delta ADIPO}$ and *Hilpda*$^{flox/flox}$ mice. Specifically, plasma leptin, adiponectin, and insulin (Fig. 6A), as well as hepatic triglyceride levels (Fig. 6B) were not significantly different between *Hilpda*$^{\Delta ADIPO}$ and *Hilpda*$^{flox/flox}$ mice on either diet. Furthermore, glucose tolerance was not significantly affected by HILPDA deficiency in the high-fat diet group (Fig. 6C). Gene expression analysis showed increased expression of inflammation-related genes in the adipose tissue of mice fed the high-fat diet compared to mice fed the low-fat diet but no differences were observed between *Hilpda*$^{\Delta ADIPO}$ and *Hilpda*$^{flox/flox}$ mice (Fig. 6D). In addition, secretion of IL6 and IL10 by adipose tissue explants were not significantly different between *Hilpda*$^{\Delta ADIPO}$ and *Hilpda*$^{flox/flox}$ mice (Fig. 6E). Collectively, these data show that the increase in adipose tissue lipolysis upon adipocyte HILPDA deficiency is not accompanied by any change in glucose tolerance, liver triglyceride content, adipose tissue inflammation, and plasma levels of several metabolic hormones in mice fed a high-fat diet.

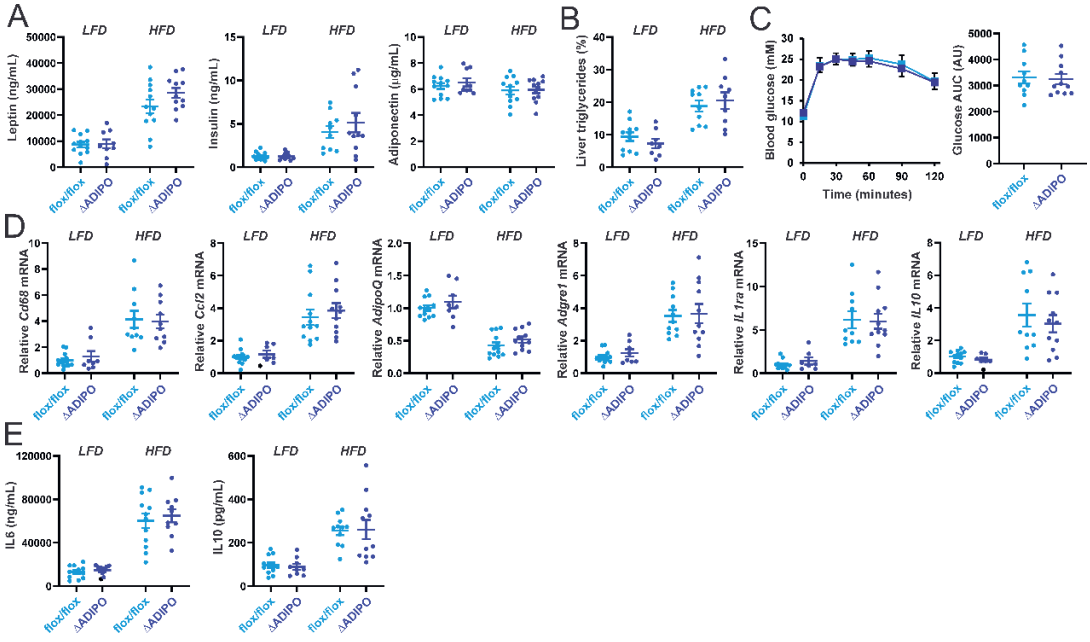

Fig 6. HILPDA does not influence HFD-induced metabolic and inflammatory complications. A) Plasma levels of metabolism-related hormones in *Hilpda*$^{flox/flox}$ and *Hilpda*$^{\Delta ADIPO}$ mice fed low-fat or high-fat diet for 20 weeks (n=9-12 per group). B) Liver triglyceride content. C) Intraperitoneal glucose tolerance test and Area Under the Curve. D) Relative mRNA expression of inflammation-related genes in epididymal white adipose tissue. E) Secretion of IL6 and IL10 by explants of epididymal white adipose tissue. In the graphs, the horizontal bar represents the mean, and the error bars represent SEM.

Another physiological condition associated with increased fatty acid load in adipose tissue is fasting and fasting/refeeding. Accordingly, *Hilpda*$^{\Delta ADIPO}$ and *Hilpda*$^{flox/flox}$ mice were subjected to a 24h fast or to a 24h fast followed by a 4h refeed. In both the fasted and refed groups, *Hilpda* mRNA (Fig. 7A) and protein levels (Fig. 7B) in adipose tissue were markedly lower in the *Hilpda*$^{\Delta ADIPO}$ mice compared to *Hilpda*$^{flox/flox}$ mice. As observed in primary adipocytes treated with DGATi, HILPDA deficiency in adipocytes was accompanied by a marked increase in ATGL protein content (Fig. 7B), which was specifically observed after fasting/refeeding. Intriguingly, DGAT2 protein content was increased by HILPDA deficiency after fasting but decreased by HILPDA deficiency after fasting/refeeding. These data suggest that HILPDA influences ATGL and DGAT2 protein content in adipose tissue but only under specific metabolic conditions.

Further analysis of the phenotype showed that body weight was significantly lower in the *Hilpda*$^{\Delta ADIPO}$ mice than in the *Hilpda*$^{flox/flox}$ mice, as was the relative weight of the gonadal, inguinal and subscapular brown adipose tissue depot (Fig. 7C). By contrast, relative liver weight was unaffected by HILPDA deficiency (Fig. 7C). To examine the metabolic effects of HILPDA deficiency in fasted and refed mice, several plasma metabolites were measured. Interestingly, plasma glycerol levels were significantly elevated in *Hilpda*$^{\Delta ADIPO}$ compared to *Hilpda*$^{flox/flox}$ mice in the fasted state (Fig. 7D). By contrast, plasma cholesterol, triglycerides, glucose, and non-esterified fatty acid levels were similar in *Hilpda*$^{\Delta ADIPO}$ and *Hilpda*$^{flox/flox}$ mice after either fasting or fasting/refeeding. The elevated glycerol levels in fasted *Hilpda*$^{\Delta ADIPO}$ mice support the observation made in mice fed a high-fat diet and suggest an increase in adipose tissue lipolysis, which in turn might account for the lower weight of various adipose depots. Liver triglyceride content was not significantly different between the *Hilpda*$^{\Delta ADIPO}$ and *Hilpda*$^{flox/flox}$ mice (Fig. 7E).

In primary adipocytes, HILPDA deficiency under conditions of a high fatty acid load was associated with increased expression of cell stress markers. To verify if this may also hold in vivo, we measured the expression of stress-associated genes in adipose tissue of fasted and refed *Hilpda*$^{\Delta ADIPO}$ and *Hilpda*$^{flox/flox}$ mice. In line with the increase in ATGL protein content, adipose tissue mRNA levels of *Grp78*, *Xbp1*, *Atf4*, and *Ern1* were modestly but significantly higher in *Hilpda*$^{\Delta ADIPO}$ mice than in *Hilpda*$^{flox/flox}$ mice, which was specifically observed after fasting/refeeding (Fig. 7F).

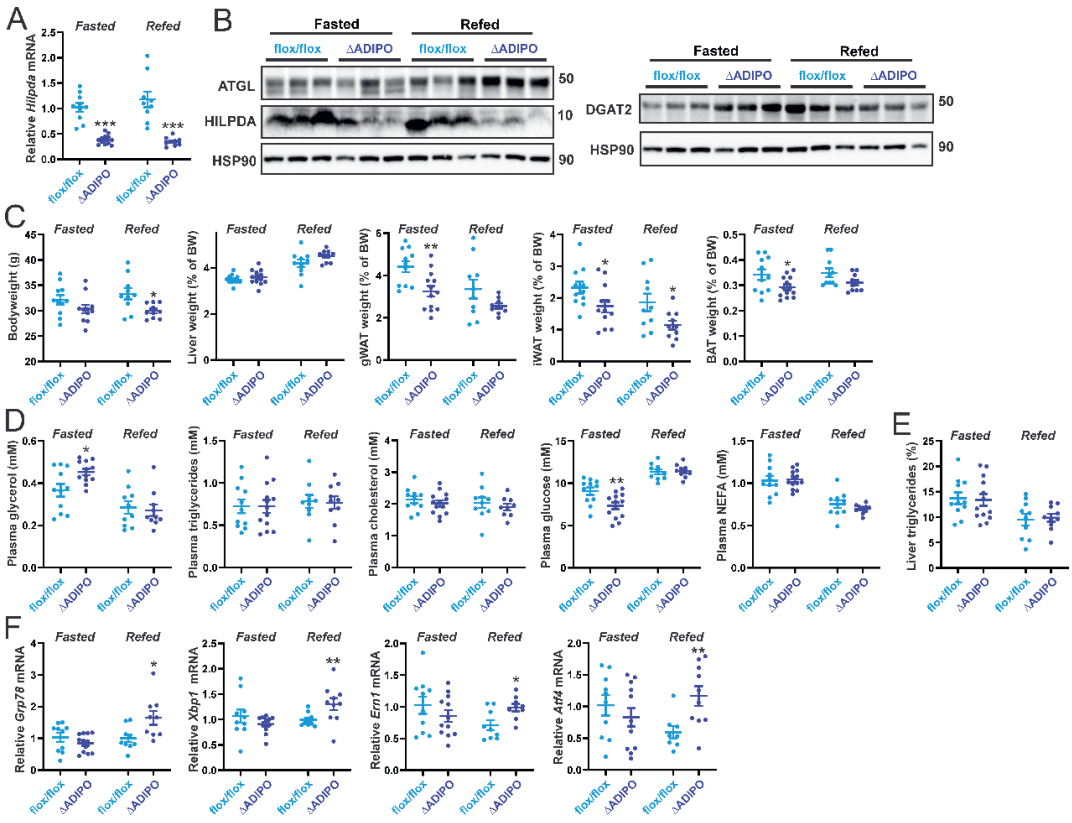

Fig 7. HILPDA alleviates ER stress in adipose tissue during refeeding. A) Relative *Hilpda* mRNA expression in epididymal white adipose tissue of *Hilpda*$^{flox/flox}$ and *Hilpda*$^{\Delta ADIPO}$ mice after 24 hours of fasting or 20 hours of fasting followed by 4 hours of refeeding with chow. B) HILPDA, ATGL, DGAT2 protein levels in epididymal white adipose tissue. C) Weight of mice and various tissues. D) Plasma metabolites. E) Liver triglyceride content (%, wt/wt). F) Relative expression of ER stress related-genes in epididymal white adipose tissue.

DISCUSSION

Previously, it was shown that fatty acids exert feedback inhibition on adipocyte lipolysis by activating GPR120 and suppressing cAMP levels (Burns et al., 1978; Fain and Shepherd, 1975; Husted et al., 2020; Kalderon et al., 2012). Here, we present evidence that the ATGL inhibitor HILPDA underlies the autocrine negative feedback regulation of adipose tissue lipolysis by NEFA via GPR120. According to this model, fatty acids generated by lipolysis activate GPR120, leading to upregulation of HILPDA. The elevated HILPDA levels in turn inhibit ATGL by downregulating ATGL protein

content, thereby decreasing ATGL-catalyzed lipolysis and concomitant release of glycerol and fatty acids. Through this mechanism, triglyceride hydrolysis in adipocytes is adjusted to the local availability of fatty acids. When this mechanism malfunctions, for instance when adipocytes are deficient in HILPDA, intracellular fatty acid levels are expected to rise, which could lead to cell stress when combined with stimuli that activate lipolysis and/or inhibit fatty acid re-esterification.

Evidence abounds indicating that HILPDA inhibits ATGL activity and associated lipolysis in various cell types (DiStefano et al., 2015; Padmanabha Das et al., 2018; van Dierendonck et al., 2020; van Dierendonck et al., 2022; VandeKopple et al., 2019; Zhang et al., 2017). In vitro studies, however, show that despite the clear physical interaction between HILPDA and ATGL, HILPDA only weakly inhibits ATGL, in particular when compared with the related protein G0S2 (Padmanabha Das et al., 2018). Interestingly, treatment of adipocytes with fatty acids increases HILPDA protein while decreasing ATGL protein levels. Furthermore, ATGL protein levels were elevated in HILPDA-deficient adipocytes, suggesting that HILPDA downregulates ATGL protein. These data are consistent with other studies showing that adenoviral-mediated overexpression of HILPDA reduces ATGL protein levels in 3T3-L1 adipocytes and that HILPDA deficiency is accompanied by an increase in ATGL protein in macrophages treated with LPS or fatty acids (Dijk et al., 2017; van Dierendonck et al., 2020; van Dierendonck et al., 2022). The suppressive effect of HILPDA on ATGL protein level in LPS-treated macrophages could be attributed to enhanced proteosomal ATGL degradation (van Dierendonck et al., 2022). Collectively, the data suggest that HILPDA reduces ATGL-mediated lipolysis, not by direct (allosteric) interference with ATGL enzymatic activity but rather by stimulating ATGL degradation and thus reducing ATGL protein levels.

Intriguingly, fatty acids still managed to decrease ATGL protein in HILPDA-deficient adipocytes. Similar results were obtained in adipocytes treated with DGAT inhibitors to raise endogenous fatty acid levels. These data point to an additional mechanism that is activated by fatty acids and regulates ATGL protein levels but is independent of HILPDA. Alternatively, a potential role of the residual HILPDA expression in the HILPDA-deficient macrophages cannot be excluded.

In cultured adipocytes, the repression of ATGL protein levels by HILPDA was mainly evident under conditions of elevated fatty acid load, such as created by the external provision of fatty acids or inhibition of fatty acid re-esterification. Under these conditions, intracellular fatty acid concentrations are expected to rise, relieving the need to produce fatty acids via hydrolysis of stored triglycerides. This is where HILPDA comes in. By downregulating ATGL, HILPDA represses lipolysis and restores homeostatic fatty acid control. HILPDA is thus a central node in the negative feedback

regulation of intracellular lipolysis by fatty acids and GPR120. Conceptually, this mechanism resembles the feedback inhibition of extracellular lipolysis by fatty acids via induction of ANGPTL4 and the resulting inhibition of lipoprotein lipase (Georgiadi et al., 2010).

Protein and mRNA levels of HILPDA in various cell types, including cancer cells, macrophages, and hepatocytes, are highly induced by fatty acids. We find that fatty acids also upregulate HILPDA protein levels in adipocytes. Since HILPDA is a target gene of the transcription factors PPARα and PPARγ, which are activated by fatty acids (Kliewer et al., 1997; Krey et al., 1997), it is tempting to attribute the induction of HILPDA by fatty acids to transcriptional regulation via PPARs. However, we found that, unlike in hepatocytes (de la Rosa Rodriguez et al., 2021), the induction of HILPDA protein by fatty acids in adipocytes is not accompanied by an increase in HILPDA mRNA. In addition, the PPARγ antagonist GW9662 failed to lower the induction of HILPDA by fatty acids. Instead, our data suggest that fatty acids raise HILPDA protein levels at least partly via GPR120. Previously, it was shown that fatty acids promote lipid droplet formation in Huh-7 hepatoma cells by activating GPR120, which initially is independent of exogenous lipid uptake (Rohwedder et al., 2014). Based on our data, it can be hypothesized that the early stimulation of lipid droplet accumulation by fatty acids may be mediated by induction of HILPDA via GPR120, leading to the growth of lipid droplets via suppression of ATGL-catalyzed triglyceride hydrolysis.

The mRNA expression of *Hilpda* was only modestly decreased in adipose tissue of *Hilpda*$^{\Delta ADIPO}$ mice compared to *Hilpda*$^{flox/flox}$ mice. Surprisingly, HILPDA protein levels even appeared to be higher in adipose tissue of *Hilpda*$^{\Delta ADIPO}$ mice compared to *Hilpda*$^{flox/flox}$ mice. A possible reason for this unexpected finding is that HILPDA expression in adipose tissue is a marker for macrophage foam cells (van Dierendonck et al., 2020), the formation of which is enhanced in adipose tissue of diet-induced obese mice (Prieur et al., 2011). Accordingly, most of the HILPDA in obese adipose tissue originates from the macrophage foam cells, explaining why myeloid-specific HILPDA deficiency markedly reduced HILPDA protein in adipose tissue of diet-induced obese mice (van Dierendonck et al., 2020), whereas adipocyte-specific HILPDA deficiency did not. By contrast, under conditions of fasting and fasting/refeeding, HILPDA mRNA and protein levels were markedly decreased in adipose tissue of *Hilpda*$^{\Delta ADIPO}$ mice compared to *Hilpda*$^{flox/flox}$ mice.

In earlier studies, adipocyte-specific HILPDA deficiency did not impact plasma NEFA and glycerol under any of the conditions examined, including fasting, cold exposure, and CL316,243 injection (Dijk et al., 2017). By contrast, in the present study, we find a modest but statistically significant increase in plasma glycerol in *Hilpda*$^{\Delta ADIPO}$ mice compared to *Hilpda*$^{flox/flox}$ mice after fasting and

high fat feeding. These data suggest that the effects of adipocyte-specific HILPDA deficiency on plasma glycerol levels are only visible under specific physiological/nutritional conditions in a well-powered study in mice with a pure genetic background.

Previously, adipocyte-specific HILPDA deficiency was found to be associated with a reduced weight of the gonadal fat depot after high-fat feeding. However, this effect was lost at thermoneutrality (DiStefano et al., 2016). In the present study performed at 21ºC, we did not observe a significant difference in weight of various adipose depots between *Hilpda*$^{\Delta ADIPO}$ and *Hilpda*$^{flox/flox}$ mice after either low- or high-fat feeding. By contrast, the weight of the various adipose depots was significantly lower in the *Hilpda*$^{\Delta ADIPO}$ mice compared to *Hilpda*$^{flox/flox}$ mice after fasting and fasting/refeeding. *Hilpda*$^{flox/flox}$ mice. In previous experiments, gonadal adipose tissue weight was not impacted by adipocyte-specific HILPDA deficiency after 24h fasting, nor after 10 days of cold exposure or injection with the β3-adrenergic agonist CL316,243. The reason for the different outcomes is unclear but may be related to the use of mice with a mixed genetic background in previous studies. Overall, the effect of adipocyte-specific HILPDA deficiency on the weight of adipose tissue depots is not very consistent and likely depends on the nutritional and physiological background.

In conclusion, we show that HILPDA is a central node in a fatty acid- and GPR120-induced autocrine feedback loop in adipocytes that aims to limit intracellular triglyceride hydrolysis under conditions of excess intra- or extracellular fatty acid supply.

REFERENCES

Bhatt-Wessel, B., Jordan, T.W., Miller, J.H., and Peng, L. (2018). Role of DGAT enzymes in triacylglycerol metabolism. Arch Biochem Biophys *655*, 1-11.

Burns, T.W., Langley, P.E., Terry, B.E., and Robinson, G.A. (1978). The role of free fatty acids in the regulation of lipolysis by human adipose tissue cells. Metabolism *27*, 1755-1762.

Chitraju, C., Mejhert, N., Haas, J.T., Diaz-Ramirez, L.G., Grueter, C.A., Imbriglio, J.E., Pinto, S., Koliwad, S.K., Walther, T.C., and Farese, R.V., Jr. (2017). Triglyceride Synthesis by DGAT1 Protects Adipocytes from Lipid-Induced ER Stress during Lipolysis. Cell Metab *26*, 407-418 e403.

Chitraju, C., Walther, T.C., and Farese, R.V., Jr. (2019). The triglyceride synthesis enzymes DGAT1 and DGAT2 have distinct and overlapping functions in adipocytes. J Lipid Res *60*, 1112-1120.

de la Rosa Rodriguez, M.A., Deng, L., Gemmink, A., van Weeghel, M., Aoun, M.L., Warnecke, C., Singh, R., Borst, J.W., and Kersten, S. (2021). Hypoxia-inducible lipid droplet-associated induces DGAT1 and promotes lipid storage in hepatocytes. Molecular metabolism *47*, 101168.

de la Rosa Rodriguez, M.A., and Kersten, S. (2020). Regulation of lipid droplet homeostasis by hypoxia inducible lipid droplet associated HILPDA. Biochimica et biophysica acta. Molecular and cell biology of lipids *1865*, 158738.

Dijk, W., Mattijssen, F., de la Rosa Rodriguez, M., Loza Valdes, A., Loft, A., Mandrup, S., Kalkhoven, E., Qi, L., Borst, J.W., and Kersten, S. (2017). Hypoxia-Inducible Lipid Droplet-Associated Is Not a Direct Physiological Regulator of Lipolysis in Adipose Tissue. Endocrinology *158*, 1231-1251.

DiStefano, M.T., Danai, L.V., Roth Flach, R.J., Chawla, A., Pedersen, D.J., Guilherme, A., and Czech, M.P. (2015). The Lipid Droplet Protein Hypoxia-inducible Gene 2 Promotes Hepatic Triglyceride Deposition by Inhibiting Lipolysis. J Biol Chem *290*, 15175-15184.

DiStefano, M.T., Roth Flach, R.J., Senol-Cosar, O., Danai, L.V., Virbasius, J.V., Nicoloro, S.M., Straubhaar, J., Dagdeviren, S., Wabitsch, M., Gupta, O.T., et al. (2016). Adipocyte-specific Hypoxia-inducible gene 2 promotes fat deposition and diet-induced insulin resistance. Molecular metabolism *5*, 1149-1161.

Fain, J.N., and Shepherd, R.E. (1975). Free fatty acids as feedback regulators of adenylate cyclase and cyclic 3':5'-AMP accumulation in rat fat cells. J Biol Chem *250*, 6586-6592.

Georgiadi, A., Lichtenstein, L., Degenhardt, T., Boekschoten, M.V., van Bilsen, M., Desvergne, B., Muller, M., and Kersten, S. (2010). Induction of cardiac Angptl4 by dietary fatty acids is mediated by peroxisome proliferator-activated receptor beta/delta and protects against fatty acid-induced oxidative stress. Circ Res *106*, 1712-1721.

Gimm, T., Wiese, M., Teschemacher, B., Deggerich, A., Schodel, J., Knaup, K.X., Hackenbeck, T., Hellerbrand, C., Amann, K., Wiesener, M.S., et al. (2010). Hypoxia-inducible protein 2 is a novel lipid droplet protein and a specific target gene of hypoxia-inducible factor-1. FASEB J *24*, 4443-4458.

Goodman, H.M., and Knobil, E. (1961). Growth hormone and fatty acid mobilization: the role of the pituitary, adrenal and thyroid. Endocrinology *69*, 187-189.

Hellerstein, M.K., Christiansen, M., Kaempfer, S., Kletke, C., Wu, K., Reid, J.S., Mulligan, K., Hellerstein, N.S., and Shackleton, C.H. (1991). Measurement of de novo hepatic lipogenesis in humans using stable isotopes. J Clin Invest *87*, 1841-1852.

Husted, A.S., Ekberg, J.H., Tripp, E., Nissen, T.A.D., Meijnikman, S., O'Brien, S.L., Ulven, T., Acherman, Y., Bruin, S.C., Nieuwdorp, M., et al. (2020). Autocrine negative feedback regulation of lipolysis through sensing of NEFAs by FFAR4/GPR120 in WAT. Molecular metabolism *42*, 101103.

Jenkins, C.M., Mancuso, D.J., Yan, W., Sims, H.F., Gibson, B., and Gross, R.W. (2004). Identification, cloning, expression, and purification of three novel human calcium-independent phospholipase A2 family members possessing triacylglycerol lipase and acylglycerol transacylase activities. J Biol Chem *279*, 48968-48975.

Kalderon, B., Azazmeh, N., Azulay, N., Vissler, N., Valitsky, M., and Bar-Tana, J. (2012). Suppression of adipose lipolysis by long-chain fatty acid analogs. J Lipid Res *53*, 868-878.

Kalderon, B., Mayorek, N., Berry, E., Zevit, N., and Bar-Tana, J. (2000). Fatty acid cycling in the fasting rat. Am J Physiol Endocrinol Metab *279*, E221-227.

Kersten, S. (2014). Physiological regulation of lipoprotein lipase. Biochim Biophys Acta *1841*, 919-933.

Klein, S., Young, V.R., Blackburn, G.L., Bistrian, B.R., and Wolfe, R.R. (1986). Palmitate and glycerol kinetics during brief starvation in normal weight young adult and elderly subjects. J Clin Invest *78*, 928-933.

Kliewer, S.A., Sundseth, S.S., Jones, S.A., Brown, P.J., Wisely, G.B., Koble, C.S., Devchand, P., Wahli, W., Willson, T.M., Lenhard, J.M., et al. (1997). Fatty acids and eicosanoids regulate gene expression through direct interactions with peroxisome proliferator-activated receptors alpha and gamma. Proc Natl Acad Sci U S A *94*, 4318-4323.

Krey, G., Braissant, O., L'Horset, F., Kalkhoven, E., Perroud, M., Parker, M.G., and Wahli, W. (1997). Fatty acids, eicosanoids, and hypolipidemic agents identified as ligands of peroxisome proliferator-activated receptors by coactivator-dependent receptor ligand assay. Mol Endocrinol *11*, 779-791.

Lass, A., Zimmermann, R., Haemmerle, G., Riederer, M., Schoiswohl, G., Schweiger, M., Kienesberger, P., Strauss, J.G., Gorkiewicz, G., and Zechner, R. (2006). Adipose triglyceride lipase-

mediated lipolysis of cellular fat stores is activated by CGI-58 and defective in Chanarin-Dorfman Syndrome. Cell Metab *3*, 309-319.

Leibel, R.L., Hirsch, J., Berry, E.M., and Gruen, R.K. (1985). Alterations in adipocyte free fatty acid re-esterification associated with obesity and weight reduction in man. Am J Clin Nutr *42*, 198-206.

Maier, A., Wu, H., Cordasic, N., Oefner, P., Dietel, B., Thiele, C., Weidemann, A., Eckardt, K.U., and Warnecke, C. (2017). Hypoxia-inducible protein 2 Hig2/Hilpda mediates neutral lipid accumulation in macrophages and contributes to atherosclerosis in apolipoprotein E-deficient mice. FASEB J *31*, 4971-4984.

Mattijssen, F., Georgiadi, A., Andasarie, T., Szalowska, E., Zota, A., Krones-Herzig, A., Heier, C., Ratman, D., De Bosscher, K., Qi, L., et al. (2014). Hypoxia-inducible lipid droplet-associated (HILPDA) is a novel peroxisome proliferator-activated receptor (PPAR) target involved in hepatic triglyceride secretion. J Biol Chem *289*, 19279-19293.

Padmanabha Das, K.M., Wechselberger, L., Liziczai, M., De la Rosa Rodriguez, M., Grabner, G.F., Heier, C., Viertlmayr, R., Radler, C., Lichtenegger, J., Zimmermann, R., et al. (2018). Hypoxia-inducible lipid droplet-associated protein inhibits adipose triglyceride lipase. J Lipid Res *59*, 531-541.

Prieur, X., Mok, C.Y., Velagapudi, V.R., Nunez, V., Fuentes, L., Montaner, D., Ishikawa, K., Camacho, A., Barbarroja, N., O'Rahilly, S., et al. (2011). Differential lipid partitioning between adipocytes and tissue macrophages modulates macrophage lipotoxicity and M2/M1 polarization in obese mice. Diabetes *60*, 797-809.

Rohwedder, A., Zhang, Q., Rudge, S.A., and Wakelam, M.J. (2014). Lipid droplet formation in response to oleic acid in Huh-7 cells is mediated by the fatty acid receptor FFAR4. Journal of cell science *127*, 3104-3115.

Strawford, A., Antelo, F., Christiansen, M., and Hellerstein, M.K. (2004). Adipose tissue triglyceride turnover, de novo lipogenesis, and cell proliferation in humans measured with 2H2O. Am J Physiol Endocrinol Metab *286*, E577-588.

van Dierendonck, X., de la Rosa Rodriguez, M.A., Georgiadi, A., Mattijssen, F., Dijk, W., van Weeghel, M., Singh, R., Borst, J.W., Stienstra, R., and Kersten, S. (2020). HILPDA Uncouples Lipid Droplet Accumulation in Adipose Tissue Macrophages from Inflammation and Metabolic Dysregulation. Cell reports *30*, 1811-1822 e1816.

van Dierendonck, X., Vrieling, F., Smeehuijzen, L., Deng, L., Boogaard, J.P., Croes, C.A., Temmerman, L., Wetzels, S., Biessen, E., Kersten, S., et al. (2022). Triglyceride breakdown from lipid droplets regulates the inflammatory response in macrophages. Proc Natl Acad Sci U S A *119*, e2114739119.

VandeKopple, M.J., Wu, J., Auer, E.N., Giaccia, A.J., Denko, N.C., and Papandreou, I. (2019). HILPDA Regulates Lipid Metabolism, Lipid Droplet Abundance, and Response to Microenvironmental Stress in Solid Tumors. Mol Cancer Res *17*, 2089-2101.

Villena, J.A., Roy, S., Sarkadi-Nagy, E., Kim, K.H., and Sul, H.S. (2004). Desnutrin, an adipocyte gene encoding a novel patatin domain-containing protein, is induced by fasting and glucocorticoids: ectopic expression of desnutrin increases triglyceride hydrolysis. J Biol Chem *279*, 47066-47075.

Yang, X., Lu, X., Lombes, M., Rha, G.B., Chi, Y.I., Guerin, T.M., Smart, E.J., and Liu, J. (2010). The G(0)/G(1) switch gene 2 regulates adipose lipolysis through association with adipose triglyceride lipase. Cell Metab *11*, 194-205.

Young, S.G., and Zechner, R. (2013). Biochemistry and pathophysiology of intravascular and intracellular lipolysis. Genes Dev *27*, 459-484.

Zhang, X., Saarinen, A.M., Hitosugi, T., Wang, Z., Wang, L., Ho, T.H., and Liu, J. (2017). Inhibition of intracellular lipolysis promotes human cancer cell adaptation to hypoxia. eLife *6*.

Zimmermann, R., Strauss, J.G., Haemmerle, G., Schoiswohl, G., Birner-Gruenberger, R., Riederer, M., Lass, A., Neuberger, G., Eisenhaber, F., Hermetter, A., et al. (2004). Fat mobilization in adipose tissue is promoted by adipose triglyceride lipase. Science *306*, 1383-1386.

CHARPTER 3

Macrophages take up VLDL-sized emulsion particles through caveolae-mediated endocytosis and excrete part of the internalized triglycerides as fatty acids

Lei Deng, Frank Vrieling, Rinke Stienstra, Guido J. Hooiveld, Anouk L. Feitsma, Sander Kersten

PLoS Biology

doi: 10.1371/journal.pbio.3001516

ABSTRACT

Triglycerides are carried in the bloodstream as part of very low-density lipoproteins (VLDL) and chylomicrons, which represent the triglyceride-rich lipoproteins. Triglyceride-rich lipoproteins and their remnants contribute to atherosclerosis, possibly by carrying remnant cholesterol and/or by exerting a pro-inflammatory effect on macrophages. Nevertheless, little is known about how macrophages process triglyceride-rich lipoproteins. Here, using VLDL-sized triglyceride-rich emulsion particles, we aimed to study the mechanism by which VLDL triglycerides are taken up, processed, and stored in macrophages. Our results show that macrophage uptake of VLDL-sized emulsion particles is dependent on lipoprotein lipase and requires the lipoprotein-binding C-terminal domain of lipoprotein lipase but not the catalytic N-terminal domain. Subsequent internalization of VLDL-sized emulsion particles by macrophages is carried out by caveolae-mediated endocytosis, followed by triglyceride hydrolysis catalyzed by lysosomal acid lipase. It is shown that STARD3 is required for the transfer of lysosomal fatty acids to the ER for subsequent storage as triglycerides, while NPC1 likely is involved in promoting the extracellular efflux of fatty acids from lysosomes. Our data provide novel insights into how macrophages process VLDL triglycerides and suggest that macrophages have the remarkable capacity to excrete part of the internalized triglycerides as fatty acids.

Keywords: Very low-density lipoproteins, endocytosis, caveolae, LPL, Macrophages

GRAPHIC ABSTRACT

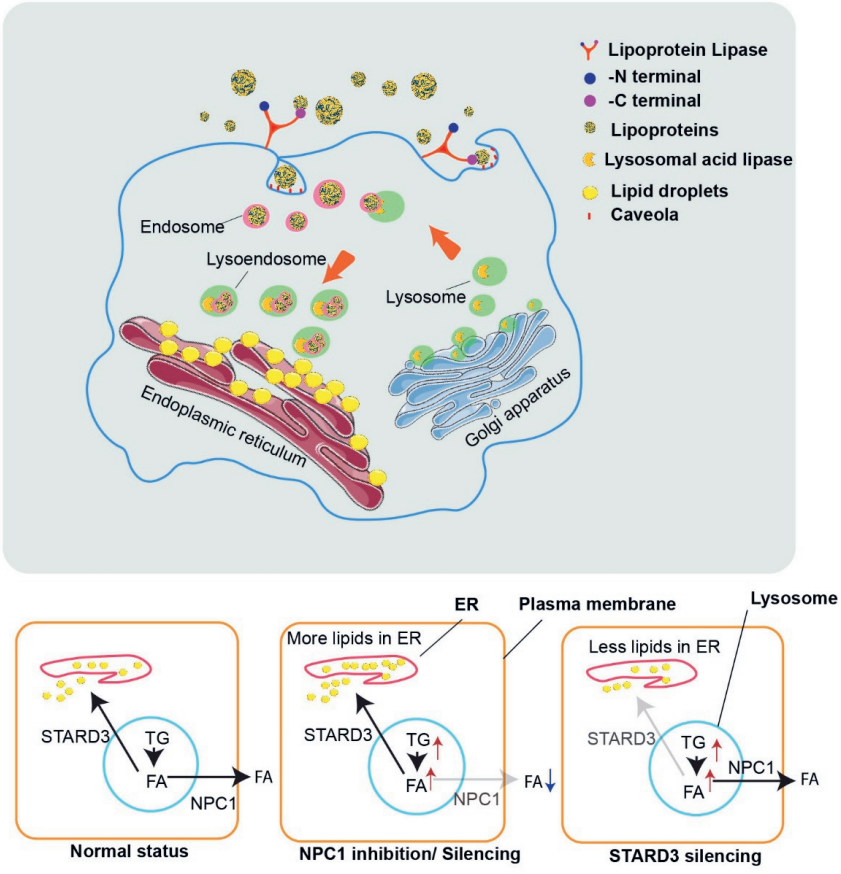

Macrophages take up VLDL-sized emulsion particles through caveolae-mediated endocytosis and excrete part of the internalized triglycerides as fatty acids. Deng et al. show that VLDL uptake by macrophages is mediated by the lipid-binding function of LPL. After endocytosis, the triglycerides in the particles are hydrolyzed by lysosomal LAL and the resulting fatty acids are excreted and stored via NPC1 and STARD3, respectively.

SUMMURY

Triglyceride-rich lipoproteins and their remnants contribute to atherosclerosis, possibly by carrying remnant cholesterol and/or by exerting a pro-inflammatory effect on macrophages. Nevertheless, little is known about how macrophages process triglyceride-rich lipoproteins.

We show that uptake by macrophages of VLDL-sized emulsion particles is dependent on the enzyme lipoprotein lipase via its C-terminal domain. Subsequent internalization of VLDL-triglycerides by macrophages is carried out by caveolae-mediated endocytosis, followed by hydrolysis by lysosomal acid lipase. STARD3 is required for the transfer of lysosomal fatty acids to the ER for lipid storage, while NPC1 likely is involved in promoting the extracellular efflux of fatty acids. Our data provide novel insights into how macrophages process VLDL-derived triglycerides and suggest that macrophages have the remarkable capacity to excrete internalized triglycerides as fatty acids.

ABSTRACT

Triglycerides are carried in the bloodstream as part of very low-density lipoproteins (VLDL) and chylomicrons, which represent the triglyceride-rich lipoproteins. Triglyceride-rich lipoproteins and their remnants contribute to atherosclerosis, possibly by carrying remnant cholesterol and/or by exerting a pro-inflammatory effect on macrophages. Nevertheless, little is known about how macrophages process triglyceride-rich lipoproteins. Here, using VLDL-sized triglyceride-rich emulsion particles, we aimed to study the mechanism by which VLDL triglycerides are taken up, processed, and stored in macrophages. Our results show that macrophage uptake of VLDL-sized emulsion particles is dependent on lipoprotein lipase and requires the lipoprotein-binding C-terminal domain but not the catalytic N-terminal domain of lipoprotein lipase. Subsequent internalization of VLDL-sized emulsion particles by macrophages is carried out by caveolae-mediated endocytosis, followed by triglyceride hydrolysis catalyzed by lysosomal acid lipase. It is shown that STARD3 is required for the transfer of lysosomal fatty acids to the ER for subsequent storage as triglycerides, while NPC1 likely is involved in promoting the extracellular efflux of fatty acids from lysosomes. Our data provide novel insights into how macrophages process VLDL triglycerides and suggest that macrophages have the remarkable capacity to excrete part of the internalized triglycerides as fatty acids.

Keywords: very low-density lipoproteins, endocytosis, caveolae, lipoprotein lipase, macrophages

INTRODUCTION

Lipids are essential for all cells, either as structural components, signaling molecules, or fuel source. Lipids are transported through the bloodstream as part of lipoproteins. Whereas cholesterol is mainly carried in high-density and low-density lipoproteins, triglycerides (TG) are predominantly transported by chylomicrons and very low-density lipoproteins (VLDL). Chylomicrons have a diameter of 75-600 nm, carry dietary TG, and are produced by enterocytes (Martins et al., 1996a). Conversely, VLDL have an average diameter of 30-80 nm, carry TG that are produced endogenously, and are synthesized in the liver (German et al., 2006a). In the fasted state, TG are present in the blood almost entirely as part of VLDL and its remnant lipoproteins.

Macrophages are innate immune cells that form the frontline in the host's defense against pathogens. They are specialized in the detection, phagocytosis, and destruction of bacteria and other harmful organisms. In addition, macrophages can present antigens and regulate inflammation by releasing cytokines. Besides phagocytizing and neutralizing pathogens, macrophages can also scavenge lipids, which after uptake can be stored in specialized organelles called lipid droplets. How macrophages scavenge VLDL and chylomicrons, and how the associated lipids are internalized and processed has not been well characterized.

Lipid uptake and storage in macrophages have primarily been investigated in the context of atherosclerosis (de Gaetano et al., 2016). Macrophages take up oxidized LDL, which is considered a key event in the pathogenesis of atherosclerotic lesions (Poznyak et al., 2020). In the past decades, evidence has been accumulating that apart from LDL particles, TG-rich lipoproteins (TRL) and their remnants also contribute to atherosclerosis (Ginsberg et al., 2021), possibly by carrying remnant cholesterol and/or by exerting a pro-inflammatory effect on macrophages (Saraswathi and Hasty, 2006a). Consistent with their purported roles in atherosclerosis, VLDL and VLDL remnants can be taken up and retained in the intima, where they can interact with macrophages (Nordestgaard et al., 1995).

The uptake of oxidized LDL and cholesterol by macrophages is mediated by a group of structurally unrelated molecular pattern recognition receptors referred to as scavenger receptors, including SCARB1, CD36, and MSR1 (Dhaliwal and Steinbrecher, 1999). However, in contrast to the uptake of oxidized LDL, little is known about how macrophages take up and process VLDL particles. It has been shown that the uptake of VLDL-TG in cultured macrophages is promoted by lipoprotein lipase (LPL) (Chang et al., 2019). Besides its lipolytic function, LPL may enhance lipid uptake by

functioning as a molecular bridge between VLDL and lipoprotein receptors and/or heparan sulfate proteoglycans (Beisiegel, 1996)(Ishibashi et al., 1990). Other steps in the uptake of VLDL-TG by macrophages remain poorly defined.

Endocytosis describes the transport of extracellular substances or particles into cells and is tightly related to the biological function of macrophages. The endocytosis pathway can be classified into several types: clathrin-dependent endocytosis, clathrin-independent endocytosis, pinocytosis, and phagocytosis (Wendland, 2001). The importance of clathrin-mediated endocytosis in the cellular uptake of lipids is well established. Indeed, the cellular uptake of LDL is mediated by the binding of LDL to the LDL receptor, followed by the formation of clathrin-coated pits and subsequent delivery of the lipid cargo to the lysosomes (Lakadamyali et al., 2006). Receptor-mediated endocytosis also mediates the uptake of native or modified LDL and remnant lipoproteins in macrophages as a key step in the pathogenesis of atherosclerosis (Wilhelm et al., 2017). In hepatocytes, receptor-mediated endocytosis is required for the uptake of VLDL- and chylomicron remnants (Zanoni et al., 2018). Whether endocytosis contributes to the uptake of VLDL-TG by macrophages is unclear.

After uptake by cells, LDL is degraded in lysosomes, releasing free cholesterol. The cholesterol binds to Niemann-Pick type C2 (NPC2) before being shuttled out of the lysosome via NPC1 (Mesmin et al., 2013) (Infante et al., 2008)(Thelen and Zoncu, 2017). Part of the cholesterol transported via this pathway may go to the plasma membrane, while another portion may go to the endoplasmic reticulum (ER). The lysosomal membrane protein STARD3 transports the cholesterol directly from the lysosome to the ER by interacting with vesicle-associated membrane protein-associated protein (VAP)A/B on the ER membrane (Alpy et al., 2013). Interestingly, STARD3 also promotes the reverse transport of cholesterol from the ER to the lysosome (Wilhelm et al., 2017), as well as the transfer of cholesterol from the lysosome to mitochondria (Charman et al., 2010). While there is thus substantial insight into how cholesterol is processed, transported, and stored in macrophages, our mechanistic understanding of the processing of VLDL-TG in macrophages is very limited.

Considering the growing recognition of the importance of TRL and their remnants in atherosclerosis (Ginsberg et al., 2021), here, using VLDL-sized TG-rich emulsion particles, we aimed to study the mechanism by which VLDL-TG are taken up and processed in macrophages.

RESULTS

VLDL-sized lipid emulsion particles are taken up by macrophages

Using a microfluidizer, TG-rich emulsion particles were prepared with a mean diameter of 60 nm, referred to as VLDL-sized emulsion particles (Fig 1a)(German et al., 2006b). Treatment of human primary macrophages with these particles for 6 hours led to marked lipid accumulation, as visualized using BODIPY 493/503 staining (Fig 1b) and quantified using flow cytometry (Fig 1c). Treatment with VLDL-sized emulsion particles also significantly increased the expression of lipid-sensitive genes as measured by real-time qPCR (Fig 1d). Heatmaps (Fig 1e) and volcano plots (Fig 1f) based on RNAseq analysis clearly showed the marked effect of the lipid emulsion particles on gene expression in macrophages. Interestingly, VLDL-sized emulsion particles reduced the expression of cholesterol biosynthesis genes (GO:0006695), which is consistent with the suppressive effect of unsaturated fatty acids on genes involved in cholesterol synthesis, illustrating the significant impact of the lipid emulsion particles on lipid metabolism in macrophages (Fig 1g) (Carroll et al., 2018)(Fukumitsu et al., 2013). In agreement with previous studies (Saraswathi and Hasty, 2006b)(Lookene et al., 2000)(den Hartigh et al., 2014)(Aflaki et al., 2012), VLDL-sized emulsion particles also modulated genes involved in the ER stress response (GO:0034976) (Figure 1h) and the inflammatory response (GO:0006954) (Fig 1i).

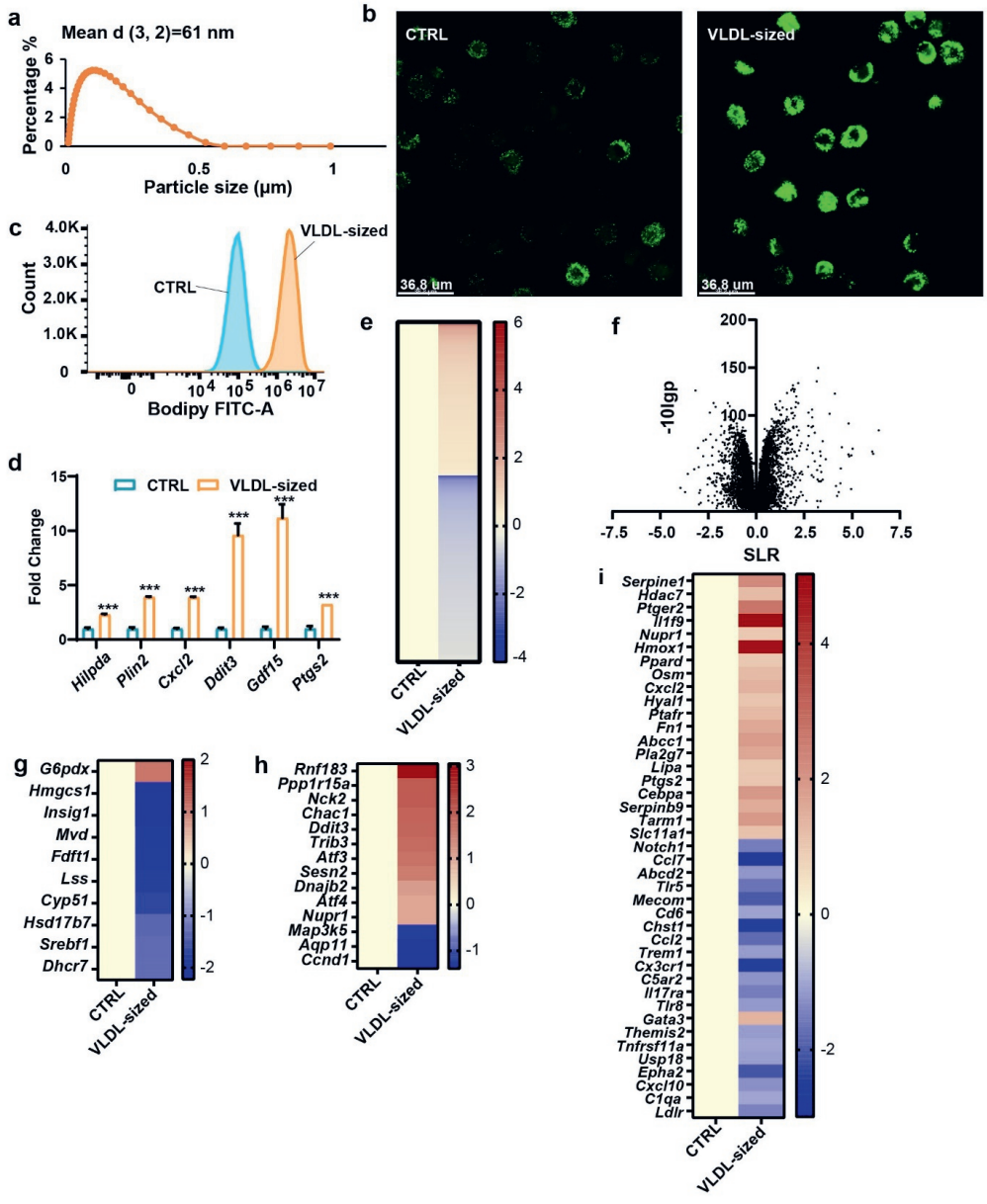

Fig 1. VLDL-sized emulsion particles promote lipid accumulation in cultured macrophages.

(a) The particle size distribution of VLDL-sized emulsion particles as determined by mastersizer 3000. (b) BODIPY 493/503 staining of intracellular neutral lipids in human primary macrophages treated with 0.5 mM VLDL-sized emulsion particles (referred to as VLDL-sized) for 6 hours (n=6). (c) Mean fluoresce intensity (FITC-A) measured by flow cytometry of mouse RAW 264.7 macrophages treated with 1 mM VLDL-sized emulsion particles for 6 hours (n=3). (d) mRNA expression of lipotoxic marker genes. (e) Heatmap and (f) Volcano plot of RNAseq data of RAW 264.7 macrophages treated with VLDL-sized emulsion particles using

all genes with q value less than 0.05 for any comparison. Heatmaps plotted with differentially expressed genes ($p<0.01$, SLR>1) involved in cholesterol synthesis (g), the ER stress response (h), and the inflammatory response (i). Bar graphs were plotted as mean±SD. Scale bar depicts signal log ratio (SLR). Data were analysed statistically using Student's t-test; *P < 0.05, **P<0.01, ***P<0.001, ***P<0.0001. (The raw data of RNA-sequencing are available under accession number GSE203250. The FACS data are available under repository ID FR-FCM-Z5K3. Other data can be found in "S1 other raw data".)

LPL is required for the uptake of VLDL-sized emulsion particles by macrophages

To determine whether LPL is required for the uptake of VLDL-sized emulsion particles by macrophages, we treated RAW 264.7 macrophages with heparin, which decreases surface LPL abundance by either releasing LPL from the cell surface or promoting internalization and degradation of LPL (CAMPOS et al., 1993). As expected, treatment with heparin markedly reduced macrophage LPL content (Fig 2a). Consistent with a role of LPL in the uptake of VLDL-sized emulsion particles, heparin reduced lipid accumulation in macrophages treated with the emulsion particles (Fig 2b-c).

To further assess the role of LPL in macrophage uptake of VLDL-sized emulsion particles, we silenced LPL in human primary macrophages using siRNA (Fig 2d). LPL silencing markedly reduced cellular lipid accumulation in macrophages treated with the emulsion particles, as visualized by BODIPY 493/503 staining (Fig 2e) and supported by flow cytometric analysis (Fig 2f). Consistent with lower lipid uptake, the induction of lipid-sensitive genes *HILPDA*, *PLIN2* and *PDK4* by the emulsion particles was significantly reduced by LPL silencing (Fig 2g). A similar suppressive effect of LPL silencing on lipid accumulation was observed in macrophages treated with human VLDL (Fig 2h-i). Overall, these data indicate that LPL is necessary for macrophage uptake of VLDL.

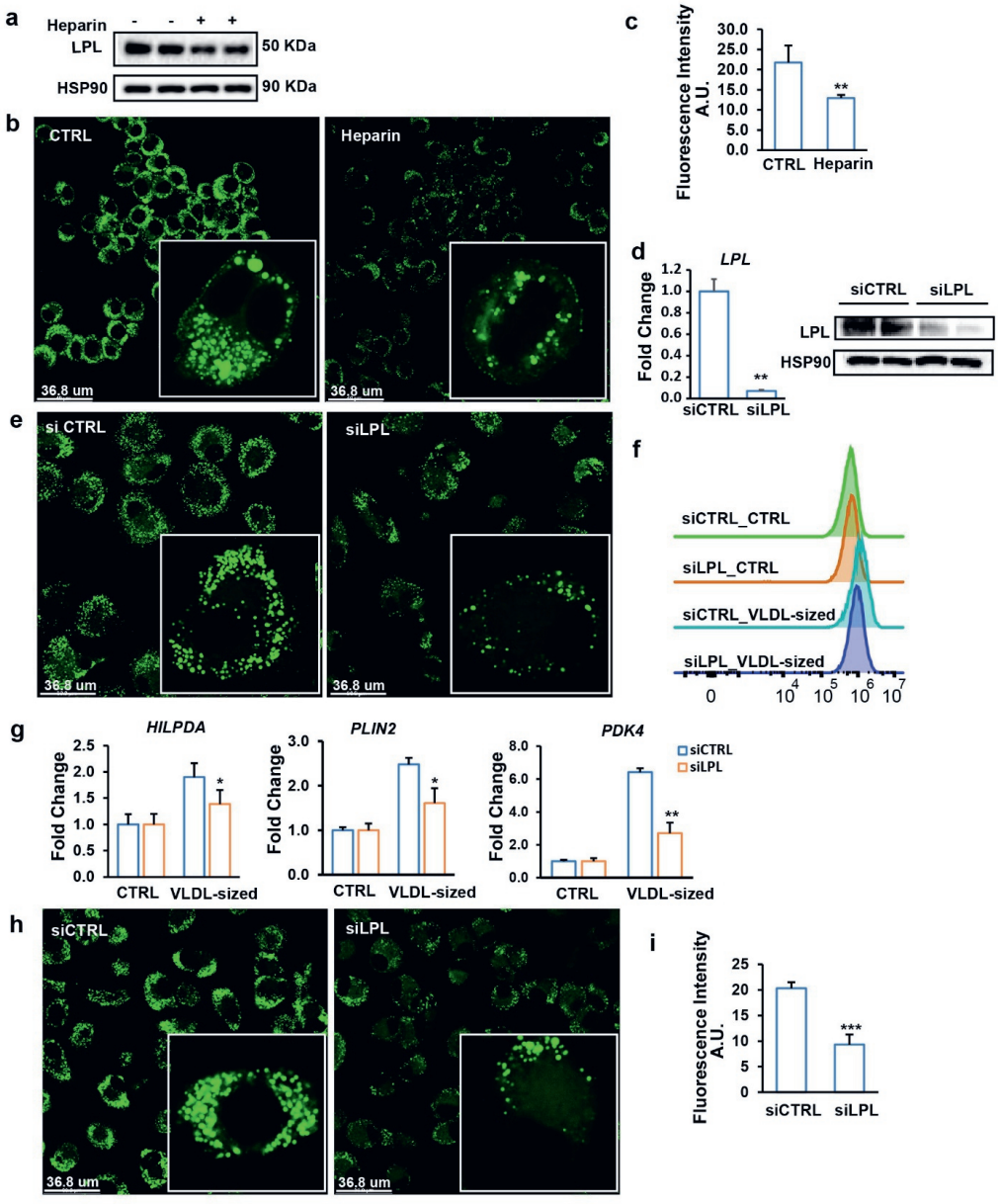

Fig 2. LPL mediates VLDL uptake in cultured macrophages.

(a) LPL protein levels in RAW 264.7 macrophages treated with 50 UI/ml Heparin for 2 hours. (b) BODIPY 493/503 staining of intracellular neutral lipids in RAW 264.7 macrophages treated with 1mM VLDL-sized emulsion particles for 6 hours in the presence or absence of 50 UI/ml human heparin (n=6). (c) Quantification of the fluorescence images by ImageJ (n=6). (d) LPL mRNA and protein levels in human primary macrophages treated with control siRNA or LPL siRNA for 48 hours. (e) BODIPY 493/503 staining of intracellular neutral

lipids in human macrophages treated with siCTRL or siLPL for 48 hours followed by treatment with 0.5 mM VLDL-sized emulsion particles for 6 hours. (f) Mean fluorescence intensity quantified by flow cytometry (n=3). (g) mRNA expression of selected lipid-sensitive genes. (h) BODIPY 493/503 staining of intracellular neutral lipids in human macrophages treated with siCTRL or siLPL for 48 hours followed by treatment with 0.5 mM human plasma-isolated VLDL for 6 hours (n=6). (i) Mean fluorescence intensity quantified by Image J (n≥4). The bar graphs were plotted as mean±SD. Asterisk indicates significantly different from control according to Student's t-test. *p<0.05, **p<0.01, ***p<0.001. (The FACS data are available under repository ID FR-FCM-Z5KY. Other data can be found in "S1 other raw data".)

Uptake of VLDL-sized emulsion particles by macrophages is dependent on the C-terminal portion of LPL

Based on our data and previous data (Saraswathi and Hasty, 2006b)(Oteng et al., 2019)(Milosavljevic et al., 2003), we hypothesized that the catalytic function of LPL is essential for macrophage uptake of VLDL. However, GSK264220A, a catalytic inhibitor of LPL, did not significantly alter lipid accumulation in RAW 264.7 cells treated with VLDL-sized emulsion particles (Fukumitsu et al., 2013) (Fig 3a-b). Also, the addition of an antibody directed against the catalytic N-terminal portion of human LPL did not noticeably influence lipid accumulation in human monocyte-derived macrophages (Fig 3c-d). These data suggest that the uptake of VLDL-sized emulsion particles by macrophages does not require the catalytic function of LPL.

The above finding raises the possibility that LPL may participate in the binding of the VLDL-sized emulsion particles to the macrophage surface. To verify this notion, human primary macrophages were co-treated with VLDL-sized emulsion particles and an antibody (5D2) directed against the C-terminal portion of LPL, which mediates the binding of TG-rich lipoproteins (Lookene et al., 2000). Interestingly, the C-terminal hLPL antibody markedly decreased intracellular lipid accumulation, supporting the notion that the C-terminal region of LPL is required for macrophage uptake of VLDL-sized emulsion particles and suggesting that LPL's role in macrophage uptake of VLDL is more as a receptor than as an enzyme (Fig 3e-f).

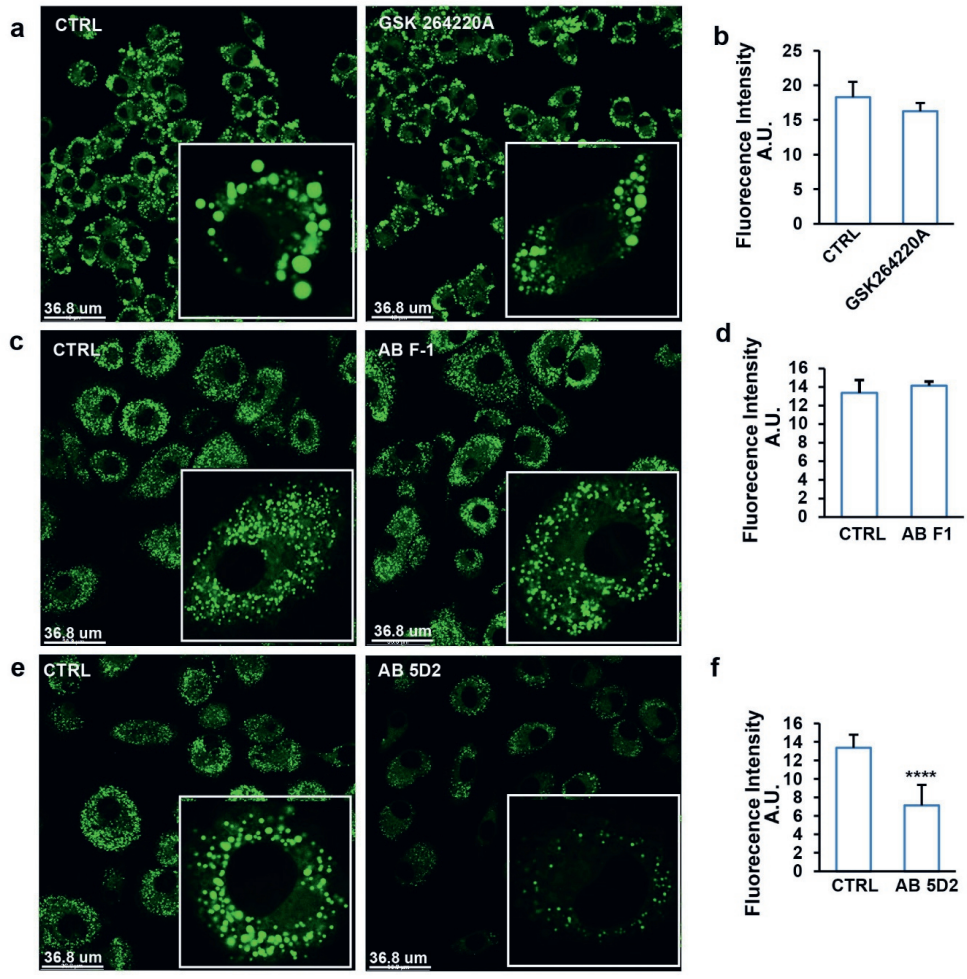

Fig 3. The C-terminal portion of LPL mediates uptake of VLDL-sized emulsion particles in cultured macrophages.

(a) BODIPY 493/503 staining of RAW 264.7 macrophages treated with 1 mM VLDL-sized emulsion particles for 6 hours in the presence or absence of 0.2 μM of the catalytic LPL inhibitor GSK264220 (n=6). (b) Mean fluorescence intensity quantified by Image J (n=4). (c) BODIPY 493/503 staining of human primary macrophages treated with 0.5 mM VLDL-sized emulsion particles for 6 hours in the presence or absence of antibody F1 targeting the N-terminal portion of LPL (2 μg/ml) (n=6). (d) Mean fluorescence intensity quantified by Image J (n≥4). (e) BODIPY 493/503 staining of human primary macrophages treated with 0.5 mM VLDL-sized emulsion particles for 6 hours in the presence or absence of antibody 5D2 targeting the C-terminal of LPL (2 μg/ml) (n=6). (f) Mean fluorescence intensity quantified by Image J (n≥4). The bar graphs

were plotted as mean±SD. Asterisk indicates significantly different from control according to Student's t-test. ****p<0.0001. (The raw data of bar graphs can be found in "S1 other raw data".)

Macrophage uptake of VLDL-sized emulsion particles is mediated by caveola-mediated endocytosis

Next, we examined whether the uptake of VLDL-sized emulsion particles was mediated by endocytosis. In agreement with this notion, early endosomes could be observed in RAW 264.7 macrophages after loading with VLDL-sized emulsion particles (Fig 4a). To determine if VLDL-sized emulsion particles are taken up by macrophages via clathrin- or caveola-mediated endocytosis, RAW 264.7 macrophages were treated with VLDL-sized emulsion particles in conjunction with the endocytosis inhibitors cholopromazine and genistein, which block clathrin- and caveola-mediated endocytosis, respectively (Vercauteren et al., 2010). Whereas cholopromazine showed little to no effect, genistein markedly reduced intracellular lipid accumulation (Fig 4b-c), suggesting that VLDL-sized emulsion particles are taken up via caveola-mediated endocytosis. Genistein similarly reduced intracellular lipid accumulation in human primary macrophages treated with the emulsion particles (Fig 4f-g).

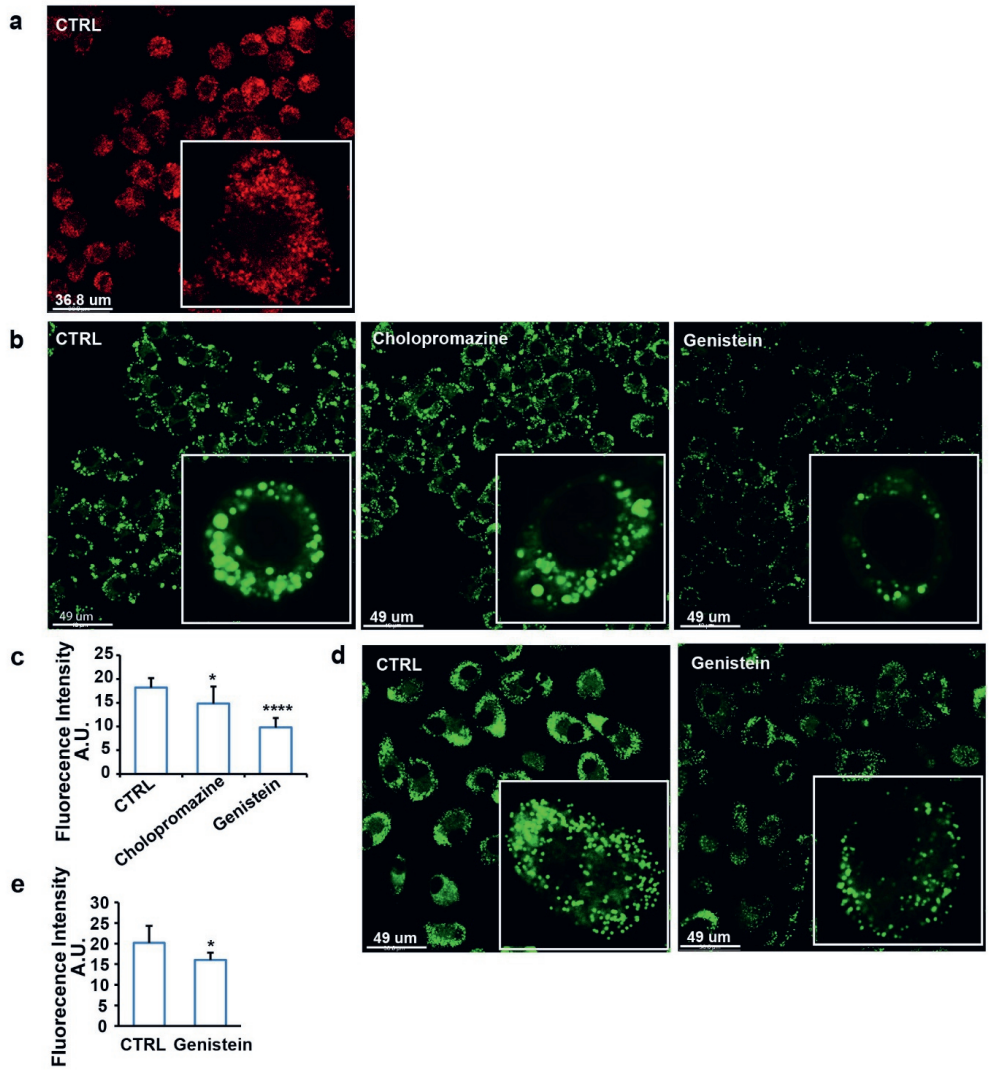

Fig 4. VLDL-sized emulsion particles are taken up by macrophages via caveola-mediated endocytosis. (a) Early endosome staining of RAW 264.7 macrophages treated with 1 mM of VLDL-sized emulsion particles for 6 hours (n=6). (b) BODIPY 493/503 staining of RAW 264.7 macrophages treated with 1 mM VLDL-sized emulsion particles for 6 hours in the presence or absence of 10 μg/ml chlorpromazine or 200 μM Genistein (n=6). (c) Mean fluorescence intensity quantified by Image J (n=6). (d) BODIPY 493/503 staining of human primary macrophages treated with 0.5 mM VLDL-sized emulsion particles for 6 hours in the presence or absence of 200 μM Genistein (n=6). (e) Mean fluorescence intensity quantified by Image J (n≥3). The bar graphs were plotted as mean±SD. Asterisk indicates significantly different from control according to Student's t-test. *$p<0.05$, ****$p<0.0001$. (The raw data of bar graphs can be found in "S1 other raw data".)

To further examine the role of caveola in the uptake of VLDL-sized emulsion particles, we silenced the *CAV1* and *CAV2* genes in human primary macrophages using siRNA (Fig 5a-b). Caveolins, encoded by *CAV1* and *CAV2*, are the main protein components of caveolae. Silencing of CAV1 and CAV2 markedly decreased intracellular lipid accumulation after loading cells with VLDL-sized emulsion particles, as visualized by confocal microscopy (Fig 5c) and quantified by flow cytometry (Fig 5d). A similar marked reduction in intracellular lipid accumulation upon CAV1 (Fig 5e-f) and CAV2 silencing (Fig 5g-h) was observed in human primary macrophages treated with human plasma-isolated VLDL. Consistent with a role of LPL, CAV1, and CAV2 in the uptake of VLDL-sized emulsion particles, the change in expression of *IL6* and *MCP1* (*CCL2*) upon treatment with VLDL-sized emulsion particles was altered by siRNA-based silencing of these genes (S1 Fig). Collectively, these results demonstrate that VLDL-sized emulsion particles are taken up via caveolae-mediated endocytosis,

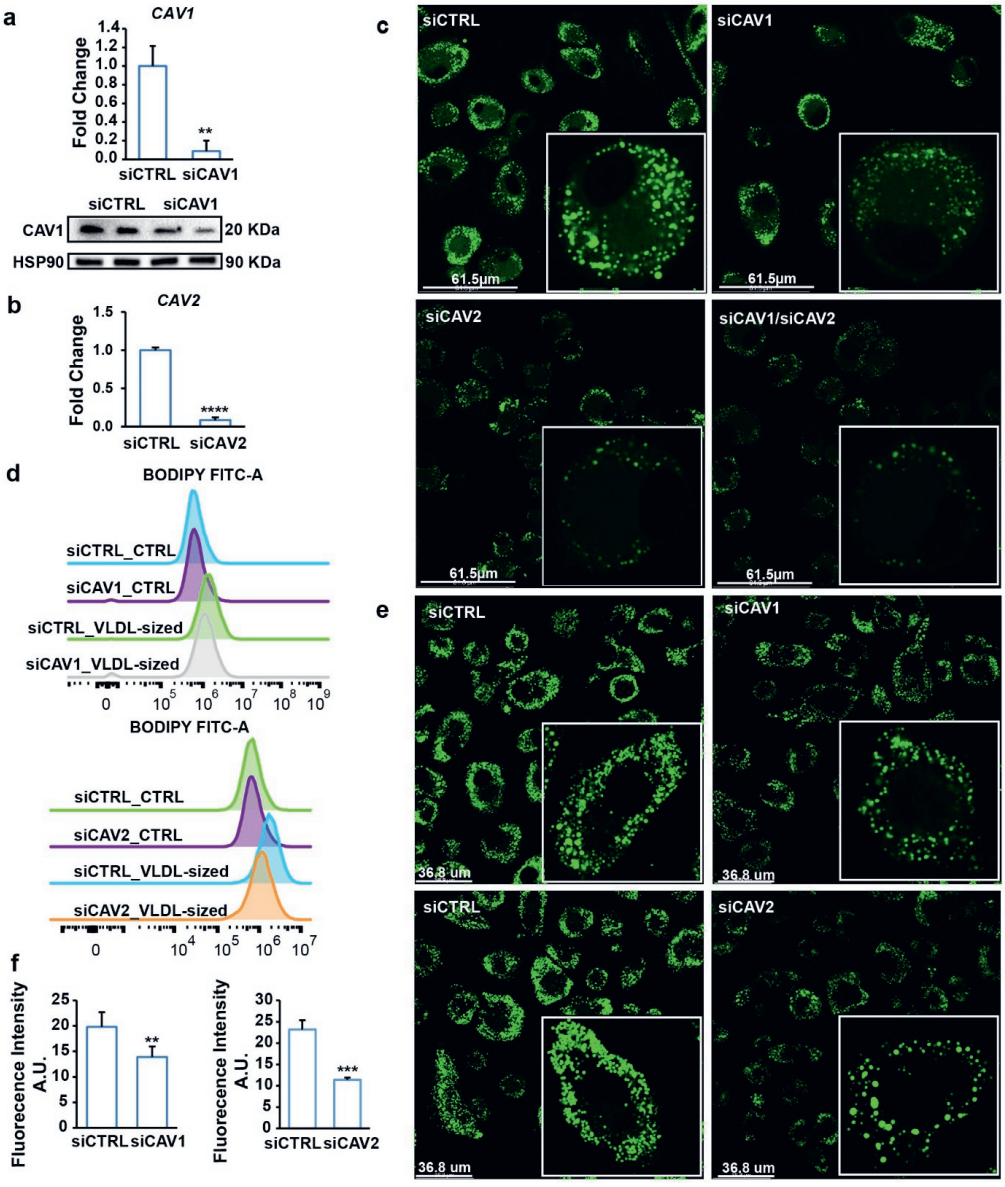

Fig 5. Silencing of Caveolin 1 and 2 impairs uptake of VLDL by macrophages.

(a) mRNA and protein levels of Caveolin 1 after 48 hour treatment with siCTRL or siCAV1. (b) mRNA expression of Caveolin 2 after 48 hour treatment with siCTRL or siCAV2. (c) BODIPY 493/503 staining of human macrophages treated with siCTRL, siCAV1, or siCAV2 for 48 hours followed by treatment with 0.5 mM VLDL-sized emulsion particles for 6 hours (n=6). (d) Mean fluorescence intensity quantified by flow cytometry (n=3). (e) BODIPY 493/503 staining of human macrophages treated with siCTRL, siCAV1, or siCAV2 for 48 hours followed by treatment with 0.5 mM human plasma-isolated VLDL for 6 hours (n=6). (f)

Mean fluorescence intensity quantified by Image J (n≥4). The bar graphs were plotted as mean±SD. Asterisk indicates significantly different from control according to Student's t-test. **p<0.01, ***p<0.001. (The FACS data are available under repository FR-FCM-Z5JV and FR-FCM-Z5KZ. Other data can be found in "S1 other raw data".)

Treatment of RAW 264.7 macrophages with VLDL-sized emulsion particles was associated with marked upregulation of genes involved in lysosomal function (Fig 6a). Endocytosed lipids destined for degradation are sorted into lysosomes, where they are digested by the enzyme lysosomal acid lipase (LAL). Strikingly, co-treatment of human primary macrophages treated with VLDL-sized emulsion particles with the LAL inhibitor Lalistat 2 markedly enhanced intracellular lipid accumulation (Fig 6b and 6c). Co-staining of lipids and lysosomes showed that the lipids appeared to be trapped in the lysosomal compartment. Minimal overlap in lipid- and lysosomal staining was observed in the absence of LAL inhibition (Figs 6d & S2). Interestingly, non-esterified fatty acids were detected in the culture medium of macrophages previously loaded with VLDL-sized emulsion particles, which was attenuated by LAL inhibition (Fig 6e). This suggests that macrophages can release non-esterified fatty acids after uptake of TG and that this release is dependent on LAL. The increase in lipid accumulation by Lalistat 2 was accompanied by reduced expression of the lipid-sensitive genes *HILPDA*, *PDK4*, *PLIN2*, *CXCL2* (Fig 6f). These data suggest that when LAL is inhibited, endocytosed lipids cannot further be processed and accumulate in lysosomes, preventing the transcriptional activation of lipid-sensitive genes. Taken together, we show that VLDL-sized emulsion particles are degraded via LAL in the lysosome. While most of the liberated fatty acids are destined for storage, a portion is released into the extracellular environment.

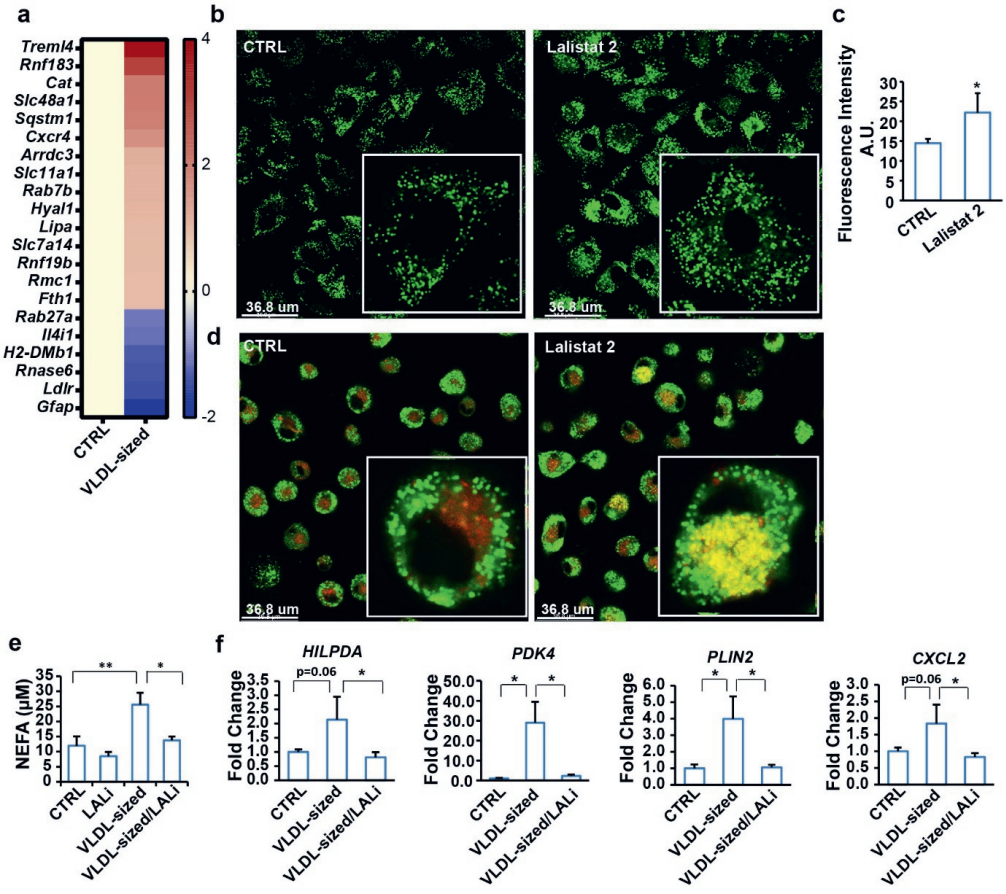

Fig 6. VLDL-sized emulsion particles are degraded by lysosomal acid lipase.

(a) Heatmap showing changes in expression of genes involved in lysosome activity in RAW 264.7 macrophages treated with 1 mM VLDL-sized emulsion particles for 6 hours ($p<0.01$, SLR>1). Scale bar depicts signal log ratio (SLR). (b) BODIPY 493/503 staining of human macrophages treated with 0.5 mM VLDL-sized emulsion particles for 6 hours in the presence or absence of 30 μM Lalistat 2 (n=6). The cells were washed twice with PBS and then incubated in fresh medium without VLDL-sized emulsion particles for another 24 hours. (c) Mean fluorescence intensity quantified by Image J (n=4). (d) Co-staining of lysosome (red) and neutral lipids (green) in human macrophages (n=6). (e) Non-esterified fatty acid levels in the medium. (f) mRNA levels of lipid-sensitive genes in human macrophages. The bar graphs were plotted as mean±SD. Asterisk indicates significantly different compared with control or in marked comparisons according to Student's t-test. *$p<0.05$, **$p<0.01$. (The raw data of RNA-sequencing are available under accession number GSE203250. Other data can be found in "S1 other raw data".)

NPC1 silencing retains lipids derived from VLDL-sized emulsion particles in the lysosomes and reduces the extracellular release of free fatty acids

Since NPC1 mediates the lysosomal export of cholesterol, we considered the possibility that NPC1 might also be involved in lysosomal export of VLDL-derived fatty acids. Interestingly, the expression of NPC1 was significantly up-regulated by VLDL-sized emulsion particles in human primary macrophages (Fig 7a). Co-treatment of human primary macrophages treated with VLDL-sized emulsion particles with a chemical inhibitor of NPC1 was associated with markedly elevated intracellular lipid accumulation (Fig 7b), as well as with more pronounced lysosomal staining (Fig 7c). To verify the notion that lipids may be partly retained in the lysosomes upon NPC1 inactivation, we silenced NPC1 in human primary macrophages treated with VLDL-sized emulsion particles and performed co-staining for lipids and lysosomes. Remarkably, NPC1 silencing (Fig 7d) markedly increased the overlap in lipid and lysosomal staining (Figs 7e & S3), suggesting that NPC1 deficiency causes lipids to be retained in lysosomes. Concurrent with the retention of lipids in the lysosomes, NPC1 silencing significantly decreased the levels of non-esterified fatty acids in the medium of macrophages treated with VLDL-sized emulsion particles (Fig 7f). Similarly, chemical inhibition of NPC1 significantly blunted the increase in non-esterified fatty acids in the medium of macrophages treated with the emulsion particles (Fig 7g), concurrent with an increase of lysosome dysfunction-related genes (Fig 7h). Although these data do not necessarily indicate that NPC1 directly mediates free fatty acid efflux from lysosomes, they do suggest that NPC1 is involved in promoting the extracellular release of fatty acids from macrophages.

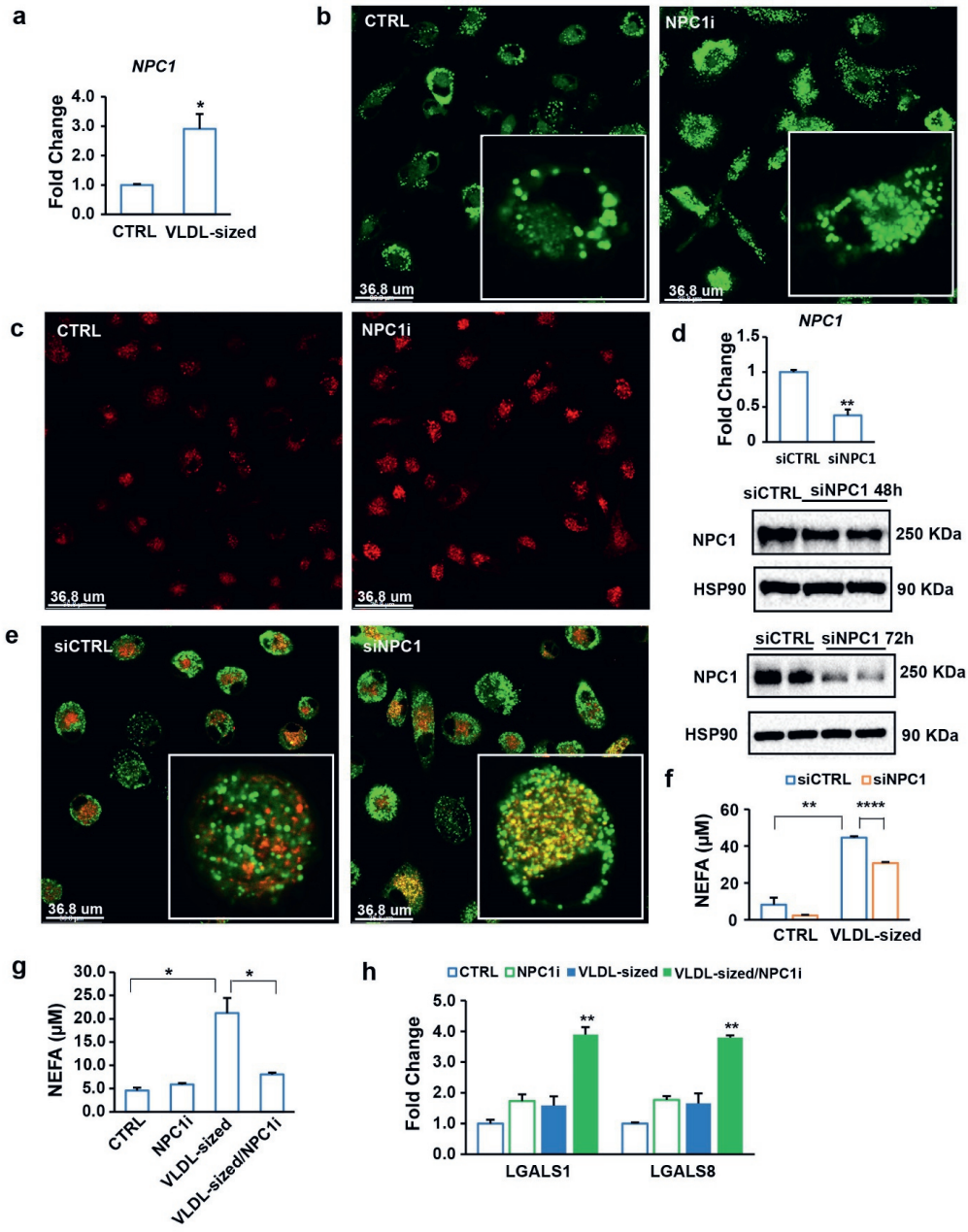

Fig 7. Part of the internalized TG in VLDL-sized emulsion particles is released from macrophages after lysosomal processing.

(a) mRNA levels of NPC1 in human macrophages treated with 1 mM VLDL-sized emulsion particles for 6 hours. Cells were washed twice with PBS and then incubate in fresh medium for 16 hours. (b) BODIPY 493/503 staining or (c) lysosomal staining of human macrophages treated with 0.5 mM VLDL-sized emulsion

particles for 6 hours in the presence or absence of 5 μM NPC1 inhibitor U18666A (n=6). (d) mRNA and protein levels of NPC1 in human macrophages treated with siCTRL or siNPC1. (e) Co-staining of lysosome (red) and neutral lipids (BODIPY 493/503, green) in human macrophages treated with siCTRL or siNPC1 for 72 hours followed by treatment with 0.5 mM VLDL-sized emulsion particles for 24 hours (n=6). Thereafter, the cells were washed twice with PBS and incubated in fresh medium without VLDL-sized emulsion particles for 24 hours. (f) Non-esterified fatty acid concentration in culture medium from human macrophages treated with siCTRL or siNPC1 for 48 hours followed by treatment with 0.5 mM VLDL-sized emulsion particles for 6 hours or (g) treatment with 0.5 mM VLDL-sized emulsion particles for 6 hours in the presence or absence of 5 μM NPC1 inhibitor U18666A. After the treatments, the cells were washed twice with PBS, followed by incubation in fresh medium without VLDL-sized emulsion particles for 16 hours. (h) mRNA levels of Galectin-encoding genes. The bar graphs were plotted as mean±SD. Asterisk indicates significantly different compared with control or in marked comparisons according to Student's t-test. *$p<0.05$, **$p<0.01$, ****$p<0.0001$. (The raw data of bar graphs can be found in "S1 other raw data".)

STARD3 is required for the lysosomal export of fatty acids derived from VLDL-sized emulsion particles

In addition to NPC1, the expression of *STARD3* was up-regulated by VLDL-sized emulsion particles in human macrophages (Fig 8a). Inasmuch as STARD3 mediates the transport of cholesterol from lysosomes to the ER (Alpy et al., 2013), we hypothesized that STARD3 may have a similar role in the intracellular trafficking of fatty acids derived from VLDL-sized emulsion particles. In line with this hypothesis, silencing of STARD3 (Fig 8b) in human macrophages treated with VLDL-sized emulsion particles increased lipid accumulation in lysosomes and reduced lipid content in the ER (Figs 8c-d, S4 & S5). Unlike silencing of NPC1, silencing of STARD3 did not increase intracellular lipid accumulation nor did it influence the efflux of fatty acids into the medium (Fig 8e). These findings are most consistent with a scenario in which STARD3 is involved in commuting fatty acids from the lysosome to the ER but does not contribute to the extracellular export of fatty acids. Taken together, our data indicate that NPC1 and STARD3 have differential roles in the transport of VLDL-derived fatty acids from the lysosome to other (extra)cellular compartments. Specifically, NPC1 somehow promotes the extracellular release of (lysosomal) fatty acids, while STARD3 is involved in the transfer of lysosomal fatty acids to the ER for subsequent storage as TG.

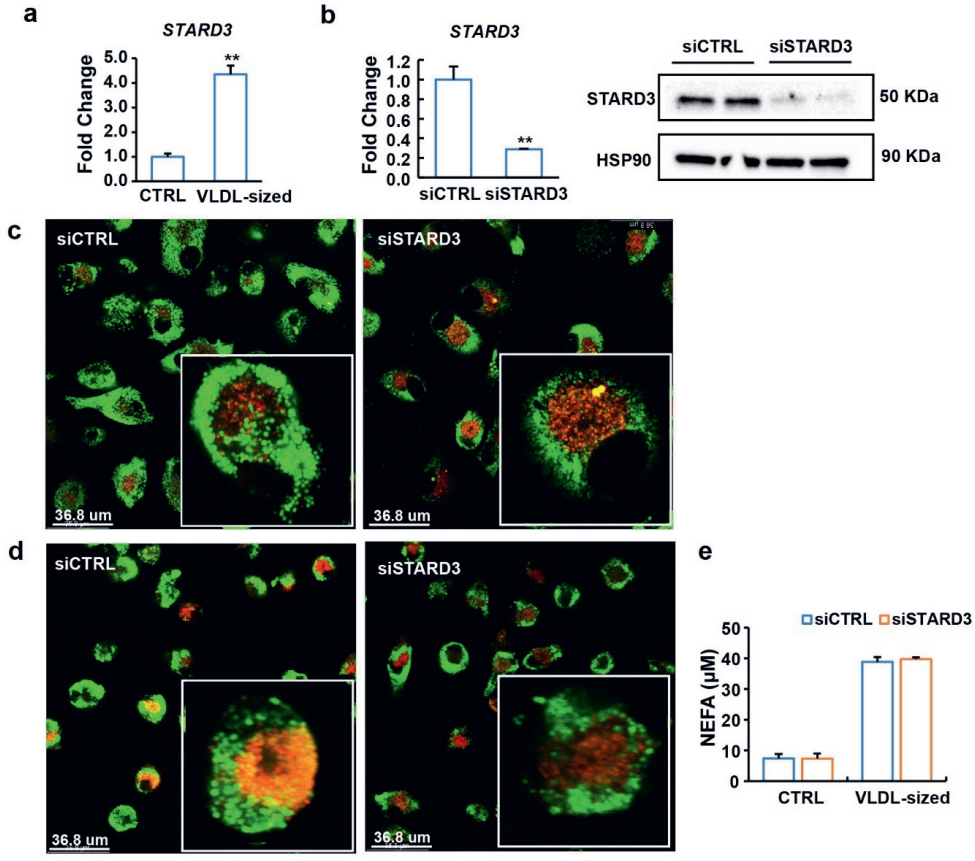

Fig 8. NPC1 and STARD3 have differential roles in the processing of VLDL-sized emulsion particles

(a) mRNA levels of STARD3 in human macrophages after treatment of 1 mM VLDL-sized emulsion particles for 6 hours. Cells were washed twice with PBS and then incubate in fresh medium for 16 hours. (b) mRNA and protein levels of STARD3 in human macrophages treated with siCTRL or siSTARD3 for 24 hours. (c) Co-staining of lysosomes (red) with neutral lipids (BODIPY 493/503, green) in human macrophages treated with siCTRL or siSTARD3 for 48 hours followed by treatment with 0.5 mM VLDL-sized emulsion particles for 24 hours (n=6). Thereafter, the cells were washed twice with PBS and incubated in fresh medium without VLDL-sized emulsion particles for 24 hours. (d) Co-staining of ER (red) and neutral lipids (BODIPY 493/503, green) in human macrophages treated with siCTRL or siSTARD3. (e) Non-esterified fatty acid concentration in culture medium from siCTRL or siSTARD3 treated human macrophages. The cells were washed twice with PBS and incubated in fresh medium without VLDL-sized emulsion particles for 16 hours. The bar graphs were

plotted as mean±SD. Asterisk indicates significantly different from control according to Student's t-test. **p<0.01. (The raw data of bar graphs can be found in "S1 other raw data".)

Macrophages take up chylomicron-sized emulsion particles via a similar mechanism as VLDL-sized emulsion particles

In contrast to VLDL, chylomicrons are not able to pass into the intima. Nevertheless, chylomicrons may come into direct contact with macrophages in the mesenteric lymph nodes. In addition, severely elevated chylomicron levels are associated with the accumulation of chylomicron-derived lipids within skin macrophages, giving rise to eruptive xanthomas. Accordingly, we asked whether the mechanism of uptake of chylomicrons by macrophages resembles the mechanism for uptake of VLDL. To that end, we repeated the studies using lipid-emulsion particles with a mean diameter of 240 nm (S6a Fig), referred to as chylomicron-sized emulsion particles, in agreement with the reported particle sizes of median-sized chylomicrons (Martins et al., 1996b). Treatment of RAW 264.7 macrophages and human primary macrophages with these particles for 6 hours led to marked lipid accumulation (S6b Fig) and increased expression of lipid-sensitive genes (S6c Fig). Similar to VLDL-sized emulsion particles, we found that LPL, but not its catalytic activity, is required for the uptake of CHYL-sized emulsion particles by macrophages (S7& S8 Figs) and that this process is driven by caveolae-mediated endocytosis (S9 Fig), involving caveolin 1 and 2 (S10 Fig). Additionally, the intracellular processing of CHYL-sized emulsion particles is mediated by LAL (S11 Fig). Taken together, these data indicate that the mechanisms for macrophage uptake of VLDL- and CHYL-sized emulsion particles are highly similar.

DISCUSSION

By virtue of its ability to enter the intima and be taken up by vascular macrophages, VLDL may contribute to atherosclerosis. Here, using artificial VLDL-sized emulsion particles and human VLDL, we studied the mechanism of uptake of VLDL particles by macrophages. We found that macrophage uptake of VLDL requires LPL and is mediated by the lipoprotein-binding C-terminal domain of LPL and not by the catalytic N-terminal domain. Subsequent internalization of VLDL-TG by macrophages was shown to occur via caveolae-mediated endocytosis, followed by TG hydrolysis by LAL in the lysosome. Intriguingly, NPC1 was found to promote the extracellular efflux of fatty acids from lysosomes, while STARD3 is involved in the transfer of lysosomal fatty acids to the ER for subsequent storage as TG. These data suggest that macrophages have the remarkable capacity to

excrete part of the internalized TG as fatty acids. Our data elaborate on the model put forward by Lindqvist and colleagues many years ago, who on the basis of studies using radiolabeled and unlabeled human VLDL proposed that incubation of macrophages with VLDL leads to TG accumulation via uptake of intact VLDL, mediated by either a receptor or a nonreceptor-mediated pathway and involving phagocytosis or endocytosis (Lindqvist et al., 1983).

LPL is mainly known for its ability to catalyze the hydrolysis of TG in VLDL and chylomicrons and thereby promote the uptake of plasma TG-derived fatty acids in tissues such as the heart, skeletal muscle, white adipose tissue, and brown adipose tissue (Martins et al., 1996b) (Goldberg, 1996). In addition to catalyzing TG hydrolysis, LPL can facilitate the binding and uptake of lipoprotein particles by cells independent of lipolysis (Stein and Stein, 2003) (Zheng et al., 2006). Through its ability to interact with lipoproteins on the one hand, and heparan sulfate proteoglycans or specific surface receptors on the other hand, LPL can function as a bridge between lipoproteins and the cell surface (Borén et al., 2001). For example, in macrophages—which are characterized by high levels of LPL expression—LPL was found to enhance the uptake of oxLDL (Hendriks et al., 1996). Previous studies have shown that LPL promotes the uptake TRL-TG and -cholesterol by macrophages *in vitro* (Lindqvist et al., 1983) (Ostlund-Lindqvist et al., 1983). However, thus far it was not fully clear whether the stimulation of TRL-TG uptake by LPL is mainly mediated by the abovementioned lipolysis-independent bridging function—leading to whole particle uptake—or requires actual TG hydrolysis followed by cellular uptake of fatty acids (Takahashi et al., 2013). Using antibodies directed against the N- or C-terminal domain of LPL, we found that macrophage uptake of TG contained in VLDL-sized emulsion particles is dependent on particle binding by LPL but not on the catalytic function of LPL. Whether binding to HSPG-bound LPL is sufficient to trigger endocytosis of the VLDL-like particles or requires an additional receptor remains to be determined.

Previous evidence suggested that LPL-catalyzed lipolysis is not required for the uptake of VLDL-TG by cultured macrophages but does have a modest stimulatory effect (Lindqvist et al., 1983). Further work is necessary to better define the role of the catalytic function of LPL in macrophage lipid metabolism. For example, it would be of interest to know the impact of the replacement of wildtype LPL by catalytically inactive mutated LPL on lipid uptake and metabolism in macrophages treated with VLDL-sized emulsion particles (Merkel et al., 1998). As an alternative, we considered the use of the LPL inhibitor orlistat. However, a major drawback of orlistat is that it also inhibits LAL (Tuohetahuntila et al., 2017), which would seriously complicate the interpretation of the data.

Our data suggest that macrophages internalize entire VLDL particles via endocytosis. Uptake of entire TRL particles has been previously observed in vascular endothelial cells of BAT and WAT (Bartelt et al., 2011)(Heine et al., 2018)(Schlein et al., 2021). In endothelial cells, the TRL are routed through the endosomal-lysosomal pathway, where they undergo LAL-mediated processing (Fischer et al., 2021). This route strongly resembles the pathway we observed for VLDL-sized emulsion particles in human primary macrophages.

It is well established that LDL and oxLDL are taken up by cells via receptor-mediated clathrin-dependent endocytosis (Maurer and Cooper, 2006)(Kibbey et al., 1998)(Garuti et al., 2005)(Ye et al., 2012)(Wei et al., 2014)(Jones and Willingham, 1999). In contrast, our data indicate that VLDL is taken up by macrophages via caveolae-mediated endocytosis. Specifically, we observed that genistein markedly reduced lipid accumulation in macrophages treated with VLDL-sized emulsion particles, whereas cholopromazine had no effect. Gene silencing of *CAV1* and especially *CAV2* also markedly reduced lipid accumulation in VLDL-treated macrophages. The difference in the type of endocytosis mediating the uptake of LDL and VLDL might be explained by the different sizes of the two types of particles or by differences in the composition of the lipid cargo (REJMAN et al., 2004). Interestingly, previous studies have found that CAV1 is enriched in lipid-droplet fractions of endothelial cells and adipocytes (Le Lay et al., 2006)(Kuo et al., 2017). It can be hypothesized that in macrophages, part of the CAV1 is similarly associated with lipid droplets, which might imply that the role of caveolins in lipid processing in macrophages may go beyond endocytosis.

The internalization and subsequent breakdown of pathogens, apoptotic cells, or particles such as lipoproteins burden the macrophage with potentially toxic macromolecules that must either be metabolized or expelled (Tabas and Bornfeldt, 2020). For example, internalized cholesterol can either be esterified to fatty acids and stored or it can be exported out of the macrophages via ABCA1 to apolipoprotein A-I to produce precursors for HDL particles. Through these mechanisms, macrophages are able to limit the toxic effects of excessive free cholesterol levels on the cell membrane. Similar to cholesterol, elevated intracellular levels of free fatty acids can also be damaging to cells. To restrict this lipotoxicity, macrophages and other cells are able to convert fatty acids into TG as well as use the fatty acids as fuel. However, in contrast to cholesterol, there is very little evidence in the literature that macrophages export fatty acids. Lindqvist and colleagues showed that the presence of bovine serum albumin in the culture medium markedly decreased TG content in lipid-laden macrophages, raising the suggestion that macrophages are capable of mobilizing its stored TG (Lindqvist et al., 1983). Consistent with these data, we found that macrophages loaded with VLDL-

sized emulsion particles release fatty acids into the medium. Moreover, we observed that this process was impaired by inactivation of LAL and NPC1. At this stage, it is unclear if extracellular fatty acid efflux is dependent on the fusion of the lysosomes with the plasma membrane or requires fatty acid transport through the cytoplasm. Since NPC1 was specifically dismissed as fatty acid transporter (Passeggio and Liscum, 2005), the decreased fatty acid release upon NPC1 inactivation is probably secondary to impaired lysosomal lipolysis due to lysosomal accumulation of cholesterol, rather than reflecting a direct role of NPC1 as fatty acid transporter. Previously, it was suggested that lipid-laden macrophages may release fatty acids via the action of a nonlysosomal (presumably cytoplasmic) neutral triglyceride lipase (von Hodenberg et al., 1984). Based on our data, we cannot exclude that the increase in fatty acid release upon NPC1 silencing was dependent on TG storage in lipid droplets and ATGL-mediated lipolysis prior to the release of the fatty acids into the medium.

Consistent with our data, Mashek and colleagues recently found that fatty acids liberated by lipophagy in lysosomes can be transported out of hepatocytes, and suggested that the effluxed fatty acids may be available for uptake by the same cell (Cui et al., 2021). Based on our data, it is impossible to say whether the extracellular efflux of lysosome-derived fatty acids is needed for the storage of VLDL-TG in macrophages via re-uptake of the fatty acids. One could wonder about the rationale for exporting fatty acids from the cell if most of the fatty acids are re-taken up. Rather, the efflux of fatty acids may be a mechanism to rid the macrophage of excess fatty acids acquired via endocytosis and phagocytosis. It can be speculated that the fatty acids released by macrophages may be used as fuel by neighboring cells, similar as has been suggested for endothelial cells (Kuo et al., 2017).

StAR-related lipid transfer domain-3 (STARD3) is a sterol-binding protein that promotes sterol transport by creating ER–endosome contact sites (Wilhelm et al., 2016). We found that STARD3 is involved in the transfer of VLDL-derived fatty acids from the lyso/endosome to the ER. Whether STARD3 directly binds fatty acids or stimulates transport by creating membrane contact sites requires further study. Our data suggest that in contrast to NPC1, STARD3 does not promote the extracellular efflux of fatty acids. NPC1 and STARD3 thus have distinct roles in the transport of VLDL-derived fatty acids from the lysosome to other (extra)cellular compartments.

Our key findings on the uptake and intracellular processing of VLDL-sized emulsion particles in macrophages were reproduced when using the larger CHYL-sized emulsion particles, suggesting that TRL are processed through a common mechanism. However, it should be noted that the range in particle sizes of our artificial CHYL-sized emulsion particles is smaller than that of human

chylomicrons. Accordingly, it cannot be excluded that human chylomicrons are also taken up via other mechanisms, such as micropinocytosis. Previous *in vitro* studies already found large similarities in the mechanism of VLDL and chylomicron uptake and degradation by macrophages, showing among other things that macrophages are able to take up intact VLDL and chylomicron particles (Lindqvist et al., 1983)(Ostlund-Lindqvist et al., 1983). The *in vivo* relevance of uptake of chylomicrons by macrophages is likely limited. In contrast to VLDL and its remnants, chylomicrons are not able to penetrate the arterial wall to be taken up by macrophages. One specific location where chylomicrons do get in direct contact with macrophages is in the mesenteric lymph nodes, where excessive uptake of chylomicrons can lead to the formation of giant macrophage foam cells, as observed in ANGPTL4-deficient mice on a high fat diet (Lichtenstein et al., 2010).

Our study also has limitations. First, most of our experiments were conducted with artificial TG-rich emulsion particles. These VLDL-mimicking particles were generated with a microfluidizer using casein as emulsifier. It should be noted, though, that our key findings were verified with human VLDL. In addition, our data on the role of LPL in VLDL-TG uptake are fully consistent with previous studies that used human VLDL. The similarity in the mechanism of uptake of human VLDL and artificial VLDL-sized emulsion particles containing casein as emulsifier suggest that macrophages recognize TRL particles on the basis of size and/or lipid content rather than a specific protein component. A second limitation of our study is that the TG in VLDL-sized emulsion particles were not radioactively or fluorescently labeled. Consequently, we cannot fully exclude that part of the stored lipids may be endogenously synthesized by the macrophage in response to treatment with VLDL-sized emulsion particles. However, this contribution likely is small. In the future and when available, fluorescently-labeled TG could be incorporated into the VLDL-sized emulsion particles to enable direct intracellular visualization of exogenous lipids.

In conclusion, our data suggest that the uptake of TRL-derived TG by macrophages is mediated by the lipid-binding function of LPL. After binding to LPL, TRL-TG are taken up by caveolin-mediated endocytosis, followed by LAL-catalyzed hydrolysis in the lysosomes. Subsequent processing of TRL-derived fatty acids towards storage requires the proteins NPC1, which was found to promote the extracellular efflux of fatty acids from lysosomes, and STARD3, which is involved in the transfer of lysosomal fatty acids to the ER for subsequent storage as TG. Our data provide key new insights into how macrophages take up and process TRL.

METHODS

Preparation of VLDL- and chylomicron- sized lipid emulsions

The VLDL- and chylomicron-sized lipid emulsions were prepared with commercial sunflower oil (Gwoon, the Netherlands) with a microfluidizer at pressures of 400 bar and 1200 bar, respectively, for five cycles. Sodium caseinate (purity 97%, Excellion, FrieslandCampina, the Netherlands) was used as an emulsifier. Caseinate was solubilized in PBS overnight at 4°C to a final concentration of 1% (w/w). Before making the nano-emulsions, 10% sunflower oil mixed with caseinate solution was pre-emulsified using an IKA Ultra turrax for 1 min at 10,000 rpm/min. The size of the droplets was measured using a Mastersizer 3000 (Malvern Panalytical, United Kingdom).

Cell culture

RAW 264.7 macrophages

RAW 264.7 macrophages were cultured in DMEM supplemented with 10% FCS and 1% p/s. Cells were seeded at a density of 52,000 cells/cm^2 and cultured overnight before treatment with emulsions for 6 hours.

Human buffy-coat primary macrophages

PBMC isolation

Human buffy-coat blood was obtained from Sanquin, the Netherlands. Briefly, 25 ml of buffy-coat blood diluted 1:1 with PBS was added to 50 ml Leucosept tubes containing 15 ml of Ficoll-Paque followed by centrifugation for 15 min at 800 RCF at room temperature. Afterwards, the PBMC layer was collected and washed with cold PBS for three times. 70 µm cell strainers were used to remove clumps/ fat residues.

Monocytes isolation

Moncytes were isolated by MojoSort CD14 positive selection kits (Biolegend, California, United States) and LS columns (Miltenyi Biotec, Bergisch Gladbach, Germany). Briefly, 10 µl CD14 Nanobeads (10x pre-diluted in MACS buffer (PBS+ 0.5%BSA+ 2mM EDTA)) and 90 µl MACS buffer were added per 1×10^7 PBMCs and incubated at 4ºC for 15 min (gently mixed every 5 min). Afterwards, the monocytes were separated by LS columns using a Miltenyi QuadroMACS Separator.

Isolated cells were cultured in RPMI medium supplemented with 10% FCS, 1% GlutaMax and 1% p/s at a density of 1×10^6 cells/ml. 5 ng/ml of Granulocyte-macrophage colony-stimulating factor (GM-CSF; Miltenyi) was used to differentiate monocytes into macrophages. After full differentiation, cells were seeded at a density of 100,000 cells per cm^2 for siRNA assay and 150,000 cells per cm^2 for the other assays.

Inhibitors and heparin assay

Cells were pre-incubated with chemical inhibitors (30 μM of Lalistat 2, 0.2 μM of GSK264220A, 200 μM of Genistein, 10 μg/ml of chlorpromazine, 5 μM of U18666A) for 1 hour and then continuously treated with lipid emulsions for 6 hours.

For the heparin assay, cells were treated with 50 UI/ml of heparin for 2 hours, followed by two times washing with PBS. Emulsions were subsequently added to the cells together with the same concentration of heparin.

Human LPL F:1 (Santa Cruz Biotechnology, Inc., California, USA) and 5D2 antibodies were added to cell culture medium 2 hours prior to emulsion loading at the concentration of 2 μg/ml (1:100 dilution).

Genistein, Lalistat 2, chlorpromazine and heparin were obtained from Sigma-Aldrich, Missouri, United States. GSK264220A was from Tocris (bio-techne), Abingdon, United Kingdom. LPL 5D2 antibody was contributed by Dr. Anne Beigneux, Department of Medicine, David Geffen School of Medicine, UCLA, USA.

Free fatty acids assay

For functional study of NPC1 and STARD3, GM-CSF derived macrophages were loaded with VLDL-sized emulsion particles. After washing the cells twice with PBS, the medium was refreshed and cells were left for 16 hours. Then medium was collected for assessment of free fatty acids using the free fatty acids kit (Instruchemie, The Netherlands) following the manufacturer's instructions.

Quantitive RT-PCR

Total RNA was isolated using TRizol Reagent (Thermo Fisher Scientific, Massachusetts, United States). cDNA was synthesized using iScript cDNA Sythesis Kit (Bio-Rad Laboratories, Inc., California, United States) following the manufacturer's protocol. Real-Time polymerase chain reaction (RT-PCR) was performed on the CFX 384 Touch Real-Time detection system (Bio-Rad

Laboratories, Inc., California, United States), using the SensiMix (BioLine, London, UK) protocol for SYBR green reactions. Mouse/human 36B4 expression was used for normalization.

Immunoblotting

The cell lysates were prepared using RIPA Lysis and Extraction Buffer (Thermo Fisher Scientific, Massachusetts, United States) or with self-prepared NP40 lysis buffer (50 mM Tris-HCl pH 8.0, 0.5% NP40, 150 mM NaCl, 5 mM $MgCl_2$) for cell membrane binding proteins (LPL, Caveolin 1) and quantified with Pierce BCA Protein Assay Kit (Buffer (Thermo Fisher Scientific, Massachusetts, United States). The cell lysates were separated by electrophoresis on pre-cast 4-15% polyacrylamide gels and transferred onto nitrocellulose membranes using a Trans-Blot Semi-Dry transfer cell (Bio-Rad Laboratories, Inc., California, United States), blocked in 5% skim milk in TBS-T (TBS buffer supplied with 1 ‰ TWEEN 20) and incubated with LPL antibody (F:1), caveolin-1 Antibody (4H312), STARD3 antibody (H-1) (sc-166215) (Santa Cruz Biotechnology, Inc., Texas, United States) and NPC1 antibody (ab134113) (Abcam, Abcam, Cambridge, United Kingdom) overnight at 4ºC. Secondary antibody incubation was performed at room temperature for 1 hour. HSP90 was used for normalization (antibody was purchased from Cell Signaling Technology, Inc., Massachusetts, United States). Images were gained using the ChemiDoc MP system (Bio-Rad Laboratories, Inc., California, United States).

RNAseq analysis

Cells were treated with 1 mM VLDL-sized or chylomicron-sized lipid emulsions for 6 hours and harvested for total RNA isolation. The experiments were performed in both biological and technical triplicates. Samples of each condition from one experiment were pooled. Transcriptome analysis by RNA-sequencing was performed by BGI Hong Kong Company Limited (Hong Kong) following a standard protocol. In brief, RNA samples were prepared using RNeasy Mini Kit (Qiagen, Hilden, Germany) following the manufacturer's instructions. Samples were then shipped to BGI for library construction and RNA sequencing runs on the BGISEQ-500 platform (Goodwin et al., 2016). Genomic DNA was removed with two digestions using Amplification grade DNAse I (Invitrogen, USA). The RNA was sheared and reverse transcribed using random primers to obtain cDNA, which was used for library construction. The library quality was determined by using Bioanalyzer 2100. Thereafter, the library was used for 150bp paired-end sequencing on the BGISEQ-500 sequencing platform. All the generated raw sequencing reads were filtered, by removing reads with adaptors, reads with more than 10% of unknown bases, and low quality reads. Clean reads were then obtained and stored as FASTQ format.

The RNA-seq reads were used to quantify transcript abundances. To this end, the tool Salmon (version 0.14.1) (Patro et al., 2017) was used to map the reads to the GRCm38.p6 mouse genome assembly-based transcriptome sequences as annotated by the GENCODE consortium (release M22) (Frankish et al., 2019). The obtained transcript abundance estimates and lengths were then imported in R using the package tximport, scaled by average transcript length and library size, and summarized on the gene-level. Such scaling corrects for bias due to correlation across samples and transcript length, and has been reported to improve the accuracy of differential gene expression analysis (Soneson et al., 2016). Differential gene expression was determined using the package limma (Ritchie et al., 2015) utilizing the obtained scaled gene-level counts. Briefly, before statistical analyses, nonspecific filtering of the count table was performed to increase detection power, based on the requirement that a gene should have an expression level greater than 10 counts, i.e. ~0.45 count per million reads (cpm) mapped, for at least 3 libraries across all 9 samples. Differences in library size were adjusted by the trimmed mean of M-values normalization method (Bourgon et al., 2010), implemented in the package edgeR (Robinson et al., 2010). Counts were transformed to log2(cpm) values and associated precision weights, and entered into the limma analysis pipeline (Law et al., 2014). Differentially expressed genes were identified by using generalized linear models that incorporate empirical Bayes methods to shrink the standard errors towards a common value, thereby improving testing power (Smyth, 2004). All sequencing data have been submitted to the Gene Expression Omnibus (GEO), and are available under accession number GSE203250.

Confocal imaging

Cells were seeded and treated in µ-Slide 8 Well Glass plates (ibidi GmbH, Planegg, Germany) and visualized with Leica SP8-SMD confocal microscope (Leica Microsystems, Wetzlar, Germany) equipped with a 63× 1.20 NA water-immersion objective lens. Images were acquired using 1,024 × 1,024 pixels with the pinhole set at 1 Airy Unit (AU). Excitation of the fluorescent probes was performed using white light laser (WLL, 50% laser output). Florescent emission was detected using an internal Hybrid (HyD) detector. At least three entire images and three single cell images were taken for each replicate. The experiments are a minimum of two biological duplicates.

Lipid droplet accumulation was measured on 3.7% formaldehyde fixed cells after 20 min incubation with 2 µg/ml BODIPY 493/503 (Thermo Fisher Scientific, Massachusetts, United States) and mounted with Vectashield-H anti-fade medium (Vector laboratories, California USA). The WLL laser line (488 nm) was set at a laser power of 2.5% and emission was detected selecting a spectral window of 505-550 nm.

Endoplasmic reticulum (ER) was stained in live cells using ER Staining Kit - Red Fluorescence - Cytopainter (ab139482) (Abcam, Cambridge, United Kingdom) following the manufacturer's protocol. The principle of the stain reagent provided by the manufacturer is binding to the sulphonylurea receptors of ATP-sensitive K+ channels, which are prominent on the ER. Briefly, cells were stained with 1.5 µl/ml Detection Reagent and cultured with colorless DMEM for 45 minutes at 37°C before detection by microscopy. The WLL laser line (596 nm) was set at a laser power of 5% and emission was detected selecting a spectral window of 670-720 nm.

Lysosome were stained in live cells using LysoTracker Deep Red (Thermo Fisher Scientific, Massachusetts, United States) following the manufacturer's protocol. The LysoTracker probes consist of a fluorophore linked to a weak base that is only partially protonated at neutral pH. This allows LysoTracker probes to freely permeate cell membranes enabling them to label live cells. LysoTracker probes are highly selective for acidic organelles. Briefly, cells were stained with 75 nM fluorescence probe and cultured with colorless DMEM for 60 minutes at 37°C before detection by microscopy. The WLL laser line (647 nm) was set at a laser power of 5% and emission was detected selecting a spectral window of 670-720 nm.

Early endosomes were stained by CellLight Early Endosomes-RFP, BacMam 2.0 Kit (Thermo Fisher Scientific, Massachusetts, United States). In brief, cells were incubated overnight with 40 µl/ml CellLight reagent, fixed with 3.7% formaldehyde and mounted with Vectashield-H anti-fade medium. The WLL laser line (555 nm) was set at a laser power of 5% and emission was detected selecting a spectral window of 565-700 nm. Human primary macrophages for co-staining assays were cultured overnight in fresh medium after the lipid treatment to allow for sufficient intracellular lipid transportation.

When performing co-staining of neutral lipids with ER, 2µg/ml BODIPY 493/503 and 1.5 µl/ml ER Detection Reagent were mixed in 1X Assay Buffy (equipped in ER kit). For lipid droplets-lysosome co-staining, the reagents were mixed in colorless DMEM. The co-staining duration followed the requirement of ER staining or lysosome staining.

All staining operations and confocal imaging were protected from light as much as possible.

Flow cytometry analysis

Human primary macrophages (GM-CSF) were seeded in 24-well plates with a density as previously described and treated with 0.5 mM lipid emulsions for 6 hours. 1 µg/ml BODIPY 493/503 was used for cellular lipid droplet staining. After 20 minutes of incubation with BODIPY at 37 ºC, cells were

twice washed with PBS and then trypsinized. Samples were measured on a CytoFLEX cytometer (Beckman Coulter, Inc, Indianapolis, USA) and data were analyzed by FlowJo (BD, Oregon, USA).

siRNA gene knock down assay

Silencing of *LPL*, *CAV1*, *CAV2*, *NPC1* and *STARD3* in GM-CSF buffy coat human macrophages was carried out using ON-TARGETplus siRNA SMARTpool kits (Horizon Discovery Research company, Waterbeach, United Kingdom) following the instructions of the manufacturer. Briefly, GM-CSF macrophages were seeded in the desired plates at the density specified before and cultured overnight. 50 nM of siRNA was applied together with Lipofectamine RNAiMAX Transfection Reagent (Thermo Fisher Scientific, Massachusetts, United States) for 48 hours. Real time-qPCR and immunoblotting were used to assess the transfection efficiency. The sequences of the siRNAs are listed in S1 Table.

Statistical Analysis

Data are presented as mean ±SD. Data analysis were performed using unpaired Student's *t* test. GO Cellular components analysis was completed by Enrichr (Xie et al., 2021)(Chen et al., 2013)(Kuleshov et al., 2016). All other plots on transcriptome data were generated by Graphpad Prism 8.

Acknowledgements

The authors would like to thank Chang Sun for helping with the screening of chemical inhibitors of endocytosis, Montserrat de la Rosa Rodriguez and Qi Zheng for helping with confocal microscope technology, and Benthe van der Lugt for helping with human monocytes isolation. We thank Anne Beigneux (UCLA) for providing the LPL antibody 5D2.

REFERENCE

Aflaki, E., Doddapattar, P., Radović, B., Povoden, S., Kolb, D., Vujić, N., Wegscheider, M., Koefeler, H., Hornemann, T., Graier, W.F., et al. (2012). C16 ceramide is crucial for triacylglycerol-induced apoptosis in macrophages. Cell Death Dis. *3*.

Alpy, F., Rousseau, A., Schwab, Y., Legueux, F., Stoll, I., Wendling, C., Spiegelhalter, C., Kessler, P., Mathelin, C., Rio, M.C., et al. (2013). STARD3 or STARD3NL and VAP form a novel molecular tether between late endosomes and the ER. J. Cell Sci. *126*, 5500–5512.

Bartelt, A., Bruns, O.T., Reimer, R., Hohenberg, H., Ittrich, H., Peldschus, K., Kaul, M.G., Tromsdorf, U.I., Weller, H., Waurisch, C., et al. (2011). Brown adipose tissue activity controls triglyceride clearance. Nat. Med. *17*, 200–206.

Beisiegel, U. (1996). New aspects on the role of plasma lipases in lipoprotein catabolism and atherosclerosis. Atherosclerosis *124*, 1–8.

Borén, J., Lookene, A., Makoveichuk, E., Xiang, S., Gustafsson, M., Liu, H., Talmud, P., and Olivecrona, G. (2001). Binding of Low Density Lipoproteins to Lipoprotein Lipase Is Dependent on Lipids but Not on Apolipoprotein B. J. Biol. Chem. *276*, 26916–26922.

Bourgon, R., Gentleman, R., and Huber, W. (2010). Independent filtering increases detection power for high-throughput experiments. Proc. Natl. Acad. Sci. U. S. A. *107*, 9546–9551.

CAMPOS, A., NÙÑEZ, R., KOENIG, C.S., CAREY, D.J., and BRANDAN, E. (1993). A lipid-anchored heparan sulfate proteoglycan is present in the surface of differentiated skeletal muscle cells: Isolation and biochemical characterization. Eur. J. Biochem. *216*, 587–595.

Carroll, R.G., Zasłona, Z., Galván-Peña, S., Koppe, E.L., Sévin, D.C., Angiari, S., Triantafilou, M., Triantafilou, K., Modis, L.K., and O'Neill, L.A. (2018). An unexpected link between fatty acid synthase and cholesterol synthesis in proinflammatory macrophage activation. J. Biol. Chem. *293*, 5509–5521.

Chang, H.R., Josefs, T., Scerbo, D., Gumaste, N., Hu, Y., Huggins, L.A., Barrett, T.J., Chiang, S.S., Grossman, J., Bagdasarov, S., et al. (2019). Role of LpL (Lipoprotein Lipase) in macrophage polarization in vitro and in vivo. Arterioscler. Thromb. Vasc. Biol. *39*, 1967–1985.

Charman, M., Kennedy, B.E., Osborne, N., and Karten, B. (2010). MLN64 mediates egress of cholesterol from endosomes to mitochondria in the absence of functional Niemann-Pick Type C1

protein. J. Lipid Res. *51*, 1023–1034.

Chen, E.Y., Tan, C.M., Kou, Y., Duan, Q., Wang, Z., Meirelles, G. V., Clark, N.R., and Ma'ayan, A. (2013). Enrichr: Interactive and collaborative HTML5 gene list enrichment analysis tool. BMC Bioinformatics *14*.

Cui, W., Sathyanarayan, A., Lopresti, M., Aghajan, M., Chen, C., and Mashek, D.G. (2021). Lipophagy-derived fatty acids undergo extracellular efflux via lysosomal exocytosis. Autophagy *17*, 690–705.

Dhaliwal, B.S., and Steinbrecher, U.P. (1999). Scavenger receptors and oxidized low density lipoproteins. In Clinica Chimica Acta, (Clin Chim Acta), pp. 191–205.

Fischer, A.W., Jaeckstein, M.Y., Gottschling, K., Heine, M., Sass, F., Mangels, N., Schlein, C., Worthmann, A., Bruns, O.T., Yuan, Y., et al. (2021). Lysosomal lipoprotein processing in endothelial cells stimulates adipose tissue thermogenic adaptation. Cell Metab. *33*, 547-564.e7.

Frankish, A., Diekhans, M., Ferreira, A.M., Johnson, R., Jungreis, I., Loveland, J., Mudge, J.M., Sisu, C., Wright, J., Armstrong, J., et al. (2019). GENCODE reference annotation for the human and mouse genomes. Nucleic Acids Res. *47*, D766–D773.

Fukumitsu, S., Villareal, M.O., Onaga, S., Aida, K., Han, J., and Isoda, H. (2013). α-Linolenic acid suppresses cholesterol and triacylglycerol biosynthesis pathway by suppressing SREBP-2, SREBP-1a and -1c expression. In Cytotechnology, (Springer), pp. 899–907.

de Gaetano, M., Crean, D., Barry, M., and Belton, O. (2016). M1- and M2-type macrophage responses are predictive of adverse outcomes in human atherosclerosis. Front. Immunol. *7*, 275.

Garuti, R., Jones, C., Li, W.P., Michaely, P., Herz, J., Gerard, R.D., Cohen, J.C., and Hobbs, H.H. (2005). The modular adaptor protein autosomal recessive hypercholesterolemia (ARH) promotes low density lipoprotein receptor clustering into clathrin-coated pits. J. Biol. Chem. *280*, 40996–41004.

German, J.B., Smilowitz, J.T., and Zivkovic, A.M. (2006a). Lipoproteins: When size really matters. Curr. Opin. Colloid Interface Sci. *11*, 171.

German, J.B., Smilowitz, J.T., and Zivkovic, A.M. (2006b). Lipoproteins: When size really matters. Curr. Opin. Colloid Interface Sci. *11*, 171.

Ginsberg, H.N., Packard, C.J., Chapman, M.J., Borén, J., Aguilar-Salinas, C.A., Averna, M., Ference, B.A., Gaudet, D., Hegele, R.A., Kersten, S., et al. (2021). Triglyceride-rich lipoproteins and their

remnants: Metabolic insights, role in atherosclerotic cardiovascular disease, and emerging therapeutic strategies-a consensus statement from the European Atherosclerosis Society. Eur. Heart J. *42*, 4791–4806.

Goldberg, I.J. (1996). Lipoprotein lipase and lipolysis: Central roles in lipoprotein metabolism and atherogenesis. J. Lipid Res. *37*, 693–707.

Goodwin, S., McPherson, J.D., and McCombie, W.R. (2016). Coming of age: Ten years of next-generation sequencing technologies. Nat. Rev. Genet. *17*, 333–351.

den Hartigh, L.J., Altman, R., Norman, J.E., and Rutledge, J.C. (2014). Postprandial VLDL lipolysis products increase monocyte adhesion and lipid droplet formation via activation of ERK2 and NFκB. Am. J. Physiol. - Hear. Circ. Physiol. *306*.

Heine, M., Fischer, A.W., Schlein, C., Jung, C., Straub, L.G., Gottschling, K., Mangels, N., Yuan, Y., Nilsson, S.K., Liebscher, G., et al. (2018). Lipolysis Triggers a Systemic Insulin Response Essential for Efficient Energy Replenishment of Activated Brown Adipose Tissue in Mice. Cell Metab. *28*, 644-655.e4.

Hendriks, W.L., Van Der Boom, H., Van Vark, L.C., and Havekes, L.M. (1996). Lipoprotein lipase stimulates the binding and uptake of moderately oxidized low-density lipoprotein by J774 macrophages. Biochem. J. *314*, 563–568.

von Hodenberg, E., Khoo, J.C., Jensen, D., Witztum, J.L., and Steinberg, D. (1984). Mobilization of stored triglycerides from macrophages as free fatty acids. Arteriosclerosis *4*, 630–635.

Infante, R.E., Wang, M.L., Radhakrishnan, A., Hyock, J.K., Brown, M.S., and Goldstein, J.L. (2008). NPC2 facilitates bidirectional transfer of cholesterol between NPC1 and lipid bilayers, a step in cholesterol egress from lysosomes. Proc. Natl. Acad. Sci. U. S. A. *105*, 15287–15292.

Ishibashi, S., Yamada, N., Shimano, H., Mori, N., Mokuno, H., Gotohda, T., Kawakami, M., Murase, T., and Takaku, F. (1990). Apolipoprotein E and lipoprotein lipase secreted from human monocyte-derived macrophages modulate very low density lipoprotein uptake. J. Biol. Chem. *265*, 3040–3047.

Jones, N.L., and Willingham, M.C. (1999). Modified LDLs are internalized by macrophages in part via macropinocytosis. Anat. Rec. *255*, 57–68.

Kibbey, R.G., Rizo, J., Gierasch, L.M., and Anderson, R.G.W. (1998). The LDL receptor clustering motif interacts with the clathrin terminal domain in a reverse turn conformation. J. Cell Biol. *142*,

59–67.

Kuleshov, M. V., Jones, M.R., Rouillard, A.D., Fernandez, N.F., Duan, Q., Wang, Z., Koplev, S., Jenkins, S.L., Jagodnik, K.M., Lachmann, A., et al. (2016). Enrichr: a comprehensive gene set enrichment analysis web server 2016 update. Nucleic Acids Res. *44*, W90–W97.

Kuo, A., Lee, M.Y., and Sessa, W.C. (2017). Lipid Droplet Biogenesis and Function in the Endothelium. Circ. Res. *120*, 1289–1297.

Lakadamyali, M., Rust, M.J., and Zhuang, X. (2006). Ligands for clathrin-mediated endocytosis are differentially sorted into distinct populations of early endosomes. Cell *124*, 997–1009.

Law, C.W., Chen, Y., Shi, W., and Smyth, G.K. (2014). Voom: Precision weights unlock linear model analysis tools for RNA-seq read counts. Genome Biol. *15*.

Le Lay, S., Hajduch, E., Lindsay, M.R., Le Lièpvre, X., Thiele, C., Ferré, P., Parton, R.G., Kurzchalia, T., Simons, K., and Dugail, I. (2006). Cholesterol-induced caveolin targeting to lipid droplets in adipocytes: A role for caveolar endocytosis. Traffic *7*, 549–561.

Lichtenstein, L., Mattijssen, F., De Wit, N.J., Georgiadi, A., Hooiveld, G.J., Van Der Meer, R., He, Y., Qi, L., Köster, A., Tamsma, J.T., et al. (2010). Angptl4 protects against severe proinflammatory effects of saturated fat by inhibiting fatty acid uptake into mesenteric lymph node macrophages. Cell Metab. *12*, 580–592.

Lindqvist, P., Ostlund-Lindqvist, A.M., Witztum, J.L., Steinberg, D., and Little, J.A. (1983). The role of lipoprotein lipase in the metabolism of triglyceride-rich lipoproteins by macrophages. J. Biol. Chem. *258*, 9086–9092.

Lookene, A., Nielsen, M.S., Gliemann, J., and Olivecrona, G. (2000). Contribution of the carboxy-terminal domain of lipoprotein lipase to interaction with heparin and lipoproteins. Biochem. Biophys. Res. Commun. *271*, 15–21.

Martins, I.J., Mortimer, B., Miller, J., and Redgrave, T.G. (1996a). Effects of particle size and number on the plasma clearance of chylomicrons and remnants. J. Lipid Res. *37*.

Martins, I.J., Mortimer, B., Miller, J., and Redgrave, T.G. (1996b). Effects of particle size and number on the plasma clearance of chylomicrons and remnants. J. Lipid Res. *37*.

Maurer, M.E., and Cooper, J.A. (2006). The adaptor protein Dab2 sorts LDL receptors into coated pits independently of AP-2 and ARH. J. Cell Sci. *119*, 4235–4246.

Merkel, M., Kako, Y., Radner, H., Cho, I.S., Ramasamy, R., Brunzell, J.D., Goldberg, I.J., and Breslow, J.L. (1998). Catalytically inactive lipoprotein lipase expression in muscle of transgenic mice increases very low density lipoprotein uptake: Direct evidence that lipoprotein lipase bridging occurs in vivo. Proc. Natl. Acad. Sci. U. S. A. *95*, 13841–13846.

Mesmin, B., Antonny, B., and Drin, G. (2013). Insights into the mechanisms of sterol transport between organelles. Cell. Mol. Life Sci. *70*, 3405–3421.

Milosavljevic, D., Kontush, A., Griglio, S., Le Naour, G., Thillet, J., and Chapman, M.J. (2003). VLDL-induced triglyceride accumulation in human macrophages is mediated by modulation of LPL lipolytic activity in the absence of change in LPL mass. Biochim. Biophys. Acta - Mol. Cell Biol. Lipids *1631*, 51–60.

Nordestgaard, B.G., Wootton, R., and Lewis, B. (1995). Selective Retention of VLDL, IDL, and LDL in the Arterial Intima of Genetically Hyperlipidemic Rabbits In Vivo. Arterioscler. Thromb. Vasc. Biol. *15*, 534–542.

Ostlund-Lindqvist, A.M., Gustafson, S., Lindqvist, P., Witztum, J.L., and Little, J.A. (1983). Uptake and degradation of human chylomicrons by macrophages in culture. Role of lipoprotein lipase. Arteriosclerosis *3*, 433–440.

Oteng, A.B., Ruppert, P.M.M., Boutens, L., Dijk, W., Van Dierendonck, X.A.M.H., Olivecrona, G., Stienstra, R., and Kersten, S. (2019). Characterization of ANGPTL4 function in macrophages and adipocytes using Angptl4-knockout and Angptl4-hypomorphic mice. J. Lipid Res. *60*, 1741–1754.

Passeggio, J., and Liscum, L. (2005). Flux of fatty acids through NPC1 lysosomes. J. Biol. Chem. *280*, 10333–10339.

Patro, R., Duggal, G., Love, M.I., Irizarry, R.A., and Kingsford, C. (2017). Salmon provides fast and bias-aware quantification of transcript expression. Nat. Methods *14*, 417–419.

Poznyak, A. V., Nikiforov, N.G., Markin, A.M., Kashirskikh, D.A., Myasoedova, V.A., Gerasimova, E. V., and Orekhov, A.N. (2020). Overview of OxLDL and Its Impact on Cardiovascular Health: Focus on Atherosclerosis. Front. Pharmacol. *11*.

REJMAN, J., OBERLE, V., ZUHORN, I.S., and HOEKSTRA, D. (2004). Size-dependent internalization of particles via the pathways of clathrin- and caveolae-mediated endocytosis. Biochem. J. *377*, 159–169.

Ritchie, M.E., Phipson, B., Wu, D., Hu, Y., Law, C.W., Shi, W., and Smyth, G.K. (2015). Limma powers differential expression analyses for RNA-sequencing and microarray studies. Nucleic Acids Res. *43*, e47.

Robinson, M.D., McCarthy, D.J., and Smyth, G.K. (2010). edgeR: a Bioconductor package for differential expression analysis of digital gene expression data. Bioinformatics *26*, 139–140.

Saraswathi, V., and Hasty, A.H. (2006a). The role of lipolysis in mediating the proinflammatory effects of very low density lipoproteins in mouse peritoneal macrophages. J. Lipid Res. *47*, 1406–1415.

Saraswathi, V., and Hasty, A.H. (2006b). The role of lipolysis in mediating the proinflammatory effects of very low density lipoproteins in mouse peritoneal macrophages. J. Lipid Res. *47*, 1406–1415.

Schlein, C., Fischer, A.W., Sass, F., Worthmann, A., Tödter, K., Jaeckstein, M.Y., Behrens, J., Lynes, M.D., Kiebish, M.A., Narain, N.R., et al. (2021). Endogenous Fatty Acid Synthesis Drives Brown Adipose Tissue Involution. Cell Rep. *34*, 108624.

Smyth, G.K. (2004). Linear models and empirical bayes methods for assessing differential expression in microarray experiments. Stat. Appl. Genet. Mol. Biol. *3*.

Soneson, C., Love, M.I., and Robinson, M.D. (2016). Differential analyses for RNA-seq: Transcript-level estimates improve gene-level inferences. F1000Research *4*.

Stein, Y., and Stein, O. (2003). Lipoprotein lipase and atherosclerosis. Atherosclerosis *170*, 1–9.

Tabas, I., and Bornfeldt, K.E. (2020). Intracellular and Intercellular Aspects of Macrophage Immunometabolism in Atherosclerosis. Circ. Res. *126*, 1209–1227.

Takahashi, M., Yagyu, H., Tazoe, F., Nagashima, S., Ohshiro, T., Okada, K., Osuga, J.I., Goldberg, I.J., and Ishibashi, S. (2013). Macrophage lipoprotein lipase modulates the development of atherosclerosis but not adiposity. J. Lipid Res. *54*, 1124–1134.

Thelen, A.M., and Zoncu, R. (2017). Emerging Roles for the Lysosome in Lipid Metabolism. Trends Cell Biol. *27*, 833–850.

Tuohetahuntila, M., Molenaar, M.R., Spee, B., Brouwers, J.F., Wubbolts, R., Houweling, M., Yan, C., Du, H., VanderVen, B.C., Vaandrager, A.B., et al. (2017). Lysosome-mediated degradation of a distinct pool of lipid droplets during hepatic stellate cell activation. J. Biol. Chem. *292*, 12436–12448.

Vercauteren, D., Vandenbroucke, R.E., Jones, A.T., Rejman, J., Demeester, J., De Smedt, S.C., Sanders, N.N., and Braeckmans, K. (2010). The use of inhibitors to study endocytic pathways of gene carriers: Optimization and pitfalls. Mol. Ther. *18*, 561–569.

Wei, J., Fu, Z.Y., Li, P.S., Miao, H.H., Li, B.L., Ma, Y.T., and Song, B.L. (2014). The clathrin adaptor proteins ARH, Dab2, and numb play distinct roles in Niemann-Pick C1-Like 1 versus low density lipoprotein receptor-mediated cholesterol uptake. J. Biol. Chem. *289*, 33689–33700.

Wendland, B. (2001). Everything you ever wanted to know about endocytosis. Nat. Cell Biol. *3*, E254–E254.

Wilhelm, L.P., Tomasetto, C., and Alpy, F. (2016). Touché! STARD3 and STARD3NL tether the ER to endosomes. Biochem. Soc. Trans. *44*, 493–498.

Wilhelm, L.P., Wendling, C., Védie, B., Kobayashi, T., Chenard, M., Tomasetto, C., Drin, G., and Alpy, F. (2017). STARD 3 mediates endoplasmic reticulum-to-endosome cholesterol transport at membrane contact sites. EMBO J. *36*, 1412–1433.

Xie, Z., Bailey, A., Kuleshov, M. V., Clarke, D.J.B., Evangelista, J.E., Jenkins, S.L., Lachmann, A., Wojciechowicz, M.L., Kropiwnicki, E., Jagodnik, K.M., et al. (2021). Gene Set Knowledge Discovery with Enrichr. Curr. Protoc. *1*, e90.

Ye, Z.J., Go, G.W., Singh, R., Liu, W., Keramati, A.R., and Mani, A. (2012). LRP6 protein regulates low density lipoprotein (LDL) receptor-mediated LDL uptake. J. Biol. Chem. *287*, 1335–1344.

Zanoni, P., Velagapudi, S., Yalcinkaya, M., Rohrer, L., and von Eckardstein, A. (2018). Endocytosis of lipoproteins. Atherosclerosis *275*, 273–295.

Zheng, C., Murdoch, S.J., Brunzell, J.D., and Sacks, F.M. (2006). Lipoprotein lipase bound to apolipoprotein B lipoproteins accelerates clearance of postprandial lipoproteins in humans. Arterioscler. Thromb. Vasc. Biol. *26*, 891–896.

Supplementary

Table S1 Target sequences for siRNA used in the study

siRNA	Contents	Target Sequence
ON-TARGETplus Human CAV1 (857) siRNA - SMARTpool	siRNA J-003467-06	CUAAACACCUCAACGAUGA
	siRNA J-003467-07	GCAAAUACGUAGACUCGGA
	siRNA J-003467-08	GCAGUUGUACCAUGCAUUA
	siRNA J-003467-09	GCAUCAACUUGCAGAAAGA
ON-TARGETplus Human CAV2 (858) siRNA - SMARTpool	siRNA J-010958-05	AGAUUGGGAUACUGUAAUA
	siRNA J-010958-06	GUAAAGACCUGCCUAAUGG
	siRNA J-010958-07	GUAGGACGAUGCUUCUCUU
	siRNA J-010958-08	UAUCAUUGCUCCAUUGUGU
ON-TARGETplus Human STARD3 (10948) siRNA - SMARTpool	siRNA J-017665-05	GCGCAGGGACCGAUACUUG
	siRNA J-017665-06	GGCAAGACGUUUAUCCUGA
	siRNA J-017665-07	CAAGGGACUUCGUGAAUGU
	siRNA J-017665-08	GGAUGGUGCUGUGGAACAA
ON-TARGETplus Human NPC1 (4864) siRNA - SMARTpool	siRNA J-008047-05	GGACAACUAUACCCGAAUA
	siRNA J-008047-06	GAAGAAAGCCCGACUUAUA
	siRNA J-008047-07	GCGAACGGCUUCUAAAUUU
	siRNA J-008047-08	GAUGAGACCAAUUGUGAUA
ON-TARGETplus Human LPL (4023) siRNA - SMARTpool	siRNA J-008970-05	GCAGGAAGUCUGACCAAUA
	siRNA J-008970-06	CAUGACAAGUCUCUGAAUA
	siRNA J-008970-07	CCUACAAAGUCUUCCAUUA
	siRNA J-008970-08	GGGCUCUGCUUGAGUUGUA

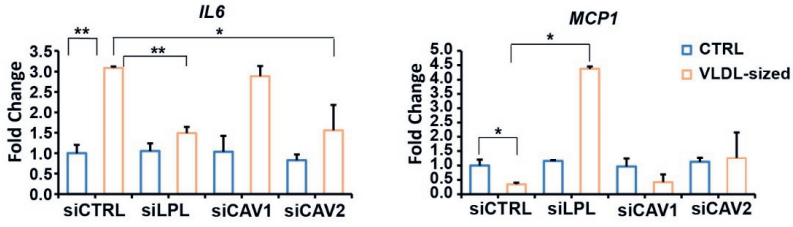

S1 Fig. Silencing of LPL, CAV1 and CAV2 modulated the expression of cytokines altered by lipid treatment. Human primary macrophages were treated with 1 mM VLDL-sized emulsion particles for 24 hours. The bar graphs were plotted as mean±SD. Asterisk indicates significantly different in the marked comparisons according to Student's t-test. *p<0.05, **p<0.01.

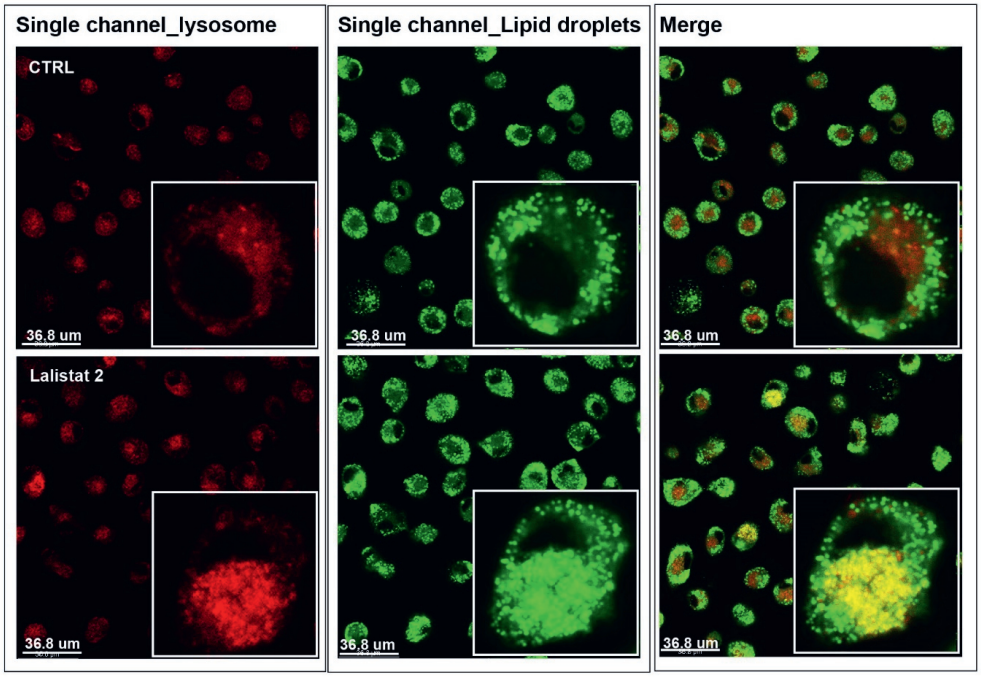

S2 Fig. Neutral lipids retained in lysosomes after inhibiting lysosomal acid lipase. The figure illustrates single channel images of co-staining of lysosome (red) and neutral lipids (BODIPY 493/503, green) in human macrophages in the presence or absence of 30 μM Laslistat 2 (n=6). Cells were treated with 0.5 mM VLDL-sized emulsion particles for 24 hours. Before imaging, cells were washed twice with PBS and cultured in fresh medium for 24 hours.

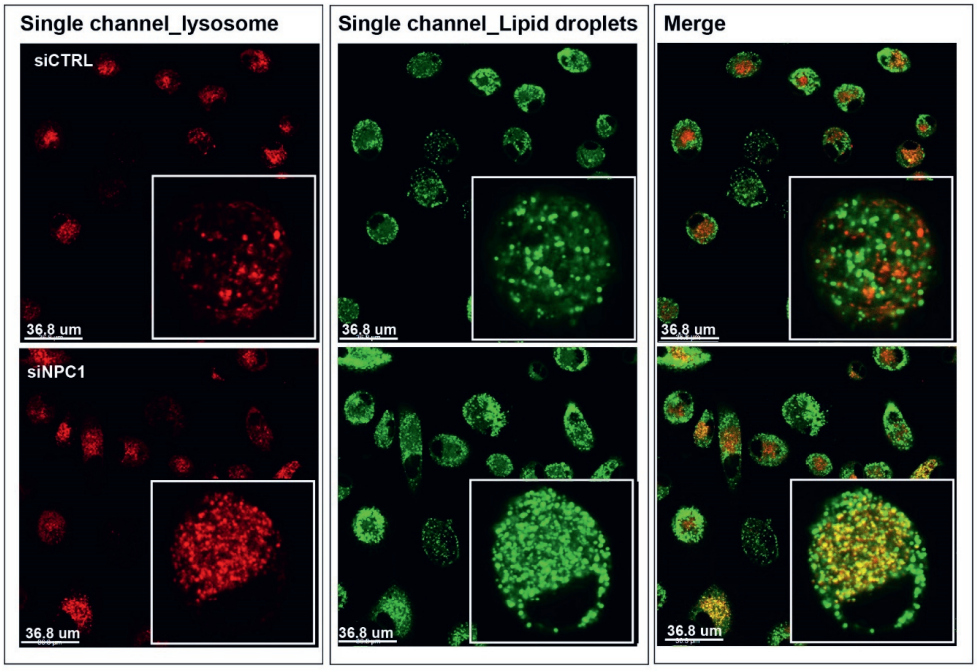

S3 Fig. Neutral lipids retained in lysosomes of siNPC1-treated human primary macrophages. The figure illustrates single channel images of co-staining of lysosome (red) and neutral lipids (BODIPY 493/503, green) in human macrophages treated with siCTRL or siNPC1 for 72 hours, followed by treatment with 0.5 mM VLDL-sized emulsion particles for 24 hours (n=6). Before imaging, cells were washed twice with PBS and cultured in fresh medium for 24 hours.

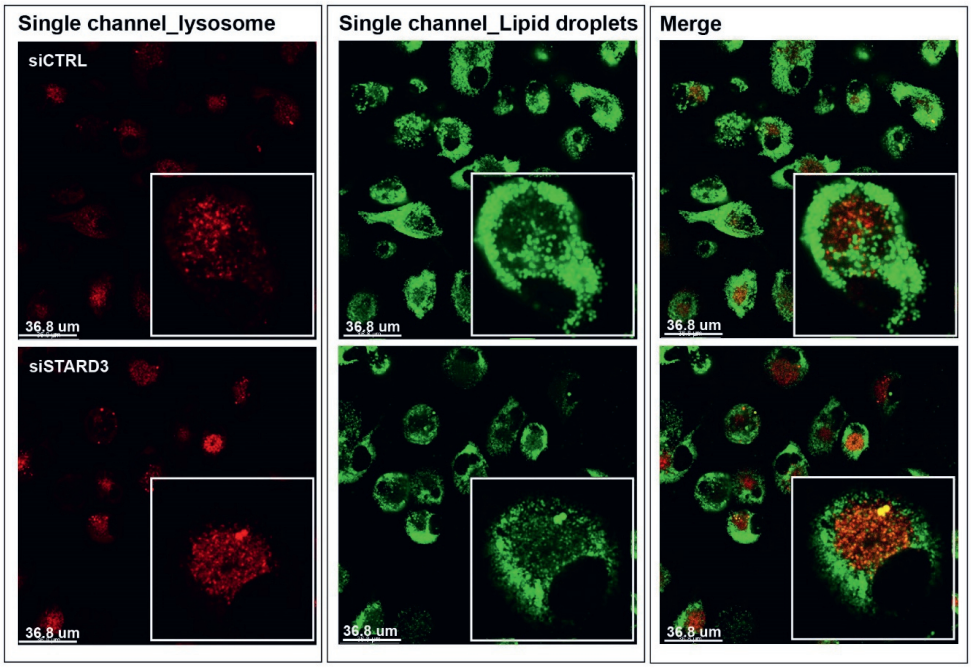

S4 Fig. Increased lipid accumulation in lysosomes by STARD3 silencing. The figure presents single channel images for co-staining of lysosomes (red) and neutral lipids (BODIPY 493/503, green) in human macrophages treated with siCTRL or siSTARD3 for 48 hours and followed by treatment with 0.5 mM VLDL-sized emulsion particles for 24 hours (n=6). Before imaging, cells were washed twice with PBS and cultured in fresh medium for 24 hours.

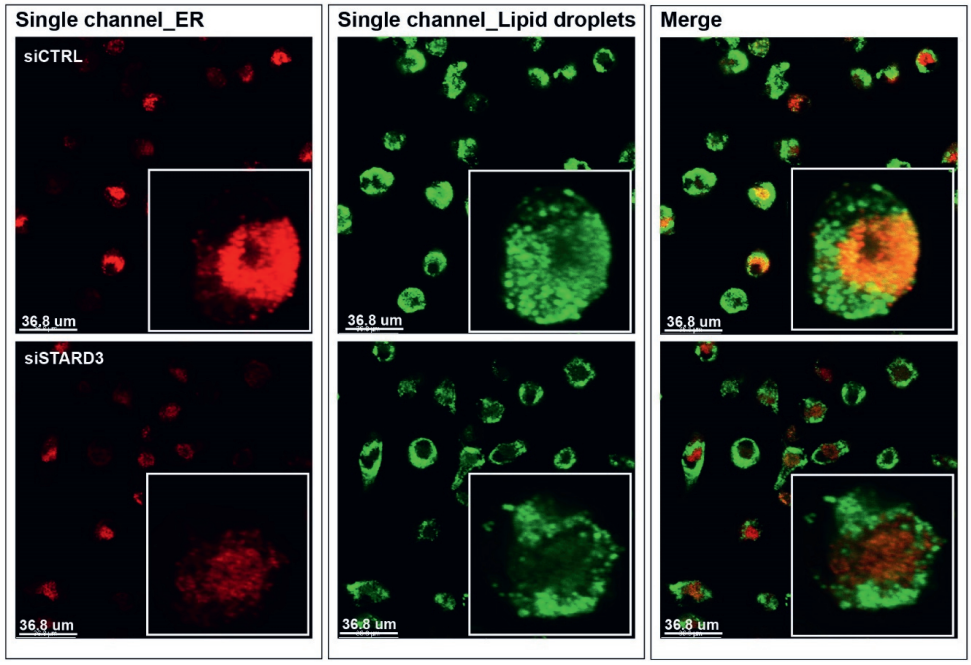

S5 Fig. STARD3 silencing impairs accumulation of neutral lipids in the ER. The figure presents single channel images for co-staining of ER (red) and neutral lipids (BODIPY 493/503, green) in human macrophages treated with siCTRL or siSTARD3 for 48 hours followed by treatment with 0.5 mM VLDL-sized emulsion particles for 24 hours (n=6).

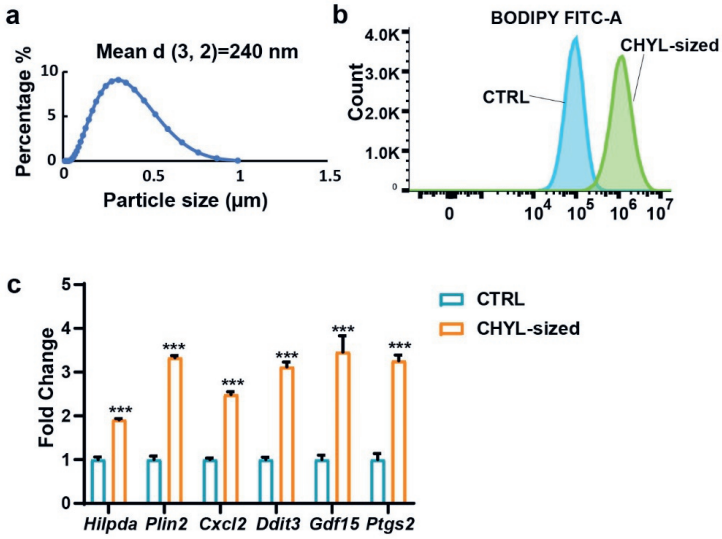

S6 Fig. CHYL-sized emulsion particles promote lipid accumulation in cultured macrophages. (a) The particle size distribution of CHYL-sized emulsion particles as determined by mastersizer 3000. (b) Mean fluorescence intensity (FITC-A) measured by flow cytometry of mouse RAW 264.7 macrophages treated with 1 mM CHYL-sized emulsion particles for 6 hours (n=3). (c) mRNA expression of lipotoxic marker genes in RAW 264.7 macrophages. Bar graphs were plotted as mean ± SD. Statistical significance was analysed using Two-way ANOVA; *p < 0.05, **p<0.01, ***p<0.001, ***p<0.0001.

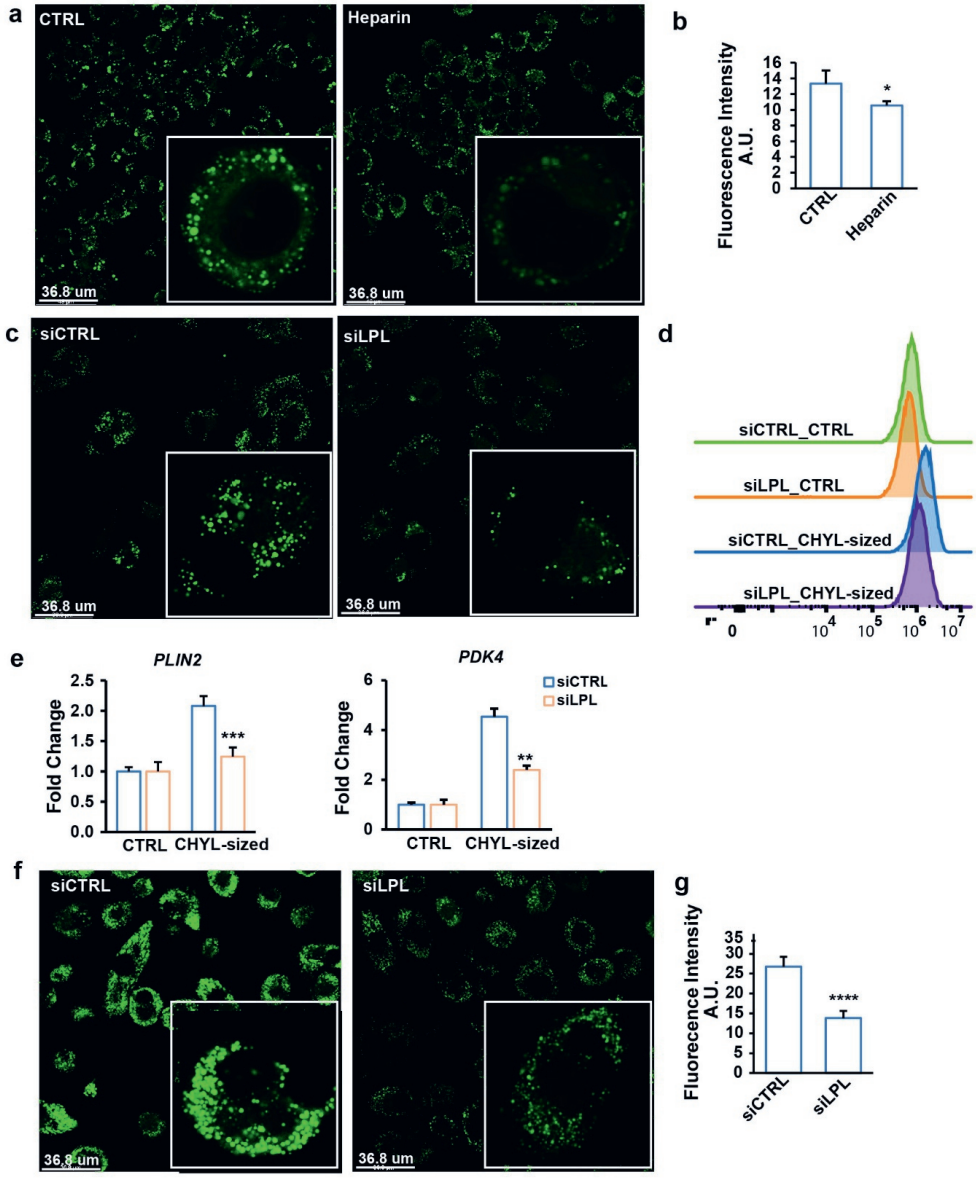

S7 Fig. LPL mediates uptake of CHYL-sized emulsion particles in cultured macrophages. (a) BODIPY 493/503 staining of intracellular neutral lipids in RAW 264.7 macrophages treated with 1 mM CHYL-sized emulsion particles for 6 hours in the presence or absence of 50 UI/ml human heparin (n=6). (b) Quantification of the fluorescence images by ImageJ (n=4). (c) BODIPY 493/503 staining of intracellular neutral lipids in human macrophages treated with siCTRL or siLPL for 48 hours followed by treatment with 0.5 mM CHYL-sized emulsion particles for 6 hours (n=6). (d) Mean fluorescence intensity quantified by flow cytometry (n=3). (e) mRNA expression of selected lipid-sensitive genes. (f) BODIPY 493/503 staining of intracellular neutral

lipids in human macrophages treated with siCTRL or siLPL for 48 hours followed by treatment with 0.5 mM human plasma isolated CHYL for 6 hours (n=6). (g) Mean fluorescence intensity quantified by Image J (n≥4). The bar graphs were plotted as mean±SD. Asterisk indicates significantly different from control according to Student's t-test. *p<0.05, **p<0.01, ***p<0.001.

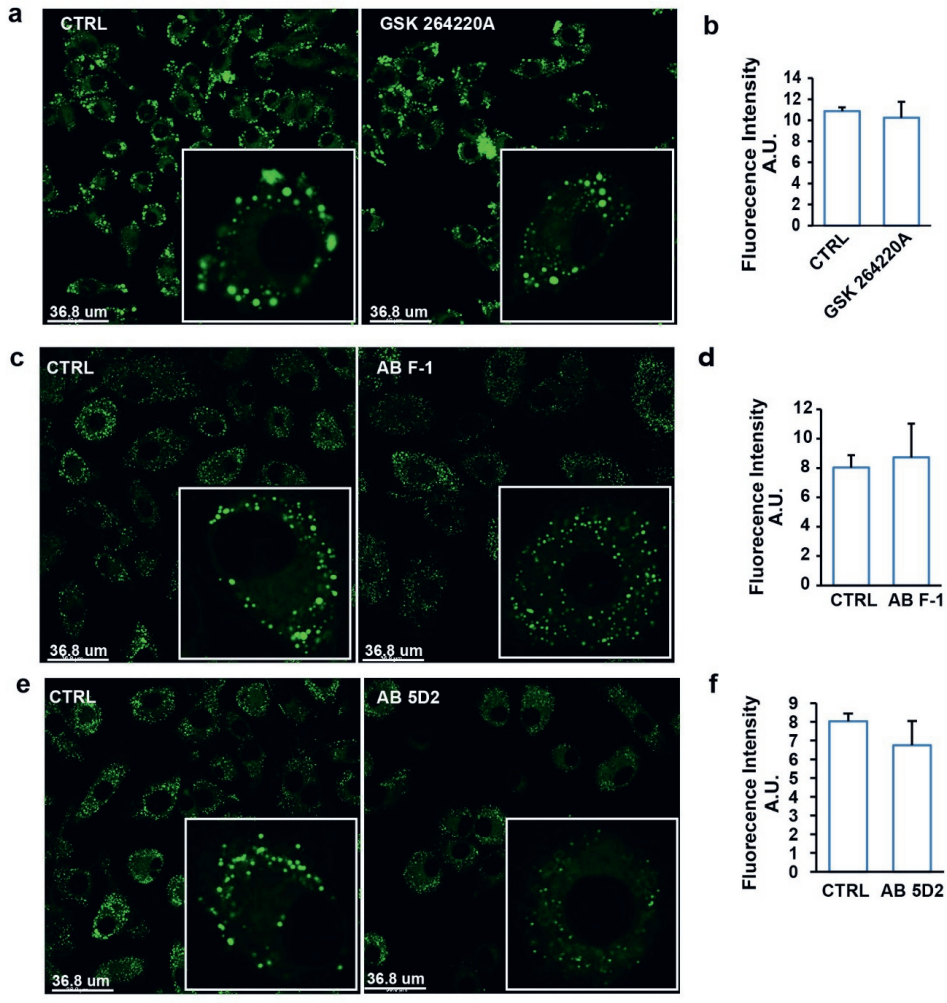

S8 Fig. The C-terminal portion of LPL mediates uptake of CHYL-sized emulsion particles in cultured macrophages. (a) BODIPY 493/503 staining of RAW 264.7 macrophages treated with 1 mM CHYL-sized emulsion particles for 6 hours in the presence or absence of 0.2 μM of the catalytic LPL inhibitor GSK264220 (n=6). (b) Mean fluorescence intensity quantified by Image J (n≥4). (c) BODIPY 493/503 staining of human primary macrophages treated with 0.5 mM CHYL-sized emulsion particles for 6 hours in the presence or absence of antibody F1 targeting the N-terminal portion of LPL (2 μg/ml) (n=6). (d) Mean fluorescence intensity quantified by Image J (n≥4). (e) BODIPY 493/503 staining of human primary macrophages treated

with 0.5 mM CHYL-sized emulsion particles for 6 hours in the presence or absence of antibody 5D2 targeting the C-terminal portion of LPL (2 µg/ml) (n=6). f) Mean fluorescence intensity quantified by Image J (n≥4). The bar graphs were plotted as mean±SD. Asterisk indicates significantly different from control according to Student's t-test. ****p<0.0001.

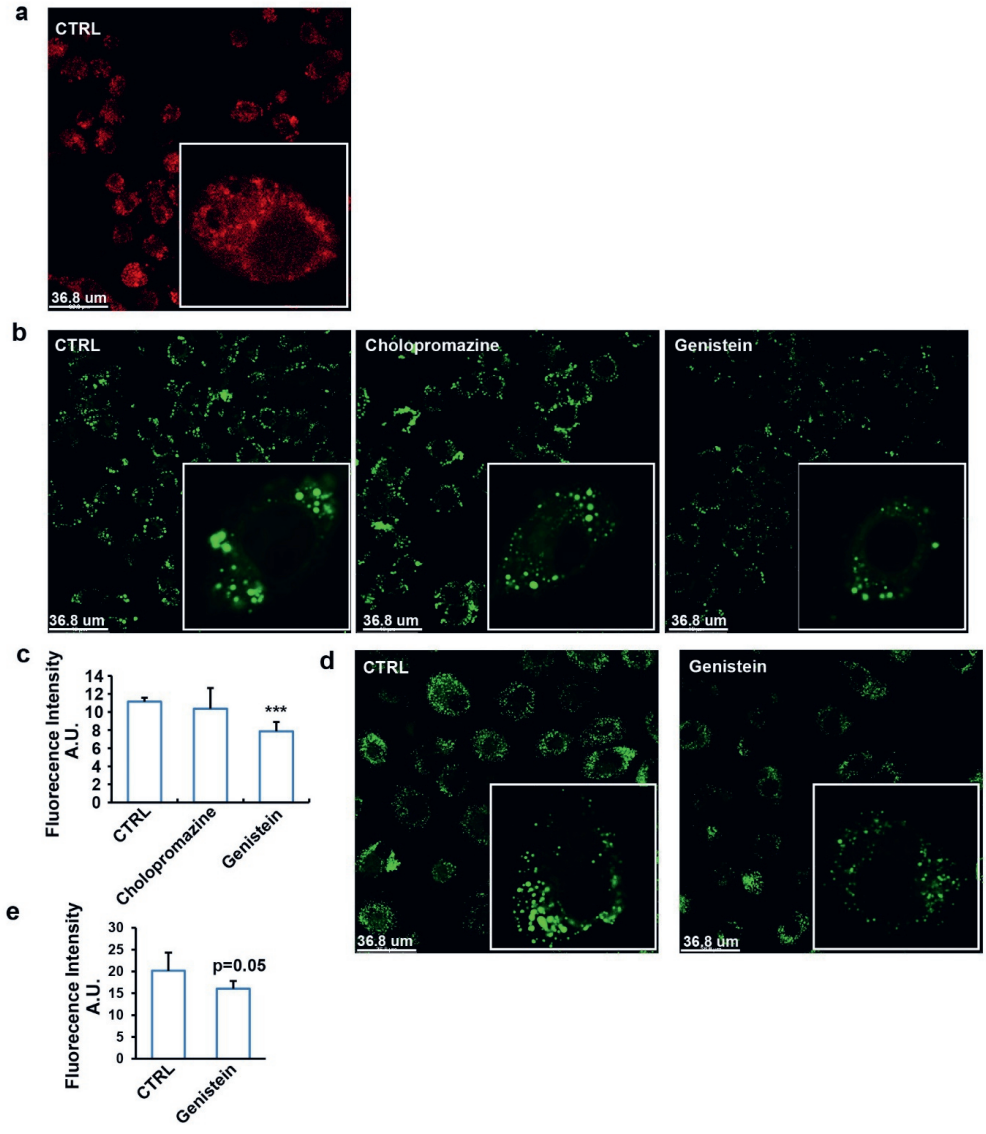

S9 Fig. CHYL-sized emulsion particles are taken up by macrophages via caveola-mediated endocytosis. (a) Early endosome staining of RAW 264.7 macrophages treated with 1 mM of CHYL-sized emulsion particles for 6 hours (n=6). (b) BODIPY 493/503 staining of RAW 264.7 macrophages treated with 1 mM CHYL-sized emulsion particles for 6 hours in the presence or absence of 10 µg/ml chlorpromazine or 200 µM Genistein

(n=6). (c) Mean fluorescence intensity quantified by Image J (n=6). (d) BODIPY 493/503 staining of human primary macrophages treated with 0.5 mM CHYL-sized emulsion particles for 6 hours in the presence or absence of 200 μM Genistein (n=6). (e) Mean fluorescence intensity quantified by Image J (n=3). The bar graphs were plotted as mean±SD. ***p<0.001.

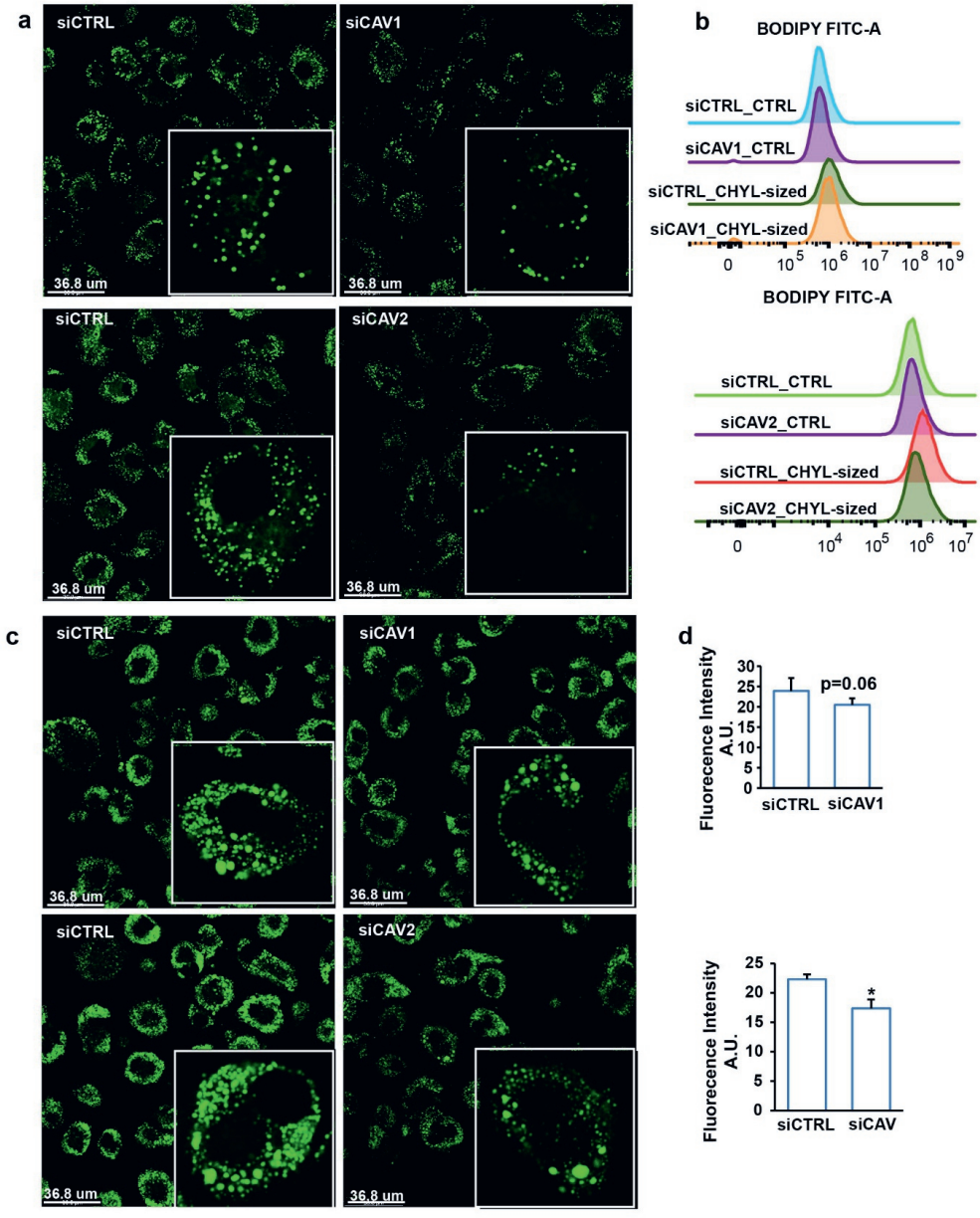

S10 Fig. Silencing of Caveolin 1 and 2 impairs uptake of CHYL-sized emulsion particles by macrophages. (a) BODIPY 493/503 staining of human macrophages treated with siCTRL, siCAV1,

or siCAV2 for 48 hours followed by treatment with 0.5 mM CHYL-sized emulsion particles for 6 hours (n=6). (b) Mean fluorescence intensity quantified by flow cytometry (n=3). (c) BODIPY 493/503 staining of human macrophages treated with siCTRL, siCAV1, or siCAV2 for 48 hours followed by treatment with 0.5 mM human plasma-isolated CHYL for 6 hours (n=6). (d) Mean fluorescence intensity quantified by Image J (n=4). The bar graphs were plotted as mean±SD. Asterisk indicates significantly different from control according to Student's t-test. *p<0.05.

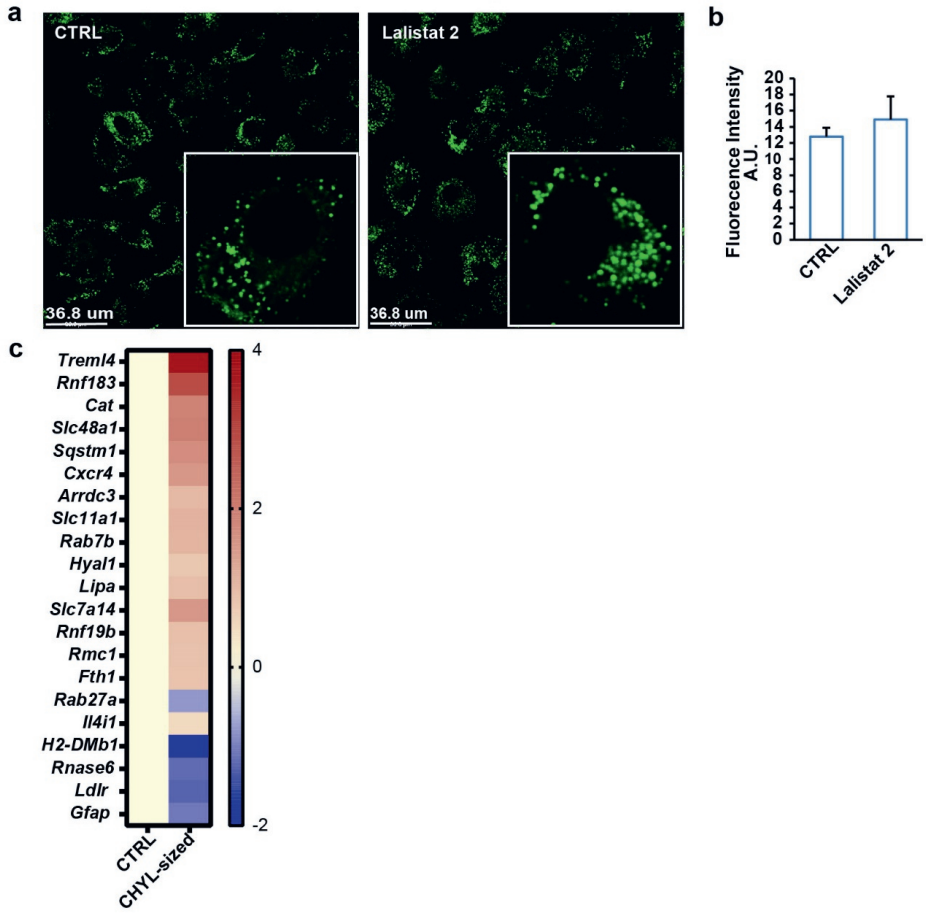

S11 Fig. TG in CHYL-sized emulsion particles are degraded by lysosomal acid lipase. (a) BODIPY 493/503 staining of human macrophages treated with 0.5 mM CHYL-sized emulsion particles for 6 hours in the presence or absence of 30 μM Lalistat 2 (n=6). (b) Mean fluorescence intensity quantified by Image J (n=6). (c) Heatmaps showing changes in the expression of genes involved in lysosome activity in RAW 264.7 macrophages treated with 0.5 mM CHYL-sized emulsion particles for 6 hours (p<0.01, SLR>1). Scale bar depicts signal log ratio (SLR).

CHARPTER 4

Impact of Milk fat on Postprandial Plasma Metabolomics: A Randomized Cross-over Human trial

Charlotte C.J.R. Michielsen, Lei Deng, Maaike den Os, Anouk L. Feitsma, Sander Kersten, Lydia A. Afman

To be submitted

ABSTRACT

Elevated postprandial lipids are associated with an increased risk of atherosclerotic cardiovascular disease. While numerous studies have examined the effect of different dietary fat sources on postprandial lipid levels, a more global analysis of postprandial plasma metabolites has been lacking. A common fat source in the Western-type diet is milk fat. Here, we aimed to investigate the acute effects of milk fat on postprandial metabolites, with a special interest in the specific properties of the milk fat globular membranes. To that end, a double-blind crossover human trial was performed in which 37 participants received in random order a high-fat shake composed of cream (CREAM), anhydrous milk fat (AMF), or vegetable fat (VEGE). Blood samples were drawn up to eight hours after consumption. At baseline, and 3 and 6 hours postprandially, plasma metabolites were quantified using NMR metabolomics. The changes in plasma fatty acids reflected the fatty acid composition of the shakes. AMF and CREAM consumption resulted in a faster postprandial increase and decrease in several fractions of VLDL and the inflammatory protein GlycA. Consumption of CREAM resulted in a more rapid increase in total triglycerides and branched chain amino acids at 3 hours and a faster decrease at 6 hours compared to the other shakes.

Overall, the consumption of shakes differing in fat sources led to altered postprandial dynamics of several metabolites. Specifically, consumption of milk fat and especially CREAM caused a steeper rise and more rapid return to baseline of numerous lipid metabolites and the inflammatory marker GlycA. Our study suggests a suppressive effect of milk fat and MFGM on postprandial lipemia and inflammation.

Keywords: Milk fat; Milk fat globule membrane; Accelerated postprandial metabolism; lipoproteins; Branched-chain fatty acids; Human study

INTRODUCTION

Triglycerides (TG) are one of the three major energy sources in our diet. After being digested in the intestine to monoglycerides and fatty acids, dietary TG are reassembled in the enterocytes and exported as part of chylomicrons. The chylomicrons are transported to peripheral tissues such as the heart, skeletal muscles, and adipose tissue, where the TG are hydrolyzed by the enzyme lipoprotein lipase (LPL). The entry of chylomicrons into the bloodstream is followed by an increase in very low-density lipoproteins (VLDL) due to competition for lipolysis by LPL between VLDL and chylomicrons. Accordingly, postprandial lipemia reflects an increase in both liver-derived VLDL and intestine-derived chylomicrons.

Elevated levels of TG after a meal are referred to as postprandial lipemia and are often caused by the consumption of high-fat meals in combination with a delay in LPL-mediated clearance of TG-rich lipoproteins. Postprandial lipemia is a risk factor for cardiovascular disease through its association with the production of cholesterol-rich and atherogenic VLDL and chylomicron remnant particles (Ginsberg et al., 2021)(Nakamura et al., 2016)(Botham and Wheeler-Jones, 2013). In addition, during prolonged postprandial lipemia, the exchange of core lipids between TG-rich lipoproteins and LDL and HDL is increased, resulting in the formation of highly atherogenic LDL particles and low levels of HDL.

Besides contributing to post-prandial lipidemia, consumption of high-fat meals can also raise postprandial plasma inflammation markers, including IL6 and IL1β (Meessen et al., 2019)(Lundman et al., 2007), as well as protein-related markers such as glycoprotein acetyls and C-reactive protein (Mazidi et al., 2021a)(Beisswenger et al., 2011). It is thought that postprandial inflammation is closely connected to postprandial lipemia (Klop et al., 2012), possibly because of the direct activation of immune cells by TG-rich lipoproteins (Alipour et al., 2008).

The consumption of dairy products has a long history, especially in western culture. In addition to providing high-quality protein and other valuable nutrients, such as calcium, potassium, and riboflavin, (whole) milk is also a major source of dietary fat. Because of its high content of saturated fatty acids, which have been shown to raise plasma levels of the atherogenic LDL, consumption of milk fat has been discouraged by numerous organizations. Indeed, the American Heart Association only recommends the consumption of low-fat or non-fat milk products (Lichtenstein et al., 2006). In recent years, however, several cohort studies have failed to find an association between the long-term consumption of (full fat) milk products and an increased risk of cardiovascular diseases (Elwood et al., 2010; Goldbohm et al., 2011; Soedamah-Muthu et al., 2011; Guo et al., 2017; Sellem et al., 2022).

These findings have led several leading nutrition scientists to argue that a policy to lower the intake of saturated fatty acids by reducing dairy consumption is likely to have limited or possibly negative effects on cardiometabolic disease risk (Astrup et al., 2019; Lovegrove and Givens, 2016). It has been recognized, though, that many uncertainties remain, and that detailed intervention studies on the metabolic impact of milk fat are needed. In particular, the possible importance of the food matrix has been emphasized (Astrup et al., 2019).

The food matrix of many dairy products such as butter, cream, and cheese is characterized by a unique encapsulation of the lipid components. Specifically, milk fat is composed of milk fat globules, which are composed of a neutral lipid core surrounded by so-called milk fat globule membranes (MFGM). These MFGM are enriched with glycerophospholipids and sphingolipids, especially sphingomyelin, phosphatidylcholine, and phosphatidylethanolamine. In addition, MFGM contain proteins, cholesterol, and other lipid species. Although several studies have pointed to positive health properties of MFGM in a variety of clinical and physiological contexts, including behavioral development, insulin sensitivity, and plasma lipid-lowering, our overall understanding of the health effects of MFGM is still very limited (Raza et al., 2021). In particular, to what extent MFGM may impact the postprandial lipemic response is unknown.

Here, we performed a randomized crossover human trial to compare the effect of a high-fat meal containing cream (containing MFGM), anhydrous milk fat (lacking MFGM), and a matched vegetable fat blend on postprandial plasma metabolites in overweight healthy adults.

MATERIALS AND METHODS

Study population

The study population consisted of 40 healthy men and women aged 40-70, with a BMI of 22-27 kg/m^2. Participants were excluded if they were suffering from any chronic metabolic, gastrointestinal, inflammatory, or another chronic disease, if they had (a history) of gastro-intestinal complaints or surgery, renal or hepatic malfunctioning (determined by ALAT, ASAT, and creatinine measurements), or if they were using any medication that may influence the study results by affecting intestinal motility. Additionally, participants were excluded if they were (wishing to become) pregnant, using soft/hard drugs, drank >14 alcohol consumptions/week, smoked, or had an unstable body weight. Lastly, participants were also excluded from the study if they were following a vegan diet or had food allergies to any of the products used in the study. All participants provided their written consent before participation in the study.

Study Design

The study was a double-blind, randomized acute intervention study (Figure 1a). Each participant visited the research unit three times, with a wash-out period of at least one week. During each study visit, the participants underwent a dietary lipid challenge test in the form of a high-fat shake. Participants were randomly assigned to a sequence of shakes.

The evening before each study visit, participants consumed a standardized meal (ad libitum) and were not allowed to eat or drink anything except water until the next day. The following day, participants appeared at the research unit in a fasted state for a minimum of 10 hours.

The study was conducted at Wageningen University, the Netherlands, from 07-01-2020 until 10-03-2020. The experimental protocol and procedures were approved by the Medical Ethical Committee of Wageningen University and were in accordance with the Helsinki declaration of 1975 as revised in 1983. The study was registered at clinicaltrials.gov as NCT04178681 'Postprandial Effects of Milk Fats (POEMI)'.

Dietary lipid challenge test

During each study visit, participants underwent a dietary lipid challenge test. In this test, participants consumed a liquid shake (0.5 L) containing 95 grams of fat from different sources (Table 1). Three types of fat were consumed during this study, namely: 100% vegetable fat blend (VEGE), 100% anhydrous milk fat (AMF, bovine milk fat), and 100% cream (CREAM) (AMF + milk fat globular membranes). The shakes were isocaloric and differed solely in their fat source, as the remaining constituents were identical. The fats were provided by FrieslandCampina in powder form (Table 2). The shakes were prepared by dissolving the fat powders in skimmed milk.

Table 1. Nutritional information on the high-fat shakes

	VEGE & AMF	CREAM
Powder (118 g)		
Fat (g)	95,0	95,0
Protein (g)	2,4	4,2
Lactose (g)	0,2	5,5
Glucose (g)	17,6	11,3
Milk +water		
Fat (g)	0,5	0,5
Protein (g)	18,5	17,0
Lactose (g)	24,5	22,5
Glucose (g)	0,0	3,2
Total		
Fat (g)	95,5	95,5
Protein (g)	20,9	21,2
Carbs (g)	42,3	42,5
Total Energy (KJ)	**4748**	

The shakes were provided to the participants in a tinted cup with an opaque straw to hide their content. Participants had to consume the shake within ten minutes and were not allowed to eat or drink anything except for water (ad libitum) unless the last blood sample was drawn. During that time frame, participants were also not allowed to engage in physical exercise.

Table 2. The ingredient list of the three different fat powders

Fat powder	Ingredients
Vegetable blend (VEGE)	Vegetable fat blend, glucose syrup, milk protein (caseinate), stabilizer (E451i: Pentasodium triphosphate), free-flowing agent (E551: silicon dioxide)
Anhydrous milk fat (AMF)	Anhydrous milk fat, glucose syrup, milk protein (caseinate), stabilizer (E451i: Pentasodium triphosphate), free-flowing agent (E551: silicon dioxide)
CREAM (AMF+MFGM)	Cream, milk protein (caseinate), glucose syrup, stabilizer (E451i: Pentasodium triphosphate), free-flowing agent (E551: silicon dioxide)

Blood collection

During each study visit, a catheter cannula was inserted in the participant's antecubital vein. Thirty minutes after the cannula insertion, blood was drawn from the catheter cannula for the baseline measurement (t=0). After this baseline measurement, participants consumed a high-fat shake. Subsequently, blood was drawn at t=1, 2, 3, 4, 5, 6, 7, and 8 hours after consumption. All EDTA blood samples were stored at -80°C until further analysis.

Metabolomics

Blood samples collected at 0 hours (baseline), 3 hours, and 6 hours were processed by Nightingale Health. This platform performs high-throughput proton Nuclear Magnetic Resonance (NMR). Details on the analysis have been described previously (Soininen et al., 2015)(Würtz et al., 2017). The analysis allows for simultaneous detection and quantification of 249 metabolites and their corresponding ratios within one experimental set-up. These include lipoprotein subclasses and constituents, their relative ratios, lipids, fatty acids, amino acids, ketone bodies, glycolysis-related metabolites, and various other low-molecular-weight metabolites.

Statistical analysis

Statistical analyses of the metabolites were performed on log2-transformed data. Differences in the postprandial responses between the three different shakes from the dietary lipid challenge test were

analyzed using linear mixed models for repeated measures. Participants were specified as subjects. Shake and time were specified as repeated measures. The delta values (t=3h-t=0h and t=6h-t=0h) of the 249 metabolites were selected as the dependent variable in the model. Shake, time, and the interaction between shake*time were included as fixed effects. A first-order autoregressive covariance structure was selected for the model. An additional LSD posthoc test was performed on metabolites with a significant shake*time effect to identify differences between the shakes and specify shake*time effects at specific time points. The linear mixed model's findings were corrected for multiple testing using Benjamini-Hochberg's FDR correction (FDR p-value 0.05) (Benjamini and Hochberg, 1995). All statistical analyses were performed using IBM® SPSS® Statistics (version 28.0.1.0). Figures were created in GraphPad Prism (Version 9.3.1) and Cytoscape (version 3.9.1).

RESULTS

Participant characteristics

Of the 40 participants that entered this study, 37 completed the study. One participant dropped out after the first study visit, and two other participants dropped out after the second study visit (Figure 1A). Data from the dropouts were still included in the analysis. The participant characteristics of the 40 participants can be found in Table 3.

Table 3. Participant characteristics of the 40 included participants in this study.

Data are presented as mean ± standard deviation.

Characteristic	
Gender (m/f)	9/31
Age (years)	57.3 ± 8.0
Weight (kg)	71.5 ± 8.5
Height (cm)	172.2 ± 7.7
BMI (kg/m^2)	24.1 ± 1.7
Waist circumference (cm)	
Men	92.2 ± 5.9
Women	81.8 ± 6.2
Hip circumference (cm)	
Men	102.6 ± 4.6
Women	102.2 ± 6.0
WHR	
Men	0.90 ± 0.05
Women	0.80 ± 0.05
Hb (mmol/L)	8.4 ± 0.6
ALAT (uL)	24.7 ± 11.8
ASAT (uL)	21.5 ± 7.3
Creatinine (umol/L)	71.6 ± 11.1

Abbreviations: alanine aminotransferase (ALAT), aspartate aminotransferase (ASAT), body mass index (BMI), hemoglobin (Hb), waist-hip ratio (WHR)

AMF, CREAM and VEGE differentially impact postprandial metabolites

The focus of the analysis was on the differential effect of the 3 fat sources on postprandial plasma metabolite levels (between shake comparison). Of the 249 metabolites measured in total, 102 metabolites were differentially changed postprandially by the three shakes. Posthoc tests were

performed to identify the differences between shakes at a specific time point. At 3 hours postprandially, 37 metabolites were significantly different between VEGE and AMF, 39 metabolites were significantly different between VEGE and CREAM, and no metabolites were significantly different between AMF and CREAM. At 6 hours postprandially, 41, 29, and 8 metabolites were identified as significantly different for the above comparisons, respectively (Figure 1b).

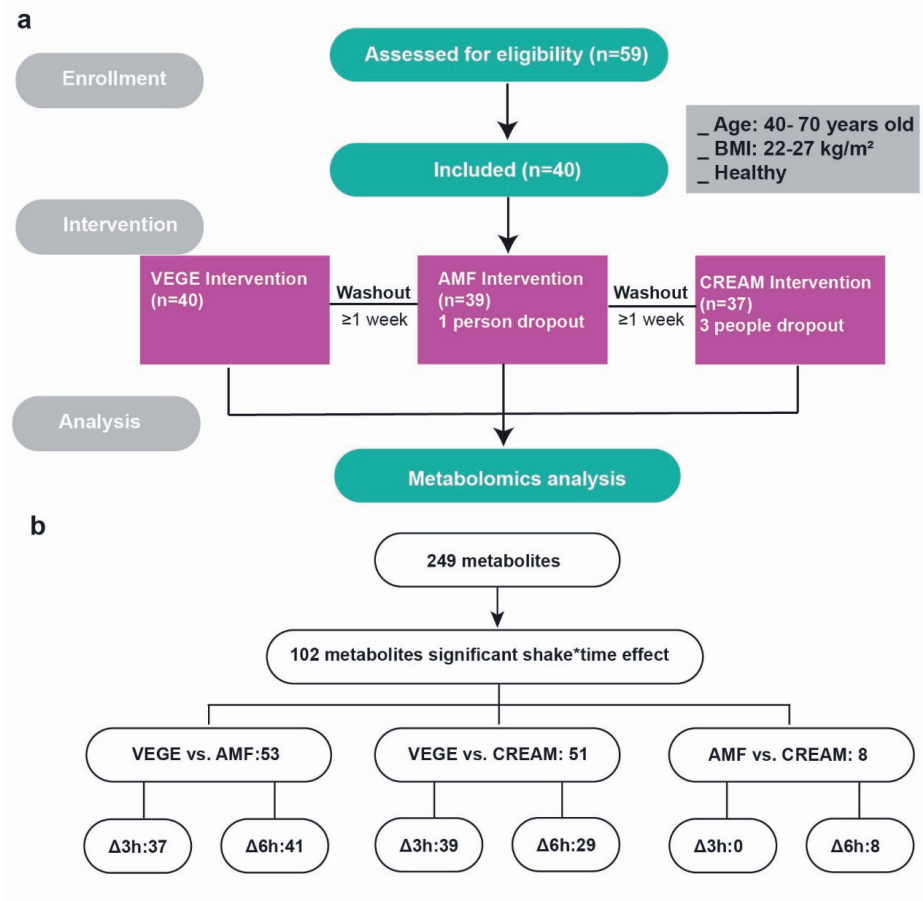

Figure 1. Differential effects of interventions on postprandial metabolites. Flowchart of a) the study design and b) the number of metabolites significantly changed in the interventions. Shake*time effect was tested using linear mixed models for repeated measures. Significant findings were corrected for multiple testing using FDR-correction (FDR p-value<0.05). A LSD posthoc test was performed on metabolites with a significant FDR p-value for shake*time to identify differences between the shakes and shake*time effects at specific time points.

Postprandial fatty acids reflect the dietary fat composition

The postprandial levels of individual fatty acids in the total lipid fraction are tightly linked to the lipid composition of the shake. Significant differences between shakes were found in the postprandial fatty acid responses for the degree of unsaturation, the ratio of polyunsaturated fatty acids to monounsaturated fatty acids, and the levels of polyunsaturated fatty acids, omega-6 fatty acids, linoleic acid, monounsaturated fatty acids, and saturated fatty acids (Figure 2 &Table S1).

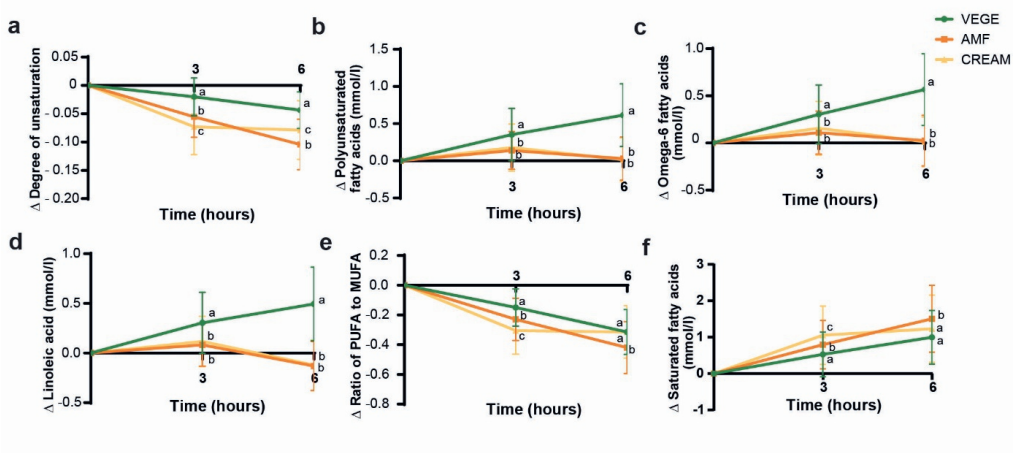

Figure 2. Postprandial fatty acids change after the consumption of three interventions. a) Degree of unsaturation. Shake*time effect in linear mixed models analysis (FDR p-value = 0.003). Significant difference between VEGE and AMF ($p<0.001$), and VEGE and CREAM ($p<0.001$). b) Polyunsaturated fatty acids (mmol/l). Shake*time effect in linear mixed models analysis (FDR p-value = 0.007). Significant difference between VEGE and AMF ($p<0.001$), and VEGE and CREAM ($p<0.001$). c) Omega-6 fatty acids (mmol/l). Shake*time effect in linear mixed models analysis (FDR p-value = 0.005). Significant difference between VEGE and AMF ($p<0.001$), and VEGE and CREAM ($p<0.001$). d) Linoleic acid (mmol/l). Shake*time effect in linear mixed models analysis (FDR p-value = 0.002). Significant difference between VEGE and AMF ($p<0.001$), and VEGE and CREAM ($p<0.001$). e) PUFA.MUFA ratio. Shake*time effect in linear mixed models analysis (FDR p-value = 0.003). Significant difference between VEGE and AMF ($p<0.001$), and VEGE and CREAM ($p<0.001$). f) Saturated fatty acids (mmol/l). Shake*time effect in linear mixed models analysis (FDR p-value = 0.010). Significant difference between VEGE and AMF ($p<0.001$), and VEGE and CREAM ($p<0.001$). a, b, c indicate significant differences between shakes for shake*time effect at specific timepoints. All values represent mean + SD.

The postprandial increase in poly-unsaturated fatty acids, omega-6 fatty acids, and linoleic acid was significantly attenuated in the AMF and CREAM groups compared to VEGE. Conversely, at 3 hours postprandially, saturated fatty acid levels went up more strongly in the AMF and CREAM groups

compared to VEGE, which was abolished for CREAM at 6 hours postprandially. Consistent with these data, at 3 and 6 hours after consumption of the shake, the degree of fatty acid unsaturation was decreased to a stronger extent in the AMF and CREAM groups as compared to VEGE. The significantly higher postprandial concentration of unsaturated fatty acids but not saturated fatty acids after consumption of VEGE compared to AMF and CREAM matches with the higher concentration of unsaturated fatty acids in the VEGE shake compared to the other shakes.

Tendency towards a smaller increase in extra large lipoprotein-lipids after consumption of CREAM

Chylomicrons contain dietary lipids and account for a major portion of postprandial lipemia. We analyzed extra large VLDL- and chylomicron-lipids, including the general concentration, total lipids, total phospholipds, free cholesterol, total cholesterol, and cholesterol ester (Figure 3a-3g, Table S1). No significant differences in postprandial levels of these various lipid fractions were observed between the shakes. Nevertheless, at 6 hours postprandially, there was a tendency towards lower levels for all lipid fractions after the CREAM shake compared to AMF and VEGE.

Total triglycerides rose significantly faster after CREAM compared to AMF and VEGE but also returned more quickly towards baseline (Figure 3h). Since chylomicron-sized lipids were not statistically different between the shakes, these data hint at a differential effect of the shakes on other lipoprotein fractions.

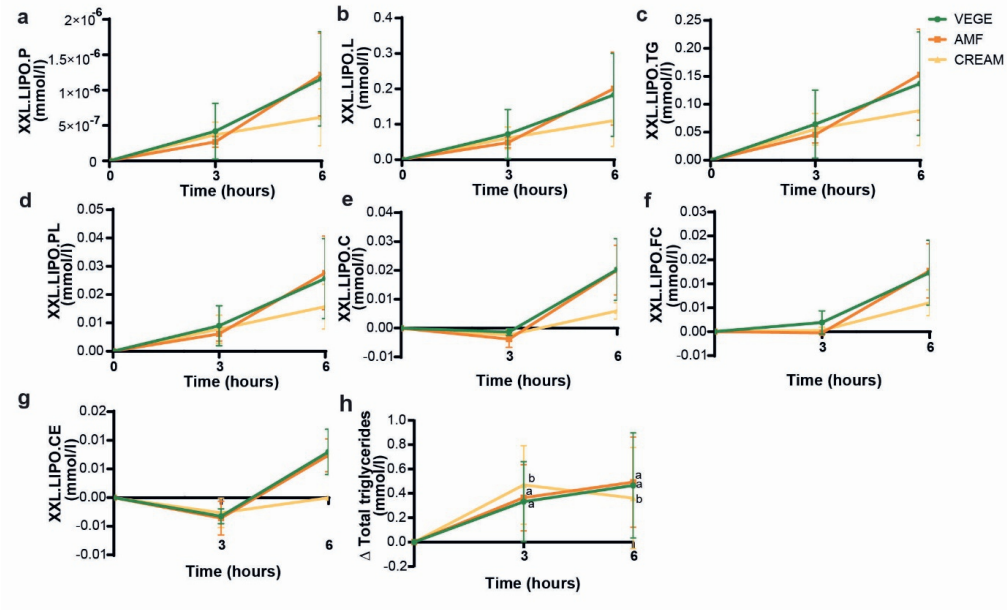

Figure 3. Delta postprandial response of XXL.LIPO. consitutuents. a) General concentration (mmol/l). b) Total lipids (mmol/l). c) Total triglycerides(mmol/l). d) Total phospholipids (mmol/l). e) Free cholesterol (mmol/l). f) Total cholesterol (mmol/l). g) cholesterol esters of extremely large lipoproteins (mmol/l). h) total triglycerides in plasma. Total triglycerides (mmol/l). Shake*time effect in linear mixed models analysis (FDR p-value = 0.008). At T=3 h, Significant difference between VEGE and CREAM (p=0.004), and AMF and CREAM (p=0.029). At T=6 h, Significant difference between VEGE and CREAM (p=0.005), and AMF and CREAM (p<0.001). a, b, c indicate significant differences between shakes for shake*time effect at specific time points. All values represent mean + SD.

VLDL-lipids more rapidly return to baseline after consumption of AMF and CREAM

Overall, most of the postprandial differences between the shakes concerned the VLDL fractions and the LDL fractions (Figure 4 & Table S1). Compared to VEGE, consumption of AMF and CREAM resulted in a significantly more rapid postprandial reduction in cholesterol and cholesterol esters in the very large and large VLDL fractions after an initial similar increase (Figure 4a-4d). The effects on the total lipids in medium VLDL of these interventions were also in line with this (Figure 4e). The consumption of AMF and CREAM significantly decreased cholesterol esters in medium VLDL compared to VEGE. However, whereas cholesterol esters in medium VLDL declined continuously after AMF, they showed a tendency towards a return to baseline after CREAM (Figure 4f).

Concerning LDL, AMF and CREAM resulted in a significantly higher increase at 3 hours postprandially compared to VEGE (Figure 4g-4h).

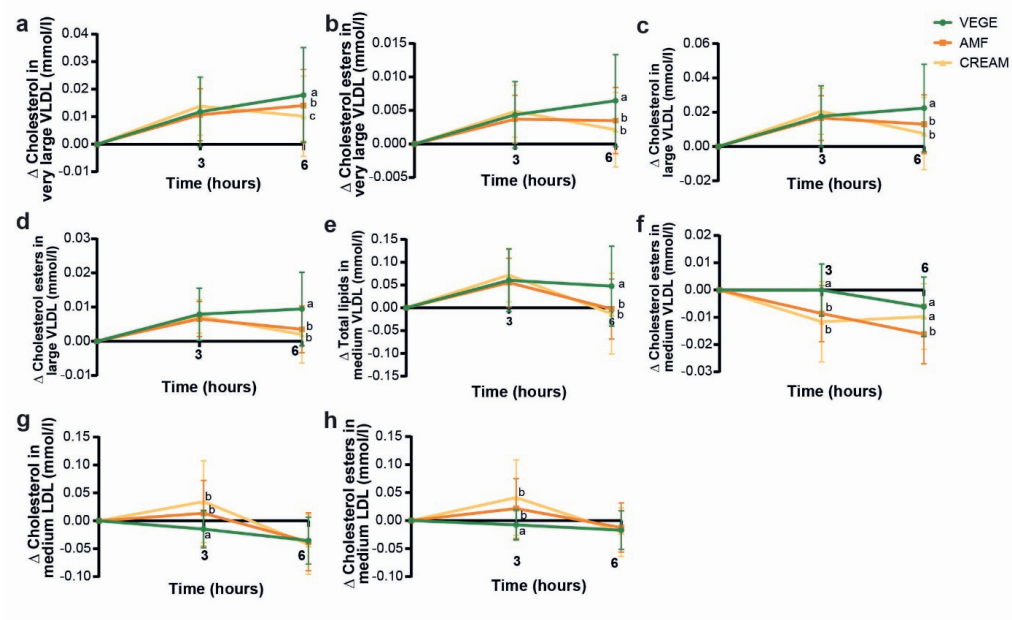

Figure 4. Delta postprandial response of (V)LDL constituents. a) Cholesterol in very large VLDL (mmol/l). Shake*time effect in linear mixed models analysis (FDR p-value = 0.011). Significant difference between VEGE and AMF (p=0.038), and VEGE and CREAM (p=0.034). b) Cholesterol esters in very large VLDL (mmol/l). Shake*time effect in linear mixed models analysis (FDR p-value = 0.011). Significant difference between VEGE and AMF (p=0.001), and VEGE and CREAM (p=0.002). c) Cholesterol in large VLDL (mmol/l). Shake*time effect in linear mixed models analysis (FDR p-value = 0.010). Significant difference between VEGE and AMF (p=0.004), and VEGE and CREAM (p=0.005). d) Cholesterol esters in large VLDL (mmol/l). Shake*time effect in linear mixed models analysis (FDR p-value = 0.014). Significant difference between VEGE and AMF (p<0.001), and VEGE and CREAM (p<0.001). e) Total lipids in medium VLDL (mmol/l). Shake*time effect in linear mixed models analysis (FDR p-value = 0.011). Significant difference between VEGE and AMF (p=0.001), and VEGE and CREAM (p=0.008). f) Cholesterol esters in medium VLDL (mmol/l). Shake*time effect in linear mixed models analysis (FDR p-value = 0.020). Significant difference between VEGE and AMF (p<0.001), and VEGE and CREAM (p<0.001). g) Cholesterol in medium LDL (mmol/l). Shake*time effect in linear mixed models analysis (FDR p-value = 0.017). Significant difference between VEGE and CREAM (p=0.043). h) Cholesterol esters in medium LDL (mmol/l). Shake*time effect in linear mixed models analysis (FDR p-value = 0.013). Significant difference between 100% VEG and CREAM (p=0.012). a, b, c indicate significant differences between shakes for shake*time effect at specific timepoints. a, b, c indicate significant differences between shakes for shake*time effect at specific timepoints. All values represent mean + SD.

CREAM consumption led to more rapid postprandial changes in the level of branched-chain amino acids

Significant differences in postprandial responses of total-branched chain amino acids, isoleucine, leucine, and valine were found between the shakes (Table S1). Postprandial levels of branched-chain amino acids significantly increased 3 hours after CREAM consumption compared to AMFand VEGE. This increase was followed by a more pronounced decrease in plasma branched-chain amino acids 6 hours after CREAM consumption (Figure 5a). The postprandial changes in plasma leucine after consumption of the three shakes followed the same tendency (Figure 5b).

Concerning the plasma levels of the other amino acids, significant differences in postprandial responses were observed between the shakes (Table S1). Compared to VEGE and AMF, CREAM consumption resulted in a significantly lower postprandial concentration of plasma phenylamine (Figure 5c) and glutamine (Figure 5d) after 6 hours.

AMF and CREAM consumption led to a more rapid decline in the postprandial increase of the inflammatory marker GlycA

GlycA is a novel biomarker of systematic inflammation and has been associated with many metabolic disorders and diseases (Ballout and Remaley, 2020; Connelly et al., 2016; Mokkala et al., 2020). Interestingly, the postprandial response of GlycA differed significantly between the three shakes (Table S1). Specifically, CREAM and AMF consumption resulted in a lower level at 6 hours postprandially compared to VEGE (Figure 5e).

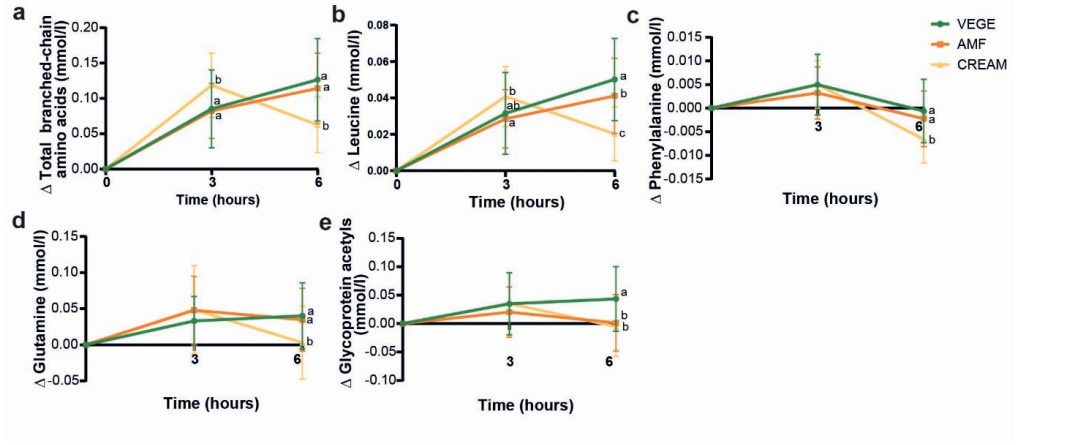

Figure 5. Delta postprandial response of amino acids and GlycA. a) Phenylalanine. Shake*time effect in linear mixed models analysis (FDR p-value = 0.010). Significant difference between VEGE and AMF

(p=0.032), and VEGE and CREAM (p<0.001). b) Glutamine. Shake*time effect in linear mixed models analysis (FDR p-value = 0.015). Significant difference between AMF and CREAM (p=0.026). c) Total branched-chain amino acids (mmol/l) Shake*time effect in linear mixed models analysis (FDR p-value = 0.001). Significant difference between VEGE and CREAM (p=0.018). d) Leucine (mmol/l). Shake*time effect in linear mixed models analysis (FDR p-value = 0.001). Significant difference between VEGE and AMF (p=0.026), and VEGE and CREAM (p<0.001). e) Delta postprandial response of glycoprotein acetyls (GlycA). All values represent mean + SD. Shake*time effect in linear mixed models analysis (FDR p-value = 0.019). Significant difference between VEGE and AMF (p<0.001). and VEGE and CREAM (p=0.003). a, b, c indicate significant differences between shakes for shake*time effect at specific timepoints. All values represent mean + SD.

DISCUSSION

This study aimed to examine the acute impact of consumption of bovine milk fats with and without milk fat globular membranes on the postprandial plasma metabolomic response, using blended vegetable fat as a reference.

With the use of targeted, quantitative NMR-based metabolomics, 102 plasma metabolites were identified that showed a significantly different postprandially response between fat sources over time. In general, we observed a more pronounced increase at 3 hours and a more pronounced subsequent decrease at 6 hours of most VLDL and LDL fractions following AMF and CREAM consumption as compared to VEGE. A similar steeper rise and more rapid return to baseline were observed for total plasma TG and BCAA following CREAM consumption as compared to AMF and VEGE. Finally, the postprandial increase in plasma GlycA more quickly returned to baseline after AMF and CREAM consumption as compared to VEGE.

The postprandial plasma metabolomic responses were much more similar between CREAM and AMF than between VEGE and dairy-based fats. Such a result could be expected considering that the fatty acid composition of CREAM and AMF are nearly identical. Nonetheless, some differences were observed between CREAM and AMF. As indicated above, plasma TG and BCAA went up and down more quickly following CREAM consumption as compared to AMF and VEGE, which thus might be explained by the MFGM. It is thought that MFGM enhances dietary TG digestion by delivering the TG to the gastric phase earlier, resulting in faster TG absorption (Bourlieu and Michalski, 2015). Similar findings were obtained by Baumgartner et al (Baumgartner et al., 2017). In their cross-over study, healthy young men received a test drink with either a commercially available, standard infant milk formula or with larger phospholipid-coated fat droplets to mimic the human milk fat globule. Similar to our findings, the experimental MFGM drink led to a more rapid increase in postprandial TG and a faster return to baseline, with a peak at three hours after consumption. Rodent studies have suggested that especially the polar lipids in the MFGM might play an important role in modulating postprandial lipemia (Lecomte et al., 2015). In addition, the lipid components of the MFGM might be responsible for the long-term benefits of human milk on obesity (Oosting et al., 2012a). Several studies have found that the provision of mice with phospholipid-coated lipid droplets during early postnatal life reduces adiposity and insulin resistance following exposure to a Western-type diet, suggesting that early exposure to MFGM positively influences obesity and metabolic health (Baars et al., 2016; Kodde et al., 2017; Oosting et al., 2012b, 2014).

It is well established that elevated post-prandial lipemia is associated with an increased risk of cardiovascular disease (Desmarchelier et al., 2019). Post-prandial hyperlipidemia is primarily the consequence of impaired plasma TG clearance due to reduced activity of LPL. The connection between LPL activity and cardiovascular disease is supported by the observation that the carrier status of a gain-of-function variant in the LPL gene is associated with a decreased risk of coronary artery disease (Wang et al., 2021). Although we only performed metabolomics at three time points, our data suggest that the postprandial TG exposure is shorter after CREAM compared to AMF and VEGE. Currently, to what extent changes in the kinetics of the postprandial TG response may be associated with altered risk of coronary artery disease is unclear. However, since especially prolonged post-prandial lipidemia is associated with increased levels of atherogenic lipoproteins, it can be hypothesized that the faster kinetics of postprandial TG after CREAM may be beneficial for cardiovascular risk.

Interestingly, CREAM also resulted in a faster return to baseline of plasma amino acids, especially the BCAA, mimicking the pattern for total TG. The faster kinetics of plasma BCAA could theoretically be explained by more rapid protein digestion, resulting in quicker entry of amino acids into the circulation. Alternatively, it may reflect a link between lipid and amino acid metabolism. It has been suggested that abnormal lipid metabolism may impair BCAA catabolism, thereby raising levels in the blood among old men (Kujala et al., 2016a). Recent studies have found an association between plasma BCAA levels and metabolic disturbances (Kujala et al., 2016b), including insulin resistance, obesity, and type 2 diabetes (Newgard, 2012) (Huffman et al., 2009; Ruiz-Canela et al., 2016; De Simone et al., 2013).

Remarkably, the concentration of the inflammation marker glycoprotein acetyls (GlycA) was almost back to baseline at 6 hours after CREAM and AMF consumption while it was still elevated after VEGE. GlycA is specifically detected by NMR spectroscopy and reflects the abundance of glycan groups of acute-phase glycoproteins. Its measurement may complement or provide advantages over existing clinical markers of systemic inflammation such as CRP (Otvos et al., 2015). In a recent study by Mazidi et al. (Mazidi et al., 2021a), the postprandial TG and GlycA responses were measured at multiple intervals after sequential mixed-nutrient meals (0 h and 4 h) in 1002 healthy adults aged 18–65 y, showing a strong association between postprandial TG and postprandial GlycA levels. In addition, a strong link was found between enhanced postprandial GlycA responses and a higher predicted cardiovascular disease risk in obese people (using the atherosclerotic disease risk score) (Mazidi et al., 2021b). The smaller overall increase in GlycA after CREAM and AMF consumption

compared to VEGE may reflect reduced postprandial inflammation in response to milk fat compared to vegetable fat. It can be speculated that the lower increment in GlycA after CREAM and AMF is directly coupled to the faster kinetics of postprandial lipemia in these groups.

Our study also has limitations. First, the metabolomics analysis was only performed at baseline and 3 and 6 hours postprandially. The use of additional time points would help to get a better overview of the kinetics of postprandial metabolites. Second, our study only looked at the acute effect of the different fat sources. Whether a similar result would be obtained after chronic consumption of CREAM, AMF, and VEGE is unclear. Third, to gain a better understanding of the effects of the different shakes on postprandial inflammation, it would have been worthwhile to assess selected plasma cytokines. However, it should be noted that plasma levels of most cytokines are extremely low in healthy people and therefore difficult to measure.

To conclude, our study reveals differences in postprandial dynamics in several metabolites after consumption of shakes varying in the fat source. Specifically, consumption of milk fat and especially CREAM resulted in a steeper rise and more rapid return to baseline of numerous lipid metabolites as well as the inflammatory marker GlycA. Overall, our study suggests a suppressive effect of milk fat and MFGM on postprandial lipemia and inflammation.

REFERENCE

Alipour, A., Van Oostrom, A.J.H.H.M., Izraeljan, A., Verseyden, C., Collins, J.M., Frayn, K.N., Plokker, T.W.M., Elte, J.W.F., and Cabezas, M.C. (2008). Leukocyte activation by triglyceride-rich lipoproteins. Arterioscler. Thromb. Vasc. Biol. *28*, 792–797.

Astrup, A., Bertram, H.C.S., Bonjour, J.P., De Groot, L.C.P., De Oliveira Otto, M.C., Feeney, E.L., Garg, M.L., Givens, I., Kok, F.J., Krauss, R.M., et al. (2019). WHO draft guidelines on dietary saturated and trans fatty acids: Time for a new approach? BMJ *366*.

Baars, A., Oosting, A., Engels, E., Kegler, D., Kodde, A., Schipper, L., Verkade, H.J., and Van Der Beek, E.M. (2016). Milk fat globule membrane coating of large lipid droplets in the diet of young mice prevents body fat accumulation in adulthood. Br. J. Nutr. *115*, 1930–1937.

Ballout, R.A., and Remaley, A.T. (2020). GlycA: A New Biomarker for Systemic Inflammation and Cardiovascular Disease (CVD) Risk Assessment. J. Lab. Precis. Med. *5*, 17–17.

Baumgartner, S., van de Heijning, B.J.M., Acton, D., and Mensink, R.P. (2017). Infant milk fat droplet size and coating affect postprandial responses in healthy adult men: a proof-of-concept study. Eur. J. Clin. Nutr. *71*, 1108–1113.

Beisswenger, P.J., Brown, W. V., Ceriello, A., Le, N.A., Goldberg, R.B., Cooke, J.P., Robbins, D.C., Sarwat, S., Yuan, H., Jones, C.A., et al. (2011). Meal-induced increases in C-reactive protein, interleukin-6 and tumour necrosis factorα are attenuated by prandial+basal insulin in patients with Type2 diabetes. Diabet. Med. *28*, 1088–1095.

Benjamini, Y., and Hochberg, Y. (1995). Controlling the False Discovery Rate: A Practical and Powerful Approach to Multiple Testing. J. R. Stat. Soc. Ser. B *57*, 289–300.

Bohl, M., Bjørnshave, A., Rasmussen, K. V., Schioldan, A.G., Amer, B., Larsen, M.K., Dalsgaard, T.K., Holst, J.J., Herrmann, A., O'Neill, S., et al. (2015). Dairy proteins, dairy lipids, and postprandial lipemia in persons with abdominal obesity (DairyHealth): A 12-wk, randomized, parallel-controlled, double-blinded, diet intervention study. Am. J. Clin. Nutr. *101*, 870–878.

Bordoni, A., Danesi, F., Dardevet, D., Dupont, D., Fernandez, A.S., Gille, D., Nunes dos Santos, C., Pinto, P., Re, R., Rémond, D., et al. (2017). Dairy products and inflammation: A review of the clinical evidence. Crit. Rev. Food Sci. Nutr. *57*, 2497–2525.

Botham, K.M., and Wheeler-Jones, C.P.D. (2013). Postprandial lipoproteins and the molecular

regulation of vascular homeostasis. Prog. Lipid Res. *52*, 446–464.

Bourlieu, C., and Michalski, M.C. (2015). Structure-function relationship of the milk fat globule. Curr. Opin. Clin. Nutr. Metab. Care *18*, 118–127.

Connelly, M.A., Gruppen, E.G., Wolak-Dinsmore, J., Matyus, S.P., Riphagen, I.J., Shalaurova, I., Bakker, S.J.L., Otvos, J.D., and Dullaart, R.P.F. (2016). GlycA, a marker of acute phase glycoproteins, and the risk of incident type 2 diabetes mellitus: PREVEND study. Clin. Chim. Acta *452*, 10–17.

Desmarchelier, C., Borel, P., Lairon, D., Maraninchi, M., and Valéro, R. (2019). Effect of nutrient and micronutrient intake on chylomicron production and postprandial lipemia. Nutrients *11*.

Elwood, P.C., Pickering, J.E., Ian Givens, D., and Gallacher, J.E. (2010). The Consumption of Milk and Dairy Foods and the Incidence of Vascular Disease and Diabetes: An Overview of the Evidence. Lipids *45*, 925.

Ginsberg, H.N., Packard, C.J., Chapman, M.J., Borén, J., Aguilar-Salinas, C.A., Averna, M., Ference, B.A., Gaudet, D., Hegele, R.A., Kersten, S., et al. (2021). Triglyceride-rich lipoproteins and their remnants: Metabolic insights, role in atherosclerotic cardiovascular disease, and emerging therapeutic strategies-a consensus statement from the European Atherosclerosis Society. Eur. Heart J. *42*, 4791–4806.

Goldbohm, R.A., Chorus, A.M.J., Garre, F.G., Schouten, L.J., and Van Den Brandt, P.A. (2011). Dairy consumption and 10-y total and cardiovascular mortality: a prospective cohort study in the Netherlands. Am. J. Clin. Nutr. *93*, 615–627.

Guo, J., Astrup, A., Lovegrove, J.A., Gijsbers, L., Givens, D.I., and Soedamah-Muthu, S.S. (2017). Milk and dairy consumption and risk of cardiovascular diseases and all-cause mortality: dose–response meta-analysis of prospective cohort studies. Eur. J. Epidemiol. *32*, 269–287.

Huffman, K.M., Shah, S.H., Stevens, R.D., Bain, J.R., Muehlbauer, M., Slentz, C.A., Tanner, C.J., Kuchibhatla, M., Houmard, J.A., Newgard, C.B., et al. (2009). Relationships between circulating metabolic intermediates and insulin action in overweight to obese, inactive men and women. Diabetes Care *32*, 1678–1683.

Karupaiah, T., Tan, C.H., Chinna, K., and Sundram, K. (2011). The chain length of dietary saturated fatty acids affects human postprandial lipemia. J. Am. Coll. Nutr. *30*, 511–521.

Klop, B., Proctor, S.D., Mamo, J.C., Botham, K.M., and Castro Cabezas, M. (2012). Understanding

postprandial inflammation and its relationship to lifestyle behaviour and metabolic diseases. Int. J. Vasc. Med. *2012*, 11.

Kodde, A., Van Der Beek, E.M., Phielix, E., Engels, E., Schipper, L., and Oosting, A. (2017). Supramolecular structure of dietary fat in early life modulates expression of markers for mitochondrial content and capacity in adipose tissue of adult mice. Nutr. Metab. *14*, 1–13.

Kujala, U.M., Peltonen, M., Laine, M.K., Kaprio, J., Heinonen, O.J., Sundvall, J., Eriksson, J.G., Jula, A., Sarna, S., and Kainulainen, H. (2016a). Branched-chain amino acid levels are related with surrogates of disturbed lipid metabolism among older men. Front. Med. *3*, 57.

Kujala, U.M., Peltonen, M., Laine, M.K., Kaprio, J., Heinonen, O.J., Sundvall, J., Eriksson, J.G., Jula, A., Sarna, S., and Kainulainen, H. (2016b). Branched-chain amino acid levels are related with surrogates of disturbed lipid metabolism among older men. Front. Med. *3*, 57.

Lecomte, M., Bourlieu, C., Meugnier, E., Penhoat, A., Cheillan, D., Pineau, G., Loizon, E., Trauchessec, M., Claude, M., Ménard, O., et al. (2015). Milk polar lipids affect in vitro digestive lipolysis and postprandial lipid metabolism in mice. J. Nutr. *145*, 1770–1777.

Lichtenstein, A.H., Appel, L.J., Brands, M., Carnethon, M., Daniels, S., Franch, H.A., Franklin, B., Kris-Etherton, P., Harris, W.S., Howard, B., et al. (2006). Diet and lifestyle recommendations revision 2006: A scientific statement from the American heart association nutrition committee. Circulation *114*, 82–96.

Lovegrove, J.A., and Givens, D.I. (2016). Dairy food products: Good or bad for cardiometabolic disease? Nutr. Res. Rev. *29*, 249–267.

Lundman, P., Boquist, S., Samnegård, A., Bennermo, M., Held, C., Ericsson, C.G., Silveira, A., Hamsten, A., and Tornvall, P. (2007). A high-fat meal is accompanied by increased plasma interleukin-6 concentrations. Nutr. Metab. Cardiovasc. Dis. *17*, 195–202.

Mazidi, M., Valdes, A.M., Ordovas, J.M., Hall, W.L., Pujol, J.C., Wolf, J., Hadjigeorgiou, G., Segata, N., Sattar, N., Koivula, R., et al. (2021a). Meal-induced inflammation: postprandial insights from the Personalised REsponses to DIetary Composition Trial (PREDICT) study in 1000 participants. Am. J. Clin. Nutr. *114*, 1028–1038.

Mazidi, M., Valdes, A.M., Ordovas, J.M., Hall, W.L., Pujol, J.C., Wolf, J., Hadjigeorgiou, G., Segata, N., Sattar, N., Koivula, R., et al. (2021b). Meal-induced inflammation: postprandial insights from the Personalised REsponses to DIetary Composition Trial (PREDICT) study in 1000 participants. Am. J.

Clin. Nutr. *114*, 1028–1038.

Meessen, E.C.E., Warmbrunn, M. V., Nieuwdorp, M., and Soeters, M.R. (2019). Human postprandial nutrient metabolism and low-grade inflammation: A narrative review. Nutrients *11*.

Mokkala, K., Houttu, N., Koivuniemi, E., Sørensen, N., Nielsen, H.B., and Laitinen, K. (2020). GlycA, a novel marker for low grade inflammation, reflects gut microbiome diversity and is more accurate than high sensitive CRP in reflecting metabolomic profile. Metabolomics *16*, 1–13.

Nakamura, K., Miyoshi, T., Yunoki, K., and Ito, H. (2016). Postprandial hyperlipidemia as a potential residual risk factor. J. Cardiol. *67*, 335–339.

Newgard, C.B. (2012). Interplay between lipids and branched-chain amino acids in development of insulin resistance. Cell Metab. *15*, 606–614.

Oosting, A., Kegler, D., Wopereis, H.J., Teller, I.C., Van De Heijning, B.J.M., Verkade, H.J., and Van Der Beek, E.M. (2012a). Size and phospholipid coating of lipid droplets in the diet of young mice modify body fat accumulation in adulthood. Pediatr. Res. *72*, 362–369.

Oosting, A., Kegler, D., Wopereis, H.J., Teller, I.C., Van De Heijning, B.J.M., Verkade, H.J., and Van Der Beek, E.M. (2012b). Size and phospholipid coating of lipid droplets in the diet of young mice modify body fat accumulation in adulthood. Pediatr. Res. *72*, 362–369.

Oosting, A., Van Vlies, N., Kegler, D., Schipper, L., Abrahamse-Berkeveld, M., Ringler, S., Verkade, H.J., and Van Der Beek, E.M. (2014). Effect of dietary lipid structure in early postnatal life on mouse adipose tissue development and function in adulthood. Br. J. Nutr. *111*, 215–226.

Otvos, J.D., Shalaurova, I., Wolak-Dinsmore, J., Connelly, M.A., Mackey, R.H., Stein, J.H., and Tracy, R.P. (2015). GlycA: A composite nuclear magnetic resonance biomarker of systemic inflammation. Clin. Chem. *61*, 714–723.

Ruiz-Canela, M., Toledo, E., Clish, C.B., Hruby, A., Liang, L., Salas-Salvado, J., Razquin, C., Corella, D., Estruch, R., Ros, E., et al. (2016). Plasma branched-chain amino acids and incident cardiovascular disease in the PREDIMED Trial. Clin. Chem. *62*, 582–592.

Sellem, L., Srour, B., Jackson, K.G., Hercberg, S., Galan, P., Kesse-Guyot, E., Julia, C., Fezeu, L., and Deschasaux-Tanguy, M. (2022). Consumption of dairy products and CVD risk: Results from the French prospective cohort NutriNet-Santé. Br. J. Nutr. *127*, 752–762.

De Simone, R., Vissicchio, F., Mingarelli, C., De Nuccio, C., Visentin, S., Ajmone-Cat, M.A., and

Minghetti, L. (2013). Branched-chain amino acids influence the immune properties of microglial cells and their responsiveness to pro-inflammatory signals. Biochim. Biophys. Acta - Mol. Basis Dis. *1832*, 650–659.

Soedamah-Muthu, S.S., Ding, E.L., Al-Delaimy, W.K., Hu, F.B., Engberink, M.F., Willett, W.C., and Geleijnse, J.M. (2011). Milk and dairy consumption and incidence of cardiovascular diseases and all-cause mortality: dose-response meta-analysis of prospective cohort studies. Am. J. Clin. Nutr. *93*, 158.

Soininen, P., Kangas, A.J., Würtz, P., Suna, T., and Ala-Korpela, M. (2015). Quantitative serum nuclear magnetic resonance metabolomics in cardiovascular epidemiology and genetics. Circ. Cardiovasc. Genet. *8*, 192–206.

Wang, Q., Oliver-Williams, C., Raitakari, O.T., Viikari, J., Lehtimäki, T., Kähönen, M., Järvelin, M.R., Salomaa, V., Perola, M., Danesh, J., et al. (2021). Metabolic profiling of angiopoietin-like protein 3 and 4 inhibition: A drug-target Mendelian randomization analysis. Eur. Heart J. *42*, 1160–1169.

Würtz, P., Kangas, A.J., Soininen, P., Lawlor, D.A., Davey Smith, G., and Ala-Korpela, M. (2017). Quantitative Serum Nuclear Magnetic Resonance Metabolomics in Large-Scale Epidemiology: A Primer on -Omic Technologies. Am. J. Epidemiol. *186*, 1084–1096.

SUPPLEMENTARY

Table S1. Overview table of postprandial responses for the 249 metabolites. Data are presented as mean + SD. Main effects were calculated using linear mixed models for repeated measures. Differences between shakes and interaction effects were tested with LSD post-hoc.

	VEGE						AMF						CREAM						MAIN EFFECTS			DIFFERENCES BETWEEN SHAKES (p-value)			INTERACTION EFFECTS T3			INTERACTION EFFECTS T6		
Metabolite	Baseline	SD	Δ3 hours	SD	Δ6 hours	SD	Baseline	SD	Δ3 hours	SD	Δ6 hours	SD	Baseline	SD	Δ3 hours	SD	Δ6 hours	SD	FDR time	FDR Shake	FDR Shake *Time	VEGE vs. AMF	VEGE vs. CREAM	AMF vs. CREAM	VEGE vs. AMF	VEGE vs. CREAM	AMF vs. CREAM	VEGE vs. AMF	VEGE vs. CREAM	AMF vs. CREAM
Total.C	5,365	0,939	-0,008	0,277	-0,012	0,281	5,406	0,821	0,010	0,265	-0,058	0,301	5,336	0,828	0,055	0,381	-0,003	0,330				0,684	0,382	0,199	0,873	0,324	0,397	0,462	0,818	0,332
non.HDL.C	3,896	0,966	-0,001	0,217	-0,060	0,213	3,907	0,875	0,009	0,205	-0,108	0,233	3,891	0,852	0,041	0,269	-0,068	0,249	0,030			0,516	0,525	0,199	0,913	0,358	0,408	0,305	0,975	0,321
Remnant.C	1,753	0,447	0,061	0,106	0,102	0,107	1,754	0,404	0,043	0,086	0,091	0,105	1,760	0,404	0,041	0,124	0,115	0,117	0,027			0,323	0,823	0,225	0,451	0,737	0,688	0,523	0,521	0,190
VLDL.C	0,747	0,248	0,069	0,072	0,101	0,086	0,739	0,225	0,039	0,049	0,066	0,065	0,763	0,244	0,040	0,053	0,067	0,069	0,029	0,015		0,000	0,011	0,327	0,028	0,180	0,493	0,003	0,042	0,495
ClinicalLDL.C	3,187	0,832	-0,088	0,193	-0,219	0,196	3,203	0,757	-0,087	0,190	-0,313	0,218	3,161	0,720	-0,067	0,266	-0,251	0,241	0,013			0,183	0,944	0,162	0,960	0,569	0,538	0,068	0,637	0,172
LDL.C	2,144	0,524	-0,062	0,127	-0,162	0,137	2,153	0,478	-0,034	0,142	-0,200	0,165	2,131	0,461	0,000	0,188	-0,183	0,177	0,009			0,701	0,445	0,252	0,505	0,098	0,316	0,227	0,557	0,536
HDL.C	1,469	0,269	-0,007	0,075	0,048	0,091	1,500	0,243	0,001	0,068	0,050	0,086	1,446	0,273	0,014	0,120	0,065	0,098	0,021			0,875	0,114	0,145	0,832	0,252	0,324	0,992	0,301	0,284
Total.TG	1,185	0,498	0,332	0,329	0,466	0,433	1,162	0,458	0,364	0,272	0,492	0,371	1,248	0,540	0,469	0,322	0,362	0,415			0,008	0,226	0,924	0,276	0,141	0,004	0,029	0,859	0,005	0,000
VLDL.TG	0,850	0,461	0,306	0,311	0,407	0,402	0,826	0,418	0,320	0,242	0,401	0,333	0,900	0,472	0,413	0,287	0,287	0,384			0,006	0,712	0,346	0,148	0,199	0,011	0,060	0,434	0,000	0,000
LDL.TG	0,135	0,025	0,006	0,010	0,013	0,014	0,136	0,024	0,011	0,014	0,020	0,020	0,139	0,032	0,017	0,019	0,015	0,019		0,018		0,004	0,003	0,690	0,068	0,001	0,023	0,028	0,702	0,084
HDL.TG	0,109	0,026	0,020	0,014	0,040	0,024	0,109	0,026	0,029	0,018	0,058	0,027	0,115	0,036	0,034	0,023	0,048	0,029	0,013	0,007	0,018	0,000	0,000	0,574	0,016	0,001	0,084	0,000	0,109	0,013
Total.PL	3,137	0,394	0,097	0,157	0,211	0,174	3,167	0,340	0,116	0,157	0,238	0,184	3,144	0,388	0,156	0,200	0,228	0,192	0,023			0,536	0,131	0,334	0,681	0,113	0,185	0,648	0,660	0,979
VLDL.PL	0,469	0,177	0,077	0,076	0,111	0,097	0,462	0,161	0,062	0,053	0,090	0,073	0,486	0,183	0,075	0,054	0,072	0,078		0,022		0,007	0,031	0,831	0,245	0,664	0,092	0,012	0,002	0,164
LDL.PL	0,725	0,161	-0,017	0,037	-0,043	0,037	0,728	0,148	-0,011	0,039	-0,053	0,043	0,722	0,143	-0,003	0,053	-0,045	0,048	0,012			0,747	0,338	0,200	0,569	0,161	0,396	0,306	0,953	0,335
HDL.PL	1,605	0,255	0,041	0,074	0,143	0,091	1,637	0,234	0,067	0,080	0,194	0,101	1,599	0,254	0,087	0,112	0,188	0,102	0,006	0,017		0,012	0,001	0,338	0,224	0,020	0,177	0,020	0,035	0,992

	VEGE						AMF						CREAM						MAIN EFFECTS			DIFFERENCES BETWEEN SHAKES (p-value)			INTERACTION EFFECTS T3			INTERACTION EFFECTS T6		
Metabolite	Baseline	SD	Δ3 hours	SD	Δ6 hours	SD	Baseline	SD	Δ3 hours	SD	Δ6 hours	SD	Baseline	SD	Δ3 hours	SD	Δ6 hours	SD	FDR time	FDR Shake	FDR Shake *Time	VEGE vs. AMF	VEGE vs. CREAM	AMF vs. CREAM	VEGE vs. AMF	VEGE vs. CREAM	AMF vs. CREAM	VEGE vs. AMF	VEGE vs. CREAM	AMF vs. CREAM
Total.CE	3,918	0,662	-0,025	0,204	-0,044	0,210	3,953	0,576	-0,010	0,194	-0,080	0,224	3,892	0,586	0,020	0,289	-0,038	0,249				0,695	0,403	0,219	0,846	0,339	0,437	0,455	0,832	0,336
VLDL.CE	0,451	0,141	0,029	0,035	0,043	0,039	0,447	0,128	0,012	0,026	0,026	0,034	0,458	0,136	0,008	0,033	0,033	0,037	0,025	0,017		0,001	0,032	0,238	0,021	0,048	0,825	0,015	0,337	0,150
LDL.CE	1,557	0,394	-0,039	0,094	-0,107	0,105	1,561	0,360	-0,006	0,114	-0,125	0,127	1,550	0,350	0,025	0,146	-0,121	0,137	0,010			0,910	0,242	0,288	0,297	0,029	0,234	0,377	0,575	0,755
HDL.CE	1,144	0,210	-0,012	0,060	0,025	0,073	1,168	0,190	-0,010	0,053	0,019	0,068	1,125	0,216	-0,001	0,095	0,032	0,078	0,026			0,739	0,280	0,152	0,982	0,400	0,390	0,622	0,520	0,244
Total.FC	1,447	0,279	0,017	0,076	0,031	0,076	1,454	0,247	0,020	0,073	0,022	0,080	1,444	0,247	0,035	0,095	0,035	0,086				0,655	0,336	0,154	0,952	0,296	0,300	0,490	0,783	0,329
VLDL.FC	0,296	0,109	0,040	0,040	0,058	0,051	0,292	0,099	0,028	0,026	0,040	0,035	0,305	0,110	0,032	0,026	0,034	0,039		0,013		0,000	0,004	0,621	0,070	0,603	0,234	0,001	0,001	0,610
LDL.FC	0,587	0,133	-0,023	0,034	-0,055	0,037	0,591	0,120	-0,027	0,034	-0,075	0,042	0,581	0,114	-0,026	0,052	-0,062	0,045	0,009			0,064	0,510	0,231	0,605	0,801	0,792	0,036	0,501	0,152
HDL.FC	0,325	0,060	0,006	0,016	0,023	0,020	0,331	0,054	0,010	0,016	0,031	0,020	0,321	0,059	0,015	0,026	0,033	0,022	0,010	0,018		0,064	0,001	0,149	0,381	0,034	0,171	0,081	0,023	0,505
Total.L	9,687	1,644	0,421	0,617	0,664	0,685	9,736	1,458	0,489	0,590	0,672	0,687	9,728	1,570	0,680	0,697	0,586	0,761				0,844	0,306	0,370	0,596	0,057	0,105	0,797	0,574	0,705
VLDL.L	2,066	0,846	0,451	0,448	0,620	0,572	2,026	0,769	0,421	0,327	0,556	0,451	2,149	0,874	0,528	0,354	0,425	0,503			0,014	0,225	0,166	0,689	0,964	0,111	0,054	0,089	0,001	0,014
LDL.L	3,004	0,704	-0,073	0,168	-0,192	0,176	3,017	0,644	-0,034	0,188	-0,232	0,217	2,991	0,626	0,013	0,250	-0,212	0,233	0,012			0,854	0,329	0,245	0,464	0,077	0,287	0,321	0,685	0,560
HDL.L	3,183	0,520	0,055	0,150	0,231	0,179	3,246	0,473	0,097	0,154	0,303	0,192	3,160	0,519	0,135	0,231	0,301	0,200	0,009	0,022		0,073	0,005	0,268	0,355	0,039	0,197	0,109	0,081	0,789
Total.P	0,018	0,002	0,000	0,001	0,000	0,001	0,018	0,002	0,000	0,001	0,000	0,001	0,018	0,002	0,000	0,001	0,000	0,001				0,977	0,323	0,335	0,601	0,145	0,337	0,630	0,939	0,686
VLDL.P	0,000	0,000	0,000	0,000	0,000	0,000	0,000	0,000	0,000	0,000	0,000	0,000	0,000	0,000	0,000	0,000	0,000	0,000				0,024	0,095	0,674	0,437	0,908	0,364	0,019	0,023	0,743
LDL.P	0,001	0,000	0,000	0,000	0,000	0,000	0,001	0,000	0,000	0,000	0,000	0,000	0,001	0,000	0,000	0,000	0,000	0,000	0,018			0,014	0,226	0,209	0,375	0,997	0,373	0,009	0,095	0,377
HDL.P	0,016	0,002	0,000	0,001	0,000	0,001	0,016	0,002	0,000	0,001	0,000	0,001	0,016	0,002	0,000	0,001	0,000	0,001				0,876	0,267	0,337	0,562	0,122	0,321	0,718	0,998	0,716
VLDLsize	38,531	1,282	0,574	0,537	0,794	0,827	38,498	1,133	0,638	0,442	0,560	0,716	38,643	1,145	0,887	0,551	0,224	0,840			0,004	0,257	0,059	0,287	0,472	0,017	0,024	0,024	0,000	0,000
LDLsize	23,974	0,060	-0,032	0,076	-0,040	0,076	23,972	0,063	-0,072	0,081	-0,051	0,103	23,970	0,051	-0,104	0,134	-0,044	0,089		0,020		0,029	0,005	0,379	0,019	0,000	0,082	0,496	0,897	0,598
HDLsize	9,696	0,204	0,040	0,026	0,105	0,030	9,708	0,188	0,039	0,028	0,134	0,039	9,687	0,199	0,045	0,033	0,137	0,040	0,000	0,011	0,014	0,002	0,000	0,184	0,786	0,403	0,220	0,000	0,000	0,535

	VEGE						AMF						CREAM						MAIN EFFECTS			DIFFERENCES BETWEEN SHAKES (p-value)			INTERACTION EFFECTS T3			INTERACTION EFFECTS T6		
Metabolite	Baseline	SD	Δ3 hours	SD	Δ6 hours	SD	Baseline	SD	Δ3 hours	SD	Δ6 hours	SD	Baseline	SD	Δ3 hours	SD	Δ6 hours	SD	FDR time	FDR Shake	FDR Shake *Time	VEGE vs. AMF	VEGE vs. CREAM	AMF vs. CREAM	VEGE vs. AMF	VEGE vs. CREAM	AMF vs. CREAM	VEGE vs. AMF	VEGE vs. CREAM	AMF vs. CREAM
Phosphoglyc	2,388	0,303	0,107	0,139	0,254	0,163	2,421	0,265	0,125	0,139	0,257	0,168	2,402	0,322	0,157	0,179	0,230	0,170	0,020			0,861	0,474	0,564	0,643	0,121	0,212	0,826	0,548	0,658
TG.PG	0,493	0,187	0,103	0,096	0,125	0,121	0,475	0,163	0,113	0,070	0,130	0,096	0,513	0,190	0,147	0,092	0,086	0,116			0,008	0,202	0,807	0,123	0,162	0,009	0,069	0,729	0,004	0,000
Cholines	2,721	0,321	0,085	0,140	0,214	0,158	2,756	0,277	0,091	0,135	0,187	0,162	2,729	0,332	0,121	0,192	0,175	0,170	0,023			0,553	0,874	0,450	0,929	0,258	0,264	0,356	0,360	0,954
Phosphatidylc	2,273	0,297	0,112	0,122	0,220	0,141	2,306	0,257	0,111	0,106	0,178	0,127	2,291	0,308	0,123	0,149	0,166	0,146	0,025			0,187	0,413	0,641	0,858	0,603	0,457	0,095	0,106	0,928
Sphingomyelins	0,501	0,060	0,000	0,024	0,008	0,026	0,504	0,051	-0,003	0,024	0,000	0,030	0,495	0,057	0,003	0,040	0,005	0,032				0,276	0,865	0,209	0,660	0,606	0,332	0,272	0,779	0,419
ApoB	0,973	0,225	0,003	0,044	-0,008	0,045	0,972	0,205	0,001	0,041	-0,025	0,048	0,974	0,201	0,007	0,051	-0,017	0,049	0,028			0,151	0,863	0,207	0,800	0,616	0,441	0,076	0,459	0,311
ApoA1	1,512	0,185	0,008	0,066	0,065	0,073	1,538	0,166	0,025	0,065	0,085	0,082	1,505	0,194	0,038	0,101	0,084	0,087	0,018			0,185	0,028	0,358	0,378	0,061	0,279	0,322	0,249	0,831
ApoB.ApoA1	0,656	0,190	-0,002	0,016	-0,033	0,025	0,643	0,177	-0,009	0,015	-0,051	0,030	0,661	0,180	-0,013	0,024	-0,047	0,033	0,002	0,005		0,000	0,000	0,516	0,032	0,014	0,507	0,000	0,001	0,119
Total.FA	12,087	2,041	1,440	1,515	2,670	1,866	12,146	1,873	1,490	1,364	2,475	1,734	12,223	2,129	2,006	1,576	1,955	1,734	0,026		0,013	0,596	0,727	0,902	0,650	0,021	0,017	0,240	0,006	0,026
Unsaturation	1,324	0,046	-0,020	0,033	-0,044	0,032	1,330	0,043	-0,056	0,036	-0,104	0,045	1,320	0,043	-0,073	0,049	-0,079	0,052	0,022	0,001	0,003	0,000	0,000	0,448	0,000	0,000	0,004	0,000	0,000	0,000
Omega.3	0,367	0,121	0,051	0,046	0,048	0,048	0,380	0,115	0,029	0,034	0,003	0,037	0,374	0,133	0,022	0,039	0,003	0,041	0,029	0,004		0,000	0,000	0,804	0,007	0,018	0,843	0,000	0,000	0,880
Omega.6	4,826	0,661	0,303	0,312	0,567	0,380	4,870	0,592	0,110	0,227	0,026	0,267	4,841	0,623	0,157	0,285	0,012	0,264		0,001	0,005	0,000	0,000	0,533	0,002	0,047	0,366	0,000	0,000	0,976
PUFA	5,193	0,733	0,353	0,352	0,615	0,422	5,250	0,660	0,138	0,255	0,029	0,291	5,216	0,698	0,179	0,317	0,014	0,294		0,002	0,007	0,000	0,000	0,574	0,002	0,035	0,433	0,000	0,000	0,996
MUFA	2,870	0,679	0,558	0,581	1,056	0,735	2,867	0,613	0,557	0,503	0,942	0,666	2,929	0,716	0,772	0,607	0,710	0,678	0,024		0,006	0,370	0,339	0,830	0,684	0,011	0,006	0,104	0,000	0,003
SFA	4,024	0,732	0,529	0,615	0,999	0,739	4,029	0,684	0,794	0,666	1,504	0,917	4,079	0,804	1,056	0,801	1,232	0,923	0,019	0,004	0,010	0,000	0,000	0,976	0,001	0,000	0,005	0,000	0,115	0,004
LA	3,890	0,677	0,305	0,307	0,495	0,371	3,946	0,625	0,082	0,214	-0,131	0,248	3,917	0,645	0,117	0,254	-0,122	0,254	0,032	0,001	0,002	0,000	0,000	0,391	0,000	0,007	0,440	0,000	0,000	0,665
DHA	0,211	0,040	0,001	0,022	-0,016	0,023	0,218	0,037	-0,014	0,029	-0,057	0,048	0,210	0,042	-0,029	0,048	-0,043	0,047	0,027	0,014		0,000	0,003	0,646	0,364	0,081	0,333	0,000	0,021	0,108

	VEGE						AMF						CREAM						MAIN EFFECTS			DIFFERENCES BETWEEN SHAKES (p-value)			INTERACTION EFFECTS T3			INTERACTION EFFECTS T6		
Metabolite	Baseline	SD	Δ3 hours	SD	Δ6 hours	SD	Baseline	SD	Δ3 hours	SD	Δ6 hours	SD	Baseline	SD	Δ3 hours	SD	Δ6 hours	SD	FDR time	FDR Shake	FDR Shake *Time	VEGE vs. AMF	VEGE vs. CREAM	AMF vs. CREAM	VEGE vs. AMF	VEGE vs. CREAM	AMF vs. CREAM	VEGE vs. AMF	VEGE vs. CREAM	AMF vs. CREAM
Omega.3Perc	3,012	0,814	0,068	0,219	-0,209	0,226	3,108	0,727	-0,121	0,236	-0,478	0,322	3,030	0,809	-0,235	0,331	-0,368	0,334	0,011	0,002		0,000	0,000	0,905	0,000	0,000	0,065	0,000	0,002	0,045
Omega.6Perc	40,182	2,389	-1,625	1,576	-3,147	1,607	40,338	2,396	-3,257	1,913	-6,228	2,205	39,972	2,809	-4,206	2,211	-4,988	2,471	0,014	0,001	0,001	0,000	0,000	0,585	0,000	0,000	0,001	0,000	0,000	0,000
PUFAPerc	43,194	2,327	-1,557	1,718	-3,356	1,734	43,446	2,231	-3,379	2,112	-6,707	2,463	43,002	2,588	-4,442	2,461	-5,356	2,737	0,013	0,001	0,002	0,000	0,000	0,644	0,000	0,000	0,001	0,000	0,000	0,000
MUFAPerc	23,558	2,137	1,313	1,077	2,698	1,355	23,433	1,723	1,343	0,977	2,264	1,288	23,713	2,058	1,904	1,141	1,513	1,282	0,025		0,003	0,157	0,047	0,407	0,821	0,011	0,005	0,031	0,000	0,000
SFAPerc	33,248	1,167	0,244	0,750	0,658	0,734	33,121	1,211	2,036	1,217	4,442	1,445	33,285	1,320	2,537	1,412	3,843	1,608	0,008	0,000	0,000	0,000	0,000	0,672	0,000	0,000	0,009	0,000	0,000	0,002
LAPerc	32,251	2,536	-0,893	1,286	-2,265	1,149	32,560	2,642	-2,708	1,702	-6,078	1,966	32,202	2,851	-3,436	1,966	-4,905	2,136	0,007	0,000	0,001	0,000	0,000	0,358	0,000	0,000	0,006	0,000	0,000	0,000
DHAPerc	1,768	0,328	-0,142	0,224	-0,395	0,225	1,809	0,288	-0,268	0,281	-0,653	0,336	1,737	0,326	-0,400	0,348	-0,495	0,323	0,024	0,016		0,001	0,006	0,680	0,346	0,039	0,169	0,000	0,105	0,052
PUFA.MUFA	1,854	0,243	-0,149	0,126	-0,315	0,151	1,869	0,217	-0,230	0,143	-0,420	0,174	1,834	0,251	-0,305	0,159	-0,314	0,177	0,018	0,005	0,003	0,000	0,000	0,503	0,003	0,000	0,001	0,000	0,732	0,000
Omega.6.Omega.3	14,446	4,470	-0,953	1,079	-0,219	1,261	13,836	4,000	-0,475	0,659	0,123	1,421	14,342	4,659	-0,561	1,315	0,117	1,303	0,020			0,040	0,034	0,893	0,086	0,044	0,651	0,237	0,392	0,793
Ala	0,348	0,071	0,043	0,047	-0,045	0,053	0,352	0,060	0,018	0,039	-0,065	0,046	0,349	0,074	0,030	0,049	-0,072	0,050	0,001	0,007		0,000	0,000	0,767	0,001	0,177	0,115	0,000	0,000	0,241
Gln	0,683	0,074	0,033	0,034	0,040	0,046	0,694	0,059	0,048	0,047	0,035	0,044	0,689	0,068	0,049	0,061	0,003	0,051	0,032		0,015	0,676	0,086	0,026	0,190	0,179	0,846	0,466	0,000	0,001
Gly	0,238	0,064	-0,023	0,021	-0,036	0,024	0,243	0,069	-0,028	0,023	-0,046	0,029	0,241	0,058	-0,033	0,025	-0,052	0,028	0,015	0,009		0,010	0,000	0,015	0,197	0,011	0,099	0,021	0,000	0,082
His	0,086	0,010	0,003	0,008	0,000	0,008	0,087	0,010	0,003	0,007	-0,002	0,007	0,084	0,008	0,005	0,008	-0,005	0,007	0,014		0,015	0,488	0,116	0,345	0,573	0,163	0,343	0,125	0,001	0,024
TotalBCAA	0,374	0,057	0,085	0,055	0,126	0,058	0,373	0,047	0,082	0,039	0,114	0,050	0,381	0,053	0,119	0,046	0,063	0,039			0,001	0,158	0,018	0,238	0,687	0,005	0,000	0,122	0,000	0,000
Ile	0,048	0,011	0,019	0,013	0,032	0,015	0,049	0,008	0,019	0,010	0,029	0,013	0,049	0,011	0,027	0,011	0,018	0,010			0,003	0,321	0,150	0,567	0,996	0,012	0,004	0,171	0,000	0,000
Leu	0,101	0,019	0,032	0,022	0,050	0,023	0,101	0,017	0,029	0,016	0,041	0,021	0,104	0,016	0,041	0,016	0,020	0,015		0,014	0,001	0,026	0,000	0,062	0,478	0,061	0,004	0,018	0,000	0,000

	VEGE						AMF						CREAM						MAIN EFFECTS			DIFFERENCES BETWEEN SHAKES (p-value)				INTERACTION EFFECTS T3				INTERACTION EFFECTS T6		
Metabolite	Baseline	SD	Δ3 hours	SD	Δ6 hours	SD	Baseline	SD	Δ3 hours	SD	Δ6 hours	SD	Baseline	SD	Δ3 hours	SD	Δ6 hours	SD	FDR time	FDR Shake	FDR Shake *Time	VEGE vs. AMF	VEGE vs. CREAM	AMF vs. CREAM	VEGE vs. AMF	VEGE vs. CREAM	AMF vs. CREAM	VEGE vs. AMF	VEGE vs. CREAM	AMF vs. CREAM
Val	0,224	0,030	0,035	0,021	0,045	0,023	0,223	0,026	0,034	0,014	0,044	0,018	0,228	0,030	0,051	0,020	0,025	0,017			0,000	0,512	0,319	0,670	0,731	0,001	0,000	0,571	0,000	0,000
Phe	0,049	0,005	0,005	0,006	-0,001	0,007	0,050	0,006	0,003	0,006	-0,002	0,006	0,051	0,005	0,005	0,005	-0,007	0,005	0,005	0,014	0,010	0,032	0,000	0,055	0,111	0,879	0,155	0,160	0,000	0,000
Tyr	0,063	0,010	0,010	0,008	0,003	0,010	0,064	0,008	0,008	0,007	0,002	0,009	0,064	0,010	0,017	0,010	-0,004	0,008	0,005		0,001	0,133	0,366	0,604	0,373	0,001	0,000	0,232	0,000	0,000
Glucose	5,419	0,375	-0,207	0,524	-0,052	0,363	5,473	0,324	-0,220	0,610	-0,150	0,337	5,510	0,398	-0,221	0,578	-0,279	0,346				0,309	0,080	0,358	0,815	0,980	0,839	0,242	0,026	0,142
Lactate	0,903	0,247	0,067	0,241	0,044	0,431	0,844	0,226	0,081	0,253	0,065	0,331	0,881	0,271	0,201	0,684	0,011	0,318				0,386	0,342	0,890	0,591	0,205	0,383	0,499	0,994	0,496
Pyruvate	0,048	0,013	0,007	0,015	-0,004	0,022	0,047	0,011	0,005	0,015	-0,005	0,019	0,047	0,013	0,010	0,036	-0,007	0,016	0,016			0,337	0,806	0,483	0,463	0,916	0,397	0,540	0,664	0,892
Citrate	0,094	0,013	0,002	0,007	0,001	0,010	0,094	0,014	0,003	0,010	0,004	0,011	0,091	0,011	0,004	0,010	0,006	0,011				0,276	0,027	0,225	0,764	0,289	0,399	0,218	0,053	0,388
bOHbutyrate	0,069	0,066	-0,022	0,060	0,293	0,164	0,058	0,050	0,011	0,049	0,308	0,194	0,056	0,056	0,021	0,071	0,306	0,183	0,000	0,010		0,000	0,000	0,616	0,000	0,000	0,716	0,405	0,311	0,738
Acetate	0,043	0,013	-0,003	0,020	-0,001	0,014	0,041	0,009	-0,004	0,012	0,002	0,014	0,040	0,013	-0,004	0,014	-0,002	0,011	0,030			0,578	0,832	0,435	0,981	0,966	0,942	0,456	0,815	0,313
Acetoacetate	0,037	0,032	-0,003	0,029	0,106	0,060	0,031	0,022	0,017	0,022	0,123	0,062	0,030	0,022	0,017	0,023	0,113	0,057	0,001	0,008		0,000	0,000	0,847	0,000	0,000	0,936	0,107	0,204	0,851
Acetone	0,020	0,008	-0,003	0,006	0,017	0,010	0,019	0,009	0,002	0,005	0,019	0,011	0,018	0,006	0,003	0,004	0,019	0,011	0,001	0,006		0,000	0,000	0,902	0,000	0,000	0,868	0,074	0,117	0,996
Creatinine	76,165	10,358	-5,175	6,420	-6,237	5,424	75,784	10,098	-4,059	4,798	-6,085	4,856	77,297	10,627	-5,145	5,614	-6,600	6,024				0,422	0,909	0,358	0,273	0,910	0,330	0,977	0,789	0,750
Albumin	40,187	2,418	-0,488	1,915	-1,455	1,871	39,977	2,627	-0,074	1,899	-1,036	1,953	39,753	2,670	0,009	2,599	-0,312	2,471	0,030			0,224	0,015	0,210	0,425	0,326	0,841	0,356	0,015	0,117
GlycA	0,788	0,093	0,035	0,055	0,043	0,057	0,780	0,079	0,020	0,044	0,001	0,050	0,778	0,100	0,035	0,054	-0,005	0,053	0,033	0,012	0,019	0,000	0,003	0,370	0,183	0,758	0,094	0,000	0,000	0,664
XXL.LIPO.P	0,000	0,000	0,000	0,000	0,000	0,000	0,000	0,000	0,000	0,000	0,000	0,000	0,000	0,000	0,000	0,000	0,000	0,000	0,029			0,466	0,121	0,320	0,420	0,950	0,381	0,845	0,040	0,026
XXL.LIPO.L	0,116	0,139	0,188	0,208	0,299	0,256	0,106	0,134	0,154	0,148	0,307	0,237	0,134	0,148	0,195	0,179	0,244	0,221	0,025			0,414	0,089	0,290	0,371	0,944	0,330	0,816	0,024	0,016
XXL.LIPO.PL	0,014	0,018	0,023	0,025	0,040	0,032	0,013	0,017	0,019	0,020	0,041	0,030	0,017	0,020	0,025	0,025	0,033	0,028				0,411	0,120	0,365	0,326	0,634	0,678	0,881	0,126	0,097
XXL.LIPO.C	0,027	0,026	0,026	0,027	0,047	0,036	0,025	0,024	0,021	0,021	0,045	0,033	0,031	0,028	0,028	0,026	0,037	0,031	0,019		0,019	0,356	0,195	0,594	0,416	0,443	0,085	0,650	0,016	0,015

	VEGE						AMF						CREAM						MAIN EFFECTS			DIFFERENCES BETWEEN SHAKES (p-value)				INTERACTION EFFECTS T3				INTERACTION EFFECTS T6		
Metabolite	Baseline	SD	Δ3 hours	SD	Δ6 hours	SD	Baseline	SD	Δ3 hours	SD	Δ6 hours	SD	Baseline	SD	Δ3 hours	SD	Δ6 hours	SD	FDR time	FDR Shake	FDR Shake *Time	VEGE vs. AMF	VEGE vs. CREAM	AMF vs. CREAM	VEGE vs. AMF	VEGE vs. CREAM	AMF vs. CREAM	VEGE vs. AMF	VEGE vs. CREAM	AMF vs. CREAM
XXL.LIPO.CE	0,015	0,014	0,012	0,013	0,023	0,018	0,014	0,013	0,011	0,010	0,022	0,016	0,017	0,015	0,015	0,013	0,017	0,016	0,022		0,017	0,371	0,318	0,809	0,915	0,118	0,046	0,263	0,005	0,021
XXL.LIPO.FC	0,012	0,011	0,013	0,014	0,024	0,018	0,011	0,011	0,010	0,011	0,023	0,017	0,013	0,013	0,014	0,014	0,019	0,016	0,020			0,428	0,287	0,714	0,229	0,887	0,174	0,914	0,127	0,063
XXL.LIPO.TG	0,075	0,096	0,139	0,157	0,212	0,188	0,068	0,093	0,113	0,108	0,221	0,174	0,086	0,100	0,142	0,129	0,175	0,163				0,028	0,066	0,825	0,090	0,514	0,344	0,168	0,080	0,522
XL.VLDL.P	0,000	0,000	0,000	0,000	0,000	0,000	0,000	0,000	0,000	0,000	0,000	0,000	0,000	0,000	0,000	0,000	0,000	0,000			0,009	0,911	0,482	0,348	0,164	0,010	0,060	0,214	0,001	0,002
XL.VLDL.L	0,185	0,132	0,078	0,085	0,110	0,111	0,178	0,121	0,084	0,068	0,110	0,092	0,198	0,133	0,110	0,083	0,082	0,108			0,009	0,668	0,550	0,264	0,139	0,008	0,068	0,368	0,001	0,001
XL.VLDL.PL	0,034	0,025	0,015	0,016	0,022	0,021	0,032	0,023	0,014	0,012	0,021	0,017	0,036	0,026	0,019	0,015	0,016	0,019			0,015	0,628	0,542	0,812	0,615	0,046	0,043	0,244	0,006	0,020
XL.VLDL.C	0,051	0,029	0,012	0,013	0,018	0,017	0,050	0,026	0,011	0,009	0,014	0,013	0,054	0,029	0,014	0,011	0,010	0,015			0,011	0,038	0,034	0,705	0,996	0,146	0,074	0,005	0,000	0,022
XL.VLDL.CE	0,030	0,015	0,004	0,005	0,006	0,007	0,029	0,014	0,004	0,004	0,003	0,005	0,031	0,015	0,005	0,004	0,002	0,006		0,015	0,011	0,001	0,002	0,991	0,723	0,358	0,147	0,000	0,000	0,143
XL.VLDL.FC	0,021	0,014	0,007	0,008	0,011	0,011	0,020	0,013	0,007	0,006	0,011	0,008	0,023	0,014	0,009	0,007	0,008	0,009			0,013	0,449	0,268	0,586	0,766	0,071	0,050	0,184	0,001	0,007
XL.VLDL.TG	0,100	0,080	0,051	0,057	0,070	0,073	0,096	0,073	0,058	0,046	0,074	0,062	0,108	0,080	0,078	0,059	0,055	0,075			0,007	0,222	0,821	0,142	0,045	0,003	0,093	0,726	0,001	0,000
L.VLDL.P	0,000	0,000	0,000	0,000	0,000	0,000	0,000	0,000	0,000	0,000	0,000	0,000	0,000	0,000	0,000	0,000	0,000	0,000			0,005	0,421	0,073	0,209	0,161	0,016	0,114	0,013	0,000	0,001
L.VLDL.L	0,344	0,201	0,084	0,090	0,101	0,124	0,335	0,180	0,095	0,072	0,079	0,091	0,363	0,199	0,124	0,082	0,048	0,118	0,031		0,006	0,367	0,094	0,310	0,128	0,013	0,126	0,006	0,000	0,004
L.VLDL.PL	0,065	0,042	0,018	0,019	0,024	0,026	0,062	0,038	0,018	0,014	0,018	0,019	0,069	0,042	0,024	0,016	0,012	0,023			0,008	0,117	0,044	0,429	0,343	0,048	0,126	0,002	0,000	0,010
L.VLDL.C	0,098	0,052	0,018	0,018	0,022	0,026	0,095	0,047	0,017	0,013	0,013	0,017	0,102	0,052	0,021	0,013	0,008	0,021		0,018	0,010	0,004	0,005	0,747	0,896	0,247	0,197	0,000	0,000	0,085
L.VLDL.CE	0,052	0,025	0,008	0,008	0,009	0,011	0,050	0,023	0,007	0,005	0,004	0,007	0,054	0,025	0,007	0,005	0,002	0,008		0,009	0,014	0,000	0,000	0,848	0,414	0,980	0,434	0,000	0,000	0,603
L.VLDL.FC	0,046	0,027	0,010	0,010	0,013	0,015	0,045	0,024	0,010	0,008	0,010	0,011	0,049	0,027	0,013	0,009	0,006	0,014			0,007	0,122	0,043	0,420	0,331	0,040	0,111	0,002	0,000	0,008
L.VLDL.TG	0,182	0,109	0,048	0,054	0,055	0,073	0,177	0,098	0,060	0,045	0,047	0,056	0,192	0,106	0,079	0,053	0,029	0,076	0,028		0,005	0,905	0,284	0,183	0,033	0,003	0,124	0,048	0,000	0,001
M.VLDL.P	0,000	0,000	0,000	0,000	0,000	0,000	0,000	0,000	0,000	0,000	0,000	0,000	0,000	0,000	0,000	0,000	0,000	0,000	0,024	0,008	0,017	0,000	0,000	0,591	0,233	0,732	0,419	0,000	0,000	0,953
M.VLDL.L	0,658	0,242	0,060	0,069	0,048	0,088	0,651	0,219	0,055	0,053	-0,002	0,066	0,673	0,233	0,072	0,059	-0,013	0,089	0,019	0,016	0,011	0,001	0,008	0,646	0,863	0,373	0,235	0,000	0,000	0,582

	VEGE						AMF						CREAM						MAIN EFFECTS			DIFFERENCES BETWEEN SHAKES (p-value)			INTERACTION EFFECTS T3			INTERACTION EFFECTS T6		
Metabolite	Baseline	SD	Δ3 hours	SD	Δ6 hours	SD	Baseline	SD	Δ3 hours	SD	Δ6 hours	SD	Baseline	SD	Δ3 hours	SD	Δ6 hours	SD	FDR time	FDR Shake	FDR Shake *Time	VEGE vs. AMF	VEGE vs. CREAM	AMF vs. CREAM	VEGE vs. AMF	VEGE vs. CREAM	AMF vs. CREAM	VEGE vs. AMF	VEGE vs. CREAM	AMF vs. CREAM
M.VLDL.PL	0,149	0,055	0,012	0,014	0,012	0,017	0,148	0,050	0,007	0,010	0,000	0,012	0,152	0,052	0,009	0,011	-0,001	0,015	0,029	0,009		0,000	0,001	0,374	0,137	0,566	0,394	0,000	0,000	0,695
M.VLDL.C	0,213	0,071	0,006	0,016	-0,001	0,016	0,212	0,064	-0,007	0,015	-0,020	0,016	0,214	0,062	-0,011	0,023	-0,012	0,019	0,029	0,004		0,000	0,000	0,175	0,001	0,000	0,677	0,000	0,028	0,020
M.VLDL.CE	0,121	0,039	0,000	0,010	-0,006	0,011	0,121	0,035	-0,009	0,010	-0,016	0,011	0,120	0,033	-0,012	0,015	-0,010	0,012	0,032	0,006	0,020	0,000	0,000	0,177	0,000	0,000	0,374	0,000	0,289	0,006
M.VLDL.FC	0,092	0,033	0,006	0,008	0,005	0,009	0,092	0,030	0,002	0,006	-0,004	0,007	0,094	0,031	0,001	0,009	-0,002	0,009	0,032	0,006		0,000	0,000	0,354	0,018	0,026	0,971	0,000	0,001	0,205
M.VLDL.TG	0,296	0,133	0,042	0,044	0,037	0,067	0,290	0,119	0,055	0,045	0,018	0,052	0,307	0,130	0,074	0,047	0,000	0,070	0,016		0,004	0,234	0,088	0,478	0,095	0,008	0,141	0,001	0,000	0,015
S.VLDL.P	0,000	0,000	0,000	0,000	0,000	0,000	0,000	0,000	0,000	0,000	0,000	0,000	0,000	0,000	0,000	0,000	0,000	0,000				0,061	0,055	0,836	0,574	0,949	0,627	0,041	0,015	0,440
S.VLDL.L	0,404	0,121	0,024	0,029	0,022	0,039	0,400	0,112	0,023	0,026	0,018	0,036	0,417	0,131	0,024	0,029	0,011	0,037				0,245	0,370	0,842	0,785	0,825	0,601	0,179	0,163	0,806
S.VLDL.PL	0,104	0,031	0,003	0,007	0,002	0,008	0,103	0,029	0,001	0,006	-0,003	0,008	0,106	0,031	0,000	0,008	-0,002	0,008	0,033	0,019		0,004	0,028	0,506	0,187	0,225	0,975	0,005	0,072	0,365
S.VLDL.C	0,163	0,051	-0,001	0,011	-0,005	0,013	0,162	0,047	-0,006	0,011	-0,007	0,014	0,166	0,050	-0,010	0,018	-0,004	0,016				0,060	0,204	0,568	0,109	0,017	0,334	0,295	0,501	0,078
S.VLDL.CE	0,097	0,031	-0,002	0,007	-0,003	0,009	0,096	0,029	-0,004	0,007	-0,002	0,009	0,099	0,031	-0,006	0,011	0,000	0,010				0,658	0,983	0,676	0,261	0,048	0,292	0,612	0,052	0,102
S.VLDL.FC	0,066	0,020	0,001	0,004	-0,001	0,005	0,066	0,018	-0,002	0,004	-0,005	0,005	0,067	0,019	-0,003	0,007	-0,003	0,006	0,034	0,013		0,000	0,003	0,438	0,032	0,005	0,452	0,001	0,176	0,066
S.VLDL.TG	0,138	0,046	0,022	0,017	0,026	0,028	0,135	0,042	0,027	0,019	0,027	0,024	0,145	0,055	0,033	0,020	0,017	0,026			0,016	0,525	0,898	0,439	0,205	0,024	0,144	0,690	0,015	0,012
XS.VLDL.P	0,000	0,000	0,000	0,000	0,000	0,000	0,000	0,000	0,000	0,000	0,000	0,000	0,000	0,000	0,000	0,000	0,000	0,000	0,008			0,624	0,742	0,406	0,295	0,139	0,573	0,718	0,055	0,085
XS.VLDL.L	0,358	0,076	0,017	0,018	0,039	0,027	0,357	0,067	0,011	0,017	0,046	0,028	0,365	0,082	0,004	0,032	0,053	0,041	0,007			0,674	0,736	0,436	0,170	0,075	0,511	0,428	0,027	0,083
XS.VLDL.PL	0,104	0,022	0,005	0,005	0,012	0,008	0,104	0,020	0,001	0,006	0,013	0,008	0,106	0,024	-0,001	0,012	0,015	0,013	0,006			0,157	0,334	0,705	0,024	0,007	0,424	0,762	0,153	0,186
XS.VLDL.C	0,195	0,045	0,009	0,011	0,020	0,015	0,195	0,039	0,003	0,010	0,020	0,018	0,196	0,042	-0,002	0,019	0,028	0,024	0,008		0,014	0,139	0,626	0,334	0,057	0,006	0,236	0,869	0,034	0,012
XS.VLDL.CE	0,136	0,032	0,006	0,008	0,013	0,011	0,136	0,028	0,003	0,007	0,015	0,013	0,137	0,029	0,000	0,013	0,021	0,016	0,007		0,012	0,450	0,768	0,289	0,110	0,014	0,268	0,583	0,005	0,010
XS.VLDL.FC	0,059	0,013	0,003	0,003	0,006	0,005	0,058	0,011	0,001	0,003	0,005	0,005	0,060	0,014	-0,001	0,007	0,007	0,008	0,011	0,019	0,020	0,003	0,033	0,470	0,014	0,001	0,191	0,083	0,606	0,022
XS.VLDL.TG	0,059	0,012	0,003	0,004	0,007	0,006	0,059	0,011	0,006	0,004	0,013	0,007	0,062	0,018	0,007	0,006	0,011	0,008	0,018	0,007		0,000	0,000	0,993	0,017	0,002	0,200	0,000	0,017	0,205
IDL.P	0,000	0,000	0,000	0,000	0,000	0,000	0,000	0,000	0,000	0,000	0,000	0,000	0,000	0,000	0,000	0,000	0,000	0,000	0,028	0,014		0,003	0,000	0,415	0,024	0,056	0,799	0,057	0,002	0,161
IDL.L	1,434	0,298	-0,012	0,072	0,006	0,085	1,446	0,264	0,005	0,064	0,046	0,079	1,428	0,255	0,004	0,103	0,073	0,090	0,027	0,019		0,054	0,002	0,222	0,422	0,363	0,876	0,055	0,001	0,118

	VEGE						AMF						CREAM						MAIN EFFECTS			DIFFERENCES BETWEEN SHAKES (p-value)			INTERACTION EFFECTS T3			INTERACTION EFFECTS T6		
Metabolite	Baseline	SD	Δ3 hours	SD	Δ6 hours	SD	Baseline	SD	Δ3 hours	SD	Δ6 hours	SD	Baseline	SD	Δ3 hours	SD	Δ6 hours	SD	FDR time	FDR Shake	FDR Shake *Time	VEGE vs. AMF	VEGE vs. CREAM	AMF vs. CREAM	VEGE vs. AMF	VEGE vs. CREAM	AMF vs. CREAM	VEGE vs. AMF	VEGE vs. CREAM	AMF vs. CREAM
IDL.PL	0,337	0,068	-0,004	0,017	0,000	0,021	0,340	0,060	-0,003	0,014	0,007	0,019	0,337	0,058	-0,003	0,021	0,012	0,021	0,026			0,230	0,022	0,235	0,847	0,812	0,949	0,136	0,004	0,110
IDL.C	1,006	0,219	-0,008	0,053	0,000	0,063	1,016	0,194	0,004	0,050	0,026	0,061	0,997	0,184	0,001	0,082	0,049	0,071	0,031	0,021		0,099	0,005	0,213	0,477	0,456	0,943	0,106	0,002	0,093
IDL.CE	0,752	0,167	-0,007	0,041	0,001	0,049	0,759	0,150	0,007	0,039	0,027	0,050	0,745	0,142	0,007	0,064	0,042	0,058	0,031	0,017		0,029	0,001	0,227	0,262	0,211	0,842	0,050	0,001	0,133
IDL.FC	0,254	0,053	-0,001	0,013	-0,001	0,016	0,256	0,045	-0,004	0,014	-0,001	0,016	0,252	0,043	-0,006	0,019	0,007	0,017	0,033			0,639	0,428	0,202	0,430	0,280	0,729	0,898	0,031	0,033
IDL.TG	0,091	0,016	0,000	0,005	0,006	0,007	0,091	0,015	0,004	0,006	0,013	0,009	0,094	0,022	0,006	0,008	0,012	0,010	0,014	0,004		0,000	0,000	0,570	0,005	0,000	0,184	0,000	0,000	0,585
L.LDL.P	0,001	0,000	0,000	0,000	0,000	0,000	0,001	0,000	0,000	0,000	0,000	0,000	0,001	0,000	0,000	0,000	0,000	0,000		0,011		0,000	0,001	0,697	0,011	0,004	0,563	0,002	0,070	0,262
L.LDL.L	1,925	0,437	-0,053	0,114	-0,133	0,115	1,937	0,395	-0,053	0,110	-0,165	0,142	1,914	0,385	-0,041	0,162	-0,139	0,149	0,017			0,434	0,774	0,285	0,981	0,622	0,601	0,280	0,927	0,323
L.LDL.PL	0,422	0,091	-0,009	0,023	-0,020	0,024	0,424	0,083	-0,009	0,023	-0,028	0,026	0,419	0,080	-0,006	0,031	-0,021	0,027	0,022			0,388	0,590	0,162	0,990	0,555	0,564	0,218	0,865	0,161
L.LDL.C	1,413	0,335	-0,045	0,089	-0,117	0,090	1,421	0,301	-0,048	0,085	-0,147	0,114	1,401	0,290	-0,041	0,128	-0,126	0,119	0,013			0,292	0,925	0,337	0,854	0,843	0,700	0,192	0,742	0,331
L.LDL.CE	1,041	0,253	-0,031	0,067	-0,087	0,069	1,046	0,228	-0,031	0,065	-0,107	0,088	1,033	0,221	-0,025	0,097	-0,094	0,093	0,013			0,373	0,999	0,373	0,951	0,718	0,667	0,232	0,719	0,407
L.LDL.FC	0,372	0,083	-0,014	0,023	-0,030	0,024	0,375	0,074	-0,017	0,021	-0,040	0,027	0,368	0,070	-0,016	0,032	-0,032	0,028	0,017			0,133	0,685	0,273	0,597	0,741	0,848	0,111	0,813	0,175
L.LDL.TG	0,091	0,016	0,000	0,004	0,004	0,007	0,092	0,016	0,004	0,007	0,010	0,011	0,093	0,021	0,007	0,010	0,008	0,011	0,031	0,010		0,000	0,000	0,493	0,035	0,001	0,052	0,004	0,097	0,316
M.LDL.P	0,000	0,000	0,000	0,000	0,000	0,000	0,000	0,000	0,000	0,000	0,000	0,000	0,000	0,000	0,000	0,000	0,000	0,000	0,019			0,174	0,021	0,312	0,067	0,001	0,105	0,937	0,907	0,840
M.LDL.L	0,740	0,198	-0,019	0,045	-0,048	0,053	0,741	0,185	0,015	0,073	-0,051	0,069	0,739	0,181	0,041	0,092	-0,057	0,072	0,010		0,018	0,323	0,050	0,309	0,044	0,001	0,098	0,525	0,414	0,824
M.LDL.PL	0,195	0,050	-0,006	0,012	-0,017	0,011	0,196	0,046	-0,002	0,013	-0,018	0,014	0,195	0,045	0,001	0,017	-0,018	0,017	0,007			0,671	0,190	0,364	0,172	0,020	0,288	0,441	0,594	0,827
M.LDL.C	0,514	0,144	-0,015	0,034	-0,035	0,042	0,514	0,134	0,014	0,059	-0,037	0,052	0,513	0,130	0,034	0,073	-0,042	0,053	0,009		0,017	0,312	0,043	0,294	0,035	0,000	0,091	0,486	0,380	0,829
M.LDL.CE	0,363	0,108	-0,008	0,027	-0,017	0,034	0,363	0,102	0,021	0,054	-0,012	0,044	0,364	0,100	0,041	0,067	-0,021	0,043	0,015		0,013	0,082	0,012	0,398	0,010	0,000	0,061	0,883	0,425	0,487
M.LDL.FC	0,151	0,037	-0,007	0,009	-0,018	0,010	0,152	0,034	-0,008	0,010	-0,025	0,012	0,149	0,032	-0,007	0,015	-0,021	0,013	0,005			0,048	0,476	0,202	0,814	0,869	0,688	0,011	0,245	0,160
M.LDL.TG	0,031	0,006	0,002	0,003	0,004	0,004	0,031	0,006	0,003	0,004	0,005	0,005	0,031	0,008	0,005	0,005	0,003	0,005			0,015	0,058	0,077	0,915	0,106	0,001	0,018	0,322	0,303	0,027
S.LDL.P	0,000	0,000	0,000	0,000	0,000	0,000	0,000	0,000	0,000	0,000	0,000	0,000	0,000	0,000	0,000	0,000	0,000	0,000	0,026			0,017	0,349	0,162	0,694	0,451	0,214	0,003	0,048	0,481
S.LDL.L	0,339	0,075	-0,001	0,016	-0,011	0,017	0,339	0,069	0,004	0,022	-0,016	0,023	0,338	0,066	0,013	0,029	-0,016	0,025	0,012			0,856	0,332	0,231	0,237	0,009	0,085	0,152	0,179	0,958

	VEGE						AMF						CREAM						MAIN EFFECTS			DIFFERENCES BETWEEN SHAKES (p-value)			INTERACTION EFFECTS T3			INTERACTION EFFECTS T6		
Metabolite	Baseline	SD	Δ3 hours	SD	Δ6 hours	SD	Baseline	SD	Δ3 hours	SD	Δ6 hours	SD	Baseline	SD	Δ3 hours	SD	Δ6 hours	SD	FDR time	FDR Shake	FDR Shake *Time	VEGE vs. AMF	VEGE vs. CREAM	AMF vs. CREAM	VEGE vs. AMF	VEGE vs. CREAM	AMF vs. CREAM	VEGE vs. AMF	VEGE vs. CREAM	AMF vs. CREAM
S.LDL.PL	0,108	0,021	-0,002	0,004	-0,006	0,004	0,108	0,019	0,000	0,005	-0,006	0,005	0,108	0,018	0,002	0,006	-0,006	0,006	0,005			0,411	0,048	0,204	0,157	0,011	0,155	0,788	0,938	0,723
S.LDL.C	0,217	0,051	-0,003	0,011	-0,010	0,012	0,217	0,047	0,001	0,016	-0,015	0,015	0,216	0,045	0,007	0,021	-0,015	0,017	0,010		0,020	0,510	0,525	0,191	0,300	0,014	0,114	0,051	0,111	0,794
S.LDL.CE	0,153	0,038	-0,001	0,009	-0,003	0,010	0,153	0,035	0,004	0,014	-0,005	0,013	0,153	0,034	0,009	0,018	-0,006	0,013	0,021		0,018	0,737	0,159	0,259	0,106	0,001	0,062	0,251	0,186	0,773
S.LDL.FC	0,064	0,014	-0,002	0,003	-0,007	0,004	0,064	0,013	-0,003	0,004	-0,010	0,004	0,064	0,012	-0,003	0,006	-0,009	0,005	0,003	0,017		0,001	0,036	0,195	0,315	0,383	0,926	0,000	0,043	0,083
S.LDL.TG	0,014	0,003	0,003	0,004	0,005	0,004	0,014	0,003	0,003	0,003	0,005	0,004	0,014	0,004	0,005	0,004	0,004	0,004			0,008	0,120	0,463	0,496	0,252	0,003	0,010	0,329	0,042	0,001
XL.HDL.P	0,000	0,000	0,000	0,000	0,000	0,000	0,000	0,000	0,000	0,000	0,000	0,000	0,000	0,000	0,000	0,000	0,000	0,000	0,002	0,017		0,218	0,001	0,013	0,468	0,253	0,038	0,016	0,002	0,170
XL.HDL.L	0,201	0,076	0,016	0,010	0,039	0,014	0,203	0,071	0,014	0,012	0,048	0,017	0,195	0,073	0,016	0,019	0,052	0,021	0,001			0,444	0,015	0,066	0,294	0,805	0,442	0,035	0,001	0,072
XL.HDL.PL	0,095	0,044	0,009	0,006	0,023	0,009	0,096	0,041	0,008	0,007	0,029	0,010	0,091	0,042	0,010	0,011	0,031	0,013	0,003			0,150	0,015	0,244	0,770	0,991	0,781	0,022	0,001	0,179
XL.HDL.C	0,101	0,032	0,005	0,004	0,013	0,006	0,102	0,030	0,003	0,005	0,014	0,007	0,097	0,031	0,004	0,008	0,017	0,008	0,002		0,020	0,252	0,157	0,009	0,031	0,241	0,396	0,564	0,003	0,005
XL.HDL.CE	0,074	0,026	0,003	0,003	0,008	0,005	0,075	0,024	0,002	0,004	0,010	0,006	0,072	0,025	0,003	0,006	0,012	0,006	0,003	0,020		0,828	0,019	0,007	0,196	0,775	0,333	0,320	0,001	0,005
XL.HDL.FC	0,027	0,006	0,002	0,002	0,005	0,002	0,027	0,006	0,001	0,001	0,005	0,002	0,026	0,007	0,001	0,002	0,005	0,002	0,004			0,010	0,481	0,069	0,001	0,015	0,639	0,708	0,132	0,039
XL.HDL.TG	0,006	0,001	0,002	0,002	0,003	0,002	0,006	0,001	0,002	0,001	0,004	0,002	0,006	0,002	0,002	0,002	0,003	0,002	0,016		0,016	0,102	0,361	0,578	0,994	0,140	0,064	0,026	0,753	0,009
L.HDL.P	0,002	0,001	0,000	0,000	0,000	0,000	0,002	0,001	0,000	0,000	0,000	0,000	0,002	0,001	0,000	0,000	0,000	0,000	0,003			0,533	0,018	0,059	0,891	0,335	0,228	0,314	0,028	0,150
L.HDL.L	0,770	0,306	0,036	0,047	0,123	0,066	0,793	0,286	0,042	0,047	0,151	0,064	0,749	0,293	0,055	0,075	0,159	0,068	0,002	0,018		0,106	0,002	0,073	0,734	0,154	0,206	0,056	0,005	0,213
L.HDL.PL	0,373	0,144	0,018	0,024	0,061	0,033	0,385	0,135	0,024	0,024	0,080	0,031	0,364	0,137	0,031	0,036	0,082	0,033	0,003	0,013		0,007	0,000	0,116	0,334	0,047	0,187	0,006	0,002	0,387
L.HDL.C	0,374	0,158	0,013	0,023	0,051	0,033	0,385	0,148	0,011	0,022	0,054	0,031	0,361	0,153	0,016	0,037	0,062	0,032	0,004			0,529	0,118	0,024	0,399	0,876	0,311	0,970	0,054	0,031
L.HDL.CE	0,290	0,123	0,007	0,018	0,035	0,025	0,299	0,115	0,005	0,017	0,034	0,025	0,280	0,120	0,008	0,030	0,041	0,025	0,004			0,176	0,427	0,030	0,276	0,810	0,410	0,418	0,193	0,026
L.HDL.FC	0,084	0,035	0,006	0,005	0,016	0,008	0,086	0,033	0,006	0,006	0,020	0,007	0,081	0,034	0,008	0,008	0,021	0,008	0,002	0,016		0,073	0,000	0,037	0,946	0,218	0,168	0,016	0,001	0,130
L.HDL.TG	0,023	0,007	0,005	0,003	0,011	0,006	0,023	0,007	0,008	0,004	0,017	0,007	0,024	0,008	0,009	0,006	0,015	0,008	0,008	0,007		0,000	0,000	0,406	0,019	0,007	0,378	0,000	0,032	0,044
M.HDL.P	0,004	0,001	0,000	0,000	0,000	0,000	0,004	0,001	0,000	0,000	0,000	0,000	0,004	0,001	0,000	0,000	0,000	0,000	0,017			0,100	0,011	0,320	0,288	0,032	0,225	0,207	0,171	0,852
M.HDL.L	1,049	0,167	0,012	0,060	0,074	0,069	1,074	0,154	0,036	0,061	0,108	0,080	1,048	0,178	0,049	0,088	0,100	0,080	0,014	0,018		0,020	0,002	0,397	0,163	0,013	0,199	0,058	0,095	0,924

	VEGE						AMF						CREAM						MAIN EFFECTS			DIFFERENCES BETWEEN SHAKES (p-value)			INTERACTION EFFECTS T3			INTERACTION EFFECTS T6		
Metabolite	Baseline	SD	Δ3 hours	SD	Δ6 hours	SD	Baseline	SD	Δ3 hours	SD	Δ6 hours	SD	Baseline	SD	Δ3 hours	SD	Δ6 hours	SD	FDR time	FDR Shake	FDR Shake *Time	VEGE vs. AMF	VEGE vs. CREAM	AMF vs. CREAM	VEGE vs. AMF	VEGE vs. CREAM	AMF vs. CREAM	VEGE vs. AMF	VEGE vs. CREAM	AMF vs. CREAM
M.HDL.PL	0,484	0,073	0,012	0,026	0,044	0,032	0,495	0,068	0,024	0,030	0,064	0,039	0,485	0,077	0,031	0,039	0,058	0,037	0,011	0,015		0,003	0,001	0,489	0,100	0,006	0,143	0,012	0,072	0,613
M.HDL.C	0,527	0,095	-0,007	0,034	0,013	0,038	0,540	0,086	0,000	0,029	0,019	0,038	0,521	0,101	0,005	0,050	0,022	0,043	0,024			0,311	0,033	0,247	0,425	0,088	0,331	0,526	0,210	0,507
M.HDL.CE	0,432	0,076	-0,008	0,027	0,007	0,032	0,443	0,069	-0,003	0,023	0,011	0,030	0,427	0,082	0,000	0,040	0,013	0,035	0,026			0,404	0,055	0,263	0,480	0,131	0,390	0,637	0,250	0,470
M.HDL.FC	0,094	0,019	0,001	0,007	0,006	0,007	0,097	0,017	0,003	0,006	0,009	0,008	0,094	0,020	0,004	0,010	0,008	0,009	0,020	0,021		0,098	0,004	0,204	0,261	0,017	0,167	0,223	0,118	0,680
M.HDL.TG	0,039	0,011	0,008	0,005	0,016	0,009	0,039	0,011	0,011	0,007	0,024	0,011	0,041	0,015	0,013	0,009	0,020	0,011	0,010	0,006		0,000	0,000	0,632	0,010	0,001	0,122	0,000	0,067	0,029
S.HDL.P	0,010	0,001	0,000	0,001	0,000	0,000	0,010	0,001	0,000	0,000	-0,001	0,001	0,010	0,001	0,000	0,001	-0,001	0,001	0,016			0,418	0,898	0,495	0,621	0,252	0,507	0,102	0,185	0,764
S.HDL.L	1,162	0,122	-0,010	0,055	-0,005	0,054	1,176	0,115	0,005	0,054	-0,004	0,067	1,168	0,147	0,014	0,080	-0,010	0,076				0,504	0,227	0,580	0,306	0,062	0,368	0,936	0,846	0,905
S.HDL.PL	0,654	0,068	0,002	0,031	0,015	0,030	0,662	0,064	0,011	0,030	0,021	0,038	0,659	0,082	0,016	0,042	0,016	0,041				0,259	0,114	0,624	0,275	0,054	0,347	0,617	0,813	0,803
S.HDL.C	0,467	0,048	-0,017	0,024	-0,029	0,025	0,473	0,045	-0,014	0,023	-0,038	0,027	0,466	0,059	-0,011	0,039	-0,036	0,035	0,015			0,577	0,847	0,453	0,551	0,245	0,571	0,167	0,373	0,621
S.HDL.CE	0,347	0,036	-0,014	0,018	-0,025	0,020	0,351	0,035	-0,014	0,018	-0,036	0,021	0,346	0,045	-0,012	0,030	-0,034	0,028	0,012			0,168	0,505	0,478	0,809	0,527	0,684	0,029	0,120	0,552
S.HDL.FC	0,120	0,013	-0,003	0,006	-0,004	0,006	0,122	0,012	0,000	0,006	-0,002	0,007	0,121	0,015	0,001	0,010	-0,002	0,008				0,065	0,010	0,465	0,102	0,010	0,355	0,327	0,269	0,914
S.HDL.TG	0,041	0,012	0,006	0,005	0,009	0,008	0,041	0,012	0,008	0,006	0,014	0,009	0,043	0,015	0,010	0,007	0,010	0,009	0,028	0,010	0,013	0,000	0,003	0,332	0,011	0,001	0,065	0,000	0,729	0,002
XXL.VLDL.PLPerc	10,352	5,340	1,833	3,916	2,743	4,714	10,151	4,716	1,184	3,201	2,714	4,155	10,584	4,544	1,391	3,567	2,612	4,237				0,194	0,484	0,667	0,179	0,638	0,468	0,670	0,666	0,891
XXL.LIPO.CPerc	31,119	17,864	-10,773	14,216	-11,987	16,704	29,031	13,140	-9,725	11,033	-11,216	12,164	27,482	11,329	-8,450	9,255	-8,447	9,035				0,465	0,142	0,018	0,845	0,522	0,334	0,420	0,215	0,023
XXL.LIPO.CEPerc	17,834	11,571	-7,311	9,777	-7,892	10,913	17,040	9,090	-6,318	7,664	-8,017	8,319	15,699	7,070	-5,115	6,001	-6,127	5,889				0,573	0,133	0,028	0,444	0,131	0,309	0,124	0,669	0,043
XXL.LIPO.FCPerc	13,284	7,666	-3,462	5,411	-4,095	7,104	11,992	4,558	-3,407	3,839	-3,199	4,343	11,783	4,857	-3,334	3,893	-2,320	3,894				0,366	0,400	0,061	0,111	0,413	0,573	0,713	0,059	0,046
XXL.LIPO.TGPerc	58,529	19,202	8,940	14,090	9,244	17,410	60,817	14,359	8,541	11,055	8,502	12,860	61,934	13,350	7,059	10,687	5,834	10,679				0,118	0,032	0,529	0,277	0,161	0,702	0,261	0,120	0,614

	VEGE						AMF						CREAM						MAIN EFFECTS			DIFFERENCES BETWEEN SHAKES (p-value)			INTERACTION EFFECTS T3			INTERACTION EFFECTS T6		
Metabolite	Baseline	SD	Δ3 hours	SD	Δ6 hours	SD	Baseline	SD	Δ3 hours	SD	Δ6 hours	SD	Baseline	SD	Δ3 hours	SD	Δ6 hours	SD	FDR time	FDR Shake	FDR Shake *Time	VEGE vs. AMF	VEGE vs. CREAM	AMF vs. CREAM	VEGE vs. AMF	VEGE vs. CREAM	AMF vs. CREAM	VEGE vs. AMF	VEGE vs. CREAM	AMF vs. CREAM
XL.VLDL.PLPerc	17,581	2,214	0,653	1,132	1,293	1,448	17,532	2,119	-0,038	1,152	0,977	1,739	17,583	2,500	0,059	1,945	1,354	2,382	0,030	0,019		0,011	0,821	0,024	0,017	0,382	0,211	0,266	0,559	0,065
XL.VLDL.CPerc	30,218	5,178	-3,808	2,900	-5,063	4,082	29,935	4,577	-5,605	3,506	-6,091	4,304	29,536	5,415	-6,257	3,861	-3,996	3,502		0,012	0,010	0,000	0,056	0,059	0,001	0,000	0,168	0,023	0,155	0,000
XL.VLDL.CEPerc	18,458	4,325	-3,355	2,523	-4,715	3,431	18,284	3,866	-4,544	3,074	-5,658	3,490	17,903	4,791	-5,083	3,645	-4,068	3,311		0,013	0,011	0,000	0,050	0,082	0,007	0,001	0,115	0,006	0,318	0,000
XL.VLDL.FCPerc	11,760	1,056	-0,453	0,572	-0,349	0,881	11,652	0,912	-1,062	0,644	-0,433	1,238	11,633	0,946	-1,174	0,628	0,072	1,136	0,017	0,015	0,009	0,000	0,161	0,041	0,000	0,000	0,619	0,409	0,031	0,001
XL.VLDL.TGPerc	52,201	5,500	3,155	2,637	3,771	4,007	52,533	4,963	5,643	3,296	5,114	4,754	52,882	4,892	6,198	2,830	2,642	3,700		0,011	0,010	0,000	0,168	0,011	0,000	0,000	0,462	0,053	0,051	0,000
L.VLDL.PLPerc	17,899	2,472	0,656	0,899	1,287	1,553	17,834	2,428	0,345	0,961	0,877	1,303	18,030	2,543	0,445	1,197	0,849	1,175		0,019		0,002	0,033	0,670	0,093	0,449	0,500	0,010	0,043	0,928
L.VLDL.CPerc	28,855	3,251	-0,983	1,355	-1,185	2,039	28,620	3,066	-2,344	1,764	-1,764	2,603	28,529	2,844	-2,748	1,501	-0,213	2,753	0,027	0,011	0,006	0,000	0,060	0,037	0,000	0,000	0,191	0,066	0,047	0,000
L.VLDL.CEPerc	15,657	2,431	-0,727	1,095	-1,163	1,655	15,500	2,204	-1,820	1,355	-1,657	2,084	15,353	2,121	-2,224	1,187	-0,297	2,179	0,034	0,010	0,004	0,000	0,037	0,037	0,000	0,000	0,082	0,032	0,036	0,000
L.VLDL.FCPerc	13,198	1,220	-0,255	0,471	-0,022	0,652	13,120	1,215	-0,525	0,631	-0,107	0,815	13,176	1,119	-0,524	0,607	0,084	0,817	0,022			0,011	0,223	0,267	0,010	0,038	0,982	0,376	0,599	0,125
L.VLDL.TGPerc	53,246	4,832	0,326	1,791	-0,103	2,812	53,546	4,734	1,999	2,209	0,887	3,171	53,441	4,461	2,303	2,191	-0,636	3,431	0,023	0,008	0,012	0,000	0,025	0,030	0,000	0,000	0,398	0,011	0,282	0,000
M.VLDL.PLPerc	22,644	1,267	-0,143	0,412	0,139	0,804	22,655	1,145	-0,717	0,570	0,153	0,973	22,562	1,090	-0,900	0,554	0,595	1,038	0,006	0,021	0,005	0,005	0,110	0,256	0,000	0,000	0,190	0,965	0,011	0,004
M.VLDL.CPerc	33,197	4,685	-1,608	1,531	-2,473	3,352	33,239	4,141	-3,576	2,230	-2,451	3,360	32,635	4,344	-4,441	2,240	-0,402	3,521	0,027	0,020	0,002	0,004	0,097	0,279	0,000	0,000	0,035	0,852	0,003	0,000
M.VLDL.CEPerc	19,087	3,615	-1,360	1,195	-2,233	2,642	19,136	3,228	-2,729	1,670	-2,134	2,473	18,591	3,448	-3,274	1,567	-0,618	2,551	0,033		0,003	0,013	0,160	0,335	0,001	0,000	0,039	0,975	0,003	0,001

	VEGE						AMF						CREAM						MAIN EFFECTS			DIFFERENCES BETWEEN SHAKES (p-value)			INTERACTION EFFECTS T3			INTERACTION EFFECTS T6		
Metabolite	Baseline	SD	Δ3 hours	SD	Δ6 hours	SD	Baseline	SD	Δ3 hours	SD	Δ6 hours	SD	Baseline	SD	Δ3 hours	SD	Δ6 hours	SD	FDR time	FDR Shake	FDR Shake *Time	VEGE vs. AMF	VEGE vs. CREAM	AMF vs. CREAM	VEGE vs. AMF	VEGE vs. CREAM	AMF vs. CREAM	VEGE vs. AMF	VEGE vs. CREAM	AMF vs. CREAM
M.VLDL.FCPerc	14,109	1,170	-0,248	0,382	-0,239	0,748	14,103	1,033	-0,847	0,597	-0,317	0,958	14,044	0,996	-1,167	0,749	0,217	1,035	0,015	0,015	0,002	0,000	0,011	0,410	0,000	0,000	0,017	0,466	0,015	0,001
M.VLDL.TGPerc	44,159	5,813	1,751	1,880	2,334	4,086	44,106	5,114	4,294	2,748	2,298	4,252	44,803	5,263	5,341	2,725	-0,193	4,475	0,020	0,021	0,002	0,009	0,671	0,033	0,000	0,000	0,174	0,848	0,000	0,000
S.VLDL.PLPerc	25,710	1,288	-0,678	0,471	-1,012	0,869	25,781	1,185	-1,131	0,603	-1,663	0,852	25,526	1,268	-1,325	0,729	-1,149	0,897		0,003	0,009	0,000	0,000	0,139	0,000	0,000	0,049	0,000	0,295	0,000
S.VLDL.CPerc	40,245	3,087	-2,429	1,622	-3,164	2,555	40,399	2,795	-3,383	1,768	-3,106	2,462	40,036	2,723	-4,268	2,313	-1,622	2,612			0,004	0,122	0,446	0,495	0,018	0,000	0,010	0,792	0,002	0,001
S.VLDL.CEPerc	23,837	1,930	-1,651	1,215	-1,948	1,734	23,899	1,758	-2,046	1,108	-1,267	1,590	23,784	1,616	-2,624	1,349	-0,419	1,815	0,023		0,004	0,357	0,242	0,692	0,163	0,002	0,017	0,008	0,000	0,004
S.VLDL.FCPerc	16,408	1,346	-0,778	0,527	-1,215	0,928	16,500	1,216	-1,337	0,727	-1,840	1,021	16,252	1,286	-1,645	1,045	-1,204	1,003		0,006	0,007	0,000	0,000	0,293	0,001	0,000	0,019	0,000	0,956	0,000
S.VLDL.TGPerc	34,045	4,311	3,107	1,944	4,175	3,343	33,820	3,920	4,514	2,302	4,769	3,221	34,438	3,922	5,593	2,962	2,771	3,387		0,022	0,005	0,007	0,342	0,096	0,008	0,000	0,049	0,270	0,008	0,000
XS.VLDL.PLPerc	28,988	0,592	0,008	0,488	0,183	0,603	29,007	0,472	-0,482	0,693	-0,021	0,480	29,114	0,726	-0,606	0,991	-0,150	0,551	0,022	0,009		0,001	0,000	0,250	0,001	0,000	0,429	0,164	0,034	0,405
XS.VLDL.CPerc	54,279	2,290	-0,066	0,846	-0,426	1,369	54,361	2,103	-0,704	0,821	-1,244	1,429	53,935	2,088	-1,195	1,390	-0,288	1,419		0,009	0,006	0,000	0,002	0,230	0,007	0,000	0,019	0,000	0,690	0,000
XS.VLDL.CEPerc	37,940	2,151	-0,090	0,800	-0,428	1,388	38,060	1,961	-0,346	0,679	-0,559	1,250	37,599	2,010	-0,634	0,903	0,158	1,093			0,009	0,148	0,964	0,165	0,191	0,009	0,080	0,488	0,011	0,000
XS.VLDL.FCPerc	16,339	0,266	0,024	0,212	0,001	0,172	16,301	0,253	-0,358	0,348	-0,685	0,530	16,336	0,237	-0,560	0,717	-0,445	0,528		0,002	0,012	0,000	0,000	0,840	0,000	0,000	0,025	0,000	0,000	0,012
XS.VLDL.TGPerc	16,733	2,085	0,058	0,642	0,243	1,009	16,631	1,972	1,186	1,042	1,265	1,417	16,951	1,998	1,801	1,973	0,437	1,499		0,003	0,007	0,000	0,000	0,315	0,000	0,000	0,022	0,000	0,610	0,000
IDL.PLPerc	23,573	0,591	-0,076	0,359	-0,082	0,578	23,518	0,566	-0,275	0,518	-0,255	0,658	23,634	0,709	-0,317	0,531	-0,306	0,781		0,020		0,013	0,008	0,684	0,065	0,072	0,824	0,106	0,089	0,732

	VEGE						AMF						CREAM						MAIN EFFECTS			DIFFERENCES BETWEEN SHAKES (p-value)			INTERACTION EFFECTS T3			INTERACTION EFFECTS T6		
Metabolite	Baseline	SD	Δ3 hours	SD	Δ6 hours	SD	Baseline	SD	Δ3 hours	SD	Δ6 hours	SD	Baseline	SD	Δ3 hours	SD	Δ6 hours	SD	FDR time	FDR Shake	FDR Shake *Time	VEGE vs. AMF	VEGE vs. CREAM	AMF vs. CREAM	VEGE vs. AMF	VEGE vs. CREAM	AMF vs. CREAM	VEGE vs. AMF	VEGE vs. CREAM	AMF vs. CREAM
IDL.CPerc	69,998	1,334	0,017	0,537	-0,299	0,828	70,108	1,053	-0,008	0,671	-0,443	1,062	69,783	1,435	-0,076	1,081	-0,174	1,272				0,517	0,975	0,498	0,926	0,607	0,619	0,420	0,579	0,152
IDL.CEPerc	52,246	1,411	-0,024	0,650	-0,120	0,925	52,353	1,277	0,338	0,930	0,160	1,399	52,052	1,566	0,392	1,268	0,275	1,466				0,041	0,015	0,577	0,099	0,103	0,836	0,226	0,118	0,570
IDL.FCPerc	17,742	0,573	0,041	0,419	-0,179	0,433	17,755	0,580	-0,346	0,429	-0,603	0,506	17,731	0,683	-0,468	0,466	-0,449	0,513	0,032	0,003		0,000	0,000	0,825	0,000	0,000	0,196	0,000	0,008	0,109
IDL.TGPerc	6,439	1,012	0,059	0,262	0,381	0,430	6,374	0,870	0,283	0,345	0,698	0,548	6,583	1,056	0,394	0,634	0,480	0,639	0,023	0,010		0,000	0,001	0,470	0,015	0,001	0,163	0,001	0,361	0,017
L.LDL.PLPerc	21,955	0,424	0,120	0,302	0,435	0,487	21,939	0,426	0,137	0,313	0,426	0,672	21,959	0,482	0,133	0,453	0,536	0,715	0,021			0,919	0,502	0,404	0,935	0,970	0,970	0,824	0,407	0,235
L.LDL.CPerc	73,197	1,099	-0,269	0,450	-1,029	0,588	73,239	1,001	-0,482	0,511	-1,408	0,736	73,121	0,921	-0,616	0,767	-1,345	0,754	0,005	0,014		0,002	0,000	0,598	0,115	0,015	0,267	0,004	0,023	0,709
L.LDL.CEPerc	53,852	1,332	-0,083	0,517	-0,763	0,766	53,833	1,211	-0,131	0,514	-0,972	0,916	53,840	1,128	-0,162	0,810	-1,033	0,970	0,008			0,274	0,116	0,586	0,818	0,630	0,772	0,192	0,100	0,634
L.LDL.FCPerc	19,345	0,580	-0,185	0,320	-0,266	0,445	19,406	0,490	-0,351	0,292	-0,437	0,420	19,281	0,676	-0,453	0,470	-0,312	0,507		0,016		0,001	0,005	0,784	0,019	0,002	0,176	0,018	0,593	0,085
L.LDL.TGPerc	4,847	0,825	0,149	0,234	0,594	0,394	4,821	0,732	0,346	0,324	0,982	0,437	4,920	0,770	0,482	0,527	0,809	0,536	0,007	0,005	0,018	0,000	0,000	0,714	0,013	0,000	0,062	0,000	0,031	0,018
M.LDL.PLPerc	26,464	0,715	-0,247	0,658	-0,657	0,850	26,511	0,636	-0,668	0,996	-0,664	0,895	26,426	0,711	-1,036	1,377	-0,448	0,735			0,016	0,122	0,034	0,538	0,036	0,000	0,060	0,935	0,368	0,307
M.LDL.CPerc	69,273	1,074	-0,141	0,817	-0,217	1,012	69,247	0,972	0,321	1,011	-0,394	1,080	69,266	0,852	0,612	1,330	-0,423	0,964	0,021		0,020	0,422	0,114	0,426	0,053	0,002	0,213	0,418	0,363	0,901
M.LDL.CEPerc	48,713	2,119	0,319	1,286	1,107	1,501	48,586	1,875	1,628	2,068	1,610	1,841	48,884	1,988	2,378	2,774	0,961	1,522		0,016	0,012	0,002	0,002	0,921	0,002	0,000	0,073	0,239	0,646	0,098
M.LDL.FCPerc	20,560	1,248	-0,460	0,595	-1,324	0,902	20,660	1,124	-1,308	1,166	-2,004	1,105	20,382	1,387	-1,766	1,547	-1,384	1,022		0,005	0,011	0,000	0,000	0,811	0,000	0,000	0,018	0,002	0,676	0,007
M.LDL.TGPerc	4,263	0,668	0,387	0,387	0,874	0,555	4,243	0,603	0,347	0,284	1,058	0,528	4,308	0,611	0,425	0,349	0,871	0,631	0,006		0,018	0,267	0,997	0,268	0,477	0,729	0,261	0,026	0,725	0,009

	VEGE						AMF						CREAM						MAIN EFFECTS			DIFFERENCES BETWEEN SHAKES (p-value)				INTERACTION EFFECTS T3			INTERACTION EFFECTS T6		
Metabolite	Baseline	SD	Δ3 hours	SD	Δ6 hours	SD	Baseline	SD	Δ3 hours	SD	Δ6 hours	SD	Baseline	SD	Δ3 hours	SD	Δ6 hours	SD	FDR time	FDR Shake	FDR Shake *Time	VEGE vs. AMF	VEGE vs. CREAM	AMF vs. CREAM	VEGE vs. AMF	VEGE vs. CREAM	AMF vs. CREAM	VEGE vs. AMF	VEGE vs. CREAM	AMF vs. CREAM
S.LDL.PLPerc	32,196	1,289	-0,297	0,756	-0,797	0,920	32,164	1,286	-0,378	0,734	-0,267	0,932	32,149	1,481	-0,704	1,116	-0,164	0,819			0,012	0,077	0,308	0,480	0,666	0,052	0,091	0,004	0,001	0,481
S.LDL.CPerc	63,776	1,265	-0,575	0,844	-0,794	0,932	63,844	1,248	-0,525	0,663	-1,534	0,875	63,712	1,384	-0,439	0,953	-1,238	0,972	0,014		0,019	0,011	0,250	0,169	0,781	0,498	0,667	0,000	0,024	0,131
S.LDL.CEPerc	44,813	1,566	-0,147	0,954	0,746	1,015	44,818	1,518	0,450	1,134	0,708	1,204	44,851	1,703	0,896	1,698	0,510	1,001			0,016	0,141	0,036	0,509	0,024	0,000	0,091	0,854	0,362	0,446
S.LDL.FCPerc	18,964	0,706	-0,428	0,367	-1,540	0,801	19,027	0,688	-0,975	0,907	-2,242	0,993	18,861	0,916	-1,335	1,319	-1,748	1,017	0,011	0,007	0,015	0,000	0,000	0,772	0,004	0,000	0,027	0,000	0,265	0,009
S.LDL.TGPerc	4,028	0,514	0,872	0,808	1,591	0,979	3,992	0,516	0,904	0,560	1,802	0,839	4,138	0,684	1,143	0,749	1,403	0,973	0,015		0,008	0,054	0,736	0,129	0,592	0,040	0,042	0,037	0,104	0,000
XL.HDL.PLPerc	45,386	4,949	0,597	1,196	2,413	1,826	45,628	4,710	1,035	0,985	3,430	2,338	45,197	5,063	0,821	2,413	3,641	2,724	0,009			0,023	0,037	0,979	0,375	0,731	0,626	0,023	0,018	0,652
XL.HDL.CPerc	51,287	3,828	-1,409	0,914	-3,222	1,917	51,103	3,637	-1,884	1,414	-4,401	2,599	51,174	3,892	-1,902	2,465	-4,192	2,807	0,006	0,013		0,000	0,002	0,809	0,222	0,188	0,707	0,000	0,009	0,480
XL.HDL.CEPerc	37,267	1,722	-1,580	1,172	-2,810	1,714	37,369	1,900	-1,602	1,314	-3,512	2,062	37,129	2,425	-1,564	2,324	-3,289	2,397	0,011			0,089	0,284	0,632	0,894	0,961	0,942	0,014	0,156	0,466
XL.HDL.FCPerc	14,019	2,443	0,171	0,701	-0,412	0,743	13,734	2,101	-0,282	0,404	-0,890	0,756	14,044	2,402	-0,338	0,621	-0,903	0,881	0,012	0,005		0,000	0,000	0,849	0,002	0,001	0,633	0,000	0,001	0,834
XL.HDL.TGPerc	3,327	1,299	0,812	1,011	0,809	0,955	3,268	1,285	0,849	0,890	0,971	1,029	3,629	1,720	1,081	1,261	0,551	0,994			0,014	0,230	0,685	0,097	0,529	0,108	0,169	0,312	0,034	0,000
L.HDL.PLPerc	48,706	1,547	0,060	0,403	0,216	0,658	48,724	1,447	0,541	0,591	0,903	0,870	48,930	1,690	0,619	0,662	0,682	0,744		0,002		0,000	0,000	0,328	0,000	0,000	0,492	0,000	0,001	0,043
L.HDL.CPerc	48,004	2,175	-0,604	0,526	-1,013	0,881	48,093	2,144	-1,422	1,106	-2,279	1,451	47,423	3,068	-1,524	1,482	-1,608	1,370	0,033	0,003		0,000	0,000	0,102	0,000	0,000	0,469	0,000	0,013	0,003
L.HDL.CEPerc	37,252	1,888	-0,864	0,602	-1,358	1,001	37,336	1,891	-1,629	1,260	-2,698	1,676	36,735	2,843	-1,768	1,624	-2,104	1,486	0,028	0,003		0,000	0,000	0,239	0,001	0,001	0,383	0,000	0,004	0,014

	VEGE						AMF						CREAM						MAIN EFFECTS			DIFFERENCES BETWEEN SHAKES (p-value)			INTERACTION EFFECTS T3			INTERACTION EFFECTS T6		
Metabolite	Baseline	SD	Δ3 hours	SD	Δ6 hours	SD	Baseline	SD	Δ3 hours	SD	Δ6 hours	SD	Baseline	SD	Δ3 hours	SD	Δ6 hours	SD	FDR time	FDR Shake	FDR Shake *Time	VEGE vs. AMF	VEGE vs. CREAM	AMF vs. CREAM	VEGE vs. AMF	VEGE vs. CREAM	AMF vs. CREAM	VEGE vs. AMF	VEGE vs. CREAM	AMF vs. CREAM
L.HDL.FCPerc	10,752	0,543	0,259	0,290	0,345	0,278	10,758	0,546	0,207	0,223	0,420	0,299	10,688	0,576	0,244	0,270	0,496	0,310	0,018			0,289	0,024	0,093	0,276	0,760	0,489	0,012	0,001	0,109
L.HDL.TGPerc	3,291	1,078	0,544	0,445	0,796	0,641	3,182	1,074	0,881	0,626	1,376	0,883	3,648	1,709	0,904	0,975	0,926	1,021	0,031	0,008		0,000	0,008	0,075	0,014	0,021	0,704	0,000	0,288	0,005
M.HDL.PLPerc	46,157	0,864	0,613	0,531	0,933	0,583	46,097	0,729	0,699	0,495	1,242	0,600	46,371	0,980	0,770	0,691	1,005	0,576	0,021	0,020		0,003	0,118	0,224	0,396	0,169	0,417	0,001	0,529	0,014
M.HDL.CPerc	50,055	1,865	-1,266	0,907	-2,095	1,216	50,219	1,662	-1,610	0,959	-2,905	1,199	49,590	2,379	-1,749	1,399	-2,333	1,308	0,017	0,011	0,019	0,000	0,012	0,160	0,091	0,035	0,355	0,000	0,265	0,005
M.HDL.CEPerc	41,106	1,614	-1,237	0,820	-2,050	1,117	41,211	1,494	-1,582	0,884	-2,810	1,075	40,697	2,124	-1,773	1,228	-2,312	1,211	0,016	0,008	0,017	0,000	0,001	0,293	0,048	0,008	0,173	0,000	0,155	0,006
M.HDL.FCPerc	8,949	0,488	-0,030	0,151	-0,045	0,201	9,008	0,384	-0,028	0,139	-0,095	0,181	8,894	0,492	0,024	0,272	-0,020	0,226				0,477	0,149	0,027	0,906	0,199	0,197	0,266	0,515	0,070
M.HDL.TGPerc	3,788	1,119	0,653	0,447	1,162	0,705	3,684	1,072	0,911	0,495	1,663	0,700	4,038	1,502	0,979	0,774	1,328	0,852	0,019	0,012		0,000	0,007	0,337	0,052	0,021	0,337	0,000	0,242	0,024
S.HDL.PLPerc	56,277	1,013	0,660	0,390	1,538	0,482	56,346	1,081	0,655	0,477	1,942	0,551	56,407	0,987	0,655	0,542	1,865	0,592	0,001	0,021	0,019	0,006	0,027	0,712	0,851	0,973	0,881	0,000	0,004	0,508
S.HDL.CPerc	40,222	0,937	-1,148	0,645	-2,346	0,985	40,227	1,032	-1,299	0,750	-3,077	0,898	39,930	1,250	-1,417	0,957	-2,734	1,092	0,004	0,012	0,017	0,000	0,003	0,478	0,403	0,129	0,321	0,000	0,022	0,050
S.HDL.CEPerc	29,868	0,932	-1,000	0,531	-2,085	0,925	29,874	0,986	-1,264	0,676	-2,971	0,839	29,609	1,287	-1,399	0,879	-2,657	1,103	0,004	0,004	0,013	0,000	0,000	0,643	0,095	0,018	0,229	0,000	0,000	0,067
S.HDL.FCPerc	10,353	0,451	-0,148	0,222	-0,261	0,247	10,353	0,386	-0,035	0,148	-0,106	0,221	10,321	0,407	-0,018	0,185	-0,077	0,230	0,030	0,002		0,000	0,000	0,188	0,000	0,001	0,478	0,000	0,000	0,275
S.HDL.TGPerc	3,501	0,813	0,488	0,389	0,808	0,626	3,428	0,764	0,644	0,375	1,135	0,590	3,663	1,033	0,762	0,568	0,868	0,653	0,024	0,012	0,016	0,000	0,014	0,213	0,059	0,009	0,155	0,000	0,598	0,002

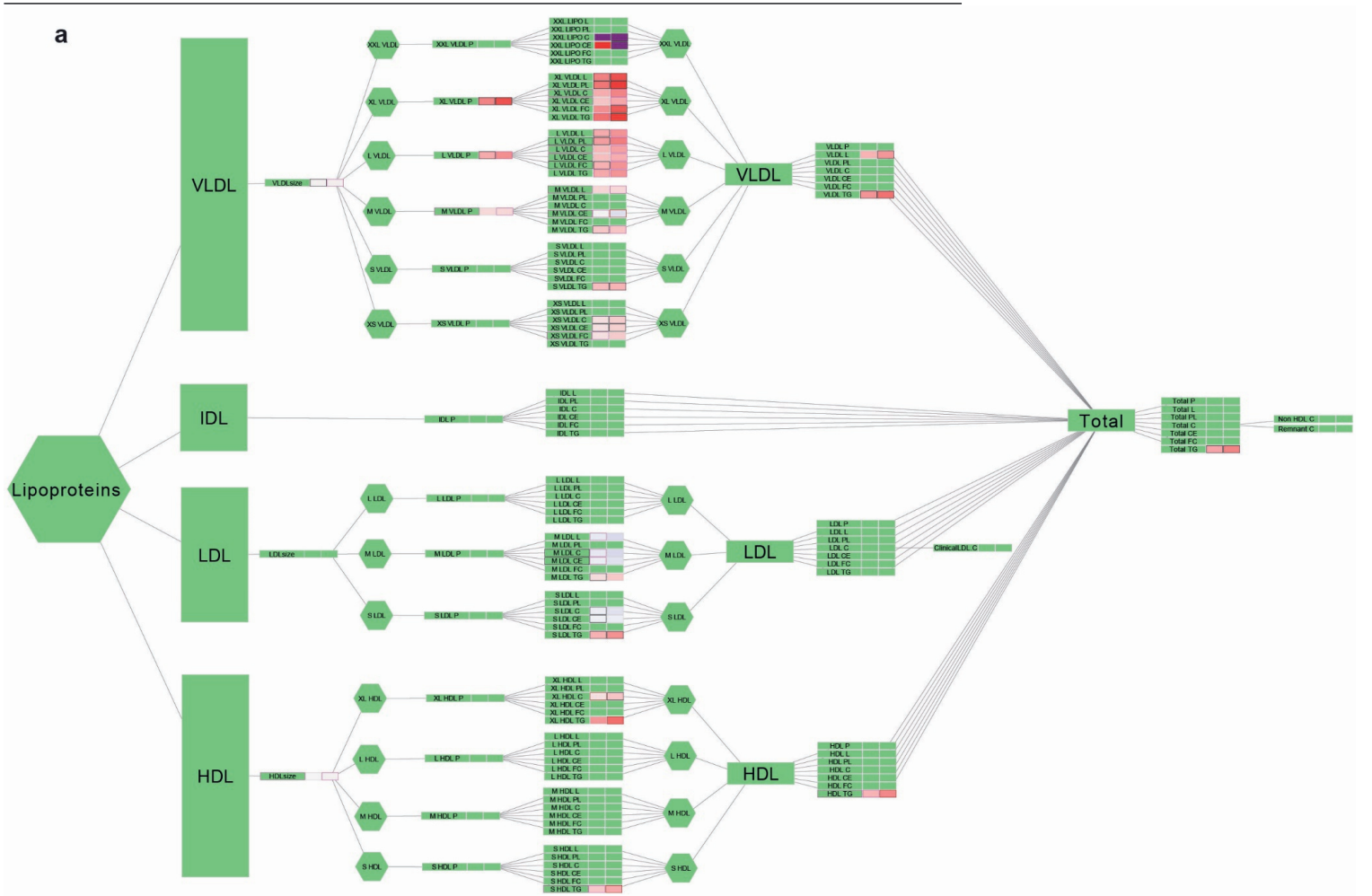
a
Lipoproteins
VLDL
IDL
LDL
HDL
VLDLsize
LDLsize
HDLsize
XXL VLDL
XL VLDL
L VLDL
M VLDL
S VLDL
XS VLDL
XXL VLDL P
XL VLDL P
L VLDL P
M VLDL P
S VLDL P
XS VLDL P
XXL LIPO L
XXL LIPO PL
XXL LIPO C
XXL LIPO CE
XXL LIPO FC
XXL LIPO TG
XL VLDL L
XL VLDL PL
XL VLDL C
XL VLDL CE
XL VLDL FC
XL VLDL TG
L VLDL L
L VLDL PL
L VLDL C
L VLDL CE
L VLDL FC
L VLDL TG
M VLDL L
M VLDL PL
M VLDL C
M VLDL CE
M VLDL FC
M VLDL TG
S VLDL L
S VLDL PL
S VLDL C
S VLDL CE
SVLDL FC
S VLDL TG
XS VLDL L
XS VLDL PL
XS VLDL C
XS VLDL CE
XS VLDL FC
XS VLDL TG
IDL P
IDL L
IDL PL
IDL C
IDL CE
IDL FC
IDL TG
L LDL P
M LDL P
S LDL P
L LDL L
L LDL PL
L LDL C
L LDL CE
L LDL FC
L LDL TG
M LDL L
M LDL PL
M LDL C
M LDL CE
M LDL FC
M LDL TG
S LDL L
S LDL PL
S LDL C
S LDL CE
S LDL FC
S LDL TG
XL HDL P
L HDL P
M HDL P
S HDL P
XL HDL L
XL HDL PL
XL HDL C
XL HDL CE
XL HDL FC
XL HDL TG
L HDL L
L HDL PL
L HDL C
L HDL CE
L HDL FC
L HDL TG
M HDL L
M HDL PL
M HDL C
M HDL CE
M HDL FC
M HDL TG
S HDL L
S HDL PL
S HDL C
S HDL CE
S HDL FC
S HDL TG
VLDL
IDL
LDL
HDL
Total
VLDL P
VLDL L
VLDL PL
VLDL C
VLDL CE
VLDL FC
VLDL TG
LDL P
LDL L
LDL PL
LDL C
LDL CE
LDL FC
LDL TG
HDL P
HDL L
HDL PL
HDL C
HDL CE
HDL FC
HDL TG
ClinicalLDL C
Total P
Total L
Total PL
Total C
Total CE
Total FC
Total TG
Non HDL C
Remnant C

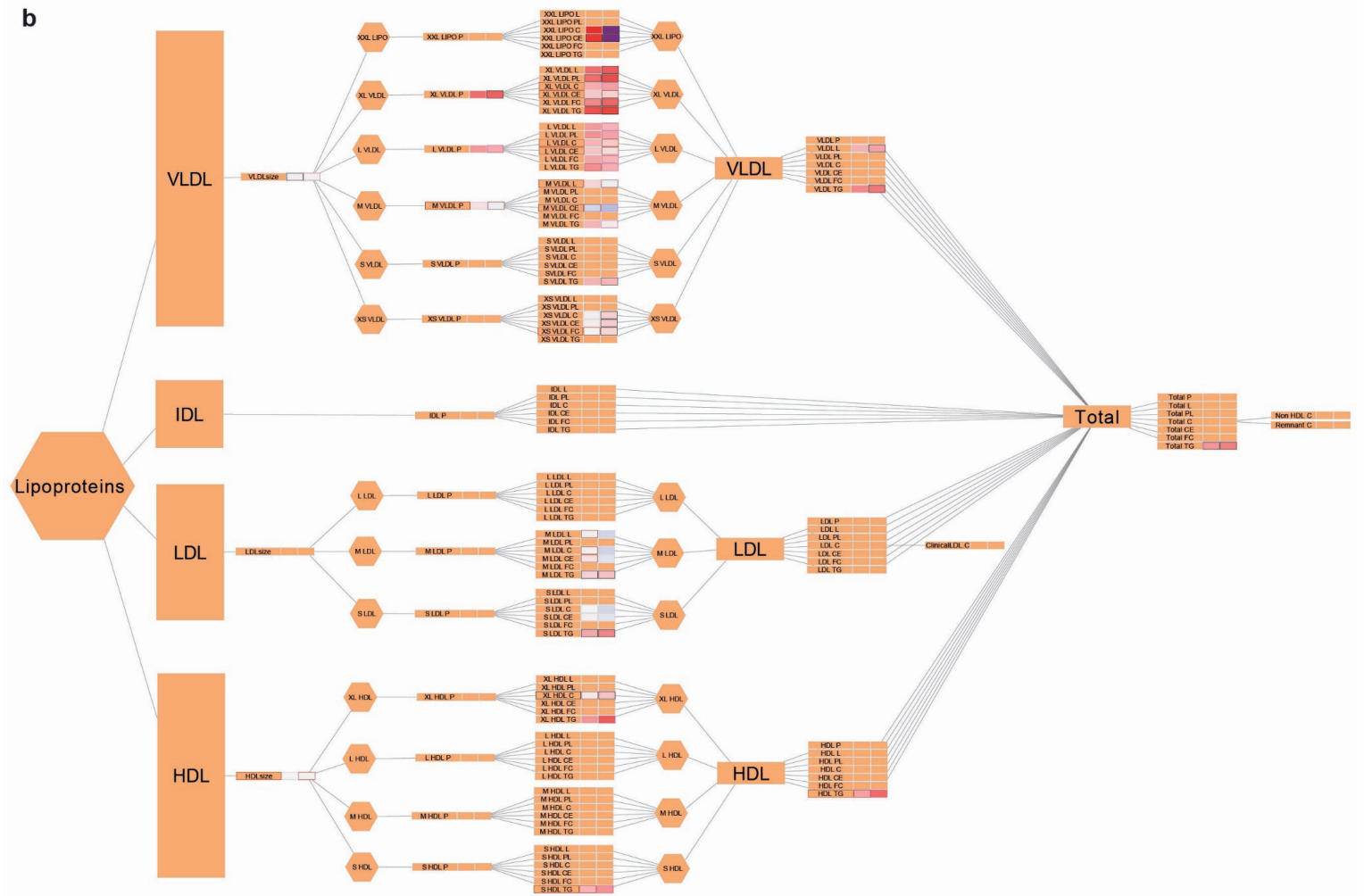
b
Lipoproteins
VLDL
IDL
LDL
HDL
VLDLsize
LDLsize
HDLsize
XXL LIPO
XL VLDL
L VLDL
M VLDL
S VLDL
XS VLDL
XXL LIPO P
XL VLDL P
L VLDL P
M VLDL P
S VLDL P
XS VLDL P
XXL LIPO L
XXL LIPO PL
XXL LIPO C
XXL LIPO CE
XXL LIPO FC
XXL LIPO TG
XL VLDL L
XL VLDL PL
XL VLDL C
XL VLDL CE
XL VLDL FC
XL VLDL TG
L VLDL L
L VLDL PL
L VLDL C
L VLDL CE
L VLDL FC
L VLDL TG
M VLDL L
M VLDL PL
M VLDL C
M VLDL CE
M VLDL FC
M VLDL TG
S VLDL L
S VLDL PL
S VLDL C
S VLDL CE
S VLDL FC
S VLDL TG
XS VLDL L
XS VLDL PL
XS VLDL C
XS VLDL CE
XS VLDL FC
XS VLDL TG
VLDL
VLDL P
VLDL L
VLDL PL
VLDL C
VLDL CE
VLDL FC
VLDL TG
IDL P
IDL L
IDL PL
IDL C
IDL CE
IDL FC
IDL TG
L LDL P
M LDL P
S LDL P
L LDL L
L LDL PL
L LDL C
L LDL CE
L LDL FC
L LDL TG
M LDL L
M LDL PL
M LDL C
M LDL CE
M LDL FC
M LDL TG
S LDL L
S LDL PL
S LDL C
S LDL CE
S LDL FC
S LDL TG
LDL
LDL P
LDL L
LDL PL
LDL C
LDL CE
LDL FC
LDL TG
ClinicalLDL C
XL HDL P
L HDL P
M HDL P
S HDL P
XL HDL L
XL HDL PL
XL HDL C
XL HDL CE
XL HDL FC
XL HDL TG
L HDL L
L HDL PL
L HDL C
L HDL CE
L HDL FC
L HDL TG
M HDL L
M HDL PL
M HDL C
M HDL CE
M HDL FC
M HDL TG
S HDL L
S HDL PL
S HDL C
S HDL CE
S HDL FC
S HDL TG
HDL
HDL P
HDL L
HDL PL
HDL C
HDL CE
HDL FC
HDL TG
Total
Total P
Total L
Total PL
Total C
Total CE
Total FC
Total TG
Non HDL C
Remnant C

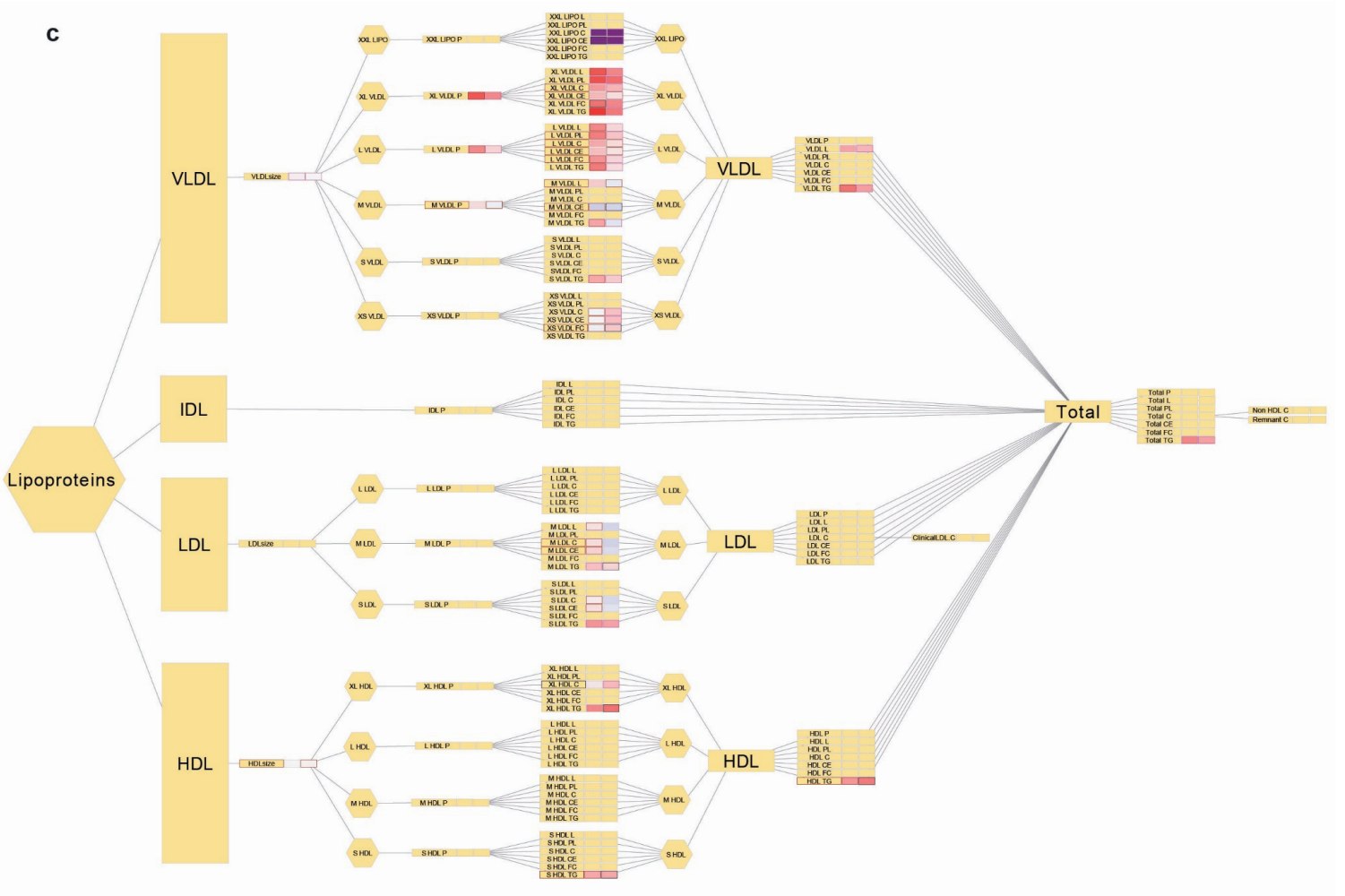
c
Lipoproteins
VLDL
IDL
LDL
HDL
VLDLsize
LDLsize
HDLsize
XXL LIPO
XL VLDL
L VLDL
M VLDL
S VLDL
XS VLDL
XXL LIPO P
XL VLDL P
L VLDL P
M VLDL P
S VLDL P
XS VLDL P
XXL LIPO L
XXL LIPO PL
XXL LIPO C
XXL LIPO CE
XXL LIPO FC
XXL LIPO TG
XL VLDL L
XL VLDL PL
XL VLDL C
XL VLDL CE
XL VLDL FC
XL VLDL TG
L VLDL L
L VLDL PL
L VLDL C
L VLDL CE
L VLDL FC
L VLDL TG
M VLDL L
M VLDL PL
M VLDL C
M VLDL CE
M VLDL FC
M VLDL TG
S VLDL L
S VLDL PL
S VLDL C
S VLDL CE
SVLDL FC
S VLDL TG
XS VLDL L
XS VLDL PL
XS VLDL C
XS VLDL CE
XS VLDL FC
XS VLDL TG
IDL P
IDL L
IDL PL
IDL C
IDL CE
IDL FC
IDL TG
L LDL P
M LDL P
S LDL P
L LDL L
L LDL PL
L LDL C
L LDL CE
L LDL FC
L LDL TG
M LDL L
M LDL PL
M LDL C
M LDL CE
M LDL FC
M LDL TG
S LDL L
S LDL PL
S LDL C
S LDL CE
S LDL FC
S LDL TG
XL HDL P
L HDL P
M HDL P
S HDL P
XL HDL L
XL HDL PL
XL HDL C
XL HDL CE
XL HDL FC
XL HDL TG
L HDL L
L HDL PL
L HDL C
L HDL CE
L HDL FC
L HDL TG
M HDL L
M HDL PL
M HDL C
M HDL CE
M HDL FC
M HDL TG
S HDL L
S HDL PL
S HDL C
S HDL CE
S HDL FC
S HDL TG
XL HDL
L HDL
M HDL
S HDL
VLDL
LDL
HDL
VLDL P
VLDL L
VLDL PL
VLDL C
VLDL CE
VLDL FC
VLDL TG
LDL P
LDL L
LDL PL
LDL C
LDL CE
LDL FC
LDL TG
HDL P
HDL L
HDL PL
HDL C
HDL CE
HDL FC
HDL TG
ClinicalLDL C
Total
Total P
Total L
Total PL
Total C
Total CE
Total FC
Total TG
Non HDL C
Remnant C

Figure S1. Postprandial lipoprotein profiles of three interventions. a) VEGE intervention; b) AMF intervention; c) CREAM intervention. [a] Border only coloured for metabolites with significant differences between shakes (post-hoc). [b] Colour inside the box represents log2 ratio and is only coloured for metabolites with a significant shake*time effect (LMM) and border only coloured for metabolites with significant shake*time at specific timepoints (post-hoc). Red border indicates significant difference between VEGE and AMF. Black border indicates significant difference between VEGE and CREAM. Pink border indicates a significant difference between VEGE, and AMF and CREAM. Abbreviations: cholesterol (C), cholesterol esters (CE), free cholesterol (FC) high-density lipoprotein (HDL) intermediate-density lipoprotein (DIL), low-density lipoprotein (LDL), lipids (L), particles (P), phospholipids (PL), triglycerides (TG), very low-density lipoprotein (VLDL).

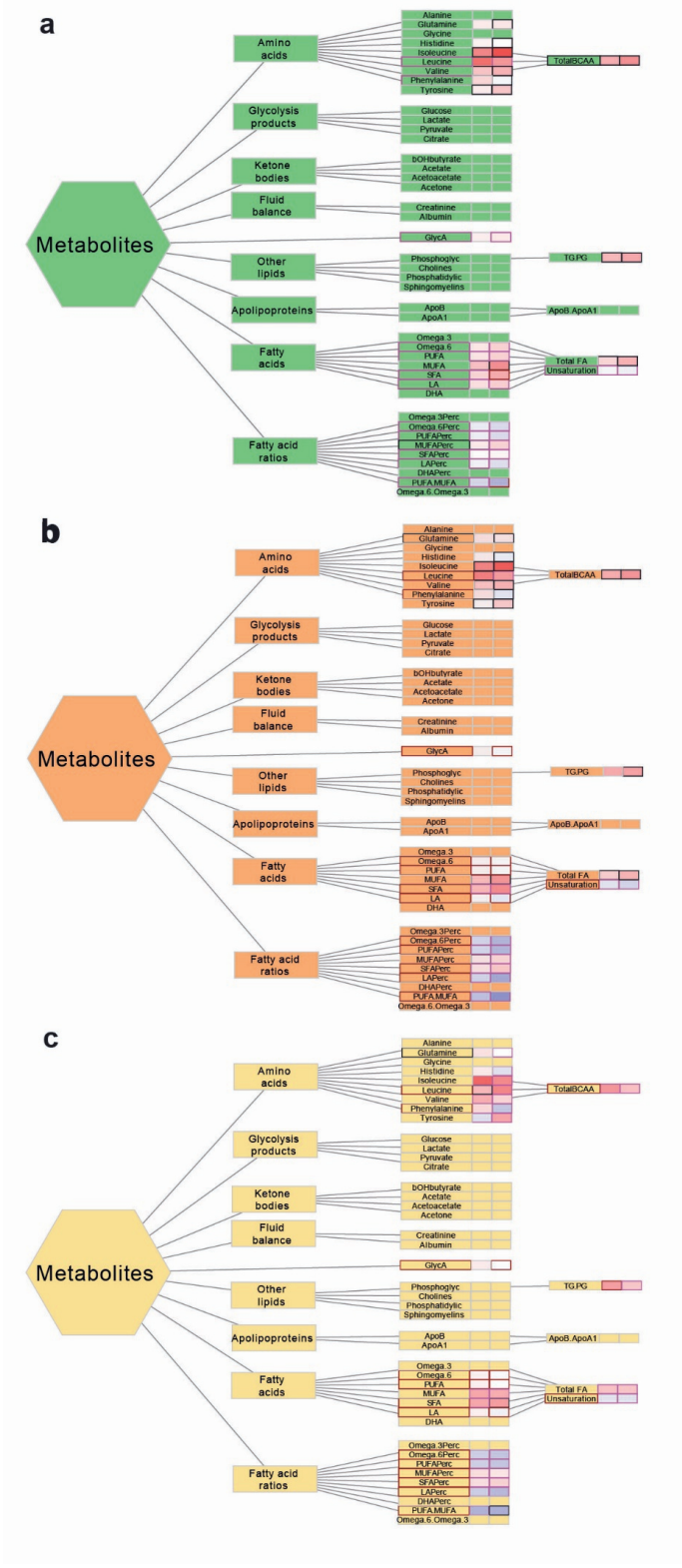
a
Metabolites
Amino acids
Alanine
Glutamine
Glycine
Histidine
Isoleucine
Leucine
Valine
Phenylalanine
Tyrosine
TotalBCAA
Glycolysis products
Glucose
Lactate
Pyruvate
Citrate
Ketone bodies
bOHbutyrate
Acetate
Acetoacetate
Acetone
Fluid balance
Creatinine
Albumin
GlycA
Other lipids
Phosphoglyc
Cholines
Phosphatidylic
Sphingomyelins
TG.PG
Apolipoproteins
ApoB
ApoA1
ApoB.ApoA1
Fatty acids
Omega.3
Omega.6
PUFA
MUFA
SFA
LA
DHA
Total FA
Unsaturation
Fatty acid ratios
Omega.3Perc
Omega.6Perc
PUFAPerc
MUFAPerc
SFAPerc
LAPerc
DHAPerc
PUFA.MUFA
Omega.6.Omega.3
b
Metabolites
Amino acids
Alanine
Glutamine
Glycine
Histidine
Isoleucine
Leucine
Valine
Phenylalanine
Tyrosine
TotalBCAA
Glycolysis products
Glucose
Lactate
Pyruvate
Citrate
Ketone bodies
bOHbutyrate
Acetate
Acetoacetate
Acetone
Fluid balance
Creatinine
Albumin
GlycA
Other lipids
Phosphoglyc
Cholines
Phosphatidylic
Sphingomyelins
TG.PG
Apolipoproteins
ApoB
ApoA1
ApoB.ApoA1
Fatty acids
Omega.3
Omega.6
PUFA
MUFA
SFA
LA
DHA
Total FA
Unsaturation
Fatty acid ratios
Omega.3Perc
Omega.6Perc
PUFAPerc
MUFAPerc
SFAPerc
LAPerc
DHAPerc
PUFA.MUFA
Omega.6.Omega.3
c
Metabolites
Amino acids
Alanine
Glutamine
Glycine
Histidine
Isoleucine
Leucine
Valine
Phenylalanine
Tyrosine
TotalBCAA
Glycolysis products
Glucose
Lactate
Pyruvate
Citrate
Ketone bodies
bOHbutyrate
Acetate
Acetoacetate
Acetone
Fluid balance
Creatinine
Albumin
GlycA
Other lipids
Phosphoglyc
Cholines
Phosphatidylic
Sphingomyelins
TG.PG
Apolipoproteins
ApoB
ApoA1
ApoB.ApoA1
Fatty acids
Omega.3
Omega.6
PUFA
MUFA
SFA
LA
DHA
Total FA
Unsaturation
Fatty acid ratios
Omega.3Perc
Omega.6Perc
PUFAPerc
MUFAPerc
SFAPerc
LAPerc
DHAPerc
PUFA.MUFA
Omega.6.Omega.3

Figure S2. Postprandial metabolite after interventions. a) VEGE intervention; b) AMF intervention; c) CREAM intervention. [a]Border only coloured for metabolites with significant differences between shakes (post-hoc).[b]Colour inside the box represents log2 ratio and is only coloured for metabolites with a significant shake*time effect (LMM) and border only coloured for metabolites with significant shake*time at specific timepoints (post-hoc). Red border indicates significant difference between VEGE and AMF. Black border indicates significant difference between VEGE and CREAM. Pink border indicates a significant difference between VEGE, and AMF and CREAM. Abbreviations: beta-hydroxybutyric acid (bOHbutyrate), docosahexaenoic acid (DHA,) fatty acid (FA), linoleic acid (LA), monounsaturated fatty acid (MUFA), polyunsaturated fatty acid (PUFA), saturated fatty acid (SFA), Total branched-chain amino acids (Total BCAA).

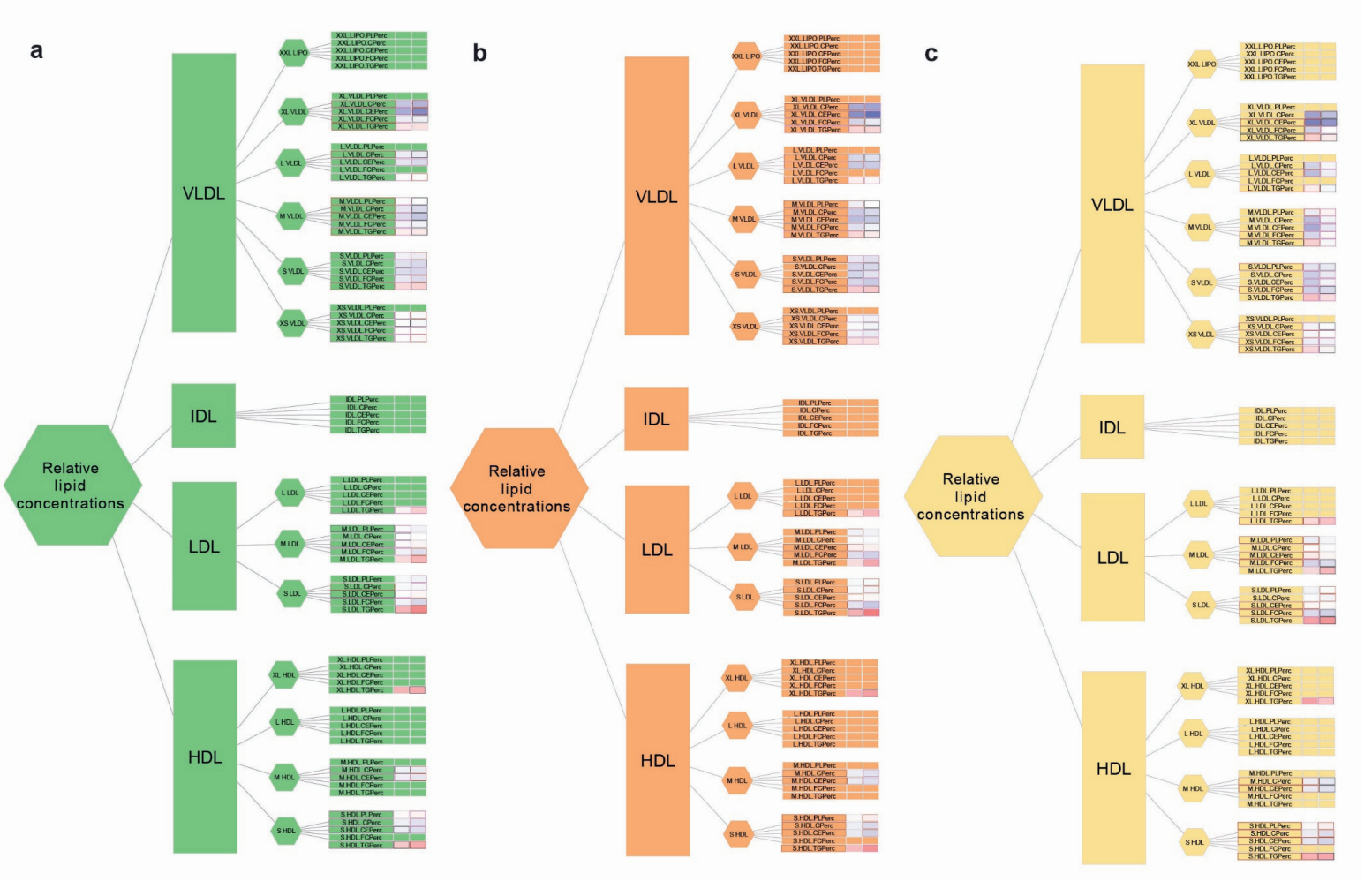
a
Relative lipid concentrations
VLDL
IDL
LDL
HDL
XXL LIPO
XL VLDL
L VLDL
M VLDL
S VLDL
XS VLDL
XXL_LIPO.PLPerc
XXL_LIPO.CPerc
XXL_LIPO.CEPerc
XXL_LIPO.FCPerc
XXL_LIPO.TGPerc
XL_VLDL.PLPerc
XL_VLDL.CPerc
XL_VLDL.CEPerc
XL_VLDL.FCPerc
XL_VLDL.TGPerc
L_VLDL.PLPerc
L_VLDL.CPerc
L_VLDL.CEPerc
L_VLDL.FCPerc
L_VLDL.TGPerc
M_VLDL.PLPerc
M_VLDL.CPerc
M_VLDL.CEPerc
M_VLDL.FCPerc
M_VLDL.TGPerc
S_VLDL.PLPerc
S_VLDL.CPerc
S_VLDL.CEPerc
S_VLDL.FCPerc
S_VLDL.TGPerc
XS_VLDL.PLPerc
XS_VLDL.CPerc
XS_VLDL.CEPerc
XS_VLDL.FCPerc
XS_VLDL.TGPerc
IDL_PLPerc
IDL_CPerc
IDL_CEPerc
IDL_FCPerc
IDL_TGPerc
L LDL
M LDL
S LDL
L_LDL.PLPerc
L_LDL.CPerc
L_LDL.CEPerc
L_LDL.FCPerc
L_LDL.TGPerc
M_LDL.PLPerc
M_LDL.CPerc
M_LDL.CEPerc
M_LDL.FCPerc
M_LDL.TGPerc
S_LDL.PLPerc
S_LDL.CPerc
S_LDL.CEPerc
S_LDL.FCPerc
S_LDL.TGPerc
XL HDL
L HDL
M HDL
S HDL
XL_HDL.PLPerc
XL_HDL.CPerc
XL_HDL.CEPerc
XL_HDL.FCPerc
XL_HDL.TGPerc
L_HDL.PLPerc
L_HDL.CPerc
L_HDL.CEPerc
L_HDL.FCPerc
L_HDL.TGPerc
M_HDL.PLPerc
M_HDL.CPerc
M_HDL.CEPerc
M_HDL.FCPerc
M_HDL.TGPerc
S_HDL.PLPerc
S_HDL.CPerc
S_HDL.CEPerc
S_HDL.FCPerc
S_HDL.TGPerc
b
Relative lipid concentrations
VLDL
IDL
LDL
HDL
c
Relative lipid concentrations
VLDL
IDL
LDL
HDL

Figure S3. Postprandial relative lipid concentrations after interventions. a) VEGE intervention; b) AMF intervention; c) CREAM intervention. [a]Border only coloured for metabolites with significant differences between shakes (post-hoc)._[b]Colour inside the box represents log2 ratio and is only coloured for metabolites with a significant shake*time effect (LMM) and border only coloured for metabolites with significant shake*time at specific timepoints (post-hoc). Red border indicates significant difference between VEGE and AMF. Black border indicates significant difference between VEGE and CREAM. Pink border indicates a significant difference between VEGE, and AMF and CREAM. Abbreviations: cholesterol (C), cholesterol esters (CE), free cholesterol (FC), high-density lipoprotein (HDL), intermediate-density lipoprotein (IDL), low-density lipoprotein (LDL), phospholipids (PL), triglycerides (TG), very low-density lipoprotein (VLDL)

CHARPTER 5

Milk fat globule membrane modulates inflammatory pathways in human monocytes: a crossover human intervention

Lei Deng, Charlotte C.J.R. Michelsen, Frank Vrieling, Guido J.E.J. Hooiveld, Rinke Stienstra, Anouk L. Feitsma, Sander Kersten, Lydia A. Afman

To be submitted

ABSTRACT

Intake of high-fat foods leads to a postprandial elevation in plasma triglycerides and inflammatory markers, which may be modulated by the type of fat ingested. Dairy products are commonly consumed but not much is known about the impact of milk fat and the milk fat globule membrane on postprandial inflammation. Here, we aimed to study the effect of milk fat with and without milk fat globule membrane on post-prandial inflammation, with a focus on blood monocyte gene expression. To that end, we performed a randomized, double-blind cross-over trial in 37 middle-aged healthy male and female volunteers. The participants consumed a meal shake containing 95.5 g of fat consisting of either a vegetable fat blend (VEGE), anhydrous milk fat (AMF), or cream (CREAM). Blood monocytes were collected at 0 hours and 6 hours postprandially and used for bulk RNA sequencing analysis and ex vivo incubation with LPS.

Consumption of all three shakes led to a significant postprandial decrease in the percentage of classic monocytes and a significant increase in the percentages of intermediate monocytes and non-classic monocytes. However, no significant differences were observed between the postprandial effects of the three interventions on monocyte subsets. Using a threshold of $P<0.01$, 787 genes were differentially regulated postprandially between the three shakes. 89 genes were differentially regulated postprandially between AMF and VEGE, while 373 genes were differentially regulated between AMF and CREAM and 667 genes between VEGE and CREAM, indicating that the effect of CREAM on monocyte gene expression was very distinct from AMF and VEGE. Pathway analyses showed that VEGE significantly activated inflammatory pathways, while this was less evident after AMF and oppositely after CREAM. CREAM significantly down-regulated energy metabolism-related pathways, such as glycolysis, TCA cycle, and oxidative phosphorylation, as well as HIF1 signaling.

In conclusion, compared to acute consumption of a vegetable fat blend and anhydrous milk fat, cream significantly downregulated energy and inflammation-related pathways in blood monocytes, suggesting a potential anti-inflammatory effect of MFGM.

Keywords: transcriptomics, milk fat, milk fat globule membrane, energy metabolism, monocytes

INTRODUCTION

Triglycerides are a major source of energy in the human diet. After a meal, dietary triglycerides enter the bloodstream packaged into large emulsion particles called chylomicrons. Most of the chylomicrons are processed in the adipose tissue, where the triglycerides are hydrolyzed by the enzyme lipoprotein lipase (LPL). Elevated levels of triglycerides after a meal, referred to as postprandial lipemia, are associated with an increased risk of cardiovascular disease (Ginsberg et al., 2021; Nakamura et al., 2016). As a consequence, major efforts are undertaken to try to develop strategies aimed at attenuating the postprandial triglyceride response, for instance by enhancing LPL-mediated lipolysis (Tall et al., 2022).

In addition to lipemia, the postprandial state is associated with postprandial inflammation. This postprandial inflammatory response may be characterized by increased plasma levels of inflammatory markers, such as IL-6, TNFa, VCAM1, ICAM1, and endotoxins (Esser et al., 2013; Lundman et al., 2007; Margioris, 2009; Meessen et al., 2019; Nappo et al., 2002), as well as altered inflammatory gene expression in PBMC and monocytes (Bouwens et al., 2010; Esser et al., 2015a; Milan et al., 2017). It is thought that postprandial inflammation is closely connected to postprandial lipemia, possibly because of the direct activation of immune cells by triglyceride-rich lipoproteins (Alipour et al., 2008). Persistently increased postprandial inflammation may potentially contribute to a state of chronic low-grade inflammation, which is a common feature of cardiometabolic diseases.

An important fat source in the Western diet is dairy. For example, in the Netherlands, nearly 20% of the total dietary fat intake and nearly 33% of the intake of saturated fatty acids is derived from dairy. Besides being rich in saturated fatty acids, milk fat is characterized by the presence of trans, branched- and odd-chain fatty acids and by the high content of butyrate. Additionally, milk fat is unique in that palmitate is enriched in the Sn-2 position, whereas in common sources of vegetable fat, palmitate is highly enriched in the Sn1,3 position. Another special property of milkfat is that it contains so-called milk fat globule membranes (MFGM). MFGM form the perimeter of the milkfat globules and are enriched with glycerophospholipids and sphingolipids, especially sphingomyelin, phosphatidylcholine, and phosphatidylethanolamine. Other components of the MFGM include proteins, cholesterol, and other lipid species. Although several studies have pointed to the positive health properties of MFGM in a variety of clinical contexts, including behavioral development, insulin sensitivity, and plasma lipids, our overall understanding of the potential health effects of MFGM is still very limited (Raza et al., 2021).

Previous studies have shown that the acute postprandial inflammatory response may depend on the type of fat ingested. We previously observed that saturated and mono-unsaturated differentially affected gene expression in human PBMC (Bouwens et al., 2010; Esser et al., 2015a). Specifically, SFA decreased the expression of cholesterol biosynthesis and uptake genes and increased cholesterol efflux genes, whereas MUFA increased inflammatory genes and PPAR-α targets involved in β-oxidation (Esser et al., 2015a). Similarly, dietary fatty acid composition substantially impacted the postprandial changes in the PBMC proteome (Camargo et al., 2013). Concerning milkfat, it was observed that fermented dairy products, especially cheese, induce a less inflammatory postprandial PBMC gene expression response than non-fermented dairy products (Rundblad et al., 2020). However, a direct comparison between milk fat and vegetable fat, as well as an investigation of the specific role of MGFM has yet to be performed.

PBMCs consist of a variety of different cell types, including T lymphocytes, B lymphocytes, and monocytes. Monocytes are innate immune cells that circulate in the blood and differentiate into macrophages after entry into tissues. After a high-fat meal, monocytes are exposed to postprandial lipemia characterized by high levels of VLDL and chylomicrons in the circulation. These triglyceride-rich lipoproteins are taken up via caveolin-mediated endocytosis, leading to the time-dependent accumulation of lipids in monocytes after a high-fat meal (Khan et al., 2016; Varela et al., 2011). This postprandial increase in monocyte lipid uptake and storage is likely associated with changes in (inflammatory) gene expression. Interestingly, however, the postprandial impact of a high-fat meal on monocyte gene expression has not yet been investigated. In addition, to what extent these effects may differ between different fat sources and may be influenced by MGFM is completely unknown.

Here, we used RNAseq to compare the postprandial effect of the consumption of a high-fat meal containing cream (containing MFGM), anhydrous milk fat (lacking MFGM), or a vegetable fat blend on monocyte gene expression in healthy overweight volunteers.

RESULTS

Participants and interventions

Of the 40 participants that entered this study, 37 completed the study. One participant dropped out after the first study visit, and two dropped out after the second study visit. The baseline characteristics of the participants are shown in table 1. Monocytes were isolated from 37 participants. We selected monocyte mRNA samples with good quality RNA for whole transcriptome analysis, which included 18 from the VEGE intervention, 18 from the AMF intervention, and 15 from the CREAM intervention. Whole transcriptome data are available from 14 participants after both VEGE and AMF interventions, 11 participants after both CREAM and VEGE, and 11 participants after all three interventions. The flowchart of the participants is shown in Figure 1a.

Table 1. Participant characteristics of the 40 included participants in this study.

Data are presented as mean ± standard deviation.

Characteristic	
Gender (m/f)	9/31
Age (years)	57.3 ± 8.0
Weight (kg)	71.5 ± 8.5
Height (cm)	172.2 ± 7.7
BMI (kg/m^2)	24.1 ± 1.7
Waist circumference (cm)	
Men	92.2 ± 5.9
Women	81.8 ± 6.2
Hip circumference (cm)	
Men	102.6 ± 4.6
Women	102.2 ± 6.0
WHR	
Men	0.90 ± 0.05
Women	0.80 ± 0.05
Hb (mmol/L)	8.4 ± 0.6
ALAT (uL)	24.7 ± 11.8
ASAT (uL)	21.5 ± 7.3
Creatinine (umol/L)	71.6 ± 11.1

Abbreviations: alanine aminotransferase (ALAT), aspartate aminotransferase (ASAT), body mass index (BMI), hemoglobin (Hb), waist-hip ratio (WHR)

Postprandial changes in monocyte subsets

Using flow cytometry, we studied monocyte populations of 34 participants after consumption of the shakes. No significant differences were observed between the postprandial effects of the three interventions on monocyte subsets (Figure 1b-1d). However, there was a significant postprandial effect of all of the three shakes. Specifically, consumption of the three shakes led to a significant postprandial decrease in the percentage of classic monocytes and a significant increase in the percentages of intermediate monocytes and non-classic monocytes (Figure 1e).

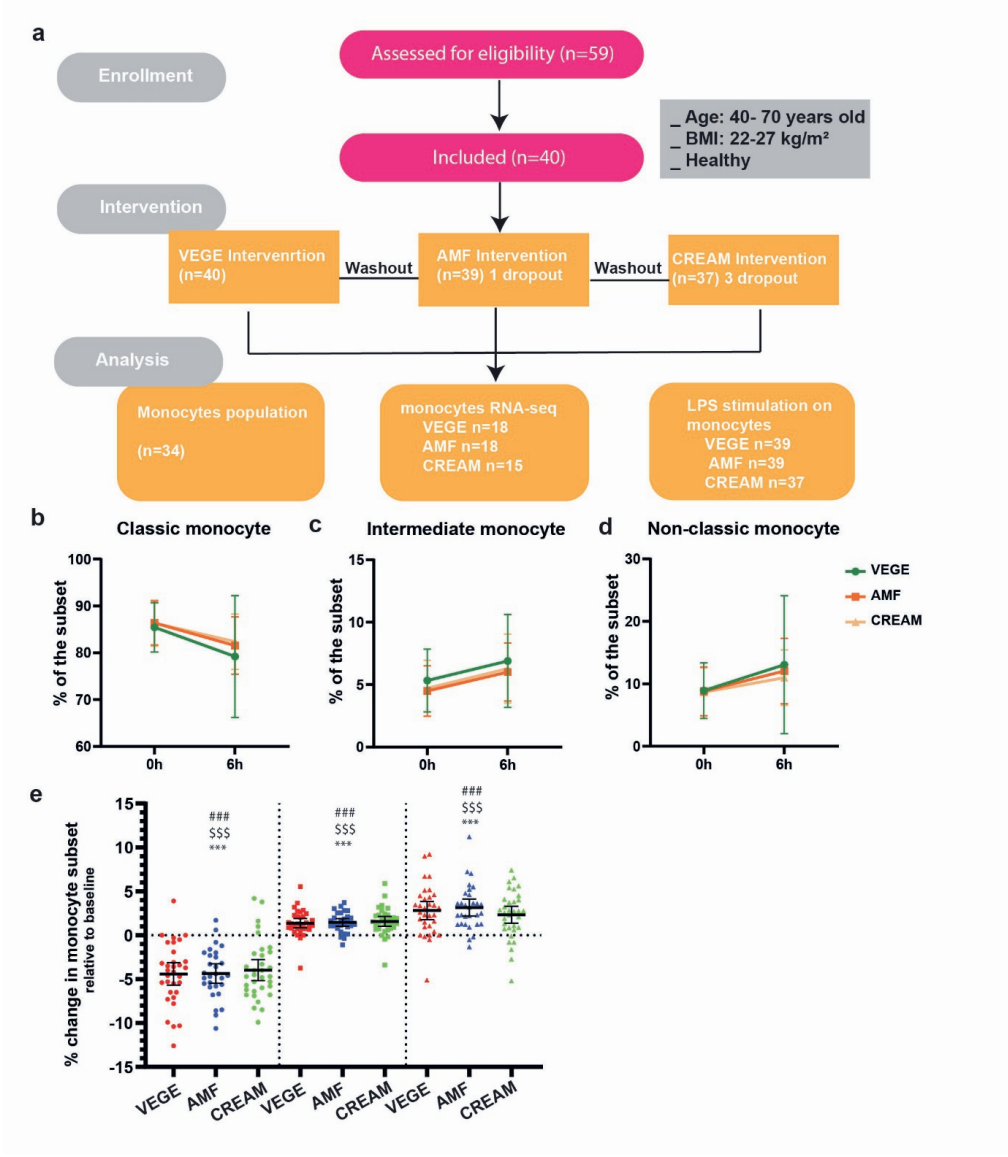

Figure 1. No regulation of three interventions on the postprandial effect of high-fat meals.

(a). Flow charts of study participants. (b-e) The changes of monocyte population of the participants after fat shake consumption. #, $ and * indicate significant postprandial change. ### p<0.001, $$$ p<0.001 and ***p<0.001

CREAM differentially modules the monocyte whole transcriptome than AMF and VEGE

The nutritional composition of the shakes, including the fatty acid composition, is depicted in Table 2 and 3. The total amount of fat was the same across the shakes. However, the VEGE shake had a lower percentage of saturated fatty acids and a higher percentage of mono- and polyunsaturated fatty acids than the milk-based shakes, whose fatty acid compositions were highly similar. Specifically, saturated fatty acids (SFA) accounted for 41.3% of the total fatty acids in VEGE, 70.4% in AMF, and 71.2% in CREAM. VEGE was rich in both monounsaturated fatty acids (MUFA, 40.0%) and polyunsaturated fatty acids (PUFA, 18.6%). Compared to VEGE, the percentage of MUFA and PUFA was much lower in AMF and CREAM at around 25.0% and 3.0%, respectively. The majority of PUFA in VEGE are omega-6 fatty acids, which accounted for 17.0% of total fatty acids. By comparison, PUFA represent 1.8% of total fatty acids in AMF and CREAM.

Table 2 Intervention shake contents

	VEGE & AMF	CREAM
Powder (118 g)		
Fat (g)	95,0	95,0
Protein (g)	2,4	4,2
Lactose (g)	0,2	5,5
Glucose (g)	17,6	11,3
Milk +water		
Fat (g)	0,5	0,5
Protein (g)	18,5	17,0
Lactose (g)	24,5	22,5
Glucose (g)	0,0	3,2
Total		
Fat (g)	95,5	95,5
Protein (g)	20,9	21,2
Carbs (g)	42,3	42,5
Total Energy (KJ)	**4748**	

Table 3 Fatty acids composition of intervention shakes

	VEGE	AMF	CREAM
C4:0		3.9	3.8
C6:0	<0.1	2.3	2.4
C8:0	1.0	1.3	1.4
C10:0	0.8	3.0	3.2
C11:0	<0.1	0.4	0.4
C12:0	11.5	3.9	4.2
C12:1w1cis		0.1	0.1
C14:0	4.1	11.4	11.6
C14:1w5cis		1.0	1.1
C15:0	<0.1	1.1	1.1
C15:iso		0.2	0.2
C15:aiso		0.4	0.4
C16:0	19.8	30.4	31.4
C16:iso	<0,1	0.2	0.2
C16:1w7cis	0.1	1.5	1.6
C17:0	<0.1	0.5	0.5
C17:iso		0.4	0.3
C17:aiso	<0,1	0.7	0.6
C17:1w7cis	<0,1	0.2	0.2
C18:0	3.3	9.7	9.1
C18:1	37.7	18.3	17.9
C18:1w7tr		1.3	1.0
C18:1w12tr		0.1	0.1
C18:1w12cis		0.8	0.7
C18:1w9tr	<0,1	0.2	0.2
C18:1w9cis	1.6	0.7	0.7
C18:1w6cis		0.8	0.7
C18:2w6cis	16.9	1.3	1.4
C18:2conj cis9t11		0.5	0.4
C18:3	1.6	0.5	0.4
C20:1	0.4	<0.1	<0.1
C22:6w3cis	<0,1	<0,1	<0,1
Summary			

Saturated fatty acids	41.3	70.4	71,2
Monounsaturated fatty acids	40.0	25.2	24.5
Polyunsaturated fatty acids	18.6	2.8	2,6
Trans fatty acids	1.6	0.7	0.6
Omega-3 fatty acids	17,0	1.8	1.8
Omega-6 fatty acids	17,0	1.8	1.8
Sn-2 palmitate	15%	45%	45%

To establish the postprandial effect of the different shakes on gene expression in monocytes, a whole transcriptome bulk RNAseq analysis was performed. After filtering, 12,770 protein-coding genes with substantial expression remained from a total of 60,232 transcripts. The focus of the analysis was on the differential effects of the three interventions, rather than on the effects of the individual shakes, which under the study design overlaps with the effect of time on gene expression. An ANOVA-like F-test was performed to analyze the differential effect of the VEGE, AMF, and CREAM interventions on whole transcriptome gene expression. Using a threshold of $p<0.01$, 787 genes were differentially regulated postprandially between the three shakes. In total, 89 genes were differentially regulated postprandially by the AMF intervention compared to the VEGE intervention, while 373 genes were differentially regulated by AMF compared to CREAM and 667 genes were differentially regulated by VEGE compared to CREAM ($p<0.01$) (Figure 2a). These numbers indicate that the effects of the CREAM intervention on monocyte gene expression were very distinct from the AMF intervention and VEGE intervention. A heatmap of the average change in expression of these genes differentially expressed between all shakes is shown in Figure 2b.

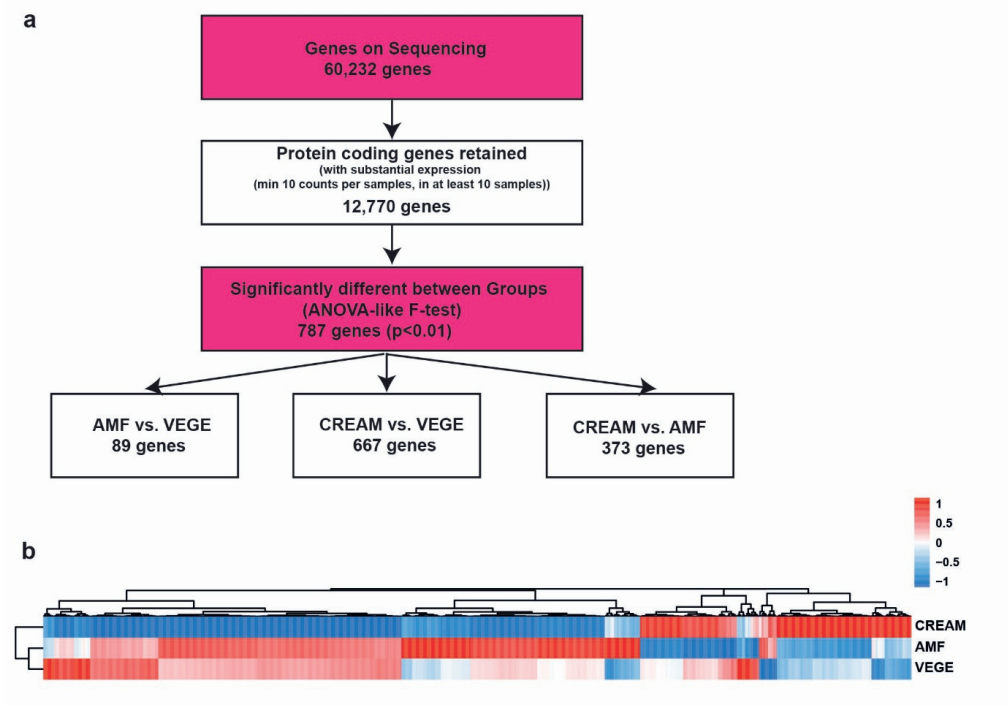

Figure 2. Distinct effects of VEGE, AMF, and CREAM intervention on the whole transcriptome of monocytes.

(a) the number of genes differentially changed between interventions (ANOVA-like F-test). (b) The heatmap of genes significantly changed in any between-shake comparisons (ANOVA-like F-test) and as well were significantly regulated by any shakes ($p<0.01$).

To gain more insight into the specific biological pathways affected by the different interventions, we performed Gene Set Enrichment Analysis (GSEA). Many pathways were commonly stimulated by the VEGE and AMF interventions (Figure 3a), while many other pathways were uniquely suppressed by the CREAM intervention (Figure 3b-3c). In the between-shake comparisons, several differentially regulated pathways (FDR $q<0.25$) were identified in the comparison of CREAM and VEGE (119 gene sets) and the comparison of CREAM and AMF (100 gene sets), whereas fewer gene sets were differentially regulated between AMF and VEGE (26 gene sets) (Figure 3d). This indicates a similarity in the postprandial effects of AMF and VEGE on monocyte gene expression and a distinct effect of CREAM. By analyzing these pathways in the different categories defined by KEGG, we found that numerous energy metabolism-related gene sets were upregulated by VEGE, not regulated by AMF, and downregulated by CREAM (Figure 4a). Gene sets related to environmental information processing and immune and metabolic pathways were specifically upregulated by VEGE or upregulated by VEGE and AMF, respectively (Figure 4b-4c).

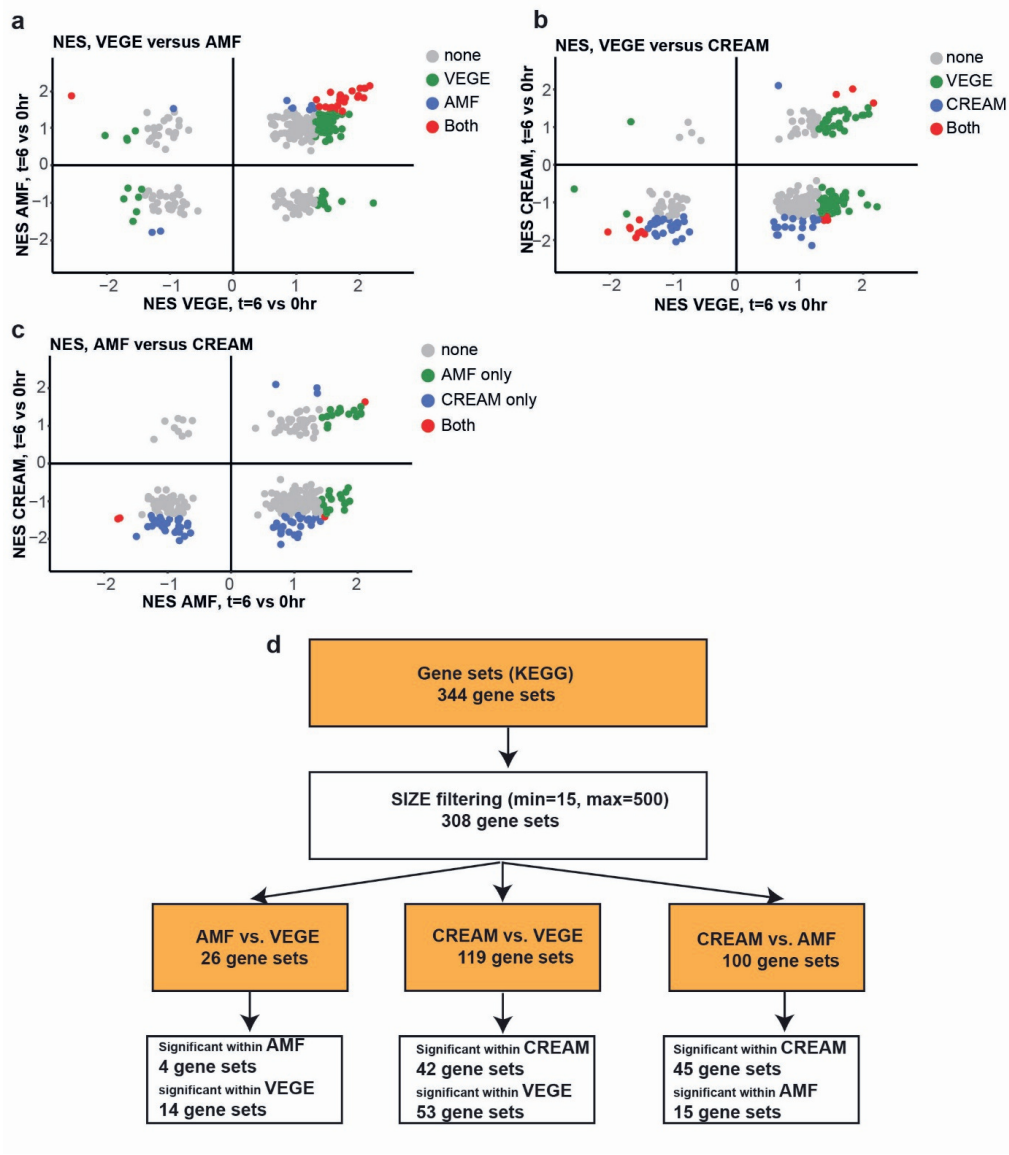

Figure 3. Differential effects of the interventions on KEGG pathways (GSEA analysis).

Similarity analysis of regulation on pathways by (a) VEGE and AMF intervention, (b) VEGE and CREAM intervention, and (c) AMF and CREAM intervention. The colored dot represents the significantly regulated pathway. (d). The flowchart shows the number of gene sets differentially changed between interventions.

Milk fat-based shakes promoted a lower postprandial inflammatory response in monocytes

A Cytoscape map was plotted to visualize the overlapping genes and highlight clusters (Figure 4d). We found that inflammation-related pathways (in cluster 1), such as the TNF signaling pathway and Toll-like receptor signaling pathway, were significantly upregulated by the VEGE shake but were not significantly altered by the AMF and CREAM shake. In line with this, a heatmap of the leading-edge genes showed an overall pattern of upregulation by VEGE, which was less pronounced or even opposite in response to the AMF and CREAM intervention, respectively (Figure 5a). The genes accounting for the 'positive regulation of the inflammatory response' (GO:0050729) were induced by the VEGE intervention, showed a partly similar response to the AMF intervention, and were generally downregulated by the CREAM intervention (Figure 5b).

To investigate the functional consequence of consumption of the different shakes on the monocytes, monocytes were isolated at baseline and 6 hours postprandially and incubated with LPS, followed by the measurement of the ex vivo release of cytokines. The LPS-induced release of TNFα by monocytes was decreased after the consumption of all three shakes compared to baseline (Figure 5c). However, no significant differences in the postprandial decrease in LPS-induced TNFα release were observed between the shakes. No significant postprandial effect was observed on LPS-induced secretion of IL- for any of the shakes (Figure 5d).

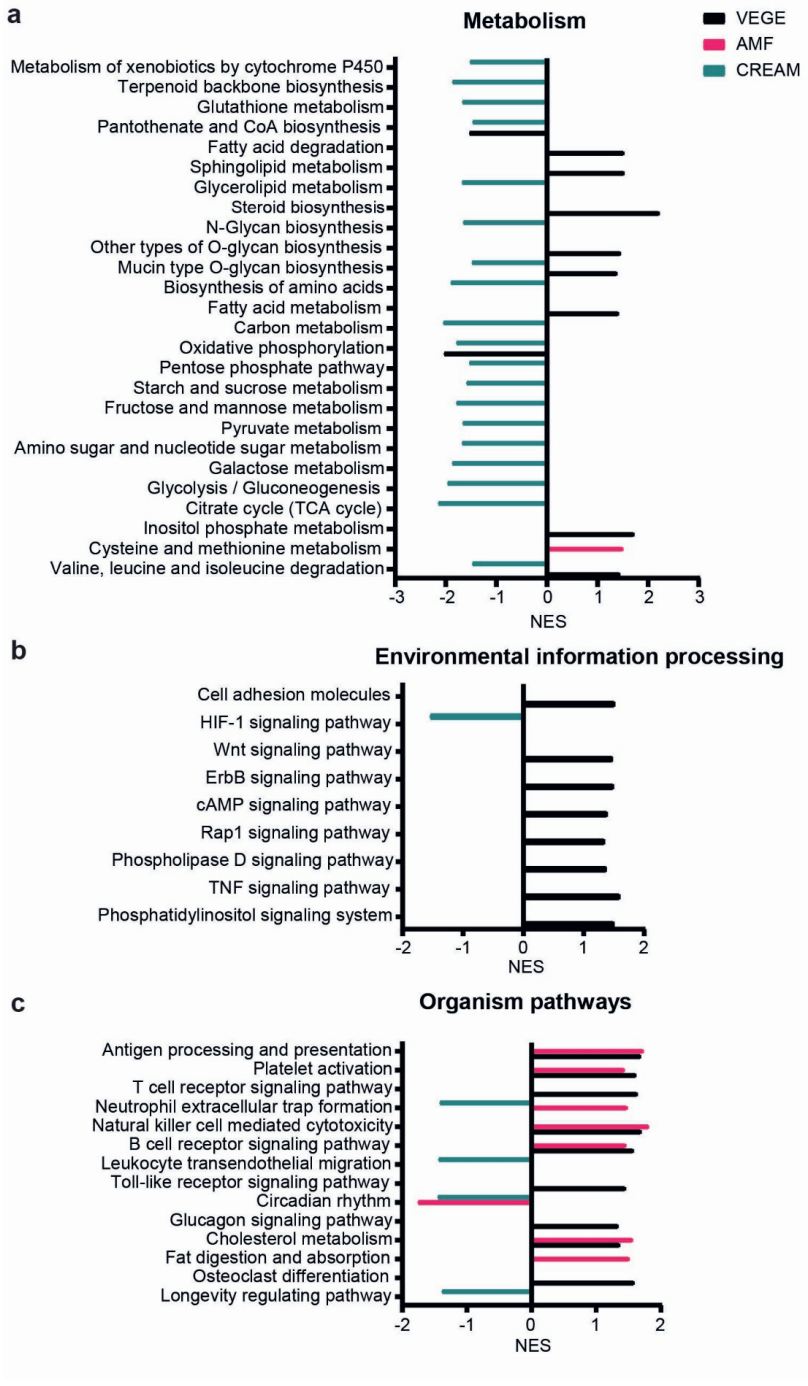
a
Metabolism
VEGE
AMF
CREAM
Metabolism of xenobiotics by cytochrome P450
Terpenoid backbone biosynthesis
Glutathione metabolism
Pantothenate and CoA biosynthesis
Fatty acid degradation
Sphingolipid metabolism
Glycerolipid metabolism
Steroid biosynthesis
N-Glycan biosynthesis
Other types of O-glycan biosynthesis
Mucin type O-glycan biosynthesis
Biosynthesis of amino acids
Fatty acid metabolism
Carbon metabolism
Oxidative phosphorylation
Pentose phosphate pathway
Starch and sucrose metabolism
Fructose and mannose metabolism
Pyruvate metabolism
Amino sugar and nucleotide sugar metabolism
Galactose metabolism
Glycolysis / Gluconeogenesis
Citrate cycle (TCA cycle)
Inositol phosphate metabolism
Cysteine and methionine metabolism
Valine, leucine and isoleucine degradation
-3 -2 -1 0 1 2 3
NES
b
Environmental information processing
Cell adhesion molecules
HIF-1 signaling pathway
Wnt signaling pathway
ErbB signaling pathway
cAMP signaling pathway
Rap1 signaling pathway
Phospholipase D signaling pathway
TNF signaling pathway
Phosphatidylinositol signaling system
-2 -1 0 1 2
NES
c
Organism pathways
Antigen processing and presentation
Platelet activation
T cell receptor signaling pathway
Neutrophil extracellular trap formation
Natural killer cell mediated cytotoxicity
B cell receptor signaling pathway
Leukocyte transendothelial migration
Toll-like receptor signaling pathway
Circadian rhythm
Glucagon signaling pathway
Cholesterol metabolism
Fat digestion and absorption
Osteoclast differentiation
Longevity regulating pathway
-2 -1 0 1 2
NES

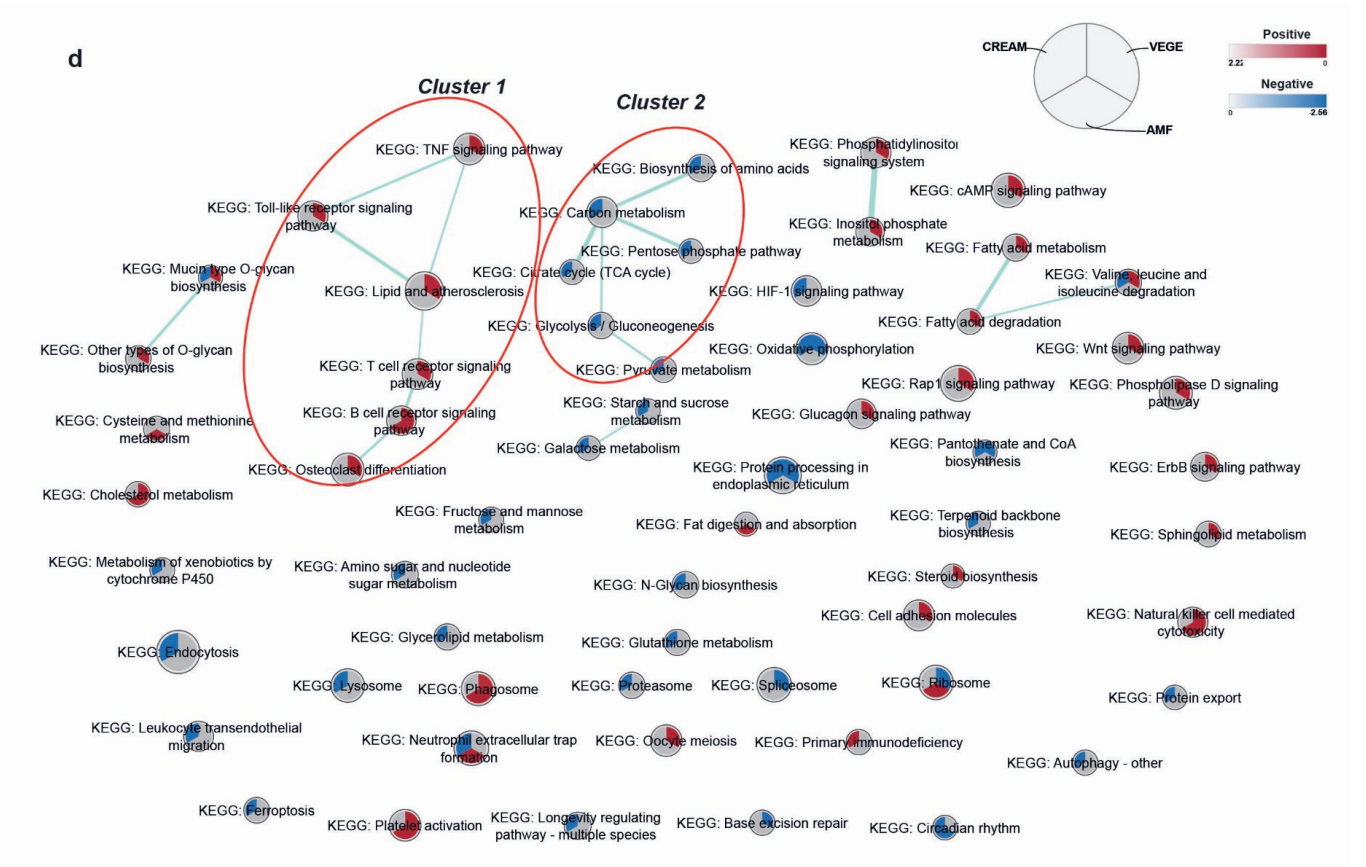
d
Cluster 1
Cluster 2
CREAM
VEGE
AMF
Positive
Negative
KEGG: TNF signaling pathway
KEGG: Toll-like receptor signaling pathway
KEGG: Mucin type O-glycan biosynthesis
KEGG: Lipid and atherosclerosis
KEGG: Other types of O-glycan biosynthesis
KEGG: T cell receptor signaling pathway
KEGG: Cysteine and methionine metabolism
KEGG: B cell receptor signaling pathway
KEGG: Osteoclast differentiation
KEGG: Cholesterol metabolism
KEGG: Biosynthesis of amino acids
KEGG: Carbon metabolism
KEGG: Pentose phosphate pathway
KEGG: Citrate cycle (TCA cycle)
KEGG: Glycolysis / Gluconeogenesis
KEGG: Pyruvate metabolism
KEGG: Starch and sucrose metabolism
KEGG: Galactose metabolism
KEGG: Fructose and mannose metabolism
KEGG: Metabolism of xenobiotics by cytochrome P450
KEGG: Amino sugar and nucleotide sugar metabolism
KEGG: Endocytosis
KEGG: Glycerolipid metabolism
KEGG: Lysosome
KEGG: Phagosome
KEGG: Leukocyte transendothelial migration
KEGG: Neutrophil extracellular trap formation
KEGG: Ferroptosis
KEGG: Platelet activation
KEGG: Longevity regulating pathway - multiple species
KEGG: Phosphatidylinositol signaling system
KEGG: Inositol phosphate metabolism
KEGG: HIF-1 signaling pathway
KEGG: Oxidative phosphorylation
KEGG: Protein processing in endoplasmic reticulum
KEGG: Fat digestion and absorption
KEGG: N-Glycan biosynthesis
KEGG: Glutathione metabolism
KEGG: Proteasome
KEGG: Spliceosome
KEGG: Oocyte meiosis
KEGG: Base excision repair
KEGG: cAMP signaling pathway
KEGG: Fatty acid metabolism
KEGG: Valine, leucine and isoleucine degradation
KEGG: Fatty acid degradation
KEGG: Wnt signaling pathway
KEGG: Rap1 signaling pathway
KEGG: Phospholipase D signaling pathway
KEGG: Glucagon signaling pathway
KEGG: Pantothenate and CoA biosynthesis
KEGG: ErbB signaling pathway
KEGG: Terpenoid backbone biosynthesis
KEGG: Sphingolipid metabolism
KEGG: Steroid biosynthesis
KEGG: Cell adhesion molecules
KEGG: Natural killer cell mediated cytotoxicity
KEGG: Ribosome
KEGG: Protein export
KEGG: Primary immunodeficiency
KEGG: Autophagy - other
KEGG: Circadian rhythm

Figure 4. Less activation or inhibitory effects of AMF and CREAM on postprandial metabolism-related pathways (GSEA analysis).

Pathways are differentially regulated in between-intervention comparisons and significantly regulated by at least one intervention (FDR q<0.25) in the KEGG category (a) metabolism, (b) environmental information process, and (c) organism systems by different interventions (FDR q<0.25). (d) Cytoscape analysis of significantly regulated pathways in between-shake comparisons.

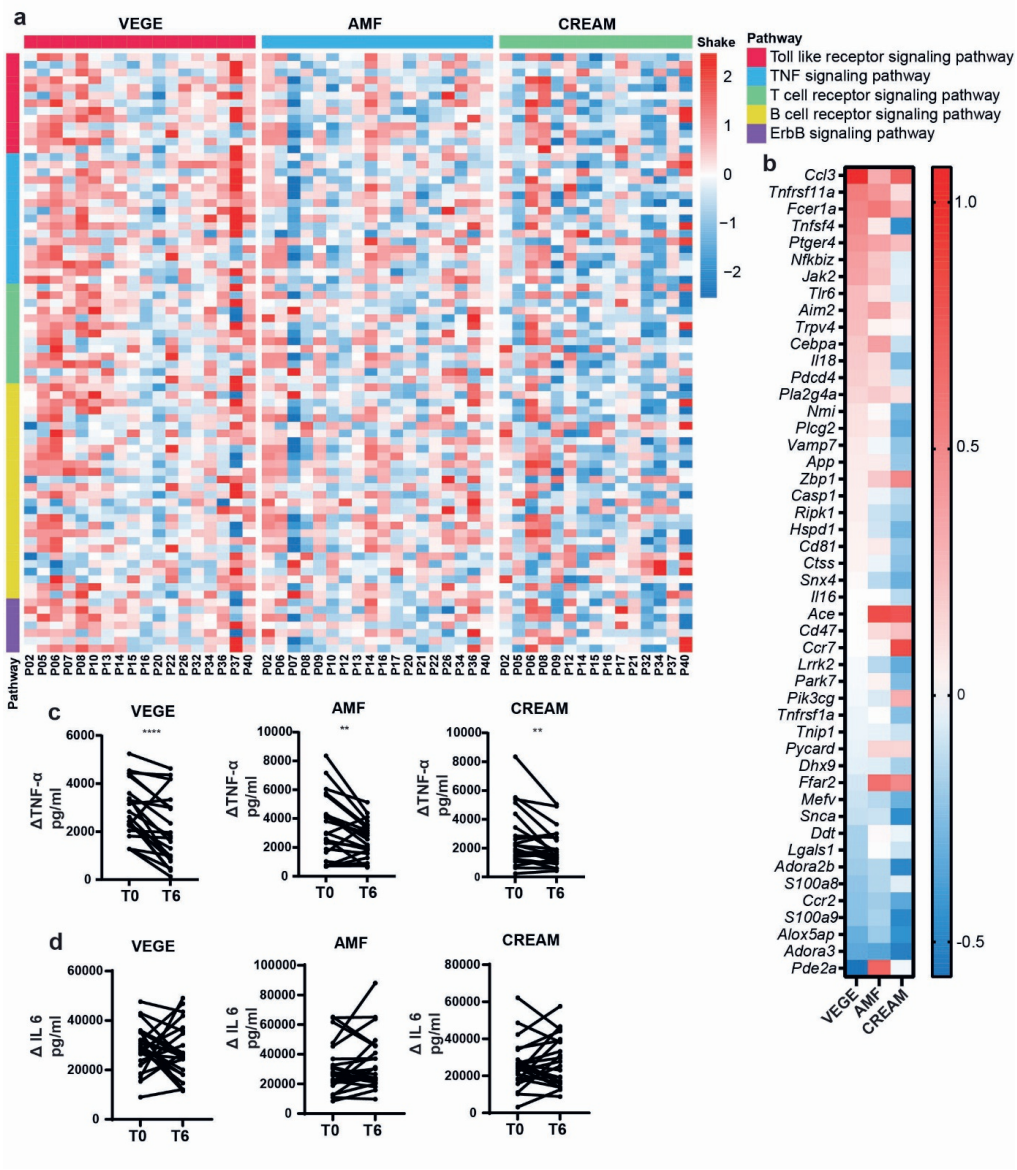

Figure 5. Less activation of inflammatory response-related pathways by AMF and CREAM intervention compared with VEGE intervention.

Heatmaps of (a) leading-edge genes in the pathways of interest with differential expression after at least one intervention ($p<0.05$), (b) genes involved in the inflammatory response and differentially regulated by at least one intervention. (c) The levels of TNFα in the culture medium of monocytes isolated from participants. (d) IL6 concentration in the culture medium.

Milk fat globule membrane suppresses energy metabolism-related signaling pathways

As shown in Figures 4a and 4d (cluster 2), the CREAM intervention downregulated energy metabolism pathways in monocytes, including glycolysis, TCA cycle, and oxidative phosphorylation, the latter suggesting a slower mitochondrial activity. This is supported by the changes in leading-edge genes involved in these pathways (Figure 6a). We also evaluated the regulation of genes involved in ATP-coupled electron transportation (Figure 6b) and oxidative stress-related pathway (Figure 6c), suggesting a decreased mitochondrial activity in response to CREAM but not the other two interventions.

Lactate, the end product of anaerobic glycolysis, is produced in high amounts by innate immune cells during inflammatory activation, including by LPS treatment (Figure 6d). However, LPS-induced lactate production did not significantly differ between baseline and 6 hours postprandially for any of the shakes.

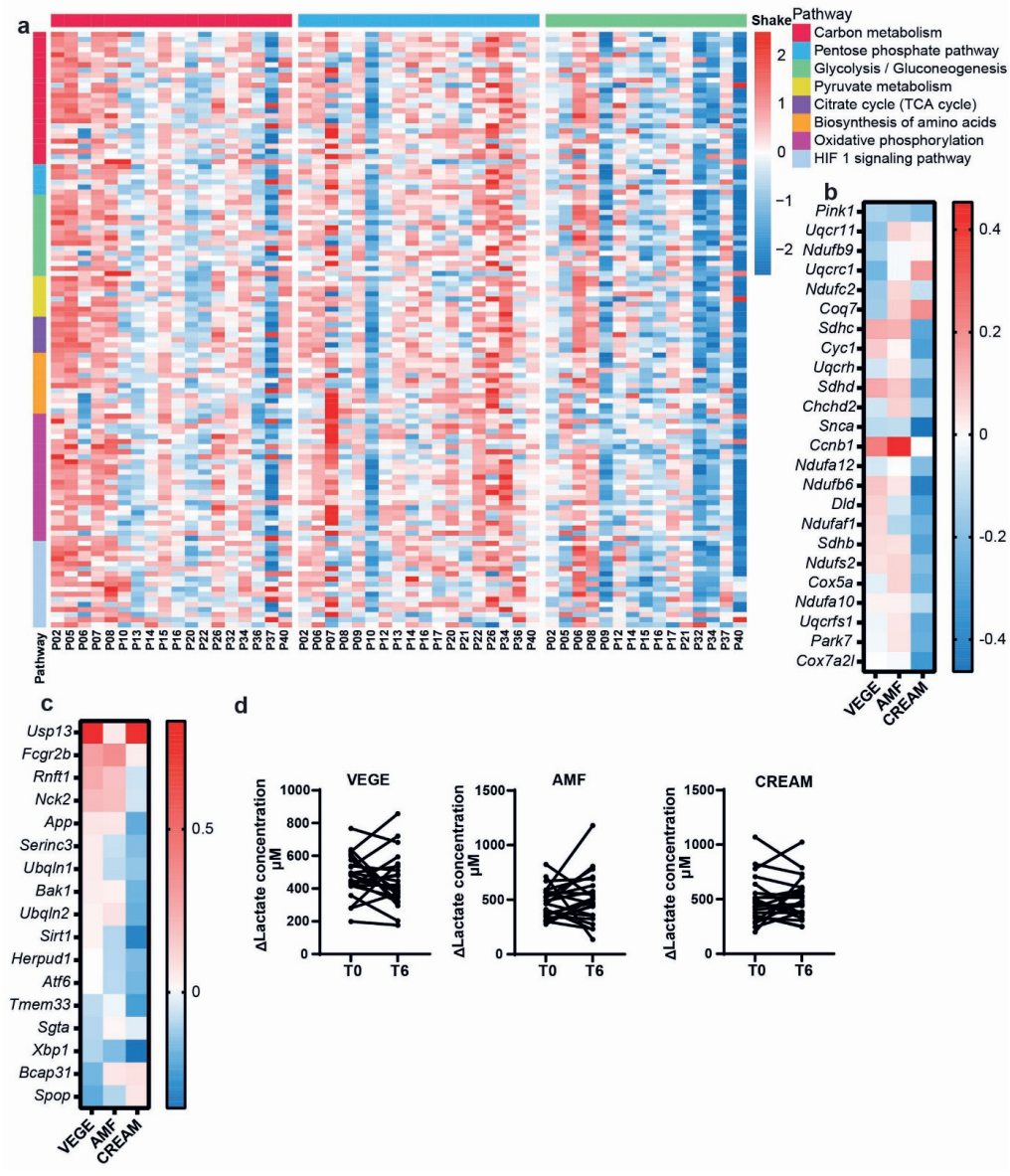

Figure 6 Inhibited effect of the CREAM intervention on energy metabolism-related pathways.

Heatmaps of (a) leading-edge genes of pathways of interest in Cytoscape and differentially regulated by at least one intervention, (b) genes involved in ATP electron coupled transportation, and (c) genes involved in oxidative stress. (d) Log2 fold change of genes related to lactate biosynthesis from pyruvate. (e) The levels of lactate in the culture medium of monocytes isolated from participants. The isolated monocytes were stimulated with 10 ng/ml LPS overnight.

Inhibited inflammation phenotype of monocytes parallels suppressed mitochondrial activity after the CREAM consumption: A prediction by Ingenuity Pathway Analysis (IPA)

Consistent with the above analysis, IPA predicted reduced secretion of several cytokines by CREAM compared to the VEGE and AMF interventions (Figure 7a). This differential effect is also demonstrated by the regulation network of transcriptome regulation (Figure S1). CSF1, one of the most important cytokines in inflammatory regulation in monocytes, was identified as the highest activated cytokine after VEGE intervention and also the most inhibited cytokine after the CREAM intervention (Figure 7a).

In the prediction of upstream transcription factors, we found that all transcription factors activated by VEGE are related to oxidative stress. These include Tcf7, SRF, SREBF2, and MRTFA (Figure 7b). In contrast, CREAM inhibited several mitochondrial homeostasis-related transcription factors, including KLF3, GPS2, and NFE2L2. NFE2L2 is an important transcription factor that responds to oxidative stress and was predicted to be one of the most highly inhibited. XBP1, a downstream transcription factor of NFE2L2, was inhibited by CREAM as well. By contrast, BACH1, which is an upstream negative regulator of NFE2L2 and XBP1, was significantly activated by CREAM (Figure 7b-7c).

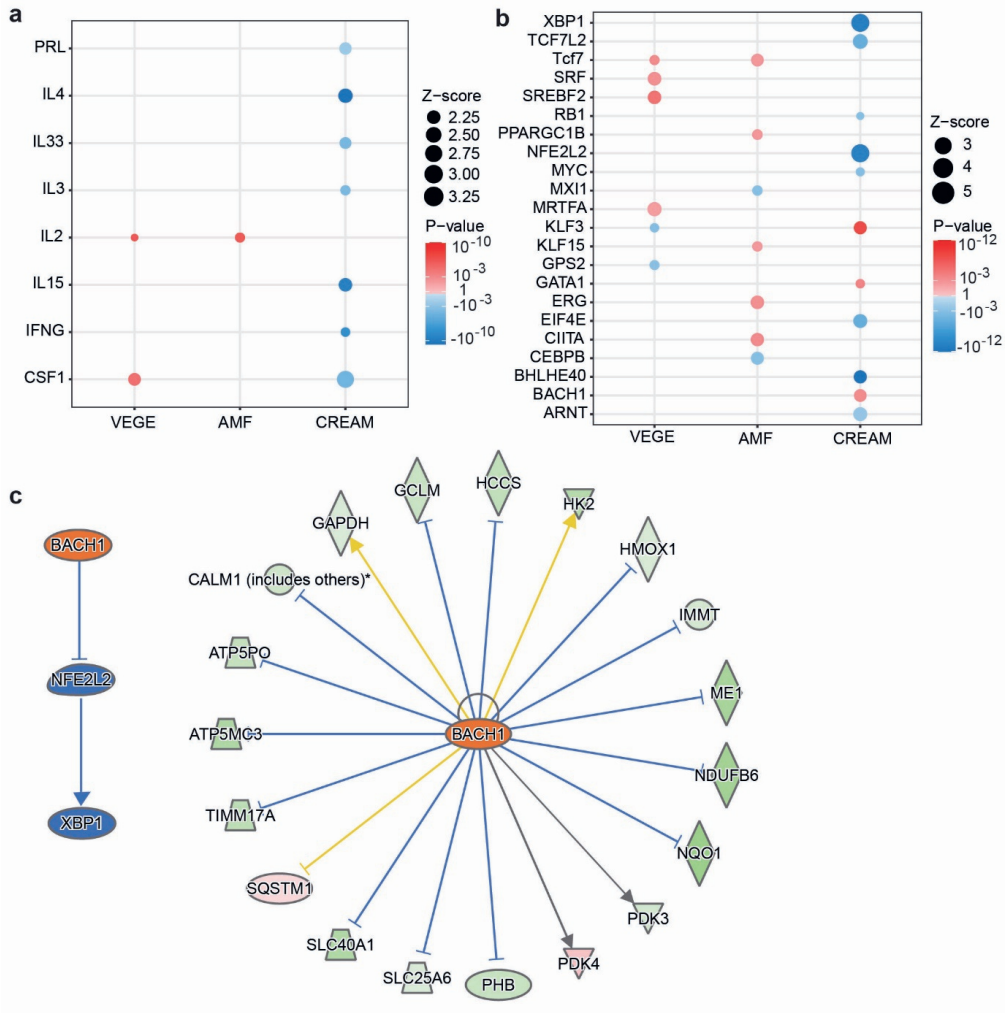

Figure 7. BACH1 is predicted as one master upstream transcription factor in mitochondrial metabolism regulation by MFGM.

IPA prediction of (a) upstream cytokines and (b) transcription factors regulated by three interventions. (c) Mechanism of prediction of the activation of BACH1 by CREAM intervention and its potential action process.

DISCUSSION

To gain more insight into the postprandial effect of milk fat on monocyte gene expression, a randomized crossover human trial was performed using high-fat shakes made with either a vegetable fat blend, anhydrous milk fat (lacking MFGM), and cream (containing MFGM). We evaluated the postprandial changes in the monocyte transcriptome after the three shakes and measured the ex vivo secretion of TNFα, IL6, and lactate by monocytes following LPS stimulation.

The three interventions differentially influenced the monocyte transcriptome. According to flow cytometry, all three shakes caused a significant shift in the monocyte population from a classic phenotype to an intermediate and non-classic phenotype. However, no differences in the postprandial effects were observed between the shakes, suggesting that the distinct postprandial effects of the three interventions on the monocyte transcriptome cannot be attributed to changes in the monocyte population. Overall, the most distinct effects were observed with CREAM. CREAM consumption was associated with inhibition of energy metabolism pathways, including oxidative phosphorylation, TCA cycle, and glycolysis. VEGE significantly activated fatty acid metabolism-related pathways, while this was not observed with AMF and CREAM consumption. One of our major findings was that consumption of VEGE led to a significant induction of inflammation-related pathways, which was observed to a much lower extent in response to AMF. By contrast, CREAM downregulated inflammatory pathways, suggesting an anti-inflammatory effect of MFGM.

The unique postprandial activation of fatty acid metabolism- and inflammation-related pathways in monocytes by VEGE is potentially linked to the high abundance of PUFA and possibly MUFA in the shake (Blaser et al., 2016; Cen et al., 2018; Frey and Brent Polk, 2014; Honda et al., 2014; Puri et al., 2013). Previously, we studied the postprandial effect of shakes rich in MUFA or SFA on the whole transcriptome in PBMCs (Esser et al., 2015b). In PBMCs, MUFA increased the expression of inflammatory genes and PPARα target genes involved in fatty acid degradation, which is in line with the observed effect of VEGE in monocytes. In PBMCs, SFA decreased the expression of genes involved in cholesterol biosynthesis and uptake. Despite the high content of SFA in milk fat, we did not observe a significant effect of AMF or CREAM on genes and pathways connected to cholesterol synthesis and uptake. These divergent results could be explained by the fact that in the present study we studied monocytes instead of PBMCs. Alternatively, they may be related to the use of milk fat as a source of SFA in the present study as compared to palm oil in the previous study.

In our study, we found that the phospholipase D signaling pathway, which can be stimulated by PUFA (Diaz-Aragon et al., 2019; Gemeinhardt et al., 2009; Ryu and Wang, 1998), was upregulated by

VEGE consumption. The phospholipase D pathway regulates intracellular signaling and metabolic pathways. Our data also show activation of cAMP signaling by VEGE, which on the one hand may be a downstream consequence of phospholipase D stimulation and on the other hand may contribute to the inflammatory response (Tavares et al., 2020).

CSF1 was predicted by IPA to be the most highly induced cytokine by VEGE. The activation of CSF-1 links to the phosphatidylinositol signaling system (Satriano et al., 1993; Varticovski et al., 1989) and the cAMP signaling pathway (Wilson et al., 1998, 2005), which were activated by VEGE in our study. In human monocytes, CSF1 acts as a key regulator of cell maturation, proliferation, and differentiation (Rathinam et al., 2011; Sweet et al., 2003; Warren and Ralph, 1986). Blocking the CSF-1 receptor has been shown to attenuate the secretion of multiple cytokines by monocytes (Sauter et al., 2016). Accordingly, it can be hypothesized that the pro-inflammatory effect of VEGE on human monocytes and the anti-inflammatory effect of CREAM are potentially mediated by the regulation of CSF-1 expression.

Intriguingly, we observed that CREAM consumption is predicted to activate the transcription factor BACH-1. Genetic BACH1 deficiency has been associated with decreased levels of various mitochondrial proteins, particularly mitochondrial complex I, and increased glycolysis and NLRP3 inflammasome activation (Pradhan et al., 2022). In addition, BACH1 was found to modulate PDK transcription, thereby decreasing the phosphorylation of pyruvate dehydrogenase in human breast cancer cells (Lee et al., 2019). The effect of the transcription factor BACH1 on mitochondrial activity follows the same pattern as HIF-1 signaling (Igarashi et al., 2021; Padilla et al., 2022). Besides hypoxia, HIF-1 is stimulated by immune cell activation and is a key regulator of mitochondrial metabolism and certain immune effector functions (Courtnay et al., 2015; Morten et al., 2013; Semenza, 2010)(Ahn et al., 2014; Mojsilovic-Petrovic et al., 2007; Oda et al., 2006). Based on these considerations, it is reasonable to hypothesize that the down-regulation of energy metabolism by CREAM is potentially linked to the activation of BACH1. Previously, BACH1 was found to function as a hypoxia-inducible repressor for the heme oxygenase-1 gene in many types of human cells (Kitamuro et al., 2003). Accordingly, activation of BACH1 may also account for the inhibition of the HIF-1 signaling pathway by CREAM. Although more direct mechanistic evidence is needed, our analysis raises the possibility that MFGM inhibits the HIF-1 signaling pathway by targeting BACH-1 with subsequent anti-inflammatory effects on human monocytes.

Our study also has limitations. The principal readouts of our study were short-term changes in gene expression, which may not translate into changes in protein levels or functional changes. In addition,

it is unclear what the long-term consequences are of the observed changes in gene expression. We also cannot rule out that the differential changes in gene expression in monocytes after consumption of the three shakes may be an indirect consequence of differences in the route and rate of metabolic processing between the three fat sources and do not reflect a direct regulatory effect of circulating lipids on monocyte gene expression. To obviate this concern, we intend to incubate human monocytes in vitro with TG-rich lipoproteins isolated from volunteers after consumption of the three shakes. Finally, we used IPA to generate hypotheses about the mechanisms underlying the observed changes in gene expression. In the future, additional studies are needed to explore the crosstalk between BACH1 and HIF-1 signaling in the modulation of energy metabolism by CREAM.

In conclusion, our study has provided detailed insight into the postprandial effect of milk fat on the monocyte transcriptome and has highlighted potential underlying mechanisms. Differential effects were found of VEGE, AMF, and CREAM on the monocyte transcriptome. Compared to acute consumption of a vegetable fat blend and anhydrous milk fat, cream significantly downregulated energy and inflammation-related pathways in blood monocytes, suggesting a potential anti-inflammatory effect of MFGM.

MATERIALS AND METHODS

Study design and subjects

The study was conducted at Wageningen University, the Netherlands, from 07-01-2020 until 10-03-2020. The experimental protocol and procedures were approved by the Medical Ethical Committee of Wageningen University and were in accordance with the Helsinki declaration of 1975 as revised in 1983. The study was registered at clinicaltrials.gov as NCT04178681 'Postprandial Effects of Milk Fats (POEMI)'. The study was a randomized, double-blind crossover intervention trial and aimed at comparing the postprandial effects of formula vegetable fat (VEGE), anhydrous milk fat (AMF), and cream on the human immune response. 59 healthy participants were screened for the trial based on the criteria: 40-70 years (age) and 22-27 kg/m^2 (BMI). Based on the power calculation to detect a significant effect on a panel of fourteen inflammatory genes to reach an effect size range from 0.089-0.283 with a power of 80% and a two-sided alpha of 0.0012 or a panel of eight cytokines including IL-8, to detect a treatment difference of 0.37 pg/ml, with a power of 80% and a two-side alpha of 0.0021, and considering 10% drop out rate tolerance, in the end, 40 participants were included. Both men and women are randomly included in the study. 40 participants were given three different shakes on different days. At least one week for washout between two interventions. On the test day, subjects arrived in the fasted state, and the concentration of C-reactive protein (CRP) in the blood was determined via a finger prick using a QuickRead CRP test (Orion Diagnostica Oy) before any blood was collected for study purposes. When the CRP concentration was below 10.0 mg/L, participants were qualified for the study, and a catheter cannula was inserted in an antecubital vein. After a 30-minute rest, fasted blood was drawn to establish baseline (t0) values for the parameters of interest. Subjects were then asked to consume a shake within 10 minutes. Blood was drawn again every additional hour post-shake, with the last blood collection taking place 8 hours
after consumption of the shake. During these 8 hours, subjects were asked to fill out a questionnaire about feelings of hunger and satiety every hour. In addition, subjects were advised to drink water regularly. Each subject consumed all three shakes in a randomized order.

Intervention diets

The three intervention fat shakes were supplied by Frislandcampina. Shake VEGE is based on the lipid formula used in infant formula. To form the shake, 118g powder was mixed with 500 ml milk for the VEGE shake and AMF shake, and 461 ml milk plus 39 ml water for the CREAM shake. Except for the existence of MFGM, shake AMF and shake cream remain the same with the milk-

sourced lipids. In summary, all shakes contain 95.5 g of fat, about 21g of protein, and about 42.3 g of carbohydrates and can supply around 4610 KJ calories (Table 3).

Identification of monocyte subsets in human whole blood

Whole blood from each subject and at each of the two time points (t=0 and t=6) was divided into two aliquots of 100 µL. One aliquot was stained with fluorescently tagged monoclonal antibodies, and the other half was left unstained to determine levels of autofluorescence. Fluorescently tagged monoclonal antibodies were obtained from BD Biosciences (CD56-PE and CD16-FITC) and Beckman Coulter (CD14-ECD, HLA-DR-PeCy5, CD45-PeCy7, and CD3-PE). The staining procedure was as follows: first, whole blood was incubated with the amount of fluorescently tagged monoclonal antibody as specified by the manufacturer on ice for 20 minutes. After lysing the red blood cells using FACS Lysing Solution (BD Biosciences), samples were incubated for 15 minutes at room temperature protected from light. We then centrifuged the samples for 5 minutes at 150 x g at room temperature and subsequently removed the supernatant. The pellet was immediately resuspended in 250 µL of FACS buffer (1% BSA in PBS, 0.22 µm filtered). All samples were analyzed on an FC500 flow cytometer (Beckman Coulter) at a medium flow rate. To identify classical, intermediate, and non-classical monocytes in whole blood based on CD14 and CD16 expression, a gating strategy described by Mukherjee et al. (Mukherjee et al., 2015) was applied.

Human monocytes isolation

8 ml of blood was collected at T=0h and T=6h using a CPT tube and centrifuging at RT for 20 min at 1800 RCF after mixing by inverting tubes. After centrifugation, the white cloudy layer was collected for further PBMC purification by washing with cold PBS three times.

Monocytes were isolated by MojoSort CD14 negative selection kits (Biolegend, California, United States) and LS columns (Miltenyi Biotec, Bergisch Gladbach, Germany). Briefly, cells were resuspended in 100 ul (per 10^7 PBMCs; the same below) MojoSort buffer. Then 5µL Human TruStain FcX™ were added to block Fc receptor Solution) and incubated at room temperature for 10 minutes. After, the cell solution was incubated on ice for 15 minutes after adding 10µL of the Biotin-Antibody Cocktail. Then 10µL Streptavidin Nanobeads were added, and incubation was continued on ice for 15 minutes. After being washed using MojoSort™ Buffer, the cells were separated by LS columns using a Miltenyi Quadro MACS Separator and the flow phase containing monocytes will be collected and centrifuged.

RNA isolation and transcriptome analysis

At least 500,000 cells were collected from each subject for every intervention and both time points (T0 and T6) for total RNA isolation using RNeasy Micro Kit (Qiagen, Hilden, Germany). Transcriptome analysis by RNA-sequencing was performed by BGI Company Limited (Laboratory of Denmark) following a standard protocol. In brief, mRNA molecules were purified from total RNA using oligo(dT)-attached magnetic beads and fragmented into small pieces using fragmentation reagent after reaction for a certain period at the proper temperature. First-strand cDNA was generated using random hexamer-primed reverse transcription, followed by second-strand cDNA synthesis. The synthesized cDNA was subjected to end-repair and then was 3' adenylated. Adapters were ligated to the ends of these 3' adenylated cDNA fragments. PCR products were purified with Ampure XP Beads (AGENCOURT) and dissolved in EB solution. The library was validated on the Agilent Technologies 2100 bioanalyzer. The double-stranded PCR products were heat-denatured and circularized by the splint oligo sequence. The single-strand circle DNA (ssCir DNA) was formatted as the final library. The library was amplified with phi29 to make DNA nanoball (DNB) which had more than 300 copies of one molecule. The DNBs was loaded into the patterned nanoarray and pair-end 100 or 150 base reads were generated in the way sequenced by synthesis.

Ex vivo monocytes culture and cytokine measurements

500, 000 monocytes were seeded in 24 well plates and cultured in RPMI medium supplied with 2 mM Glutamax, 1% p/s, and 1mM Pyruvate. After short incubation for 1h to get monocytes adherent, we stimulated cells with 10 ng/ml LPS for 24 hours. The culture medium was collected afterward for cytokine analysis according to the manufacturer's protocol.

Data Analysis

The obtained transcript abundance estimates and lengths were imported in R using the package tximport, scaled by average transcript length and library size, and summarized on the gene level. Such scaling corrects for bias due to correlation across samples and transcript length and has been reported to improve the accuracy of differential gene expression analysis (Soneson et al., 2016). Differential gene expression was determined using the package limma (Ritchie et al., 2015) utilizing the obtained scaled gene-level counts. Briefly, before statistical analyses, nonspecific filtering of the count table was performed to increase detection power, based on the requirement that a gene should have an expression level greater than 10 counts, i.e. ~0.45 count per million reads (cpm) mapped, for at least 3 libraries across all 9 samples. Differences in library size were adjusted by the trimmed mean of M-values normalization method (Bourgon et al., 2010), implemented in the package edgeR (Robinson et al., 2010). Counts were transformed to log2(cpm) values and associated precision weights and

entered into the limma analysis pipeline (Law et al., 2014). Differentially expressed genes were identified by using generalized linear models that incorporate empirical Bayes methods to shrink the standard errors towards a common value, thereby improving testing power (Smyth, 2004). ANOVA-like F-test was performed to determine the significance.

For gene set enrichment analysis (GSEA), 344 KEGG gene sets were considered. After filtering out the sets that contain genes that are not measured and below the minimum size of 15 genes or above the maximum size of 500 genes, 308 gene sets were kept.

Ingenuity Pathway Analysis (IPA) is a web-based software application that allows searches for targeted information on genes, proteins, chemicals, and drugs and the building of interactive models of experimental systems. The software is backed by the Ingenuity Knowledge Base of highly structured, detail-rich biological and chemical findings. To predict the upstream regulators of the differential modulations on the transcriptome of monocytes, IPA was performed. The genes differentially expressed with $p<0.05$ in the comparisons were considered.

REFERENCE

Ahn, G.O., Seita, J., Hong, B.J., Kim, Y.E., Bok, S., Lee, C.J., Kim, K.S., Lee, J.C., Leeper, N.J., Cooke, J.P., et al. (2014). Transcriptional activation of hypoxia-inducible factor-1 (HIF-1) in myeloid cells promotes angiogenesis through VEGF and S100A8. Proc. Natl. Acad. Sci. U. S. A. *111*, 2698–2703.

Alipour, A., Van Oostrom, A.J.H.H.M., Izraeljan, A., Verseyden, C., Collins, J.M., Frayn, K.N., Plokker, T.W.M., Elte, J.W.F., and Cabezas, M.C. (2008). Leukocyte activation by triglyceride-rich lipoproteins. Arterioscler. Thromb. Vasc. Biol. *28*, 792–797.

Blaser, H., Dostert, C., Mak, T.W., and Brenner, D. (2016). TNF and ROS Crosstalk in Inflammation. Trends Cell Biol. *26*, 249–261.

Bourgon, R., Gentleman, R., and Huber, W. (2010). Independent filtering increases detection power for high-throughput experiments. Proc. Natl. Acad. Sci. U. S. A. *107*, 9546–9551.

Bouwens, M., Bromhaar, M.G., Jansen, J., Müller, M., and Afman, L.A. (2010). Postprandial dietary lipid-specific effects on human peripheral blood mononuclear cell gene expression profiles. Am. J. Clin. Nutr. *91*, 208–217.

Camargo, A., Rangel-Zúñiga, O.A., Peña-Orihuela, P., Marín, C., Pérez-Martínez, P., Delgado-Lista, J., Gutierrez-Mariscal, F.M., Malagón, M.M., Roche, H.M., Tinahones, F.J., et al. (2013). Postprandial changes in the proteome are modulated by dietary fat in patients with metabolic syndrome. J. Nutr. Biochem. *24*, 318–324.

Cen, X., Liu, S., and Cheng, K. (2018). The role of toll-like receptor in inflammation and tumor immunity. Front. Pharmacol. *9*, 878.

Courtnay, R., Ngo, D.C., Malik, N., Ververis, K., Tortorella, S.M., and Karagiannis, T.C. (2015). Cancer metabolism and the Warburg effect: the role of HIF-1 and PI3K. Mol. Biol. Rep. *42*, 841–851.

Diaz-Aragon, R., Ramirez-Ricardo, J., Cortes-Reynosa, P., Simoni-Nieves, A., Gomez-Quiroz, L.E., and Perez Salazar, E. (2019). Role of phospholipase D in migration and invasion induced by linoleic acid in breast cancer cells. Mol. Cell. Biochem.

Esser, D., Oosterink, E., op 't Roodt, J., Henry, R.M.A., Stehouwer, C.D.A., Müller, M., and Afman, L.A. (2013). Vascular and Inflammatory High Fat Meal Responses in Young Healthy Men; A Discriminative Role of IL-8 Observed in a Randomized Trial. PLoS One *8*.

Esser, D., van Dijk, S.J., Oosterink, E., Lopez, S., Müller, M., and Afman, L.A. (2015a). High fat challenges with different fatty acids affect distinct atherogenic gene expression pathways in immune cells from lean and obese subjects. Mol. Nutr. Food Res. *59*, 1563–1572.

Esser, D., van Dijk, S.J., Oosterink, E., Lopez, S., Müller, M., and Afman, L.A. (2015b). High fat challenges with different fatty acids affect distinct atherogenic gene expression pathways in immune cells from lean and obese subjects. Mol. Nutr. Food Res. *59*, 1563–1572.

Frey, M.R., and Brent Polk, D. (2014). ErbB receptors and their growth factor ligands in pediatric intestinal inflammation. Pediatr. Res. *75*, 127–132.

Gemeinhardt, A., Alfalah, M., Gück, T., Naim, H.Y., and Fuhrmann, H. (2009). The influence of linoleic and linolenic acid on the activity and intracellular localisation of phospholipase D in COS-1 cells. Biol. Chem. *390*, 253–258.

Ginsberg, H.N., Packard, C.J., Chapman, M.J., Borén, J., Aguilar-Salinas, C.A., Averna, M., Ference, B.A., Gaudet, D., Hegele, R.A., Kersten, S., et al. (2021). Triglyceride-rich lipoproteins and their remnants: Metabolic insights, role in atherosclerotic cardiovascular disease, and emerging therapeutic strategies-a consensus statement from the European Atherosclerosis Society. Eur. Heart J. *42*, 4791–4806.

Honda, T., Egen, J.G., Lämmermann, T., Kastenmüller, W., Torabi-Parizi, P., and Germain, R.N. (2014). Tuning of Antigen Sensitivity by T Cell Receptor-Dependent Negative Feedback Controls T Cell Effector Function in Inflamed Tissues. Immunity *40*, 235–247.

Igarashi, K., Nishizawa, H., Saiki, Y., and Matsumoto, M. (2021). The transcription factor BACH1 at the crossroads of cancer biology: From epithelial–mesenchymal transition to ferroptosis. J. Biol. Chem. *297*, 101032.

Khan, I.M., Pokharel, Y., Dadu, R.T., Lewis, D.E., Hoogeveen, R.C., Wu, H., and Ballantyne, C.M. (2016). Postprandial monocyte activation in individuals with metabolic syndrome. J. Clin. Endocrinol. Metab. *101*, 4195–4204.

Kitamuro, T., Takahashi, K., Ogawa, K., Udono-Fujimori, R., Takeda, K., Furuyama, K., Nakayama, M., Sun, J., Fujita, H., Hida, W., et al. (2003). Bach1 Functions as a Hypoxia-inducible Repressor for the Heme Oxygenase-1 Gene in Human Cells *. J. Biol. Chem. *278*, 9125–9133.

Law, C.W., Chen, Y., Shi, W., and Smyth, G.K. (2014). Voom: Precision weights unlock linear model analysis tools for RNA-seq read counts. Genome Biol. *15*.

Lee, J., Yesilkanal, A.E., Wynne, J.P., Frankenberger, C., Liu, J., Yan, J., Elbaz, M., Rabe, D.C., Rustandy, F.D., Tiwari, P., et al. (2019). Effective breast cancer combination therapy targeting BACH1 and mitochondrial metabolism. Nature *568*, 254–258.

Lundman, P., Boquist, S., Samnegård, A., Bennermo, M., Held, C., Ericsson, C.G., Silveira, A., Hamsten, A., and Tornvall, P. (2007). A high-fat meal is accompanied by increased plasma interleukin-6 concentrations. Nutr. Metab. Cardiovasc. Dis. *17*, 195–202.

Margioris, A.N. (2009). Fatty acids and postprandial inflammation. Curr. Opin. Clin. Nutr. Metab. Care *12*, 129–137.

Meessen, E.C.E., Warmbrunn, M. V., Nieuwdorp, M., and Soeters, M.R. (2019). Human postprandial nutrient metabolism and low-grade inflammation: A narrative review. Nutrients *11*.

Milan, A.M., Pundir, S., Pileggi, C.A., Markworth, J.F., Lewandowski, P.A., and Cameron-Smith, D. (2017). Comparisons of the postprandial inflammatory and endotoxaemic responses to mixed meals in young and older individuals: A randomised trial. Nutrients *9*.

Mojsilovic-Petrovic, J., Callaghan, D., Cui, H., Dean, C., Stanimirovic, D.B., and Zhang, W. (2007). Hypoxia-inducible factor-1 (HIF-1) is involved in the regulation of hypoxia-stimulated expression of monocyte chemoattractant protein-1 (MCP-1/CCL2) and MCP-5 (Ccl12) in astrocytes. J. Neuroinflammation *4*.

Morten, K.J., Badder, L., and Knowles, H.J. (2013). Differential regulation of HIF-mediated pathways increases mitochondrial metabolism and ATP production in hypoxic osteoclasts. J. Pathol. *229*, 755–764.

Mukherjee, R., Kanti Barman, P., Kumar Thatoi, P., Tripathy, R., Kumar Das, B., and Ravindran, B. (2015). Non-Classical monocytes display inflammatory features: Validation in Sepsis and Systemic Lupus Erythematous. Sci. Rep. *5*.

Nakamura, K., Miyoshi, T., Yunoki, K., and Ito, H. (2016). Postprandial hyperlipidemia as a potential residual risk factor. J. Cardiol. *67*, 335–339.

Nappo, F., Esposito, K., Cioffi, M., Giugliano, G., Molinari, A.M., Paolisso, G., Marfella, R., and Giugliano, D. (2002). Postprandial endothelial activation in healthy subjects and in type 2 diabetic patients: Role of fat and carbohydrate meals. J. Am. Coll. Cardiol. *39*, 1145–1150.

Oda, T., Hirota, K., Nishi, K., Takabuchi, S., Oda, S., Yamada, H., Arai, T., Fukuda, K., Kita, T., Adachi, T., et al. (2006). Activation of hypoxia-inducible factor 1 during macrophage differentiation.

Am. J. Physiol. - Cell Physiol. *291*.

Padilla, J., Lee, B.-S., Zhai, K., Rentz, B., Bobo, T., Dowling, N.M., and Lee, J. (2022). A Heme-Binding Transcription Factor BACH1 Regulates Lactate Catabolism Suggesting a Combined Therapy for Triple-Negative Breast Cancer. Cells *11*, 1177.

Pradhan, P., Vijayan, V., Cirksena, K., Buettner, F.F.R., Igarashi, K., Motterlini, R., Foresti, R., and Immenschuh, S. (2022). Genetic BACH1 deficiency alters mitochondrial function and increases NLRP3 inflammasome activation in mouse macrophages. Redox Biol. *51*.

Puri, K.D., Di Paolo, J.A., and Gold, M.R. (2013). B-cell receptor signaling inhibitors for treatment of autoimmune inflammatory diseases and B-cell malignancies. Int. Rev. Immunol. *32*, 397–427.

Rathinam, C., Poueymirou, W.T., Rojas, J., Murphy, A.J., Valenzuela, D.M., Yancopoulos, G.D., Rongvaux, A., Eynon, E.E., Manz, M.G., and Flavell, R.A. (2011). Efficient differentiation and function of human macrophages in humanized CSF-1 mice. Blood *118*, 3119–3128.

Raza, G.S., Herzig, K.H., and Leppäluoto, J. (2021). Invited review: Milk fat globule membrane—A possible panacea for neurodevelopment, infections, cardiometabolic diseases, and frailty. J. Dairy Sci. *104*, 7345–7363.

Ritchie, M.E., Phipson, B., Wu, D., Hu, Y., Law, C.W., Shi, W., and Smyth, G.K. (2015). Limma powers differential expression analyses for RNA-sequencing and microarray studies. Nucleic Acids Res. *43*, e47.

Robinson, M.D., McCarthy, D.J., and Smyth, G.K. (2010). edgeR: a Bioconductor package for differential expression analysis of digital gene expression data. Bioinformatics *26*, 139–140.

Rundblad, A., Holven, K.B., Øyri, L.K.L., Hansson, P., Ivan, I.H., Gjevestad, G.O., Thoresen, M., and Ulven, S.M. (2020). Intake of Fermented Dairy Products Induces a Less Pro-Inflammatory Postprandial Peripheral Blood Mononuclear Cell Gene Expression Response than Non-Fermented Dairy Products: A Randomized Controlled Cross-Over Trial. Mol. Nutr. Food Res. *64*.

Ryu, S.B., and Wang, X. (1998). Increase in free linolenic and linoleic acids associated with phospholipase D-mediated hydrolysis of phospholipids in wounded castor bean leaves. Biochim. Biophys. Acta - Lipids Lipid Metab. *1393*, 193–202.

Satriano, J.A., Shuldiner, M., Hora, K., Xing, Y., Shan, Z., and Schlondorff, D. (1993). Oxygen radicals as second messengers for expression of the monocyte chemoattractant protein, JE/MCP-1, and the monocyte colony-stimulating factor, CSF-1, in response to tumor necrosis factor-α and

immunoglobulin G. Evidence for involvement of reduced nico. J. Clin. Invest. *92*, 1564–1571.

Sauter, K.A., Waddell, L.A., Lisowski, Z.M., Young, R., Lefevre, L., Davis, G.M., Clohisey, S.M., McCulloch, M., Magowan, E., Mabbott, N.A., et al. (2016). Macrophage colony-stimulating factor (CSF1) controls monocyte production and maturation and the steady-state size of the liver in pigs. Am. J. Physiol. - Gastrointest. Liver Physiol. *311*, G533–G547.

Semenza, G.L. (2010). HIF-1: upstream and downstream of cancer metabolism. Curr. Opin. Genet. Dev. *20*, 51–56.

Smyth, G.K. (2004). Linear models and empirical bayes methods for assessing differential expression in microarray experiments. Stat. Appl. Genet. Mol. Biol. *3*.

Soneson, C., Love, M.I., and Robinson, M.D. (2016). Differential analyses for RNA-seq: Transcript-level estimates improve gene-level inferences. F1000Research *4*.

Sweet, M.J., HUME M Sweet, D.A., Hume, D.A., and Immunological Regulator, as (2003). CSF-1 as a regulator of macrophage activation and immune responses Citation for CSF-1 as a Regulator of Macrophage Activation and Immune Responses. Arch. Immunol. Ther. Exp. (Warsz). *51*, 169–177.

Tall, A.R., Thomas, D.G., Gonzalez-Cabodevilla, A.G., and Goldberg, I.J. (2022). Addressing dyslipidemic risk beyond LDL-cholesterol. J. Clin. Invest. *132*.

Tavares, L.P., Negreiros-Lima, G.L., Lima, K.M., E Silva, P.M.R., Pinho, V., Teixeira, M.M., and Sousa, L.P. (2020). Blame the signaling: Role of cAMP for the resolution of inflammation. Pharmacol. Res. *159*, 105030.

Varela, L.M., Ortega, A., Bermudez, B., Lopez, S., Pacheco, Y.M., Villar, J., Abia, R., and Muriana, F.J.G. (2011). A high-fat meal promotes lipid-load and apolipoprotein B-48 receptor transcriptional activity in circulating monocytes. Am. J. Clin. Nutr. *93*, 918–925.

Varticovski, L., Druker, B., Morrison, D., Cantley, L., and Roberts, T. (1989). The colony stimulating factor-1 receptor associates with and activates phosphatidylinositol-3 kinase. Nature *342*, 699–702.

Warren, M.K., and Ralph, P. (1986). Macrophage growth factor CSF-1 stimulates human monocyte production of interferon, tumor necrosis factor, and colony stimulating activity. J. Immunol. *137*.

Wilson, N.J., Jaworowski, A., Ward, A.C., and Hamilton, J.A. (1998). cAMP Enhances CSF-1-Induced ERK Activity and c-fosmRNA Expression via a MEK-Dependent and Ras-Independent Mechanism in Macrophages. Biochem. Biophys. Res. Commun. *244*, 475–480.

Wilson, N.J., Cross, M., Nguyen, T., and Hamilton, J.A. (2005). cAMP inhibits CSF-1-stimulated tyrosine phosphorylation but augments CSF-1R-mediated macrophage differentiation and ERK activation. FEBS J. *272*, 4141–4152.

SUPPLYMENTARY

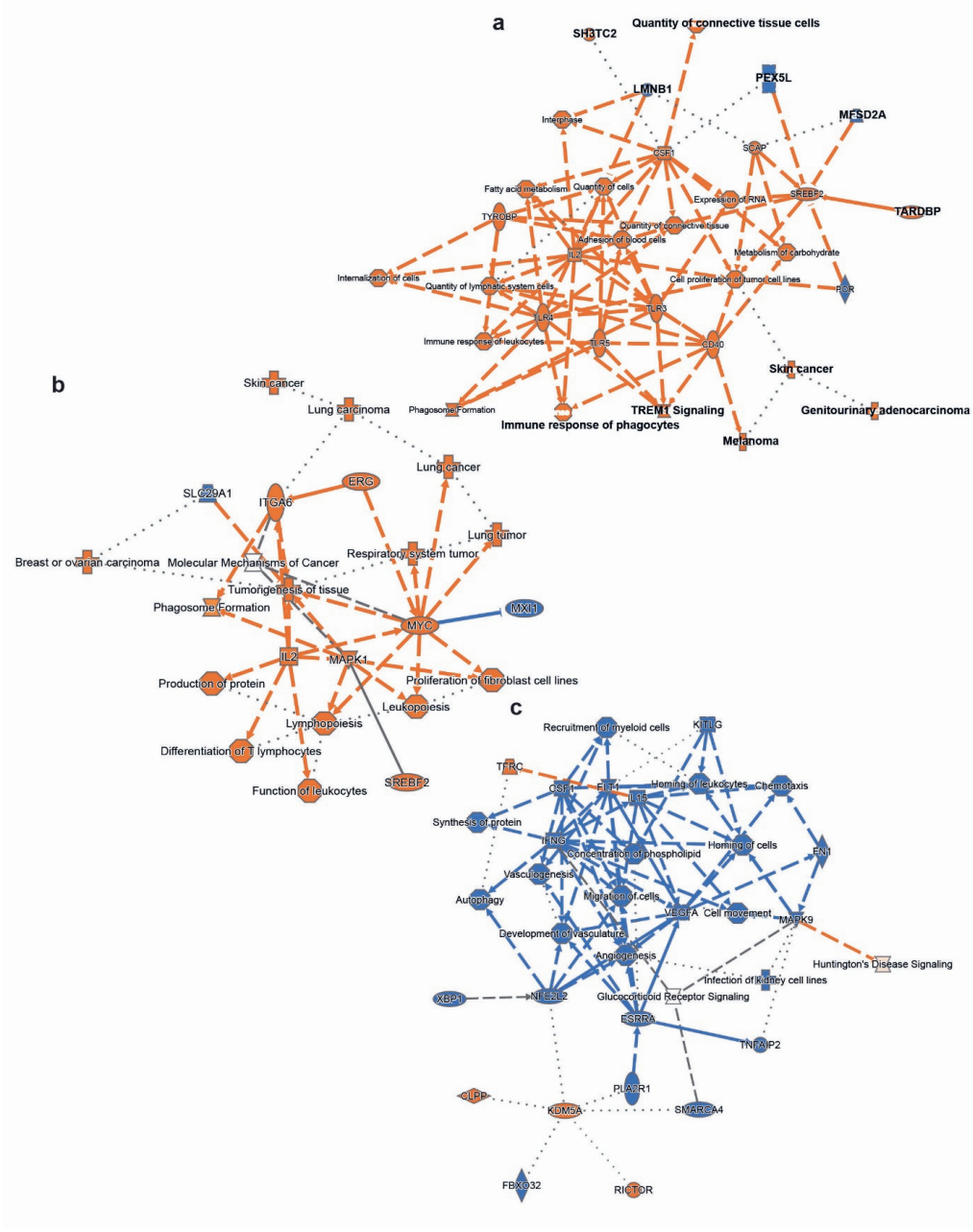

Figure S1. Differential regulations of the whole transcriptome of monocytes (IPA analysis). The regulation network of a) VEGE intervention b) AMF intervention and c) CREAM intervention. The orange color indicates an activation regulation, and the blue color indicates an inhibitory regulation.

CHARPTER 6

General discussion

In this thesis, we investigated the principles and regulations of lipid metabolism in adipocytes and immune cells to better understand the interactive dialogues between lipid metabolism and immunology. Diet is the major source of lipids for the human body. Accordingly, dietary lipid intake greatly influences metabolic homeostasis, which further affects immune health. Disturbances in lipid metabolism are at the root of many metabolic and possibly also immune-related disorders.

The main role of adipocytes is to store lipids under conditions of energy abundance and mobilize lipids under conditions of energy shortage. Accordingly, after a meal, adipocytes actively take up fatty acids to store them as triglycerides (TG). By contrast, upon transitioning to the post-absorptive state, adipocytes switch from net TG storage to net TG breakdown, resulting in the release of fatty acids into the bloodstream. Both TG synthesis and degradation are subject to detailed regulation by various signaling pathways, which relay the messages of numerous internal and external cues. The ultimate aim of these signaling pathways is to support the role of adipocytes in storing and mobilizing energy under specific environmental circumstances without incurring any cellular damage and thereby maintaining the long-term viability of the cell.

Although immune cells have a very different biological function than adipocytes, the basic metabolic pathways that operate in these cells are extremely similar. Similar to adipocytes, macrophages can store and mobilize TG. However, in contrast to the situation in adipocytes, in macrophages, these processes are mainly supportive of internal demand for fuel, at least so we think. In both types of cells, though, the buildup of specific lipid species needs to be avoided and fatty acids need to be rapidly converted, oxidized, excreted, or stored as TG to prevent lipotoxicity and associated cellular damage. Multiple signaling pathways are active in adipocytes and macrophages that are triggered by fatty acids and initiate adaptive changes in enzyme activity to compensate for changes in fatty acid supply.

In this chapter, we will discuss and integrate our findings on the metabolism of lipids in adipocytes and macrophages and the postprandial effects of different lipids on the metabolome and transcriptome of monocytes in humans.

HILPDA as a central mediator in lipid homeostasis

HILPDA regulates lipid metabolism in multiple cells

Cellular lipid homeostasis is important for supporting the basic functions of nearly all cells. Maintenance of cellular lipid homeostasis requires a balance between lipid uptake and lipid disposal.

Adipose tissue is the primary organ responsible for lipid storage and fueling other tissues in the body. Lipolysis and TG synthesis are two important pathways in adipocytes.

One of the proteins involved in the regulation of lipid homeostasis in cells is the lipid droplet-associated protein HILPDA. In hepatocytes, HILPDA was shown to promote TG synthesis by enhancing the activity of the DGAT1 enzyme. Using Förster resonance energy transfer-fluorescence lifetime imaging microscopy, a direct physical interaction between HILPDA with DGAT1 was demonstrated (de la Rosa Rodriguez et al., 2021). In macrophages, HILPDA was found to inhibit the ATGL enzyme and thereby suppress lipolysis. Again, using Förster resonance energy transfer-fluorescence lifetime imaging microscopy, as well as other molecular tools, a direct physical interaction between HILPDA and ATGL was demonstrated (van Dierendonck et al., 2020, 2022; Padmanabha Das et al., 2018). Rather than directly inhibiting ATGL enzymatic activity, which HILPDA does rather weakly, HILPDA likely interferes with ATGL action by promoting the degradation of ATGL in the proteasome.

In this thesis, we found that treatment of adipocytes with fatty acids markedly increased HILPDA protein levels. Similarly, activation of lipolysis in adipocytes led to a strong increase in HILPDA levels, which was abolished by ATGL inhibition, suggesting that fatty acids released by lipolysis stimulate HILPDA. A major portion of the fatty acids released by lipolysis in adipocytes is released into the medium. However, many fatty acids are re-esterified to TG in the cell. Inhibition of fatty acid re-esterification by blocking DGAT1/DGAT2 under conditions of activated lipolysis further raised HILPDA levels. The high sensitivity of HILPDA to changes in intracellular and extracellular fatty acid levels is fully consistent with an important role of HILPDA in lipid homeostasis in adipocytes. Linking our current findings (**chapter 2**) to our previous studies in macrophages and hepatocytes, we believe that HILPDA plays an important role in the feedback regulation of adipocyte lipolysis.

HILPDA mediates GPR120-induced autocrine negative feedback regulation of lipolysis

Adipocytes strive to maintain a healthy balance between TG synthesis and TG degradation. Postprandially, adipocytes take up excess fatty acids and store them as TG. In the post-absorptive state, the stored TG is hydrolyzed to release fatty acids. When lipolysis is overactivated or fatty acid esterification is blocked, fatty acids can accumulate in cells, potentially leading to lipotoxicity and associated ER stress (Chitraju et al., 2017), which in turn can further impair cellular function. ATGL is one of the key enzymes in lipolysis. To protect against the excess intracellular buildup of fatty acids and ensuing damage, hydrolyzed fatty acids inhibit ATGL to limit cellular lipolysis (Burns et al., 1978; Fain and Shepherd, 1975; Kalderon et al., 2012). Recently, the fatty acid receptor GPR120 was

shown to mediate autocrine negative feedback regulation of lipolysis (Husted et al., 2020a). However, little is known about the underlying mechanisms explaining how GPR120 regulates lipolysis inhibition and whether ATGL is the target enzyme. Our previous study found that HILPDA inhibits AGTL and promotes lipid storage in macrophages (van Dierendonck et al., 2020, 2022). Extending this previous work, we now show (**chapter 2**) that HILPDA is at the center of the GPR120-mediated regulation of lipolysis. It was found that activation of GPR120 inhibited lipolysis in wild-type adipocytes but failed to do so in HILPDA-deficient adipocytes. These data indicate that the regulatory role of GPR120 in lipolysis in adipocytes is dependent on HILPDA. In **chapter 2**, we also demonstrate the involvement of ATGL in the feedback pathway. It was found that activation of GPR120 by either a natural or synthetic agonist downregulated ATGL protein levels in wildtype adipocytes but not in HILPDA-deficient adipocytes. These data not only reveal a direct regulation of ATGL by HILPDA but also extend our understanding of how GPR120 signaling regulates lipolysis in adipocytes, which was not described in previous studies.

HILPDA alleviates ER stress after refeeding

We found in our study that ER stress-related genes were significantly increased in adipose tissue of adipocyte-specific HILPDA-deficient mice compared with wild-type mice but only in the refed state (**chapter 2**), suggesting a protective role of HILPDA in the switch from fasting to refeeding. During the switch from fasting to refeeding, specific signals such as insulin may transcriptionally downregulate *ATGL* to suppress the lipolysis of stored TG (Chakrabarti et al., 2013). It could be hypothesized that the transcriptional downregulation of ATGL during refeeding may be complemented by the downregulation of ATGL protein levels. Interestingly, our studies suggest a role of HILPDA in suppressing ATGL protein levels in the refed state. Specifically, we found that ATGL protein levels were markedly increased in adipose tissue of adipocyte-specific HILPDA-deficient mice compared to wild-type mice but only in the refed state. Presently, it is not clear why and how HILPDA only downregulates ATGL protein levels in the refed state (**chapter 2**). Similarly, it is not clear why HILPDA only suppresses the expression of ER stress-related genes in the refed state. We expected that HILPDA deficiency would mainly impact ATGL protein levels and ER stress-related genes in the fasted state. (**chapter 2**).

Reactive oxygen species may bridge GPR120 activation and the HILPDA-mediated ATGL inhibition

As alluded to above, the free fatty acid receptor GPR120 was found to play a central role in the negative feedback regulation of lipolysis by fatty acids in adipocytes (Husted et al., 2020b). Such a

mechanism is expected to be most important under conditions of excessive fatty acid release. However, no clear insights and guidance were provided on how GPR120 signaling may interact with the lipolysis pathway. Our studies (**chapter 2**) illustrate that the negative feedback regulation by GPR120 signaling is dependent on HILPDA via inhibition of ATGL expression in adipocytes. However, our studies have not yet revealed the mechanism through which GPR120 signaling regulates HILPDA.

In principle, the signal transmission from GPR120 sensing to HILPDA has to be via a second messenger. One of the most common consequences of the accumulation of fatty acids in the cell is the generation of ROS. ROS has been investigated as a special second messenger involved in many cellular processes, including redox regulation, cell proliferation, and differentiation (Linley et al., 2012; Sauer et al., 2001; Tsubata, 2020). Interestingly, ROS also has a direct regulatory impact on the HIF-1 subunit, HIF1α (Bonello et al., 2007; Movafagh et al., 2015). As HILPDA is a protein that is induced by hypoxia via HIF1α, it could be speculated that ROS might be the second messenger that mediates signal transmission between GPR120 and HILPDA. Previously, our group found that LPS treatment markedly upregulates HILPDA levels in macrophages (van Dierendonck et al., 2022). Since ROS is involved in the Toll-like receptor-dependent NF-κB activation by LPS (Asehnoune et al., 2004), the suggestion could even be raised that ROS mediates HILPDA regulation by both LPS and fatty acid/GPR120, conceivable via HIF1α. Consistent with such a scenario, ROS has been suggested to be involved in sensing intracellular FAs and regulating lipolysis via ATGL ubiquitination (Ding et al., 2021; Lettieri Barbato et al., 2014). Taking together, we propose that, as a second messenger, ROS may be the crucial link between the HILPDA-mediated ATGL inhibition and the negative feedback regulation of lipolysis via GPR120 activation.

The newly identified fatty acid excretion by macrophages

Macrophages treat TG-rich lipoproteins the “same” as pathogens

Macrophages were first identified as a type of immune cell that engulfs and digests pathogens and were only later discovered to perform other cellular functions, such as antigen presentation, reflecting its role in adaptive immunity. Since then it has been shown that the functional phenotypes of macrophages are crucial for the initiation, development, and progression of many types of metabolic diseases, such as atherosclerosis. For example, it is well established that macrophages contribute to atherosclerosis by taking up naïve and modified LDL (Wendland, 2001).

When macrophages ingest a pathogen, the pathogen becomes trapped in a phagosome, which thereafter fuses with a lysosome and is digested by enzymes and toxic peroxides. However, the

endocytosis capability of macrophages is also important for handling lipoproteins. The importance of clathrin-mediated endocytosis in lipid uptake by numerous cells is well established. Indeed, the cellular uptake of LDL is mediated by the binding of LDL to the LDL receptor, followed by the formation of clathrin-coated pits and subsequent delivery of the lipid cargo to the lysosomes (Lakadamyali et al., 2006). Receptor-mediated endocytosis also mediates the uptake of native or modified LDL in macrophages as a key step in the pathogenesis of atherosclerosis (Wilhelm et al., 2017). In hepatocytes, receptor-mediated endocytosis is required for the uptake of VLDL- and chylomicron remnants (Zanoni et al., 2018).

However, the uptake of TG-rich lipoproteins (VLDL and chylomicrons) by macrophages has been poorly studied. Our study (**chapter 3**) has revealed that macrophage uptake of VLDL and chylomicrons is mediated by LPL. However, unlike the conventional enzymatic function of LPL, which is carried out by the N-terminal portion of the protein, the uptake of TG-rich lipoprotein is mediated by the bridging role of LPL, which is carried by the C-terminal region of LPL. The bridging role of LPL in lipoprotein uptake by macrophages has been discussed for many years, many in the context of uptake of oxidized LDL (Beisiegel, 1996)(Ishibashi et al., 1990). However, no direct studies have been performed to validate the role of the bridging function of LPL in macrophage uptake of TG-rich lipoproteins. In our study (**chapter 3**), we tested this by either silencing the whole molecule of LPL or by using antibodies to specifically block the C- or N-terminal region. By monitoring the changes of intracellular neutral lipids, we concluded that the bridging role of LPL mediates VLDL and chylomicron uptake by macrophages.

Unlike the receptor-mediated uptake of LDL/oxLDL by macrophages, we found that macrophages endocytose VLDL and chylomicrons via caveola (**chapter 3**). Although it is difficult to specifically prove that a receptor is not required, our data suggest that uptake of VLDL and chylomicrons by macrophages may not be dependent on receptors.

The fate and the intracellular physiology of the internalized TG-rich lipoproteins by macrophages

The internalized lipoproteins and the products of digestion may be toxic to the cells and must either be metabolized, stored, or expelled (Tabas and Bornfeldt, 2020). For instance, the cholesterol derived from the digestion of LDL can be either esterified or exported to produce precursors of HDL particles. Similar to cholesterol, elevated intracellular levels of free fatty acids can be damaging to cells, for instance by inducing ER stress and oxidative stress (Weinberg, 2006). To restrict this lipotoxicity, macrophages and other cells can convert fatty acids into TG as well as use the fatty acids as fuel.

After being hydrolyzed in the lysosome, the LDL-derived cholesterol is exported from the lysosome in two different directions. STARD3 is responsible for commuting the cholesterol between the ER and the lysosomes (Alpy et al., 2013); Thelen and Zoncu, 2017). We found it is also involved in the transfer of VLDL-derived fatty acids from the lyso/endosome to the ER for esterification (**chapter 3**). Besides STARD3, NPC1 is another protein involved in the lysosomal export of cholesterol (Pfeffer, 2019). In our study (**chapter 3**), we found that macrophages loaded with VLDL-sized and chylomicrons-sized emulsion particles release fatty acids into the medium, and this process was impaired by the inactivation of lysosomal acid lipase and NPC1. However, it is still unknown whether the efflux of fatty acids is dependent on the fusion of the lysosomes with the plasma membrane or requires fatty acid transport through the cytoplasm.

Our data cannot reveal whether the extracellular efflux of lysosome-derived fatty acids is needed for the storage of VLDL-TG in macrophages via re-uptake of the fatty acids. It seems more plausible that the efflux of fatty acids allows macrophages to get rid of excess fatty acids acquired via endocytosis and phagocytosis. The effluxed fatty acids may be used by neighboring cells as fuel. Since fatty acid transport across the cell membrane is essentially driven by a concentration gradient, all cells should in principle be able to export fatty acids if the intracellular free fatty acid concentration exceeds the extracellular fatty acid concentration. The intracellular fatty acid concentration is normally kept low because any fatty acids formed are quickly activated to acyl-CoA. However, if intracellular TG hydrolysis is very active, as occurs in adipocytes and lipid-laden macrophages, a positive fatty acid gradient can be generated, leading to efflux of fatty acids.

The classical role of macrophages as phagocytosing cells is in innate immunity. In addition, macrophages support the function of other immune cells by secreting numerous cytokines and presenting antigens. As discussed above, macrophages are also able to take up lipoproteins, such as chylomicrons, oxLDL, and VLDL. The behavior of macrophages to take up these lipoproteins was physiologically considered to be aimed at acquiring fuel and removing toxicants. However, in our study (**chapter 3**), we discovered that macrophages could excrete part of the internalized TG as fatty acids. This biological process is mediated by lysosomal hydrolysis of the internalized TG, as a significant attenuation of fatty acid efflux was observed upon inhibition of lysosomal acid lipase. Macrophages are co-residing in tissues with many types of cells, which in theory could take up the released fatty acids, use them as fuel, or use them for other purposes.

Full fat milk should not always be out of the choice

Polyunsaturated fatty acids: good or bad?

While saturated fatty acids (SFAs) exert a pro-inflammatory effect in several different cell types, including macrophages, unsaturated fatty acids (UFAs) usually have the opposite effect. This included oleic acid, which is a monounsaturated fatty acid (MUFA) abundant in olive oil and the Mediterranean diet (Sales-Campos et al., 2013; Santamarina et al., 2021).

Most studies on polyunsaturated fatty acids (PUFAs) have been focused on ω-3 fatty acids, including ALA, EPA, and DHA, of which the latter two are enriched in fish oil. Several pre-clinical and clinical trials have revealed the benefits of fish oil in different inflammatory and auto-immune diseases in humans, such as rheumatoid arthritis, Crohn's disease, multiple sclerosis, and neurodegenerative disorders (Giacobbe et al., 2020; Simopoulos, 2002). By contrast, the anti-inflammatory effect of ω-6 fatty acids is still under discussion. The predominant ω-6 fatty acids are linoleic acid and arachidonic acid. The latter can be converted to prostaglandins, leukotrienes, and other lipoxygenase or cyclooxygenase products. These products are important regulators of cellular functions and carry anti/pro-inflammatory, atherogenic, and prothrombotic properties (Bagga et al., 2003; Schmitz and Ecker, 2008). Because long-chain ω-3 fatty acids can be converted to antithrombotic anti-inflammatory eicosanoids, whereas ω-6 fatty acids cannot, it has been proposed that the ratio of ω-3/ω-6 fatty acids may reflect the anti-inflammatory impact of a diet (Delpech et al., 2015; Kiecolt-Glaser et al., 2007). However, this concept is increasingly being abandoned. It was found that intake of both ω-3 and ω-6 fatty acids is associated with a reduced risk of cardiovascular disease (Wang, 2018). Moreover, ω-6 fatty acids do not inhibit the anti-inflammatory effects of ω-3 fatty acids (Pischon et al., 2003; Willett, 2007). Linoleic acid and arachidonic acid also lower plasma LDL levels (Choo et al., 2010), which is associated with protection against cardiovascular diseases.

We performed a randomized cross-over human trial to investigate the postprandial effects of different fat blends on specific aspects of human immune health using fat shakes, containing vegetable fat, milk fat with MFGM, and milk fat without MFGM (**chapter 4 and chapter 5**). Compared to milk fat, the vegetable fat blend used in our studies contained about 18% more oleic acid, 15% more linoleic acid, and 11% less palmitic acid, compared to milk fat-based shakes. In **chapter 4**, we described the acute postprandial effects of vegetable fat consumption and milk fat consumption on the lipid profile in the plasma. We found that 6 hours postprandially, VLDL fractions were significantly higher after vegetable fat consumption than after consumption of milk fat, either with or without MFGM. In contrast, the levels of HDL fractions were generally lower after the vegetable fat blend, especially compared to cream (milk fat with MFGM) consumption.

Consistent with the plasma GlycA data, the transcriptome data of the monocytes (**chapter 5)** revealed that several pathways related to inflammation (or monocytes activation) were significantly activated by vegetable fat consumption, which was not observed after the milk fat-based interventions. Taken together, it is reasonable to consider that the higher content of ω-6 fatty acids in vegetable fat may account for the inflammation-related postprandial effect of vegetable fat consumption. However, with this study, it is impossible to assign the observed effects to specific fatty acids.

Should the high abundance of saturated fatty acids in milkfat be a concern?

As SFA are considered to be pro-inflammatory and raise plasma LDL levels in human clinical trials, consumption of fats rich in SFA is generally discouraged. Indeed, consumers have been encouraged to limit full-fat dairy consumption in favor of reduced-fat dairy products. For example, the 2010 dietary guideline for Americans released by the USDA advises people to consume non-fat or low-fat milk. However, recent studies have questioned the correlation between milk fat consumption and inflammation. A systematic review based on 52 clinical trials that investigated inflammatory markers following the consumption of dairy products strongly pointed to an anti-inflammatory effect of dairy consumption in subjects with metabolic disorders (Bordoni et al., 2017). Both low-fat and high-fat products, as well as fermented products, showed anti-inflammatory activity.

In **chapter 4** and **chapter 5** of this thesis, we compared the postprandial effects of AMF, which contains 70% SFA, to VEGE, which contains 40% SFA. As shown in **chapter 4**, VEGE consumption caused a delayed postprandial change (increase and return) of several metabolites, including VLDL and LDL fractions, compared to AMF consumption. In addition, this was in parallel with the changes of postprandial plasma glycoprotein acetyls, a low-grade inflammation marker. We also studied the postprandial effect of these shakes on the monocyte transcriptome (in **chapter 5**). VEGE consumption induced multiple inflammation-related pathways, such as the TNF signaling pathway and Toll-like receptor pathway, which were not activated by the milk fat-based shake. Despite the much higher content of SFA, consumption of milk fat was not associated with elevated inflammatory markers. On the other hand, VEGE consumption, despite being high in UFA, was associated with elevated inflammatory markers such as GlycA.

In conclusion, although the underlying mechanism remains elusive, we observed that consumption of milk fat is not associated with postprandial inflammation.

Milkfat globule membrane: a potential candidate to regulate mitochondrial metabolism

The presence of MFGM has been suggested to confer anti-inflammatory properties to milk fat. Because of the processing procedures, MFGM are only intact in full-fat dairy products and are lost completely or partially in fat-free and reduced fat products. It has been shown that heating and homogenizing milk disrupt the structure and composition of the MFGM. One of the lipid fractions in MFGM that may exert an anti-inflammatory activity are the phospholipids (Rogers et al., 2017; Zhang et al., 2019). However, little is known about the underlying mechanisms. By studying the postprandial effects of milk fat with and without MFGM on the monocyte transcriptome (**chapter 5**), we were able to generate some insights. We found that in comparison with milk fat without MFGM, milk fat with MFGM suppressed general energy metabolism pathways, such as glycolysis, oxidative phosphorylation, TCA cycle, and pyruvate metabolism. Considering that the two types of shake were completely identical except for the presence of MFGM, it is reasonable to argue that the MFGM are the bioactive components responsible for the suppression of the abovementioned pathways.

Most of these pathways occur in the mitochondria. Accordingly, it can be hypothesized that the changes in these functional pathways reflect the suppression of mitochondrial activity. One of the most important side effects of mitochondrial fatty acid oxidation is the generation of reactive oxygen species (ROS), thereby activating Toll-like receptors, which primes multiple immune processes (Chakrabarti and Visweswariah, 2020). Compared to AMF, the general mitochondrial activity was suppressed by CREAM, which is expected to inhibit mitochondrial ROS synthesis and which in turn may account for the inhibition of Toll-like receptor signaling and TNF signaling (**chapter 5**). Our data thus raise the possibility that CREAM and in particular MFGM can regulate inflammation through the modulation of mitochondrial metabolism.

How does MFGM regulate mitochondrial metabolism in monocytes? Although there is no direct evidence to support one particular pathway, our data hint at a role of the HIF-1 signaling pathway. As reported, HIF-1 signaling is activated to increase intracellular oxygen and up-regulate glucose transport to augment aerobic glycolysis (Courtnay et al., 2015; Semenza, 2007). Additionally, HIF1α activates lactase dehydrogenase A (LDHA) by binding to its promoter (Firth et al., 1995; Semenza et al., 1996), thereby promoting the interconversion of lactate and pyruvate. Emerging evidence shows that the circulating lactate is an important carbon source feeding the TCA cycle in certain immune cells (Brooks, 2018; Hui et al., 2017), which implies that the inhibition of the convention from lactate to pyruvate decreases mitochondrial metabolism. The effect of the transcription factor BACH1 on mitochondrial activity follows the same pattern as HIF-1 signaling (Igarashi et al., 2021; Padilla et al., 2022). Interestingly, BACH1 was found to function as a hypoxia-inducible repressor for the heme oxygenase-1 gene in many types of human cells (Kitamuro et al., 2003). Our data (**chapter 5**) indicate

that CREAM significantly inhibited BACH1 and HIF-1 signaling, which suggests that BACH1-HIF-1 signaling may potentially account for the regulation of mitochondrial metabolism by CREAM.

As for whether the mitochondrial regulation effect of MFGM is conferred by the bioactive phospholipids, more investigations are needed.

Conclusion

In this thesis, we uncovered the essential role of hypoxia-inducible lipid droplet-associated (HILPDA) protein in the feedback regulation of lipolysis by fatty acids and GPR120 in adipocytes. Our data not only revealed a direct regulation of ATGL by HILPDA but also extend our understanding of how GPR120 signaling regulates lipolysis in adipocytes, which was not described in previous studies. We also studied how macrophages take up TG-rich lipoproteins. We found that macrophages take up VLDL- and chylomicron-sized lipid particles through caveolae to mediate endocytosis and partly excrete fatty acids from the internalized TG. These findings provide us with new insights into how macrophages metabolize TG, which may be helpful in the design of new therapies for cardiovascular diseases. The investigation of the postprandial effects of milk fat in humans established that milk fat consumption is not associated with postprandial inflammation, despite the high abundance of saturated fatty acids. Besides the anti-inflammatory effect, the CREAM intervention also suppressed mitochondrial metabolism, which suggests an interesting effect of MFGM. Although the evidence is preliminary, our systematic analysis of the transcriptome data suggested that this effect might be mediated by BACH1 activation, which further inhibits HIF-1 signaling.

REFERENCE

Alpy, F., Rousseau, A., Schwab, Y., Legueux, F., Stoll, I., Wendling, C., Spiegelhalter, C., Kessler, P., Mathelin, C., Rio, M.C., et al. (2013). STARD3 or STARD3NL and VAP form a novel molecular tether between late endosomes and the ER. J. Cell Sci. *126*, 5500–5512.

Asehnoune, K., Strassheim, D., Mitra, S., Kim, J.Y., and Abraham, E. (2004). Involvement of Reactive Oxygen Species in Toll-Like Receptor 4-Dependent Activation of NF-κB. J. Immunol. *172*, 2522–2529.

Bagga, D., Wang, L., Farias-Eisner, R., Glaspy, J.A., and Reddy, S.T. (2003). Differential effects of prostaglandin derived from ω-6 and ω-3 polyunsaturated fatty acids on COX-2 expression and IL-6 secretion. Proc. Natl. Acad. Sci. U. S. A. *100*, 1751–1756.

Beisiegel, U. (1996). New aspects on the role of plasma lipases in lipoprotein catabolism and atherosclerosis. Atherosclerosis *124*, 1–8.

Bonello, S., Zähringer, C., BelAiba, R.S., Djordjevic, T., Hess, J., Michiels, C., Kietzmann, T., and Görlach, A. (2007). Reactive oxygen species activate the HIF-1α promoter via a functional NFκB site. Arterioscler. Thromb. Vasc. Biol. *27*, 755–761.

Bordoni, A., Danesi, F., Dardevet, D., Dupont, D., Fernandez, A.S., Gille, D., Nunes dos Santos, C., Pinto, P., Re, R., Rémond, D., et al. (2017). Dairy products and inflammation: A review of the clinical evidence. Crit. Rev. Food Sci. Nutr. *57*, 2497–2525.

Brooks, G.A. (2018). The Science and Translation of Lactate Shuttle Theory. Cell Metab. *27*, 757–785.

Burns, T.W., Langley, P.E., Terry, B.E., and Robinson, G.A. (1978). The role of free fatty acids in the regulation of lipolysis by human adipose tissue cells. Metabolism *27*, 1755–1762.

Chakrabarti, S., and Visweswariah, S.S. (2020). Intramacrophage ROS Primes the Innate Immune System via JAK/STAT and Toll Activation. Cell Rep. *33*.

Chakrabarti, P., Kim, J.Y., Singh, M., Shin, Y.-K., Kim, J., Kumbrink, J., Wu, Y., Lee, M.-J., Kirsch, K.H., Fried, S.K., et al. (2013). Insulin Inhibits Lipolysis in Adipocytes via the Evolutionarily Conserved mTORC1-Egr1-ATGL-Mediated Pathway. Mol. Cell. Biol. *33*, 3659–3666.

Chitraju, C., Mejhert, N., Haas, J.T., Diaz-Ramirez, L.G., Grueter, C.A., Imbriglio, J.E., Pinto, S., Koliwad, S.K., Walther, T.C., and Farese, R. V. (2017). Triglyceride Synthesis by DGAT1 Protects

Adipocytes from Lipid-Induced ER Stress during Lipolysis. Cell Metab. *26*, 407-418.e3.

Choo, J., Ueshima, H., Curb, J.D., Shin, C., Evans, R.W., El-Saed, A., Kadowaki, T., Okamura, T., Nakata, K., Otake, T., et al. (2010). Serum n-6 fatty acids and lipoprotein subclasses in middle-aged men: The population-based cross-sectional ERA-JUMP study. Am. J. Clin. Nutr. *91*, 1195–1203.

Courtnay, R., Ngo, D.C., Malik, N., Ververis, K., Tortorella, S.M., and Karagiannis, T.C. (2015). Cancer metabolism and the Warburg effect: the role of HIF-1 and PI3K. Mol. Biol. Rep. *42*, 841–851.

Delpech, J.C., Madore, C., Joffre, C., Aubert, A., Kang, J.X., Nadjar, A., and Layé, S. (2015). Transgenic increase in n-3/n-6 fatty acid ratio protects against cognitive deficits induced by an immune challenge through decrease of neuroinflammation. Neuropsychopharmacology *40*, 525–536.

van Dierendonck, X.A.M.H., de la Rosa Rodriguez, M.A., Georgiadi, A., Mattijssen, F., Dijk, W., van Weeghel, M., Singh, R., Borst, J.W., Stienstra, R., and Kersten, S. (2020). HILPDA Uncouples Lipid Droplet Accumulation in Adipose Tissue Macrophages from Inflammation and Metabolic Dysregulation. Cell Rep. *30*, 1811-1822.e6.

van Dierendonck, X.A.M.H., Vrieling, F., Smeehuijzen, L., Deng, L., Boogaard, J.P., Croes, C.A., Temmerman, L., Wetzels, S., Biessen, E., Kersten, S., et al. (2022). Triglyceride breakdown from lipid droplets regulates the inflammatory response in macrophages. Proc. Natl. Acad. Sci. U. S. A. *119*, e2114739119.

Ding, L., Sun, W., Balaz, M., He, A., Klug, M., Wieland, S., Caiazzo, R., Raverdy, V., Pattou, F., Lefebvre, P., et al. (2021). Peroxisomal β-oxidation acts as a sensor for intracellular fatty acids and regulates lipolysis. Nat. Metab. *3*, 1648–1661.

Fain, J.N., and Shepherd, R.E. (1975). Free fatty acids as feedback regulators of adenylate cyclase and cyclic 3':5' AMP accumulation in rat fat cells. J. Biol. Chem. *250*, 6586–6592.

Giacobbe, J., Benoiton, B., Zunszain, P., Pariante, C.M., and Borsini, A. (2020). The Anti-Inflammatory Role of Omega-3 Polyunsaturated Fatty Acids Metabolites in Pre-Clinical Models of Psychiatric, Neurodegenerative, and Neurological Disorders. Front. Psychiatry *11*, 122.

Hui, S., Ghergurovich, J.M., Morscher, R.J., Jang, C., Teng, X., Lu, W., Esparza, L.A., Reya, T., Zhan, L., Yanxiang Guo, J., et al. (2017). Glucose feeds the TCA cycle via circulating lactate. Nature *551*, 115–118.

Husted, A.S., Ekberg, J.H., Tripp, E., Nissen, T.A.D., Meijnikman, S., O'Brien, S.L., Ulven, T.,

Acherman, Y., Bruin, S.C., Nieuwdorp, M., et al. (2020a). Autocrine negative feedback regulation of lipolysis through sensing of NEFAs by FFAR4/GPR120 in WAT. Mol. Metab. *42*.

Husted, A.S., Ekberg, J.H., Tripp, E., Nissen, T.A.D., Meijnikman, S., O'Brien, S.L., Ulven, T., Acherman, Y., Bruin, S.C., Nieuwdorp, M., et al. (2020b). Autocrine negative feedback regulation of lipolysis through sensing of NEFAs by FFAR4/GPR120 in WAT. Mol. Metab. *42*, 101103.

Igarashi, K., Nishizawa, H., Saiki, Y., and Matsumoto, M. (2021). The transcription factor BACH1 at the crossroads of cancer biology: From epithelial–mesenchymal transition to ferroptosis. J. Biol. Chem. *297*, 101032.

Ishibashi, S., Yamada, N., Shimano, H., Mori, N., Mokuno, H., Gotohda, T., Kawakami, M., Murase, T., and Takaku, F. (1990). Apolipoprotein E and lipoprotein lipase secreted from human monocyte-derived macrophages modulate very low density lipoprotein uptake. J. Biol. Chem. *265*, 3040–3047.

Kalderon, B., Azazmeh, N., Azulay, N., Vissler, N., Valitsky, M., and Bar-Tana, J. (2012). Suppression of adipose lipolysis by long-chain fatty acid analogs. J. Lipid Res. *53*, 868–878.

Kiecolt-Glaser, J.K., Belury, M.A., Porter, K., Beversdorf, D.Q., Lemeshow, S., and Glaser, R. (2007). Depressive symptoms, omega-6:omega-3 fatty acids, and inflammation in older adults. Psychosom. Med. *69*, 217–224.

Kitamuro, T., Takahashi, K., Ogawa, K., Udono-Fujimori, R., Takeda, K., Furuyama, K., Nakayama, M., Sun, J., Fujita, H., Hida, W., et al. (2003). Bach1 Functions as a Hypoxia-inducible Repressor for the Heme Oxygenase-1 Gene in Human Cells *. J. Biol. Chem. *278*, 9125–9133.

de la Rosa Rodriguez, M.A., Deng, L., Gemmink, A., van Weeghel, M., Aoun, M.L., Warnecke, C., Singh, R., Borst, J.W., and Kersten, S. (2021). Hypoxia-inducible lipid droplet-associated induces DGAT1 and promotes lipid storage in hepatocytes. Mol. Metab. *47*, 101168.

Lakadamyali, M., Rust, M.J., and Zhuang, X. (2006). Ligands for clathrin-mediated endocytosis are differentially sorted into distinct populations of early endosomes. Cell *124*, 997–1009.

Lettieri Barbato, D., Aquilano, K., Baldelli, S., Cannata, S.M., Bernardini, S., Rotilio, G., and Ciriolo, M.R. (2014). Proline oxidase-adipose triglyceride lipase pathway restrains adipose cell death and tissue inflammation. Cell Death Differ. *21*, 113–123.

Linley, J.E., Ooi, L., Pettinger, L., Kirton, H., Boyle, J.P., Peers, C., and Gamper, N. (2012). Reactive oxygen species are second messengers of neurokinin signaling in peripheral sensory neurons. Proc. Natl. Acad. Sci. U. S. A. *109*.

Movafagh, S., Crook, S., and Vo, K. (2015). Regulation of hypoxia-inducible Factor-1a by reactive oxygen species: New developments in an old debate. J. Cell. Biochem. *116*, 696–703.

Padilla, J., Lee, B.-S., Zhai, K., Rentz, B., Bobo, T., Dowling, N.M., and Lee, J. (2022). A Heme-Binding Transcription Factor BACH1 Regulates Lactate Catabolism Suggesting a Combined Therapy for Triple-Negative Breast Cancer. Cells *11*, 1177.

Padmanabha Das, K.M., Wechselberger, L., Liziczai, M., De La Rosa Rodriguez, M., Grabner, G.F., Heier, C., Viertlmayr, R., Radler, C., Lichtenegger, J., Zimmermann, R., et al. (2018). Hypoxia-inducible lipid droplet-associated protein inhibits adipose triglyceride lipase. J. Lipid Res. *59*, 531–541.

Pfeffer, S.R. (2019). NPC intracellular cholesterol transporter 1 (NPC1)-mediated cholesterol export from lysosomes. J. Biol. Chem. *294*, 1706–1709.

Pischon, T., Hankinson, S.E., Hotamisligil, G.S., Rifai, N., Willett, W.C., and Rimm, E.B. (2003). Habitual dietary intake of n-3 and n-6 fatty acids in relation to inflammatory markers among US men and women. Circulation *108*, 155–160.

Rogers, T.S., Demmer, E., Rivera, N., Gertz, E.R., German, J.B., Smilowitz, J.T., Zivkovic, A.M., and Van Loan, M.D. (2017). The role of a dairy fraction rich in milk fat globule membrane in the suppression of postprandial inflammatory markers and bone turnover in obese and overweight adults: an exploratory study. Nutr. Metab. *14*, 1–9.

Sales-Campos, H., Reis de Souza, P., Crema Peghini, B., Santana da Silva, J., and Ribeiro Cardoso, C. (2013). An Overview of the Modulatory Effects of Oleic Acid in Health and Disease. Mini-Reviews Med. Chem. *13*, 201–210.

Santamarina, A.B., Pisani, L.P., Baker, E.J., Marat, A.D., Valenzuela, C.A., Miles, E.A., and Calder, P.C. (2021). Anti-inflammatory effects of oleic acid and the anthocyanin keracyanin alone and in combination: Effects on monocyte and macrophage responses and the NF-κB pathway. Food Funct. *12*, 7909–7922.

Sauer, H., Wartenberg, M., and Hescheler, J. (2001). Reactive oxygen species as intracellular messengers during cell growth and differentiation. Cell. Physiol. Biochem. *11*, 173–186.

Schmitz, G., and Ecker, J. (2008). The opposing effects of n-3 and n-6 fatty acids. Prog. Lipid Res. *47*, 147–155.

Semenza, G.L. (2007). HIF-1 mediates the Warburg effect in clear cell renal carcinoma. J. Bioenerg.

Biomembr. *39*, 231–234.

Simopoulos, A.P. (2002). Omega-3 fatty acids in inflammation and autoimmune diseases. J. Am. Coll. Nutr. *21*, 495–505.

Tabas, I., and Bornfeldt, K.E. (2020). Intracellular and Intercellular Aspects of Macrophage Immunometabolism in Atherosclerosis. Circ. Res. *126*, 1209–1227.

Thelen, A.M., and Zoncu, R. (2017). Emerging Roles for the Lysosome in Lipid Metabolism. Trends Cell Biol. *27*, 833–850.

Tsubata, T. (2020). Involvement of Reactive Oxygen Species (ROS) in BCR Signaling as a Second Messenger. In Advances in Experimental Medicine and Biology, (Springer), pp. 37–46.

Wang, D.D. (2018). Dietary n-6 polyunsaturated fatty acids and cardiovascular disease: Epidemiologic evidence. Prostaglandins Leukot. Essent. Fat. Acids *135*, 5–9.

Weinberg, J.M. (2006). Lipotoxicity. Kidney Int. *70*, 1560–1566.

Wendland, B. (2001). Everything you ever wanted to know about endocytosis. Nat. Cell Biol. *3*, E254–E254.

Wilhelm, L.P., Wendling, C., Védie, B., Kobayashi, T., Chenard, M., Tomasetto, C., Drin, G., and Alpy, F. (2017). STARD 3 mediates endoplasmic reticulum-to-endosome cholesterol transport at membrane contact sites. EMBO J. *36*, 1412–1433.

Willett, W.C. (2007). The role of dietary n-6 fatty acids in the prevention of cardiovascular disease. In Journal of Cardiovascular Medicine, p.

Zanoni, P., Velagapudi, S., Yalcinkaya, M., Rohrer, L., and von Eckardstein, A. (2018). Endocytosis of lipoproteins. Atherosclerosis *275*, 273–295.

Zhang, D., Wen, J., Zhou, J., Cai, W., and Qian, L. (2019). Milk Fat Globule Membrane Ameliorates Necrotizing Enterocolitis in Neonatal Rats and Suppresses Lipopolysaccharide-Induced Inflammatory Response in IEC-6 Enterocytes. J. Parenter. Enter. Nutr. *43*, 863–873.

SUMMARY

SUMMARY

Fat is one of the three macronutrients in our diet, which is used either as an energy source or as a structural component of membranes and other cellular structures. Once taken up into the body, lipids are transported and metabolically processed to fulfill these two major roles. Although adipocytes and monocytes/macrophages have very different functions in the body, they each can take up, store, and catabolize lipids. Altered lipid metabolism in adipocytes and monocytes/macrophages is a hallmark of several major diseases, including obesity and cardiovascular disease.

Lipids are transported in the circulation in particles called lipoproteins, which include chylomicrons, VLDL, LDL, and HDL. The levels of these lipoproteins can vary depending on the nutritional state. After a meal, plasma levels of chylomicrons and to a lesser extent VLDL, are increased, a situation referred to as postprandial lipemia. The lipid in these lipoprotein particles can be taken up by adipocytes and monocytes/macrophages. To maintain intracellular lipid homeostasis, the adipocytes and monocytes/macrophages respond to changes in lipid uptake by promoting lipid storage and degradation, as well as activating other metabolic pathways. An overload of lipids or a failure to properly activate these pathways may impair the function of the adipocytes and monocytes/macrophages and lead to cell stress. How adipocytes and monocytes/macrophages handle excess lipid exposure, either in vivo or in isolated cells, and how exposure to lipids influences the function of the cells are not clearly understood. Hence, the goal of this thesis was to fill these knowledge gaps via studies in isolated adipocytes and monocytes/macrophages, laboratory animals, and humans.

Chapter 1 summarizes the principles of lipid metabolism and its regulation at the organismal and cellular levels. It describes the importance of lipid metabolism in immune cells to human health and discusses the potential immunomodulatory effects of dairy fat consumption.

The majority of dietary fat is in the form of triglycerides (TG), complemented by small amounts of cholesterol and phospholipids. After digestion in the intestine and packaging into chylomicrons, dietary fat is distributed across various organs, where it can contribute to the production of other lipoproteins, including VLDL, LDL, and IDL. Adipocytes are cells that are specialized in storing energy as TG. When tissues need lipids as fuel, the TG stored in adipocytes are broken down into fatty acids and released into circulation. In normal physiology, lipolysis and TG synthesis are well balanced and are adjusted based on cellular and whole-body needs. Non-homeostatic lipid metabolism in adipocytes is associated with cellular stress, such as ER stress. Proper self-regulation of lipid metabolism is important for cells to maintain lipid homeostasis. For example, by sensing the levels of fatty acids, activation of GPR120 initiates a negative feedback regulation of lipolysis in

adipocytes. TG are stored in cells in special organelles called lipid droplets. Several non-enzymatic proteins physically associated with lipid droplets have been identified that play a role in maintaining lipid droplet integrity, either by stabilizing enzymes involved in TG synthesis or by inhibiting lipolytic enzymes, such as adipose tissue triglyceride lipase (ATGL). Excess availability of lipids as well as aberrant lipid metabolism in adipocytes and monocytes/macrophages can contribute to the development of metabolic diseases. Macrophages can take up lipoproteins and store the lipids in lipid droplets. The uptake of lipoprotein requires endocytosis and may be facilitated by specific receptors as well as auxiliary proteins, such as LPL. Uptake of lipids by immune cells can not only fuel the cells but also affect their functional phenotype. Accordingly, dietary fats with different fatty acid compositions may differentially impact postprandial inflammation.

HILPDA is a lipid droplet-associated protein that is involved in maintaining the integrity of lipid droplets. In **chapter 2** of this thesis, we investigated the participation of HILPDA in the autocrine feedback regulation of lipolysis in adipocytes. Primary adipocytes were isolated from *Hilpda*$^{flox/flox}$ mice and *Hilpda*$^{\Delta ADIPO}$ mice and were treated with fatty acids and the synthetic GPR120 agonist, TUG 891. Both fatty acids and TUG891 induced HILPDA protein expression along with a decrease in ATGL levels. However, the effects of fatty acids and TUG 891 on ATGL were markedly blunted in HILPDA-deficient adipocytes. This indicates that the autocrine negative regulation of lipolysis by GPR120 is dependent on HILPDA and involves inhibition of ATGL expression. Similarly, raising intracellular fatty acids by inhibiting fatty acid re-esterification induced HILDPA and reduced ATGL levels in adipocytes, which was markedly blunted in HILPDA-deficient adipocytes. Consequently, HILPDA deficiency in combination with inhibition of fatty acid re-esterification increased the expression of ER stress genes, suggesting that HILPDA alleviates ER stress in adipocytes by regulating lipolysis via inhibiting ATGL. In mice that fasted for 20 hours followed by 4 hours of refeeding, HILPDA deficiency in adipocytes was associated with a marked increase in ATGL protein level, concurrent with increased expression of ER stress-related genes. This indicates that HILPDA has an important role in the homeostatic control of lipolysis by downregulating the ATGL protein.

Triglycerides are mainly carried in the bloodstream as part of very low-density lipoproteins (VLDL) and chylomicrons, which represent the TG-rich lipoproteins. TG-rich lipoproteins and their remnants contribute to atherosclerosis, possibly by carrying remnant cholesterol and/or by exerting a pro-inflammatory effect on macrophages. **Chapter 3** of the thesis examined the mechanism by which macrophages process TG-rich lipoproteins. Using VLDL-sized emulsion particles, our results show that macrophage uptake of VLDL-sized emulsion particles is dependent on LPL and requires the C-terminal domain but not the catalytic N-terminal domain of LPL. Subsequent internalization of

VLDL-sized emulsion particles by macrophages is carried out by caveolae-mediated endocytosis, followed by TG hydrolysis catalyzed by lysosomal acid lipase. It is shown that STARD3 is required for the transfer of lysosomal fatty acids to the ER for subsequent storage as TG, while NPC1 contributes to exporting fatty acids from lysosomes. Our data provide novel insights into how macrophages process VLDL triglycerides and show that macrophages can excrete part of the internalized TG as fatty acids.

Elevated postprandial lipids are associated with an increased risk of atherosclerotic cardiovascular disease. While numerous studies have examined the effect of different dietary fat sources on postprandial lipid levels, a more global analysis of postprandial plasma metabolites is missing. A common fat source in the Western-type diet is milk fat. In **chapter 4**, we described the investigation of the acute effects of milk fat on postprandial metabolites via a double-blind crossover human trial. In this trial, 37 participants received in random order a high-fat shake composed of cream (CREAM), anhydrous milk fat (AMF), or vegetable fat (VEGE). Blood samples were drawn up to eight hours after consumption. At baseline, and 3 and 6 hours postprandially, plasma metabolites were measured using NMR metabolomics. It was found that AMF and CREAM consumption resulted in a faster postprandial increase and decrease in several fractions of VLDL and the inflammatory protein GlycA. Consumption of CREAM resulted in a more rapid increase at 3 hours and a faster decrease at 6 hours postprandially compared to the other shakes. Consumption of CREAM resulted in a more rapid increase in total TG and branched-chain amino acids at 3 hours and a faster decrease at 6 hours compared to the other shakes.

Within the same study as mentioned above, we also explored the postprandial effect of these shakes on the whole transcriptome of monocytes (**chapter 5**). Blood monocytes were collected at 0 hours and 6 hours postprandially and used for whole RNA sequencing analysis and ex vivo incubation with LPS.

Using a threshold of $P<0.01$, 787 genes were differentially regulated postprandially between the three shakes. 89 genes were differentially regulated postprandially between AMF and VEGE, while 373 genes were differentially regulated between AMF and CREAM and 667 genes between VEGE and CREAM, indicating that the effect of CREAM on monocyte gene expression was very distinct from AMF and VEGE. Pathway analyses showed that VEGE significantly activated inflammatory pathways while this was less evident after the AMF intervention and not observed after consumption of CREAM. In addition, CREAM significantly down-regulated energy metabolism-related pathways,

such as glycolysis, TCA cycle, and oxidative phosphorylation, as well as HIF1 signaling, which transcriptionally regulates mitochondrial metabolism and inflammatory pathways.

In conclusion, in this thesis, we revealed how lipolysis in adipocytes is suppressed by fatty acids via GPR120. It is shown that HILPDA is essential for an autocrine negative feedback regulation by inhibiting ATGL expression, thereby protecting against lipid-induced cell stress (**chapter 2**). In **chapter 3** we uncovered how macrophages take up TG-rich lipoprotein particles. We show the role of LPL and caveolae-mediated pathways and demonstrate that macrophages excrete part of the internalized triglycerides as fatty acids. Moving from basic cellular lipid physiology to human nutritional lipidology, we found that milk fat consumption led to a faster increase and a faster return of postprandial VLDL and the inflammation marker GlycA in humans, compared to a vegetable fat blend (**chapter 4**). In **chapter 5**, an analysis of the transcriptome in monocytes from the participants shows that the consumption of milk fat is not associated with postprandial inflammation. Furthermore, the consumption of CREAM significantly inhibited energy and inflammation-related pathways, which may result in a suppression of monocyte activation. The collective data are integrated and discussed in **chapter 6**.

ACKNOWLEDGMENT

Acknowledgement

Time flies. It seems it did not take quite long to be here, as I can still recall the moment Sander picked me up at the reception on the first day of my arrival. Then my first day started… Couldn't find where the toilet is; didn't know how to get some water although was super thirsty; didn't know whether I can touch my phone in the office… But now, it seems I know everything on the second floor, except for the most basic question—do you indeed like Danny? If your answer is "yes", then congratulations! You can continue reading this part and looking for your nice name. ☺

There is an old saying in China—one-day teacher, life-long parent, which means we should always be grateful to people who give us knowledge and teach us how to grow up. Here I would like to sincerely thank **prof. dr. Sander Kersten**. Thank you, Sander, for all the support and help in these nearly five years. You offered me the chance to study here and helped me get a CSC scholarship. I really appreciate this. Your support indeed made this process very smooth and impressive. I was the first MSc student in my previous institute who applied for a CSC scholarship. I heard many times from junior students that our nice example has been inspiring others to pursue the opportunity of studying abroad, which for sure is of great importance for personal development. Personally, you are the most important person who guides me into science and allows me the potential to be an excellent scientist in the future. I was from food science and had limited knowledge of biology. It is your extremely patient and motivating supervision that guides me more and more in the field and allows the possibility that I can be awarded a doctorate in the molecular biology field. Of course, yourself is automatically an amazing example as well. The critical way you think, the rigorous attitude toward research, and the enthusiasm for science, fuel me a lot and make me always be energetic in science and I am pretty sure I can benefit from this for my whole life. I and my wife were also inspired by the saying that you posted that you need to make a good example for your students and children. We now also decided to do so as well. We are always paying attention to our behavior and being as proper as possible. Thank you!

Dr. Lydia Afman, thanks for the kind and patient supervision in the past years. You always look good, confident, and intelligent. In the beginning, when you joined the supervising team, I thought your expertise is in human intervention and frankly I was not very open to discussing the mechanistic data with you, but gradually I found I was completely wrong. The way you think about the research and the broad knowledge you have in metabolism, immunology, and data science is indeed impressive as well. I learned a lot from you as well. And of course, thank you for inviting me to join the group meeting and nice BBQs at your home. I am grateful for this. You know, someone never invites me and maybe that is the reason why we are struggling to get his name on board. ☺

Dr. Rinke Stienstra, I would like to publicly announce that your supervision is substantial, continuous, and extremely important during my PhD, although I just can pronounce your cool last name at the end of my PhD. It seems I asked more questions and help even more than your "official students". Thank you a lot for your patience and efficient help all the time. This is very much appreciated. **Mr. Stienstra**, you also set a nice example for our new family about how to smartly improve our financial status. I have already convinced my wife to work in a company to support our finance and she promised she will get me a TESLA as well if I can contribute to science as much as you. I truly believe we can have a TESLA racing someday in the future. As you said, one of the most exciting things for a man is driving a fancy car in a crowded street with a beautiful wife aside.

Dr. Anouk Feisma, thank you for supervising me continuously over the last 4.5 years. The first thing I would like to say you and Frislandcampina refreshed my knowledge about how professional a researcher in a company can be and how much a company can input into innovation. This is something our Chinses industry certainly needs to improve now. In the beginning, I thought you being one member of the supervision team was just the need for cooperation. However, this changes as you can always ask professional questions and give nice suggestions at our meetings. I would like to say you are a combined scientist in both food science and immunology. Thank you very much for your support all the time.

Merel and **Antwi**, as I said always, I do consider you two as my daily supervisors, especially in the first year of my Ph.D. Without you two, I cannot manage to master the necessary practical tools in molecular biology very fast. This is a good base for my research work and also a good base for the supervisors to help me. I am very grateful for this. **Merel**, you have all the features of an excellent teacher, which I almost told all of my students. I truly believe you will impact and inspire many students or junior researchers now and in the future. **Antwi**, I still often recall the moments we discussed my results, even at this moment when you have become my ex-colleague already for more than 3 years. You have set a very good example of how to interpret data and plan the next experiment. Thank you for being there all the time when I have any questions and wish you very smooth in your research.

My dear paranymphs, **Brecht** and **Frank**, first of all, I would like to sincerely thank you accept my invitation to be my paranymphs. I worried in the first year that if no one is willing to be my paranymph, I will be extremely embarrassed. **Brecht**, I enjoyed our coffee breaks, and we shared a lot always. You are the first colleague who invited me for a walk during a work break. I am really appreciative of this, which gives me a feeling that I indeed successfully integrated into this non-Chinese

environment. Yes, you are a really good baker, and please keep going. I am always willing to do a sensory experiment for you ☺. **Dr. Frank**, thank you for the chance to let me experience a Dutch wedding, which is quite nice. You and Maria also inspire me that we need to seek more chances to do more for this world. I am very grateful for this. Of course, your supports for all the experiments are also very appreciated. As said, your coming upgraded the technologies and models used in my thesis.

My dear officemates, of course, I would like to thank you for the free, relaxed, and happy atmosphere you contributed to. **Karin,** our office plant expert, it is very nice that I can always get nice suggestions about plants from you. We cultured three plants from one loquat fruit. What a magic thing! I hope we can get a lot of loquats one day and then the department doesn't need to buy daily fruit anymore! ☺ **Marlies,** you are always very busy, but my feeling is that no matter how busy you are, you always keep your sunny smiles on your face, which makes me very relaxed. I am sorry for your bad experience with the Chinese company about your order. I hope you will solve the issue soon. **Peter,** very nice to see you again in our office. Although we didn't have many talks, I found somehow, I still miss you during Covid-19 time. I wish you all the best now and in the future! **Yan,** I think you are doing a quite good job. You adapted yourself rapidly to this new environment and successfully integrate yourself in the group and I can see your efforts all the time. You also work hard and efficient. I believe that you will have a very fruitful achievement during your PhD. And thanks for the wedding gift. Yours is the first! We really appreciate that. Cheers! **Walid,** you are always kind to everyone and warmly greet people. This is very impressive. Enjoy your new fancy house and all the best!

Thank you, **Guido**, a rich guy who even has a road named after **Hooiveld**. It was you who was always trying to talk to me when was surrounded by Dutch language at the beginning, which made me feel much easier when newly joined the group. You are always kind and willing to help, especially at the beginning, which makes me faster to adapt to the new environment here. You know it was the first time for me to be abroad. I have to admit that it was not very easy at the beginning, although I behaved as such. You helped a lot! However, I still want to address that I strongly disagree with you about some of your opinions on China. Wait for my invitation, I will invite you to experience a real China soon. I will persuade you through what you can see, instead from the so-called unbiased medias.

Benthe, I am very glad you still work in helix, which gives me the feeling we still work together. It is very appreciated that you were always trying to get me to be in the group lunch, which I still consider that is extremely necessary for fast integration into the group for new arrivers, especially for non-Dutch students. Thank you as well for your very kind help not only in lab work but also for

explaining to me the Dutch culture, which also helps to have a good adaption. Thank you and wish you a happy journey in life and work.

Xanthe, As I mentioned before, your protocols and data are always trustable to me. I really appreciate that every time the way you answer my questions. Always much more than I asked. Your patience and extra care have always deeply moved me. It is very lucky of me that can have a colleague like you! You are always serious and good at framing things. During the writing of my thesis, I always keep yours and Merel's in my hand, which helped a lot. Wish you all the best in your current position and in helping patients with your professional knowledge.

Montse and **Philip**, we had several nice meals together. I really enjoyed them, although the meals were always later than scheduled, which caused my stomachache all the time. You guys have been supporting me all the time in the lab. Thank you, **Philip,** for teaching me the skills and knowledge in adipocytes, which is certainly one of the most important parts of my thesis. And **Montse**, you helped a lot with confocal technology, which I used throughout my first paper. Thank you, guys!

Anouk, you are always happy and smiling. Do you still remember that I said you have an Asian face when I just arrived? Forget about it. I don't think so as well. I enjoy all the relaxed talk with you. You are always frank. What keep in my mind is what you said – bikes have the highest priority in the Netherlands. I absolutely believed in you until an old gentleman yelled at me in the street, when I was cycling in a walking area ☹. **Charlotte**, it was very nice that we performed the POEMI study together. I am quite grateful that you asked me every day, what kind of dinner should prepare for myself, especially when I was super starving. Thanks a lot! Hope our fruits will mature soon! **Patrick**, you are indeed a tiger, no, maybe a leopard. You know I am trying to pick up the right word to describe your talent in athletics. I have never seen a person in reality as great as you, especially among those who are in research. Impressive! **Judith**, actually I just realized we are not in the same chair group several months ago. I was trying and always failed to figure out who is your supervisor at NMG for quite a long time. For me, you are already a fixed member of the group. You are always kind and smiling whenever we talk. I think it is quite relaxing when talking to you.

Shohreh, I was impressed by your energetic hairstyle on the first day I came. You are always warm-hearted and helpful in everything. You made a lot of urgent orders for me. I am really grateful for this. **Jenny**, it seems you never have bad moods. Always smiling, except the moments you found sensimix disappeared in the "secret" place (although I think many people know this). Thank you very much for helping us out with RNA isolation from numerous samples. I know it was tough, but finally, it is good. Keep smiling and enjoy happy life every day! **Mechteld**, you are really an expert in making

cotton candy (BBQ style) (I still don't know the Dutch name). That was the best I had eaten! Amazing! And also thank you for arranging nice wedding gifts with other colleagues. That was indeed a great inspiration for the young couple. I wish you all the best and can buy more holidays in the coming years (also wish Lydia will be fine with this ☺).

Bryan, you know what, every time when we use our dishwasher, we will appreciate your nice contribution. Thanks a lot for inviting me to a celebration at DOPPIO on my wedding day. I will remember that forever. **Mark**, you always dress well and with a decent hairstyle. I think you are the colleague I meet most outside work hours. **Michel**, thanks for being the officemate of Walid and Marlies, and then we almost greet each every day. Your daughter is impressively cute. Very nice to meet her in Lidl! **Wilma**, thanks a lot for your nice suggestion for job hunting. I proved it very useful! And also appreciate the chance you allowed me to be involved in the practical course. I learned a lot! Good luck with everything!

Mara, your name was so friendly for me at beginning when I was struggling with all difficult names. You are always very friendly and happy. It was also unbelievable that you visited so many cities in China in a short time, which I think even more than me! Hope I can have a chance to guide you a trip in China in the future. Thanks for all the help in the past years! Good luck with everything! **Monique**, you did quite nice with the "shrimp dance", which is definitely impressive for me. I am recalling this all the time when I see shrimps! Yes, indeed, they are so cute. The only pity is that till now we still don't have you play piano at impulse! Hope that will come true soon!

Mieke, I enjoyed a lot talking to you. The moment I saw the "Danny" centrifuge, I realized that I indeed have a big name and am very proud of myself. Thanks a lot. One suggestion Mieke, you should be more confident in yourself. All my nice words about you are absolutely true. I am not a "SLIMBAL" ☺. There is still one thing I need to check, which is making Sander mad, and tell him Mieke told me this. I guess this will work ☺. **Lisa**, I look forward to working for "Smeehuijzen lab". Please make sure you can give me a good salary ☺. Thanks for all the nice talks and jokes all the time, which always make my day. An important thing maybe remember is never to ask people like me to float in the Rine ☺. Thanks for your medium which supports all my monocytes/macrophages experiments. Good luck with everything! **Tessa**, I enjoyed the time we joined PhD week together. At that moment, I was still shy and appreciated you, and Laura always encourage me to join all kinds of activities. Thanks a lot! By the way, I do eat more tomatoes after you start your project. Wish you everything smooth with the thesis finishing. **Ainna**, you are new to the group. I am impressed a lot by your motivation to learn Dutch, which I planned for many years already, but never started. Thanks a lot

for the detailed suggestions for the Barcelona trip. It was very helpful! Wish you all the best with your study!

Mingjuan, thanks a lot for the help in the past years. I am grateful and appreciate a lot. You are smart and learning things very fast. I wish you continuously good in research and all the best!

Meirong, and **Ruolei**, you are doing a good job and I am pretty sure you will manage all the difficulties during your Ph.D. Looking forward to reading your amazing papers in the future. Cheers!

I also would like to thank all of my students: **Chuang Sun**, **Mingqian Xu**, **Morena Bertuzzi**, **Valerio Taggi**, **Xuan Shi**, **Ajit Pratihast**, **Lobke Zijlstra** and **Maria Aroutionouva** during these years. The accomplishment of my thesis cannot be without support from you.

我要感谢我的本科导师刘学波教授，是您为我打开了科学研究的大门并使我对之兴趣盎然！初入大学时，您展现出来的一位优秀科研工作者的精神风貌和治学态度深深地感染了学生！谢谢您！以及无比感恩于硕士导师王强研究员的求真务实的指导，是您的严谨治学，社会责任感以及对学生弥足珍贵的鼓励让我在科研这条路上坚持下来并乐在其中！铭记师恩！

借这个难得的正经机会，我要诚挚的感谢我在瓦村以及不在瓦村的中国朋友们 （避免你们争风吃醋，此处不具名，不排名了哈☺ 接下来小邓厨房的邀请会让你们看到我的诚意的☺）。感谢这四年以来你们的陪伴，帮助以及不离不弃！

感谢我的妻子刘宇思女士，是你的帮助与陪伴让我平稳而又激情澎湃地拼搏！回过头来看，牵手这 11 年里，自己变化良多且满意于此间蜕变，我想大多得益于你的包容与陪伴。愿来日方长，幸福绵延。说到这，应该也要感谢我的岳父刘俊强先生和岳母郝红格女士！谢谢您们一直以来的支持与信任，以及培养出这么好的女儿！感激感恩！

我也要感谢我的父母，邓卫华先生和吕启美女士，是你们营造的美满温馨的家庭让我在岁月静好中砥砺前行。常说，一个人的天赋决定了他能走多快，但他背后的家庭以及耳濡目染的教育能决定他走多远！我来源于农村，祖辈三代务农，时至今日，很欣然于自己所站立的位置。我想这与您们给与我的家庭与教育是分不开的。很小的时候就常常骄傲于有这样的父母。 当其他的农村妈妈们只算计着地间田头时，我的妈妈却有着记日记的习惯；当其他的务工爸爸光膀子喝啤酒时，我的爸爸穿着体面看书学习。我想正是骄傲于有这样优秀与众不同的父母，才会在内心深处根植着与众不同的梦想并为之奋斗！谢谢您们，亲爱的爸爸妈妈！

最后我要向中国留学基金委致以崇高的敬意！我想说这是一个弥足珍贵的机会让我这个出生于普通家庭的孩子有了出国学习的机会。这四年有余的学习让我受益良多，也养成了严谨，务实，勤于思考，敏于科研的态度和习惯，并收获了继续深耕的勇气！感恩铭记！

October 2022 in Wageningen

The Author

About the author

Short biography

Lei Deng was born on 29 November 1990 in Jiangsu, China. He grew up in a beautiful and mild village, which is famous for the production of rice and fish. Inspired by his father, a construction worker, and his mother, a traditional farmer, he made his dream to be a scientist when he was in primary school. Benefiting from his parents' continuous motivation and the happy family, he had been working hard and finally successfully start his bachelor's study at Northwestern University of Agricultural and Forestry Science and Technology (Yangling, Shannxi province), which is a key national comprehensive university. In 2014, he moved to the Chinese Academy of Agricultural Sciences (Beijing) and started his master's studies after obtaining his bachelor's degree in *Food Science and Technology*. From 2014 to 2017, he had been exploring the sleep-promoting effect of peanut stems and leaves under the supervision of Prof. Dr. Qiang Wang. During his master's thesis work, he felt a lack of knowledge of molecular biology and thus had been following the research activity of Prof. Dr. Sander Kersten's lab. Being impressed by Sander's amazing work in Nutrition, Metabolism, and Genomics, he applied to be a Ph.D. student in Sander's team at Wageningen University and Research in the year 2018 with financial support from China Scholarship Council and FrieslandCampina. During his Ph.D. study, Lei has been exploring the regulatory pathways of lipids in adipocytes, and monocytes/ macrophages using in vitro, ex vivo, and in vivo models. These studies make him realize the importance of metabolism regulation to not only metabolic homeostasis, but also balanced immunity for humans, and raised his great interest in immunometabolism. Now Lei has finished his Ph.D. thesis and is ready to continue his scientific adventure with a lot of passion.

List of publications

Deng, L., Vrieling, F., Stienstra, R., Hooiveld, G., Feitsma AL., Kersten, S. (2022). Macrophages take up VLDL-sized emulsion particles through caveolae-mediated endocytosis and excrete part of the internalized triglycerides as fatty acids. ***PLOS Biology,*** 20(8): e3001516.

Montserrat, A., **Deng, L.**, Gemmink, A., van Weeghel, M., Aoun, M. L., Warnecke, C., ... & Kersten, S. (2021). Hypoxia-inducible lipid droplet-associated induces DGAT1 and promotes lipid storage in hepatocytes. ***Molecular metabolism***, 47, 101168.

Dierendonck, X., Vrieling, F., Smeehuijzen, L., **Deng, L.**, Boogaard, J., Croes, C.,…& Stienstra, R. (2022). Triglyceride breakdown from lipid droplets regulates the inflammatory response in macrophages", ***PNAS***, 2114739119.

Ruppert, P. M., **Deng, L.**, Hooiveld, G. J., Hangelbroek, R. W., Zeigerer, A., & Kersten, S. (2021). RNA sequencing reveals niche gene expression effects of beta-hydroxybutyrate in primary myotubes. ***Life science alliance***, 4(10).

Overview of completed training activities

Discipline specific activities

Conferences and symposia

- Lipid Meeting, 2019

Institute of Laboratory Medicine, Leipzig, Germany

- ISSFAL congress 2021/AOCS Annual meeting&Expo, 2021

ISSFAL & AOCS, Online

- Dutch translational metabolism Seminar, 2021

Dutch Translational Metabolism Conference, Online

- Keystone Symposia: Lipidomics of Health and Disease, 2021

Keystone Symposia, Online

- 44th Annual Scientific meeting of the ELC, 2021

European Lipoprotein Club, Tutzing, Germany

- 38th International Symposium on Diabetes and Nutrition, 2021

European association for the study of diabetes, Online

- Translational immunometabolism, 2022

Cell symposium, Basel, Switzerland

General courses

- VLAG PhD week, 2018

  VLAG, Baarlo, The Netherlanders

- WGS PhD Carousel, 2018/2022

  WGS, Wageningen, The Netherlands

- Bridging across cultural differences, 2018

  WGS, Wageningen, The Netherlands

- Introduction to R, 2018

  VLAG, Wageningen, The Netherlands

- English Pronunciation and Fluency, 2018

  Wageningen in'to Languages, Wageningen, The Netherlands

- Scientific writing, 2021

  WGS, Wageningen, The Netherlands

- Supervising BSc & MSc thesis students, 2021

  WGS, Wageningen, The Netherlands

- Create your data management plan, 2022

  HNH, Wageningen, The Netherlands

Assisting in teaching and supervision activities

- Practical tools in molecular nutrition research, 2018

Wageningen University and Research, Wageningen, The Netherlands

- Supervision of MSc students, 2018-2022

Wageningen University and Research, Wageningen, The Netherlands

Other activities

- Preparation of research proposal, 2018

HNH-NMG, Wageningen, The Netherlands

- Biweekly journal club team Sander Kersten, 2018-2022

HNH-NMG, Wageningen, The Netherlands

- Weekly meeting NMG and NB group, 2018-2022

HNH-NMG and NB group, Wageningen, The Netherlands

- Monthly discussion with Friesland Campina, 2018-2022

HNH-NMG, Wageningen, The Netherlands

The research described in this thesis was financially supported by FrieslandCampina (PACMAN 181102) and a CSC Scholarship (201703250072) funded by China Scholarship Council.

Financial support from Wageningen University for printing this thesis is gratefully acknowledged.

Cover design: 李幼润 | 勤研科研绘图

Printed by: Digiforce | Proefschriftmaken.nl